



TEXAS TECH UNIVERSITY

Multidisciplinary Research in Transportation™

# Study of Elastomeric Bearings for Superelevated U-Beam Bridges

Authors: Charles D. Newhouse, Scott A. Bole, W.R. Burkett, Phillip T. Nash, Mostafa El-Shami

Performed in Cooperation with the Texas Department of Transportation  
and the Federal Highway Administration

Research Project 0-5834  
Research Report 0-5834-1  
<http://www.techmrt.ttu.edu/reports.php>

## **Notice**

The United States Government and the State of Texas do not endorse products or manufacturers. Trade or manufacturers' names appear herein solely because they are considered essential to the object of this report.

### Technical Report Documentation Page

1. Report No.:  FHWA/TX -09-5834-1	2. Government Accession No.:	3. Recipient's Catalog No.:	
4. Title and Subtitle: Study of Elastomeric Bearings for Superelevated U-Beam Bridges		5. Report Date: October 2009	
		6. Performing Organization Code:	
7. Author(s): Charles D. Newhouse, Scott A. Bole, W. R. Burkett, Phillip T. Nash, Mostafa El-Shami		8. Performing Organization Report No. 0-5834-1	
9. Performing Organization Name and Address: Texas Tech University College of Engineering Box 41023 Lubbock, Texas 79409-1023		10. Work Unit No. (TRAIS):	
		11. Contract or Grant No. : Project 0-5834	
12. Sponsoring Agency Name and Address Texas Department of Transportation Research and Technology Implementation Office P. O. Box 5080 Austin, TX 78763-5080		13. Type of Report and Period Cover: Technical Report 09/2007 – 08/2009	
		14. Sponsoring Agency Code:	
15. Supplementary Notes: Project performed in cooperation with the Texas Department of Transportation and the Federal Highway Administration			
16. Abstract: The primary objective of this research was to determine the best way to consider the effects of transverse superelevation on uniform-height steel-reinforced elastomeric bearing pads for U-Beam bridges. Existing TxDOT design provisions did not specifically account for the effects of the transverse superelevation. A nationwide survey of Departments of Transportation (DOTs) revealed that the country was nearly evenly split on whether or not superstructure elements such as U-Beams should be placed on a transverse superelevation. Specific modifications to the AASHTO Method "A" design of elastomeric bearing equations were developed to account for the transverse superelevation. The proposed modifications were evaluated over typical U-Beam span/spacing combinations for both the U-40 and U-54 sections. The ability of the proposed modifications to predict actual behavior was evaluated by inspecting existing bridges and performing full-scale laboratory testing. Both the field inspections and the laboratory testing validated the need for the proposed revisions. These proposed revisions have been submitted as suggested revisions to the TxDOT LRFD Bridge Design Manual. The feasibility of electronic monitoring in-situ bearings that have experienced significant transverse deflections was investigated. The bulging on the sides of the bearings made monitoring unreliable. Instead, a method to manually record pertinent information during the routine bridge inspection is recommended.			
17. Key Words; superelevation, transverse, transverse slope, u-beam, elastomeric bearing		18. Distribution Statement No restrictions. This document is available to the public through the National Technical Information Service, Springfield, VA 22161, www.ntis.gov	
19. Security Classif. (of this report) Unclassified	20. Security Classif. (of this page) Unclassified	21. No. of Pages	22. Price



# Study of Elastomeric Bearings for Superelevated U-Beam Bridges

by

Charles D. Newhouse, Scott Bole, W.R. Burkett,  
Phillip T. Nash, Mostafa El-Shami

Report Number  
0-5834-1

Conducted for

Texas Department of Transportation  
in cooperation with the  
U.S. Department of Transportation  
Federal Highway Administration

by the

Center for Multidisciplinary Research in Transportation

## **AUTHOR'S DISCLAIMER**

The contents of this report reflect the views of the authors who are responsible for the facts and the accuracy of the data presented herein. The contents do not necessarily reflect the official view of policies of the Texas Department of Transportation or the Federal Highway Administration. This report does not constitute a standard, specification, or regulation.

## **PATENT DISCLAIMER**

There was no invention or discovery conceived or first actually reduced to practice in the course of or under this contract, including any art, method, process, machine, manufacture, design or composition of matter, or any new useful improvement thereof, or any variety of plant which is or may be patentable under the patent laws of the United States of America or any foreign country.

## **ENGINEERING DISCLAIMER**

Not intended for construction, bidding, or permit purposes.

## **TRADE NAMES AND MANUFACTURERS' NAMES**

The United States Government and the State of Texas do not endorse products or manufacturers. Trade or manufacturers' names appear herein solely because they are considered essential to the object of this report.

## ACKNOWLEDGEMENTS

Researchers are grateful for the opportunity to thank the project monitoring committee for this research project, including Project Director John Holt of the TxDOT Bridge Division, as well as Jeff Cotham, Amy Eskridge, Dacio Marin, and Keith Ramsey, also from the TxDOT Bridge Division, and Walter Fisher III, TxDOT Dallas District Office. Much thanks is also due to Frank Wyatt and Doug Haynes of the Texas Tech University Department of Civil and Environmental Engineering for their assistance in the laboratory testing, and to Adam Davidson for his assistance in laboratory testing as well.

Prepared in cooperation with the Texas Department of Transportation and the U.S. Department of Transportation, Federal Highway Administration.

# Table of Contents

Technical Documentation Page .....	i
Title Page .....	iii
Disclaimers .....	iv
Acknowledgements.....	v
Table of Contents .....	vi
List of Figures .....	x
List of Tables .....	xiii
<b>1. Introduction .....</b>	<b>1</b>
1.1 General.....	1
1.2 Research Objectives.....	3
1.2.1 Research Objective No. 1 .....	3
1.2.2 Research Objective No. 2 .....	4
1.3 Report Organization.....	5
<b>2. Background .....</b>	<b>6</b>
2.1 Literature Review.....	6
2.1.1 History of the Texas U-Beam .....	7
2.1.2 Background of Elastomeric Bearing.....	7
2.1.3 AASHTO Bearing Design Requirements .....	9
2.1.4 TxDOT Bearing Design Requirements.....	10
2.1.5 Triaxial or Multi-Axial Behavior Studies of Elastomeric Bearings .....	11
2.1.6 Full Scale Testing Completed on Elastomeric Bearings.....	15
2.1.7 Performance of Elastomeric Bearings at Low Temperatures .....	16
2.1.8 Previous Finite Element Analysis Studies .....	17
2.1.9 National Cooperative Highway Research Program Report 596 .....	19
2.1.10 Conclusions.....	23
2.2 DOT Questionnaire Survey.....	24
2.2.1 Question No. 1 .....	24
2.2.2 Question No. 2 .....	26
2.2.3 Question No. 3 .....	26
2.2.4 Question No. 4 .....	28
2.3 Pontis Element No. 310 – Elastomeric Bearing.....	28
<b>3. AASHTO Design Provisions .....</b>	<b>34</b>
3.1 Current Design Provisions .....	34
3.2 Theory of the Proposed Modifications to Current Provisions .....	36
3.3 Limits Considered.....	38
3.4 Design Example with Proposed Modifications.....	40
3.4.1 Discussion of Design Example .....	48
3.5 Summary of Design States.....	48
3.5.1 Discussion of Summarized Design States.....	65
<b>4. Observations and Testing.....</b>	<b>66</b>
4.1 Overview of Tests Performed .....	66
4.2 Wichita Falls Bridge Inspection.....	66

4.2.1	Documentation of the Inspection .....	67
4.2.2	Comparison of Predicted Values .....	71
4.2.3	Summary of Wichita Falls Inspection.....	71
4.3	US 82 Bos-W Ramp Overpass at East 4 <sup>th</sup> Street in Lubbock, TX Field Test.....	72
4.3.1	Testing Program Overview .....	73
4.3.2	Testing Performed.....	77
4.3.3	Results – Visual Observations .....	77
4.3.4	Results – Strain Gage Readings.....	78
4.3.5	Summary of US 82 Bos-W Ramp Overpass Tests .....	80
4.4	Laboratory Testing.....	81
4.4.1	Testing Program.....	81
4.4.1.1	<i>Design of Experimental Apparatus</i> .....	81
4.4.1.2	<i>Test Frame</i> .....	81
4.4.1.3	<i>Concrete Blocks</i> .....	81
4.4.1.4	<i>Hydraulic Cylinders</i> .....	84
4.4.1.5	<i>Bearings</i> .....	84
4.4.1.6	<i>Strain Gages</i> .....	85
4.4.1.7	<i>Pressure Gages</i> .....	86
4.4.1.8	<i>Linear Displacement Gages</i> .....	87
4.4.1.9	<i>Vishay Micro-Measurements System 5000 Data Recorder</i> .....	87
4.4.1.10	<i>Test Matrix and Procedure</i> .....	89
4.4.1.11	<i>Simulation of Forces</i> .....	90
4.4.1.12	<i>Data Recorded</i> .....	91
4.4.2	Single Pad Test Results.....	92
4.4.3	Dual Pad Test Results .....	98
4.4.4	Summary of Observations.....	98
4.5	Finite Element Modeling .....	104
4.5.1	Description of the Finite Element Model.....	104
4.5.2	Comparison of FEA to Laboratory Testing .....	106
4.5.3	Summary of Observations.....	110
<b>5.</b>	<b>Comparison of Testing/Observations to Modified Design Provisions .....</b>	<b>111</b>
5.1	Combination of Transverse and Longitudinal Displacement .....	111
5.2	Prediction of Transverse and Longitudinal Deflections .....	126
5.2.1	Analysis of Transverse Angles Observed .....	126
5.2.2	Analysis of Longitudinal Angles Observed.....	130
5.2.3	Regression Analysis of Laboratory Results.....	139
5.2.4	Summary of Transverse and Longitudinal Displacements .....	144
5.3	Prediction of Uplift and/or Slipping .....	144
5.3.1	Measurement of Slip.....	144
5.3.2	Analysis of Slip Data .....	147
5.3.3	Regression Analysis for Slip.....	154
5.3.4	Measurement of Uplift.....	159
5.3.5	Analysis of Uplift.....	160
5.3.6	Prediction of Uplift .....	163
5.3.7	Summary of Uplift and Slip.....	164
5.4	Prediction of Damage .....	164
5.4.1	Reporting of Observed Damage to Bearings .....	164
5.4.2	Categorization of Observed Damage .....	165

5.4.3 Analysis of Damage .....	168
5.4.4 Summary of Damage Analysis .....	171
5.5 Finite Element Analysis .....	171
<b>6. Conclusions and Recommendations .....</b>	<b>176</b>
6.1 Research Objective No. 1 (New Design) .....	176
6.2 Research Objective No. 2 (Existing Bearings) .....	178
<b>References .....</b>	<b>181</b>

## List of Figures

1.1	Typical Transverse Displacement on a Standard U-Beam Bearing.....	2
2.1	Transverse Component of the Reaction .....	6
2.2	Typical TxDOT U-Beam, from Detail UBND (TxDOT 2006).....	8
2.3	Typical Plan of an Elastomeric Bearing .....	9
2.4	Inclined Compression Test (AASHTO M-251, Appendix A).....	16
2.5	Final Questionnaire Survey.....	25
2.6	Responses to Question No. 1 .....	26
2.7	Responses to Question No. 2 .....	27
2.8	Responses to Question No. 3 .....	27
2.9	Responses to Question No. 4 .....	28
3.1	Transverse Component $P\theta$ for $\Delta_1$ Displacement.....	38
3.2	Geometric Displacement $\Delta_2$ Caused by $Y_{bott\theta}=\Delta_2$ .....	38
3.3	Single and Double Bearing Plan Configurations .....	39
3.4	Dead and Live Loads .....	44
3.5	Bearing Pad Properties.....	45
3.6	$\Delta_1$ and $\Delta_2$ Displacements .....	46
3.7	Single Pad Configuration Checks .....	47
3.8	Single Pad Configuration Checks (Continued).....	48
4.1	Protractor Used to Measure Transverse Angles.....	68
4.2	Elevation of Bearing A .....	69
4.3	Close-Up of Bearing C.....	69
4.4	Section thru Shear Key for Alignment ‘C’ .....	70
4.5	Plan for US 82 BOS W Ramp.....	74
4.6	Erection Sheet for US 82 BOS W Ramp .....	75
4.7	Rosette Strain Gage (left) and Bondable Terminal (right).....	76
4.8	Fully Gaged Single Bearing.....	76
4.9	Change in Strain for the Precision Resistor .....	78
4.10	Change in Strain for Vertical Gages on Double Bearings .....	79
4.11	Change in Strain for Horizontal Gages on Double Bearings .....	80
4.12	Elevation View of Testing Frame .....	82
4.13	Elevation View of Longitudinal Rams .....	82
4.14	Application of Transverse Load.....	83
4.15	Standard Single and Double Bearings .....	84
4.16	Double Bearing Strain Gage Placement .....	85
4.17	Single Bearing Strain Gage Placement .....	85
4.18	Strain Gage Placement on Transverse Placement.....	85
4.19	Strain Gage Installed, 32 in. by 9 in. Bearing.....	86
4.20	Cable Extension Displacement Sensor – Transverse Direction.....	87
4.21	Cable Extension Displacement Sensors – Longitudinal Direction .....	88
4.22	Vishay Model 5000.....	88
4.23	Wiring for Vishay Model 5000.....	89
4.24	Example of Manual Data Recording Sheet.....	93
4.25	ANSYS SOLID186 Element .....	105
4.26	ANSYS Model of Bearing, Transverse Face .....	106
4.27	Pad Model with Rigid Extreme Layers.....	106
4.28	Strain Profile in Z-Direction, Rear Transverse Face, 6% Superelevation,	

	Double Pad Configuration .....	108
4.29	Strain Profile in Z-Direction, Front Transverse Face, 6% Superelevation, Double Pad Configuration .....	108
4.30	Strain Profile in z-direction, Front Longitudinal Face, 6% Superelevation, Double Pad Configuration .....	109
4.31	Strain Profile in z-direction, Rear Transverse Face, 6% Superelevation, Double Pad Configuration .....	109
5.1	Cycle 1 Transverse Results for 4% Test .....	112
5.2	Cycle 1 Longitudinal Results for 4% Test .....	113
5.3	Transverse Results for All 14 Cycles.....	114
5.4	Longitudinal Results for all 14 Cycles.....	114
5.5	Transverse Ratios versus Cycles.....	115
5.6	Longitudinal Ratios versus Cycles.....	115
5.7	Single Pad Longitudinal Results for 0% Test .....	116
5.8	Single Pad Transverse Results for 2% Test .....	117
5.9	Single Pad Longitudinal Results for 2% Test .....	117
5.10	Single Pad Transverse Results for 4% Test .....	118
5.11	Single Pad Longitudinal Results for 4% Test .....	118
5.12	Single Pad Transverse Results for 6% Test .....	119
5.13	Single Pad Longitudinal Results for 6% Test .....	119
5.14	Single Pad Transverse Results for 8% Test .....	120
5.15	Single Pad Longitudinal Results for 8% Test .....	120
5.16	Double Pad Longitudinal Results for 0% Test .....	121
5.17	Double Pad Transverse Results for 2% Test.....	122
5.18	Double Pad Longitudinal Results for 2% Test .....	122
5.19	Double Pad Transverse Results for 4% Test.....	123
5.20	Double Pad Longitudinal Results for 4% Test .....	123
5.21	Double Pad Transverse Results for 6% Test.....	124
5.22	Double Pad Longitudinal Results for 6% Test .....	124
5.23	Double Pad Transverse Results for 8% Test.....	125
5.24	Double Pad Transverse Results for 8% Test.....	125
5.25	Summary of Transverse Displacement, Single Bearing Configuration .....	126
5.26	Summary of Transverse Displacement, Double Bearing Configuration .....	127
5.27	Summary of Transverse Displacement, 2% Single Pad Configuration .....	128
5.28	Summary of Transverse Displacement, 4% Single Pad Configuration .....	128
5.29	Summary of Transverse Displacement, 6% Single Pad Configuration .....	129
5.30	Summary of Transverse Displacement, 8% Single Pad Configuration .....	129
5.31	Summary of Transverse Displacement, 2% Double Pad Configuration.....	131
5.32	Summary of Transverse Displacement, 4% Double Pad Configuration.....	131
5.33	Summary of Transverse Displacement, 6% Double Pad Configuration.....	132
5.34	Summary of Transverse Displacement, 8% Double Pad Configuration.....	132
5.35	Summary of Longitudinal Displacement, Single Pad Configuration .....	133
5.36	Summary of Longitudinal Displacement, Double Pad Configuration .....	133
5.37	Summary of Longitudinal Displacement, 0% Single Pad Configuration .....	134
5.38	Summary of Longitudinal Displacement, 2% Single Pad Configuration .....	134
5.39	Summary of Longitudinal Displacement, 4% Single Pad Configuration .....	135
5.40	Summary of Longitudinal Displacement, 6% Single Pad Configuration .....	135
5.41	Summary of Longitudinal Displacement, 8% Single Pad Configuration .....	136

5.42	Summary of Longitudinal Displacement, 0% Double Pad Configuration ....	136
5.43	Summary of Longitudinal Displacement, 2% Double Pad Configuration ....	137
5.44	Summary of Longitudinal Displacement, 4% Double Pad Configuration ....	137
5.45	Summary of Longitudinal Displacement, 6% Double Pad Configuration ....	138
5.46	Summary of Longitudinal Displacement, 8% Double Pad Configuration ....	138
5.47	Regression Summary for Model 7, Transverse Angle.....	140
5.48	Regression Summary for Model 11, Transverse Angle.....	141
5.49	Regression Summary for Model 5, Longitudinal Angle.....	142
5.50	Regression Summary for Model 7, Longitudinal Angle.....	143
5.51	Illustration of Slip, Transverse Front .....	145
5.52	Illustration of Slip, Transverse Back .....	146
5.53	Slip Measurement Locations.....	146
5.54	Bearing Corner Undergoing Curling .....	147
5.55	Summary of Slip Results, 6% Transverse Slope, Double Pad Configuration	148
5.56	Summary of Slip Results, 8% Transverse Slope, Double Pad Configuration	148
5.57	Summary of Slip Results, 2% Transverse Slope, Single Pad Configuration.	149
5.58	Summary of Slip Results, 4% Transverse Slope, Single Pad Configuration.	149
5.59	Summary of Slip Results, 6% Transverse Slope, Single Pad Configuration.	150
5.60	Summary of Slip Results, 8% Transverse Slope, Single Pad Configuration.	150
5.61	Summary of Slip Results, Single Bearing Configuration .....	152
5.62	Summary of Slip Results, Double Bearing Configuration.....	152
5.63	Regression Summary for Model 2 .....	156
5.64	Regression Summary for Model 4 .....	157
5.65	Regression Summary for Model 6 .....	158
5.66	Regression Summary for Model 7 .....	158
5.67	Example of Observed Transverse Top Uplift .....	160
5.68	Uplift Summary, Test Series S6A.....	161
5.69	Uplift Summary, Test Series S8A.....	162
5.70	Uplift Data for Test Series D4A .....	162
5.71	Uplift Summary, Test Series D6A .....	163
5.72	Uplift Summary, Test Series D8A .....	163
5.73	Hairline Surface Cracks on Elastomeric Bearing .....	166
5.74	Heavy Surface Cracking on an Elastomeric Bearing.....	166
5.75	Tension Debonding at Shims .....	167
5.76	Delamination of Elastomer .....	168
5.77	Exposure of Shims .....	168
5.78	Strains in Z-direction (Transverse Face), 0% Single Pad Configuration.....	172
5.79	Strains in Z-direction (Transverse Face), 4% Single Pad Configuration .....	173
5.80	Strain in Z-direction (Transverse Face), 8% Single Pad Configuration .....	173
5.81	Strain in Z-direction (Transverse Face), 0% Double Pad Configuration.....	174
5.82	Strains in Z-direction (Transverse Face), 4% Double Pad Configuration .....	174
5.83	Strains in Z-direction (Transverse Face), 8% Double Pad Configuration .....	175

## List of Tables

2.1	Comparison of AASHTO Methods B, A and TxDOT Modified .....	12
2.2	List of State Element Data (Pontis) Documents .....	30
2.3	Condition State No. 1 for Element No. 310.....	31
2.4	Condition State No. 2 for Element No. 310.....	32
2.5	Condition State No. 3 for Element No. 310.....	33
3.1	Standard TxDOT U-Beam Sheets.....	35
3.2	U-Beam Recommended Spacings for LRFD.....	40
3.3	Design Limit State Abbreviations.....	50
3.4	U40 with 0% Transverse Slope.....	51
3.5	U40 with 2% Transverse Superelevation.....	52
3.6	U40 with 4% Transverse Superelevation.....	53
3.7	U40 with 6% Transverse Superelevation.....	54
3.8	U40 with 8% Transverse Superelevation.....	54
3.9	U54 with 0% Transverse Slope.....	56
3.10	U54 with 2% Transverse Superelevation.....	58
3.11	U54 with 4% Transverse Superelevation.....	60
3.12	U54 with 6% Transverse Superelevation.....	62
3.13	U54 with 8% Transverse Superelevation.....	64
4.1	Location of Bearings Inspected .....	67
4.2	Summary of Wichita Falls Inspection Data .....	68
4.3	Predicted Transverse Deflections for Select Locations .....	71
4.4	Tests Performed for US 82 Bos-W Ramp Overpass.....	77
4.5	Laboratory Test Matrix .....	90
4.6	Summary of Testing Procedure .....	91
4.7	Single Pad Displacement and Damage Recorded: 0% and 2% Slopes.....	94
4.8	Single Pad Displacement and Damage Recorded: 4%, 6% and 8% Slopes ...	95
4.9	Single Pad Displacement Forces Applied: 0% and 2% Slopes.....	96
4.10	Single Pad Displacement Forces Applied: 4%, 6% and 8% Slopes.....	97
4.11	Double Pad Displacement and Damage Recorded: 0% and 2% Slopes .....	100
4.12	Double Pad Displacement and Damage Recorded: 4%, 6% and 8% Slopes..	101
4.13	Double Pad Displacement Forces Applied: 0% and 2% Slopes .....	102
4.14	Double Pad Displacement Forces Applied: 4%, 6% and 8% Slopes.....	103
4.15	Comparison of Wichita Falls Bridge Data to Laboratory Data .....	104
4.16	Comparison of Lubbock Bridge Data to Laboratory Data.....	104
4.17	Angular Deformations in Pads at 390 kip Vertical Load.....	107
5.1	Predictor Variables used in Regression Analysis .....	139
5.2	Slip Summary for Test Series, 390 Kip Load .....	153
5.3	Summary of Slip Details, 390 Kip Load.....	154
5.4	Raw Summary of Damage by Test Series .....	169
5.5	Percentage Based Summary of Damage by Test Series .....	170
5.6	Progressive Damage Summary by Test Series .....	170
6.1	Recommended Revisions to “Elements” Field Inspection and Coding Manual – Element No. 310 .....	180



# 1. INTRODUCTION

## 1.1. General

The Bridge Division of the Texas Department of Transportation (TxDOT) developed the current Texas U-beam sections in the mid-1980's as an aesthetic alternative to conventional I-shaped girders. Although the improved aesthetics resulted in a "modest increase in cost" over other superstructure alternatives, the Bridge Division still has a desire to use the Texas U-beam sections. (TxDOT 2001)

As standard practice, the Bridge Division requires that the Texas U-beam sections be supported by three steel-reinforced elastomeric bearings, one larger bearing at one end and two smaller bearings at the other end. The Bridge Division designed standard bearings for most span/beam arrangements in order to ensure consistency and to reduce both design and fabrication errors. When the Texas U-beam sections are used on relatively flat grades (longitudinally) and negligible superelevation (transversely) the standard bearings typically perform well. However, as the transverse superelevation increases, a noticeable transverse displacement is induced into the bearings.

Figure 1.1 shows a typical U-beam bridge in Wichita Falls, Texas built with a transverse slope of up to 6.0%. The pier caps were designed to be parallel with the roadway surface, thus allowing the use of uniform-height standard steel-reinforced elastomeric bearing pads. The top sketch shows two U54 sections placed parallel to the 6.0% slope of the deck. The bottom photo shows an 18° transverse displacement in the steel-reinforced elastomeric bearing. This displacement is caused primarily by the gravity component of the end reaction parallel to the bearing seat.

Transverse displacements of this magnitude are not uncommon. A displacement of this magnitude by itself would most likely not be considered problematic. However, once this displacement is considered in conjunction with the longitudinal displacement, whether it is acceptable or not is not nearly as clear. The overall aim of this research project was to clarify the role of the transverse displacements in the steel-reinforced elastomeric bearings used for the Texas U-beam sections.

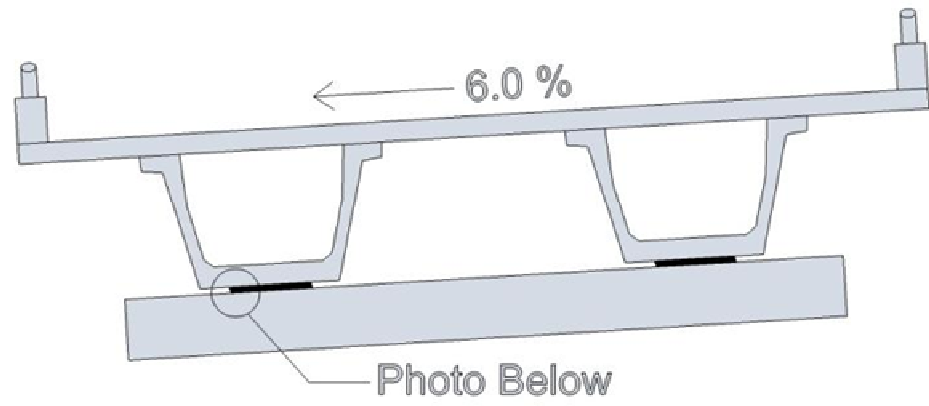


**Figure 1.1** – Typical Transverse Displacement on a Standard U-Beam Bearing

## **1.2. Research Objectives**

The original Research Project Statement provided the following concise description of the problem: (Holt 2006)

*Elastomeric bearings supporting superelevated U-beams have substantial transverse shear deformation, due to the dead load of the structure. Calculated shear deformation, in the transverse direction, for superelevated U-beams can easily approach the AASHTO-specified limits for the elastomer thickness used in TxDOT's standard U-beam bearings. These bearings are normally designed to accommodate thermally-induced shear deformation, which is usually greatest in the direction of the long axis of the bridge. Research is needed to determine if there is a need to account for the above as well as transverse shear deformations in bearing design and, if so, how.*

Two primary research objectives were developed based on the above Research Project Statement, the Texas Tech University Center for Multidisciplinary Research in Transportation's (TechMRT) response, results of a questionnaire survey sent to all 49 states and the District of Columbia, and meetings/conversations with representatives from the Bridge Division of TxDOT.

### **1.2.1. Research Objective No. 1**

The first objective was to determine if there was a need to consider the transverse superelevation in design, and if so, how it should be considered.

Superficially, this may seem a simple objective to fulfill. However, some bridge designers argue that superelevation has to always be considered while others argue that the commonly used transverse superelevation values (even up to about 8%) are low enough to be ignored in design. Strict adherence to the former group often leads to an analysis that concludes that standard size bearings are not acceptable to be used on any significant transverse slope. The latter group, however, often contends that regardless of transverse superelevation, as long as the bearing is designed for the combination of vertical load and longitudinal deformations, there is no need to consider transverse superelevation.

A second issue complicating this objective is the way steel-reinforced elastomeric bearings are viewed by different bridge designers. Some view the bearings as crucial elements

that, if not properly designed, may cause significant problems with the long-term performance of the superstructure. Others view the bearings as nearly indestructible and therefore not needing sophisticated design. The relatively low cost of the bearings in relation to the overall bridge is often used as justification for not worrying about their performance. However, if the labor and cost to the traveling public due to a bridge closure is considered, the cost needed to replace a bearing becomes significant.

A third complicating factor arises from the fact that the overall width of a Texas U-beam section and its relatively wide (1'-3 ¾") top flanges make it difficult to place a U-beam section level when the roadway is superelevated transversely. If a U-beam section were placed level no transverse force would be generated. However, placing a section level would require a significant "haunch" or "build-up" on the up-slope side to account for the roadway slope. Forming and placing concrete for such a large haunch would be difficult and is generally not recommended by TxDOT designers.

A fourth complicating factor is the use of tapered bearing pads. The width of the standard single bearing is 32 in. If such a pad were to be tapered at an 8% superelevation, the taper required would be over 2.5 in. Such an excessive taper often makes this option unfeasible.

### **1.2.2. Research Objective No. 2**

The second objective was to determine if there was a need to address existing U-beam bridges that have already been constructed on a significant transverse superelevation using standard steel-reinforced elastomeric bearing pads. If a need was determined, then recommendations for inspecting and documenting the condition were to be developed.

Bridge contractors have reported to TxDOT that when a U-beam is initially set on a bridge designed with a transverse superelevation, the bearings immediately deform transversely downhill. This can lead to difficulty aligning adjacent spans and matching formwork at the ends of a span. To alleviate this problem, shear keys are sometimes designed to resist this movement. Inspections were performed to identify the potential concerns associated with the existing condition.

### **1.3. Report Organization**

This report is divided into six chapters. Chapter 2 provides a more in-depth background of the problem starting with the Literature Review section which presents research primarily relevant to the topic of transverse displacements. A significant amount of literature has been written concerning the behavior of elastomeric bearings subjected to temperature extremes. Although this topic was considered throughout the project, it was not the primary variable to be considered. The results of a questionnaire survey sent to all 49 states and the District of Columbia are then presented. The chapter concludes with the current element data or Pontis coding for elastomeric bearing pads.

Chapter 3 presents the American Association of Transportation Officials (AASHTO) current recommended design provisions. The TxDOT modifications to these design provisions are then detailed and presented. Once the current method of design is established, a method to specifically include the influence of the transverse superelevation is presented. The ramifications of this proposed modification on current TxDOT practice are then presented.

Chapter 4 presents the results of the field and laboratory testing performed for the project. The results of an inspection on a set of bridges in Wichita Falls, Texas are presented as an example of the recording needed to establish a baseline inspection. The bearings for a second U-beam bridge in Lubbock, Texas were instrumented and monitored throughout the construction process. The resulting changes in the strains in the bearings throughout the construction process are presented in this chapter. Based on the currently used load and span arrangements presented in Chapter 3, a testing schedule was developed to test both the single and double bearing configurations throughout the anticipated range of load and deformations (both transverse and longitudinal) . The bearings were purchased, strain gages were applied, and the bearings were tested in the Structures and Materials Laboratory at Texas Tech. The results of the laboratory testing are presented. Lastly, results of Finite Element Modeling are presented.

Chapter 5 compares the predicted behavior to the observed behavior. Based on this comparison, the ability of the proposed AASHTO modifications are evaluated. This evaluation leads to the Conclusions and Recommendations provided in Chapter 6.

## 2. BACKGROUND

### 2.1. Literature Review

The TxDOT U-beams work well in practice when little or no transverse superelevation or cross slope exists. Difficulties may occur when the U-beam section is used on a roadway with a significant transverse superelevation or cross slope. When this occurs, the beam develops a transverse component to its dead load as shown in Figure 2.1. This transverse component, when transferred to the bearing pad may cause the pad to shear transversely. Also, a transverse moment may be introduced due to the vertical load acting a distance over from the centerline of the bearing.

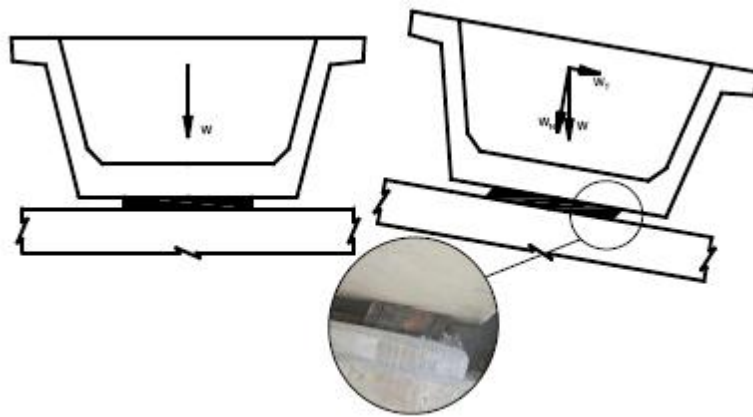


Figure 2.1– Transverse Component of the Reaction

The transverse shear depicted in Figure 2.1 may or may not be significant by itself. However, since the bearing is required to allow the U-beam to move longitudinally to accommodate thermal movements, longitudinal stresses and strains in addition to the transverse stresses and strains will be introduced into the bearing. The combination of transverse shear and moment, longitudinal shear and moment, and vertical compression may need to be considered as a worst-case triaxial state of loading.

This literature review narrowly focuses on this triaxial state of loading. The following areas were investigated: the history of the U-beam's use within the Texas Department of Transportation, background data on elastomeric bearings, national requirements on the use of elastomeric bearings including allowable stresses and strains, TxDOT design standards for elastomeric bearings, reports done for TxDOT or other agencies on elastomeric bearings, current

projects accounting for the triaxial loading of elastomeric bearings, projects that have completed full-scale testing of elastomeric bearings, and relevant articles on the finite elemental analysis of elastomeric bearings.

### **2.1.1. History of the Texas U-beam**

The Bridge Division of the Texas Department of Transportation initially developed the current Texas U-beam sections in the mid 1980s. The first bridge constructed with the current U-beam section was finished in 1993 (TxDOT, 2001). The U-section offers district designers an aesthetic alternative to the typical I-shaped girders. Many districts use the more aesthetic section despite the alternative's modest cost increase over the standard prestressed I-beams.

U-beams are tub shaped with a web section that slopes inward. As shown in Figure 2.1, this inward slope adds to the aesthetics, providing the sense that the superstructure is thinner than its I-beam counterparts. Standard depths for the U-beams are 40 in. and 54 in., allowing for maximum span lengths of 105 ft and 120 ft respectively. A typical U-beam section is shown in Figure 2.2. While TxDOT (2007) indicates that individual U-beams are more expensive than individual I- sections, U-beams may add economy to the overall system by generally requiring fewer beams. TxDOT indicates that the U-beam sections provide a clean, aesthetically pleasing appearance when used in practice. In 2004, the "pre-topped" U-beam debuted. This modification of the standard U-beam contains a 7-inch slab cast by the fabricator. This allows the contractor to rapidly construct the bridge deck on top of the beams, allowing for more economy during construction with the U-beams.

Standard details for the TxDOT U-beam sections exist allowing for the placement of the U-beam at various skew-angles and various superelevations. Skew-angles are allowed up to 45 degrees while superelevations currently are allowed up to 8% (TxDOT, 2006.) A list of the most pertinent standard details is included in section 3.1.

### **2.1.2. Background on Elastomeric Bearings**

Du Pont, in 1959, created one of the first design provisions for elastomeric bearings entitled "Design of Neoprene Bearing Pads." (Du Pont - Elastomer Chemical Department April 1959) Du Pont's procedures detailed in the provisions were adopted as the basis for many design

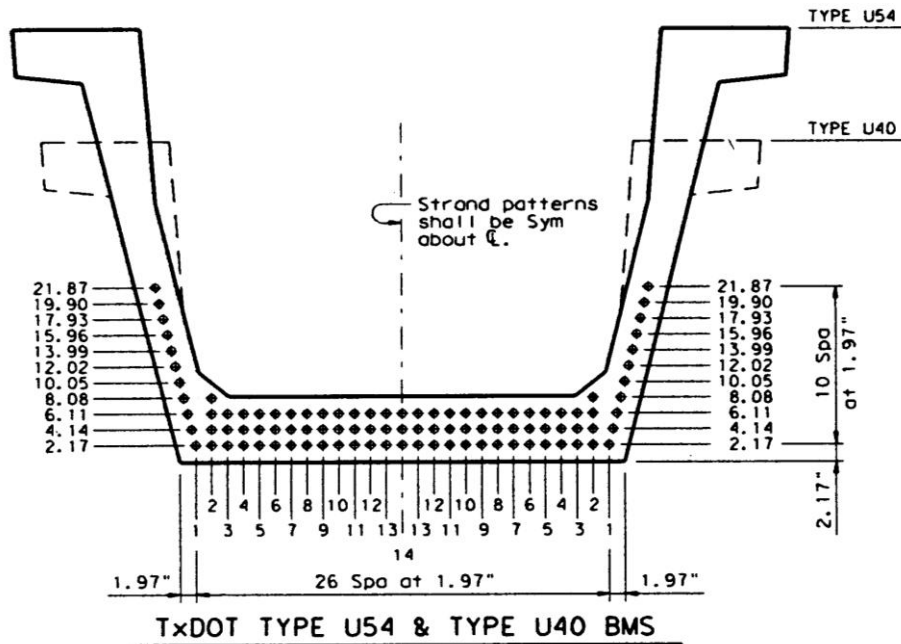


Figure 2.2 – Typical TxDOT U-beam, From Detail UBND (TxDOT, 2006)

procedures used today. Elastomeric bearings have proven to be a reliable and economical exterior application used in a variety of manners, especially in bridges. The bearing capacity for early Dupont bearings was 800 psi with compressive strains allowed up to 15%. Early on, stability was ensured by limiting the smallest plan dimension of a bearing to a minimum of 5 times the bearings thickness. Bearing slip was believed to not occur as long as the shear stress did not exceed one-fifth of the compressive stress (English et al., 1994). While the design criteria for bearings has changed over time due to a better understanding of bearing behavior, the Dupont standards are still regarded as one of the bases for today's codes.

Elastomeric bearings can be plain or reinforced and can be manufactured from natural rubber or a synthetic material (neoprene is the most common elastomer). The purpose of the elastomeric bearing is to transfer the vertical loads from bridge beams to the substructure while accommodating horizontal (usually longitudinal) movement of the beams due to thermal effects in addition to allowing for prestressing, creep, and shrinkage of the superstructure (Abe, Yoshida, and Fujino, 2004).

Bearings typically undergo three types of loading: axial compression resulting from the transfer of loads from the superstructure to the substructure, rotation from the displacement of

the beams due to their loads, and longitudinal shear displacement due to the thermal effects on the beams themselves (English et al., 1994). When a beam is superelevated transversely, a second shear displacement (in the transverse X direction) and moment in the transverse direction (about the Z axis) may develop as shown in Figure 2.3. In Figure 2.3, W is the dimension of the bearing perpendicular to the girder's length while L is the dimension parallel to the girder's length.

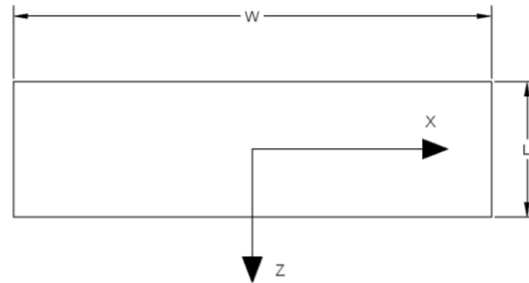


Figure 2.3 – Typical Plan of an Elastomeric Bearing

Elastomeric bearings can fail in various ways. According to English et al. (1994), bearings fail from fatigue, stability, delamination, yield/rupture, or serviceability issues. The TxDOT report by English et al. details the different failure methods and identifies the key issue to be slippage. Fatigue can be accounted for, delamination is not a critical failure mode, and stability can be considered during design to ensure that buckling/instability does not occur. Historically, slippage has been the most common failure method for TxDOT bridges.

Slippage occurs when the effect of the horizontal forces developed from the thermal influence on a beam exceeds the coefficient of friction between the beam and the bearing pad or the pad and the top of the bearing seat (Heymsfield et al., 2001). Slippage is commonly referred to as walking and was noted to have occurred in both Louisiana and Texas. In Texas, slippage appears to be limited to natural rubber bearings with span lengths greater than 100 feet and girders that are subject to extreme thermal effects (Muscarella and Yura, 1995). Muscarella and Yura found no evidence of walking with neoprene bearings.

### 2.1.3. AASHTO Bearing Design Requirements

The AASHTO LRFD process requires the designer to consider the three-dimensional effects of translational moments and rotations in the design of the bearing. Both instantaneous

and long-term effects should be considered throughout the design. Depending on the complexity of the situation governing the bearing's use, the effects of curvature, skew, rotations and support restraints should be included in the design process. The girder's material properties including the type of material and prestressing effects should also be considered. Current design provisions for bearings originate from the Allowable Stress Design service load conditions instead of factored loads. As such, the load factor for the design of bearings is usually taken as one. In addition, an allowance exists for the overstressing of the bearing during the construction process. The design of bearings has become more detailed with the release of the more recent editions of the AASHTO LRFD Bridge Design Specifications.

AASHTO bearing design allows for the use of two methods: Method A and Method B. Method A is a more conservative approach and generally results in a lower bearing capacity. Method B requires additional testing of bearings and quality control for the materials. While it may yield a more economical design from a material standpoint, bearings are typically not a high initial percentage cost in bridge design.

#### **2.1.4. TxDOT Bearing Design Requirements**

The provisions for design of the steel-reinforced elastomeric bearings are provided in the TxDOT LRFD Bridge Design Manual. (TxDOT, LRFD Bridge Design Manual 2007) TxDOT currently requires that the design of the bearings follow Design Method A, with TxDOT modifications using the AASHTO LRFD Bridge Design Specifications (3<sup>rd</sup> Edition). Additional specific details of the bearing design and the TxDOT modifications to AASHTO are presented in Section 3.1 of this document.

For typical design situations, TxDOT requires three bearings to support each U-beam section. Two smaller bearings are used on one end of the beam and one larger bearing is used on the other end. The standard size for each of the smaller bearings is a plan size of 1'-4" by 9" and a total thickness of 2.5 in. including 5 steel shims. The standard size for each of the larger bearings is a plan size of 2'-8" by 9" and a total thickness of 2.5 in. including 5 steel shims. Six standard sheets released in a TxDOT memorandum dated July 27, 2006 have been created to show details of the bearings and the U-beams. These standard sheets are available on-line and are included in section 3.1 and Appendix 3-1 of this report. (TxDOT, TxDOT Expressway British Standards (English) 2009)

The standard bearing sheet UBEB dated July 2006 contains a note to “See Bearing Pad Taper Report sheet for Fabricator’s Report of Bearing Pad Taper.” These provisions can be used to address longitudinal slope. However, there are no specific provisions on the sheet or elsewhere to address transverse slope.

According to the TxDOT LRFD Bridge Design Manual, tapered bearings are allowed as long as the slope of the taper is does not exceed 5.5%. Muscarella and Yura (1995) showed that tapered bearings have been in use in Texas prior to the AASHTO prohibition of tapered bearings in 1992. No serious issues have arisen from the use of tapered bearings in Texas and TxDOT maintains that it is easier to facilitate span end elevation differences with tapered bearings versus the contractor determining an alternate method to account for the differences. According to Hamzeh, Tassoulas, and Becker (1998), research has shown that there is no evidence that tapered bearings (less than 4% slope) perform any less successful than flat bearings. The results of their finite element study support this conclusion.

Considering lift-off, Muscarella and Yura (1995) report that “zero lift-off” limits the ability of the bearing to reach its full capacity and is an overly conservative approach to bearing design. Rotational capacity is a function of the axial stiffness of the bearing. Research conducted by the aforementioned authors at the University of Texas indicates that 20% lift-off is not detrimental to the performance of the bearing. As such, the TxDOT LRFD Bridge design manual allows the rotational capacity to be based on 20% lift-off.

General provisions require the use of 50 durometer hardness with a shear modulus between 95 and 175 psi. A summary of pertinent design criteria is shown in Table 2.1. This summary is provided so that the reader can get a sense of the differences in the methods and is not intended to be used for design since variables are not defined. Specific design provisions related to proposed changes to the AASHTO standards are included in Chapter 3 of this report.

#### **2.1.5. Triaxial or Multi-Axial Behavior Studies of Elastomeric Bearings**

Little research appears to have been conducted on the behavior of elastomeric bearings under a triaxial load. Abe, Yoshida, and Fujino (2004) conducted a study about the experimental application of loads. In their 2004 article, they set out with the following research objectives:

Table 2.1 – Comparison of AASHTO Methods B, A and TxDOT Modified

Parameter	AASHTO Method B	AASHTO Method A	TxDOT LRFD Modified
Tapered Bearings	Not Allowed	Not Allowed	Taper OK, slope not to exceed 5.5%. If slope exceeds 5.5%, use a beveled sole plate to accommodate the slope
Cover Layers	≤ 0.7 internal layer thickness	≤ 0.7 internal layer thickness	0.25-inch thick outer layers. If using 0.25-inch thick inner layers, disregard AASHTO requirement in Article 14.7.6.1
Shear Modulus (G)	80 psi ≤ G ≤ 175 ksi	80 psi ≤ G ≤ 175 ksi	95 psi ≤ G ≤ 175 ksi
Hardness Specification	None	50 to 60 durometer	50 durometer
Elastomer Material Specification	None	None	neoprene
Thermal Effects	DT determined through Article 14.7.5.2		DT = 70°
Compressive Stress Limit, bearing subjected to shear deformation	$\Theta_s \leq 1.66 \text{ GS} \leq 1.6 \text{ ksi}$	$\Theta_s \leq 1.00 \text{ GS} \leq 1.0 \text{ ksi}$ for steel reinforced bearing	$\Theta_s \leq 1.2 \text{ GS} \leq 1.2 \text{ ksi}$ (DL only); $\Theta_s \leq 1.5 \text{ GS} \leq 1.5 \text{ ksi}$ (Total Load)
Compressive Stress Limit, bearing fixed against shear deformation	$\Theta_s \leq 2.00 \text{ GS} \leq 1.75 \text{ ksi}$	Increase 10% of above limits	$\Theta_s \leq 1.2 \text{ GS} \leq 1.2 \text{ ksi}$ (DL only); $\Theta_s \leq 1.5 \text{ GS} \leq 1.5 \text{ ksi}$ (Total Load)
Shear Deformation	$h_{rt} \geq 2.0 \Delta_s$	$h_{rt} \geq 2.0 \Delta_s$	$h_{rt} \geq 2.0 \Delta_s$
Rotation, Steel Reinforced Bearing	$\Theta_s > 1.00 \text{ GS} (\Theta_s/n)$ $(B/h_{ri})^2$ and $\Theta_s < 1.875 \text{ GS} [1 - 0.2(\Theta_s/n) (B/h_{ri})^2]$	$\Theta_s \geq 0.50 \text{ GS} (\Theta_s/n)$ $(B/h_{ri})^2$ and $\Theta_s \geq 0.5 \text{ GS} (W/h_{ri})^2 (\Theta_{sz}/n)$	$\delta \geq (\Theta_{LL} + 0.005) (0.8L) / 2$
Lift-off	None	None	≤ 20% Longitudinal Dimension of Bearing
Stability	Cumbersome, See Article 14.7.5.3.6	$h_{rt} \leq \text{minimum} (L/3, W/3, \text{ or } D/4)$	$h_{rt} \leq \text{minimum} (L/3, W/3, \text{ or } D/4)$

- 1) Understanding the restoring force characteristics of laminated rubber bearings in large and small amplitude and construct a database of multi-axial loading conditions, which is useful to the designers.
- 2) The development of an accurate mathematical model, which is universal to these laminated rubber bearings for multi-axial loading conditions.

The above objectives were presented in two separate articles in the *Journal of Structural Engineering* in August 2004. The first objective is discussed below while the second objective is discussed under the finite element section of this chapter.

Past experiments on properties of bearings were conducted with single direction applied shear under constant vertical load. While the research conducted was satisfactory, the research was limited in application to “unidirectional horizontal deformation with large amplitude.” Previous research did not allow for good models of multi-directional shear (biaxial or triaxial conditions). Also, most early models for bearings did not include the hardening behavior exhibited by the elastomer under large deformations. Mozkah (1990) experimented with Teflon friction bearings under triaxial loads and proposed a model for the bearing. However, Mozkah focused only on the Teflon bearings and did not investigate the effects of triaxial loading on natural rubber or neoprene laminated bearings.

Abe, Yoshida, and Fujino (2004) subjected both natural rubber and neoprene bearings to four types of loading. During the pre-loading portion of their experiment, bearings were loaded independently in each horizontal direction to the expected maximum shear displacement under a vertical load. The objective of the pre-loading phase was to eliminate any virgin effects on the bearing. It was suggested that uniform results during further tests could be achieved if the bearings were independently loaded and unloaded in order to stabilize the hysteric loops in the shear strain versus load diagrams. Results from this testing indicated that elastomers tend to exhibit isotropic behavior after undergoing an initial deformation in a single direction.

Next, the trio investigated the effects of low amplitude cyclic deformations. The loading was intended to simulate loads resulting from traffic loads on a bridge with load deformations of 0.5% to 20% used. Thermal strains were also introduced to simulate the cyclic loading with the effect of thermal expansion/contraction of the girders. The goal of this portion was to investigate

the stiffness and damping of each bearing. The results suggest that the shear strain for natural rubber bearings is only slightly affected by the axial stress on the bearing.

Biaxial loading consisted of cyclic deformations under a constant vertical load to obtain the basic behaviors of bearings. This section of the report concentrates on determining properties of bearings so that the triaxial loading can be better understood. The shape of the hysteric loops shows the non-linear properties of the elastomer in that some hardening does occur.

Finally, triaxial loading was conducted for the bearings. To conduct this, bidirectional horizontal displacement paths were followed while the bearing was subjected to a constant axial compressive force. An important conclusion in the report was that there is a coupling effect in the two horizontal shear directions.

While this article is one of the few articles discussing triaxial loading of bearings, the basis of the article seems to apply more toward the use of bearings for earthquake loading rather than focusing on natural rubber bearings used in bridge applications. Nonetheless, the finite element model discussed in the companion paper is a good reference. It is also important to note that TxDOT requires the use of neoprene elastomeric bearings rather than natural rubber bearings.

Research by Yura et al. (2001) briefly mentioned triaxial limit states for elastomeric bearings. It was reported that the triaxial stress should not exceed six times the shear modulus as it leads to an instability as a result of cavitation. The susceptibility of caving is related to the elastomer's material property (i.e. Young's Modulus) rather than the strength of the rubber.

The yielding of the laminate material was also discussed. Yura et al. (2001) suggest that yielding occurs when the Von Mises Stress limit is reached and that the limit state is reached when the Von Mises Stress represented in the following exceeds the yield limit of the elastomer:

$$\sigma = \sqrt{\frac{(\sigma_1 - \sigma_2)^2 + (\sigma_2 - \sigma_3)^2 + (\sigma_3 - \sigma_1)^2}{2}} \quad \text{Equation 2.1}$$

where  $\sigma$  represents stress and the subscripts represent the three principal directions.

### 2.1.6. Full-Scale Testing Completed on Elastomeric Bearings

Topkaya and Yura (2002) investigated a unique way to determine the shear modulus of an elastomeric bearing. The shear modulus, according to Topkaya and Yura, is the most important material property that designers need. In 1997, AASHTO approved two methods to determine the shear modulus of elastomeric bearings. One method consisted of full-scale testing while the other used smaller test pieces.

The small sample quad shear test (ASTM D-4014) consisted of loading four smaller test pieces in shear up to fifty percent strain. Quad Shear tests are performed without a companion compressive load. The shear modulus is calculated based on the shear stress at 25% strain. Research tends to indicate that the shear modulus obtained from this test is significantly higher than that predicted from full-scale testing.

In a typical full-scale test (AASHTO 1996, 1997), two full-size bearings are sandwiched between three plates. Bearings are subjected to a compressive load which is held constant, then subjected to a shearing force in addition to the compressive force. The shear modulus is usually defined by the secant definition which relates the shear modulus to the slope of the line originating at the origin of a displacement versus load graph. If the shear force is applied independently in both directions, the shear modulus is taken as the slope of the line between the points on the graph at a strain of  $\pm 50\%$ . The secant definition of the shear modulus accounts for the non-linearity of the elastomer. These full-scale tests are more costly than the Quad Shear Tests and require an extensive apparatus to load the bearings in both compression and shear.

The inclined shear test proposed by the authors is an alternative test similar to the full-scale test mentioned above. The primary difference is that the plates the bearings are sandwiched between are sloped rather than flat. This allows for the bearings to be loaded in both compression and shear at the same time using only a compressive load shown in Figure 2.4. The shear modulus can be calculated based on the equation:

$$\frac{sWh_{rt}}{A\Delta_s} = G \quad \text{Equation 2.2}$$

where  $G$  is the Shear Modulus,  $h_{rt}$  is the total elastomer thickness of the bearing,  $s$  is the slope of the plates,  $W$  is the measured compressive force, and  $\Delta_s$  is the measured horizontal movement of

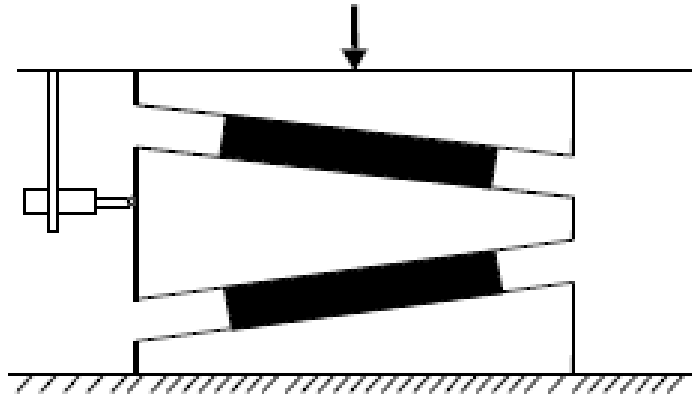


Figure 2.4 – Inclined Compression Test (From AASHTO M-251, Appendix A)

bearing. A 1:20 slope is recommended as it appears to give the best results except for bearings with a high stiffness.

The authors concluded that the inclined test can accurately determine the shear modulus of steel-reinforced laminated elastomeric bearings and is a good alternative to the Quad-Shear test. The shear modulus at 50% strain was recommended for use as the bearing's shear modulus since this is generally accepted as the upper limit of shear strain. The inclined compression test has its limitations as it does not yield favorable results for natural rubber bearings. Nonetheless, the inclined compression test is an acceptable test method for determining shear modulus according to AASHTO M251 (AASHTO, 2006).

### **2.1.7. Performance of Elastomeric Bearings at Low Temperatures**

Yakut and Yura (2002) investigated the performance of elastomeric bearings at low temperatures. They identified two types of stiffening that occur when bearings are subjected to cold temperatures. Instantaneous thermal stiffening associated with the change in temperature and crystallization of the elastomer which occurs if the low temperature is experienced over an extended time period. Research showed that crystallization is more of a concern than the instantaneous thermal stiffening. Stiffening is a concern because as a bearing stiffens, more shear force for a given movement is transferred to the substructure. In addition, the shear force may exceed the static friction limit and the bearing may slip. Yakut and Yura (2002) investigated the effect of temperature and time as parameters that influenced bearing response.

Final results answered some of the questions. According to the authors, cyclic loadings (both traffic and thermal) have little or no effect of the shear modulus. A bearing's creep rate is higher at low temperatures, but the overall effect was less than at warm temperatures. The loading rate was also found to be important. The authors recommended decreasing shear modulus for design by 30% for rubber and 20% for natural rubber to account for the load rate.

To account for low temperature effects, bearings are rejected if the  $G_{\text{cold}}/G > 4$  where  $G_{\text{cold}}$  is the shear modulus of the bearing at the specified low temperature and  $G$  is the shear modulus for the bearing at room temperature (Yura, Yakut, Becker, and Collingwood, 2001). AASHTO (2006) states that  $G$  shall be taken as the shear modulus of the bearing at 73 degrees Fahrenheit.

#### **2.1.8. Previous Finite Element Analysis Studies**

Hermann, Ramaswamy, and Hamidi (1989) provided one of the earliest finite element analysis of elastomeric bearings. Finite element analysis can be an economical means to predict the overall response characteristics of interest for bearings. Items of interest included axial force versus axial deflection and moment curvature of the bearing surface. Two computer codes, a 2-d and 3-d analysis, were developed. Because of the extensive execution time required for the 3-d analysis, it is recommended for research only. The 2-d analysis, which has a shorter execution time, is more appropriate for design. While little data about the modeling techniques can be deciphered, the research showed that finite element analysis can be a useful tool for conducting studies on design parameters of bearings. Finite element analysis can be a good means to predict overall bearing response and internal stresses in the elastomeric and reinforcement layers. One additional result is the desire to consider limiting the height of the bearing to prevent buckling/instability as can be seen in current design standards today published by both TxDOT and AASHTO.

Yazdani, Eddy, and Cai (2000) conducted a study on the behavior of bearings loaded by AASHTO precast Type III and IV girders. The bearings were modeled as eight noded cube linear elements using ANSYS 5.4 software. Individual spring stiffness values were calculated using the appropriate tributary area. The sum of the spring stiffness for each portion of the bearing was equal to the total stiffness of the bearing from the 1996 AASHTO Standards. The general trend in an early application of finite element analysis was that the results of the finite

element analysis predicted higher responses than shown in field tests. The conclusion was that skew angle may have an impact on bearing stiffness as well as the fact that bridges may be “stiffer in practice than theoretical analysis may suggest.” Nonetheless, the finite element analysis and field tests validated the AASHTO specifications.

Similarly, Green, Yazdani, Spainhour, and Chi (2001) conducted a study to utilize finite element analysis to model the Florida bulb tee 78 girder and investigate the loading response under established boundary conditions. The software used to conduct the finite element analysis was ANSYS Version 5.5, University High Option. The girders were modeled as well as the bearing pads. COMBIN14 spring elements from ANSYS were used to model the bearing pads. The spring elements accounted for the non-linear behavior of the elastomer. Each pad was broken into 9 sections as developed in the paper with appropriate spring constants for the bearings obtained through AASHTO values. Type V bearing pads (50 durometer with G between 0.655 MPa and 6.895 MPa) with the dimensions of 254 mm by 610 mm were tested at skew angles of 15, 30, 45 and 60 degrees. The results indicated that an increased deflection (strain) of the bearing pad occurred with increased skew angles. As the skew angle increased, bearing pads with higher a shear modulus were needed to keep the deflections and stresses within limits. In contrast, bearings with lower skew angles have been found to be more susceptible to “lift-off.”

Abe, Youshida and Fujino (2004) developed a finite element model based on their research discussed earlier in the triaxial stress portion of this literature review. It was used to model the “bidirectional behaviors of the bearings under a constant vertical load” which is defined as a triaxial loading state. The finite element model used by the authors was based upon a three-dimensional constitutive law of the Ozdemir model and the modeling of the elastomer as a nonlinear viscoelastic material. After further development of this model, the authors developed their finite element based on an elastoplastic model of the material. This model was used to predict the restoring forces of the bearings used as seismic isolation bearings. While this is not directly related to the use of elastomeric bridge bearings, the assumptions about the material may prove useful.

Hamzeh, Tassoulas, and Becker (1998) took earlier non-linear finite element modeling based on the work of Herman (1995) and others and modified the homogenized continuum model used at the time. Hamzeh et al. (1998) worked with a p-version finite element model

where they accounted for the material non-linearities and geometric non-linearities result from large deformations and large strains. Elastomeric bearings are subjected to large deformations and strain. The elastomer was modeled as an incompressible, hyperelastic material. The use of virtual work and Lagrange multipliers enforced the incompressible boundary condition of the elastomer. Finally, J2 flow theory with isotropic hardening was used to model the steel reinforcement as a bilinear, elastoplastic material. The authors concluded that this finite element is a good fit for the behavior of elastomeric bearings and that tapered bearings do not exhibit unusual behavior for slopes up to four percent when compared to the behavior of flat bearings. The finite element model is discussed in detail in TxDOT Research Report Number 1304-5 (Hamzeh, Tassoulas, and Becker, 1998).

#### **2.1.9. National Cooperative Highway Research Program Report 596**

National Cooperative Highway Research Program (NCHRP) Report 596, Rotation Limits for Elastomeric Bearings, contains information pertaining to the calculation of stresses within a bearing. The publication, released in 2008, provides several suggested updates to the American Association of State Highway Transportation Officials (AASHTO) design methods for elastomeric bearings. As indicated previously, elastomeric bearings are the bearings of choice for bridge designers due to their ability to accommodate the loads and rotations transferred between the superstructure and the substructure while allowing for the required movements and rotations.

Stanton et al. (2008) described the failure modes for steel-reinforced elastomeric bearings. The first mode identified was tension debonding at the ends of the shims. This occurs when the tensile forces in the elastomer cause the elastomer to separate from its bond with the steel shim. Debonding is seen where the smaller, individual bulges of the elastomer combine to form a single, larger bulge. Upon further loading or more cyclic repetitions, tension debonding may lead to shear delamination which is the continuation of the tension debonding inward along the length of the shim. Shear delamination is accompanied by cracking in the elastomer along the same level as the shim/elastomer interface. Finally, internal rupture or failure of the steel shims can occur under large loads. Internal rupture is believed to be limited to cases where the bearings are attached to steel bonding plates.

NCHRP Report 596 (2008) also described the implications of the different failure modes for steel-reinforced elastomeric bearings. In general, it is believed that tension debonding has no discernable impact on the bearing's performance. However, as tension debonding is described as the first sign of the progressive failure modes, it is an important phenomenon to note. On the other hand, shear delamination can cause serious consequences. Shear delamination could lead to the elastomer walking out from between the bearing's shims. While this situation will not likely result in a catastrophic failure, it is a serviceability failure from which the economic impacts associated with the solution would be significant. The final failure method is internal rupture. Internal rupture is the yielding or fracture of one or more steel shims within the elastomeric bearing. It is difficult to distinguish between tension debonding and delamination without destructively cutting into the bearing. Considering this fact, the authors of the NCHRP report associate the failure of a bearing with the onset of tension debonding.

Currently the design standards for bearings come from the AASHTO Bridge Design Manual. Two methods are available to complete the design. Most states choose to use Method A (Stanton et al., 2008). The standards work well for designing the bearings; however, a few concerns exist. One concern is that Method A and Method B do not require the same checks for a design to be acceptable. In some cases, a bearing meeting design requirements under Method B will fail under the provisions of Method A. The other problem is with the "no lift-off" provision in the design procedures. According to the authors of NCHRP 596 (2008), the original reason to include the no lift-off provision in the standard was to prevent internal rupture of the bearing. However, this provision may cause elastomeric bearings to be too thick and thus unstable, requiring the use of mechanical bearings when an elastomeric bearing would perform acceptably.

While not allowing lift-off was the original intent of the AASSTO design standards, many states chose to modify or ignore the provision (Statnton, et al., 2008). While experience and current bearing performance does not show any severe failures from lift-off, the true effects remain unknown. As such Stanton et al., through research conducted at the University of Washington, set out to see if a more universal design provision could be created to better allow for lift-off and to determine the true effects of lift-off on bearing performance.

Stanton et al.'s (2008) research consisted of testing elastomeric bearings of multiple sizes under various combinations of static and cyclic axial loads and rotations. A specific case under

investigation was the low axial load associated with a high rotation that was thought to cause lift-off failures according to the current AASHTO design standards. Testing was conducted and bearings were inspected with any resulting damage documented. In addition, a finite element analysis was conducted in order to find a sufficient model to predict what might occur. Stanton et al. (2008) believe that measurement of strains within the bearing or on the edges of the bearing with conventional strain gages is nearly impossible due to the magnitudes of the strains present and the stress concentrations present at the edges of the elastomer. Furthermore, the presence of the strain gages would alter the strain field present within the elastomer. A final complication is the lack of uniformity of the strain throughout the bearing. Finally, hand calculations are very tedious due to the non-linearity of the material properties of the elastomer.

The finite element model was created with the aid of the MSC.Marc 2003r2 program by MSC software. A two-dimensional analysis was conducted using large deformation plane strain in a LaGrange setting. The material modeled was non-linear, elastic, nearly incompressible with the Bulk Modulus,  $K$ , estimated from Holownia's paper, "The effect of various types of carbon black on elastic constants of elastomers," published in *Plastics and Rubber: Materials and Applications* in August of 1980. The reasonable analysis range for Stanton's research at the University of Washington was  $0 < \sigma/GS < 2$  and  $0 < \theta_y < 0.006$ . While conducting the finite element analysis, local mesh distortion inhibited the ability to calculate shear strain at the very end of the shim. This shear strain was extrapolated from the value  $\frac{1}{4}$  inch from the shim's end.

Testing completed consisted of bearings with various dimensions with the most common bearing size used being 22-in. by 9-in. This bearing size was deemed by the researchers to be the most typical bridge bearing used in practice today (Stanton et al., 2008). Testing and finite element analysis completed included both bearings with and without a bonded sole plate. Testing consisted of various loads and rotations and various cycles of each. Large shear strains associated with rotation, axial load, and shear deformation resulted in tensile debonding, followed by shear delamination, and in some test cases, yielding or fracture of the shim occurred. In general, the tests verified that the principle of superposition of strains is valid for the analysis of bearings. While this simplified analysis is not technically accurate, comparison between hand computations and finite element analysis resulted in a difference of less than 7.5 percent. Furthermore, the researchers found that non-linear effects lessen as the shape factor increases and become negligible for bearings with shape factors greater than twelve. For bearings with a

bonded sole plate, hydrostatic tension stresses that occur within the vicinity of the edge of the shim agreed closely with hand predictions.

From the finite element analysis, a few important concepts have been noted. Stanton and the other authors note that bearings with a higher durometer and a higher shape factor tend to perform better under loads. In addition, they also noted that bearings with a high shape factor do not perform particularly well under high rotations. Next, Stanton and his colleagues concluded that the approximate linear theory proposed by Gent and others in previous studies seems to match well with the finite element analysis. Evidence suggests that repeated cyclic loads result in more damage to the bearing. Lastly, for bearings with a bonded sole plate, hydrostatic tension stresses that occur within the vicinity of the edge of the shim agreed closely with hand predictions.

The effects of axial rotation and axial force are influenced by lift-off of a bearing. In the unloaded region of the bearing where lift-off occurs, the shear strain is small and constant throughout. In contrast, the remaining loaded region of the bearing undergoes a dramatic increase in shear strain with the redistribution of axial load. This change is considered a non-linear effect since the dimensions of the loaded area change with the onset and propagation of lift-off (Stanton et al., 2008).

The design procedure proposed in NCHRP Report 596 focuses on peak shear strains. The authors postulate that the compression shear and rotations each cause shear strains if applied individually and that these strains can be additive. The maximum strains will typically occur near the edge of the shims. The proposed procedure uses service loads instead of factored loads.

The new design procedure proposes changes to both Method A and Method B of the AASHTO design procedure. Two additional provisions are recommended for Method A. Stanton et al. (2008) recommend that Method A not apply in cases where an external bond plate is used or if  $S^2/n$  is greater than 16. The latter provision is aimed at avoiding excessive shear strain at edges with large rotation. For Method B, Stanton et al. (2008) recommend the removal of the no lift-off provision for bearings (except in the case of the bonded external plate where hydrostatic tension must be investigated). Instead, they recommend that the strains from cyclic loads be multiplied by an amplification factor of 2 to account for their effects on bearing damage. Finally, the authors propose to delete the absolute axial stress provision but keep the

limit in terms of GS as a final check. The author's models are provided in Chapter 3 of their report.

NCHRP Report 596 concludes that steel-reinforced elastomeric bearings are robust and can sustain visible damage while still carrying the required vertical load to prevent catastrophic failure. The report clarifies that tension debonding has no adverse effect on performance of bearing; however, it is the precursor to delamination and as such has been used to determine if a serviceability failure has occurred. Shim edges that are rounded or burred perform better than those that are orthogonal (Stanton et al., 2008).

The authors recommend that the effect of creep of the elastomer should be investigated and considered in design if deemed necessary. Lastly, while the testing in their report consisted primarily of applying axial loads and rotations to the bearing, the authors concluded that shear deformation up to 30% did not significantly reduce the number of cycles required for failure.

#### **2.1.10. Conclusions**

This literature review provides the background information regarding uniform height steel-reinforced elastomeric bearings used for Texas U-beam sections placed on a cross slope matching the superelevation of the bridge. The history of the Texas U-beam, behavior of elastomeric bearings, design criteria from both AASHTO and TxDOT including recent suggested changes, and previous finite element models is provided. From this information, the following conclusions exist:

1. Elastomeric bearings continue to be successful elements for transmitting forces from the superstructure of a bridge to its substructure while allowing for required deflections and rotations of the girders.
2. Some, but not much, information exists pertaining to the triaxial state of stress in an elastomeric bearing. Much of the information that does exist pertains to natural rubber bearings. TxDOT currently specifies the use of neoprene bearings.
3. Placing the TxDOT U-beam on a superelevated (or cross) slope may load an elastomeric bearing in a triaxial state introducing a force and rotation in the transverse direction. Further

investigation into the state of stress of a triaxially loaded bearing is needed to determine the full extent of the effects of this loading.

4. Finite Element Analysis exists as a tool for an economical analysis of the state of stress in elastomeric bearings. A finite element model for the state of stress in a triaxially loaded neoprene bearing may prove to aid in the design of the bearings. The model would need to be validated with experimental results.

5. Damage to elastomeric bearings is progressive. Tension debonding and delamination are hard to distinguish without destructive investigations. Thus, tension debonding is the more conservative representation of the onset of a serviceability failure.

## **2.2. DOT Questionnaire Survey**

A single page questionnaire survey was sent to all 49 states (excluding Texas) plus the District of Columbia, for a total of 50 questionnaire surveys. The final version of the questionnaire survey is shown in Figure 2.5. The response rate for the survey was good, with 80% of the surveys returned. The only departments of transportation that did not return the survey were:

California, Connecticut, District of Columbia, Georgia, Indiana, Iowa, Kentucky, Massachusetts, New Hampshire, and Vermont.

The full responses to the survey are provided in Appendix 2.1. Although the survey did not provide specific answers to the two research objectives, the information provided did prove useful. A summary of the responses to the four questions asked follows.

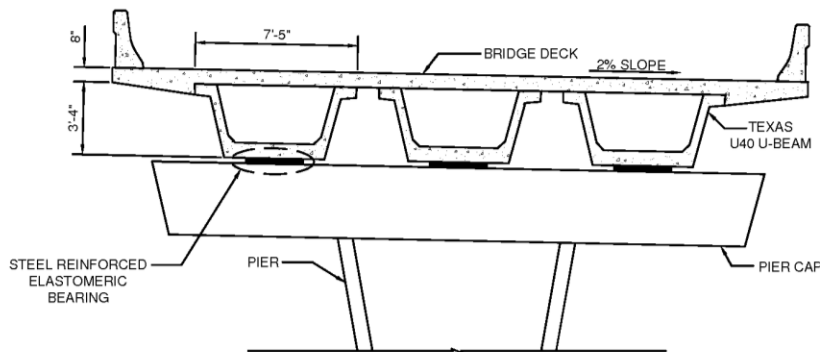
### **2.2.1. Question No. 1**

The first question was: “Does your state use a precast, prestressed U or Tub section similar to the Texas U40 U-Beam shown Above?” As shown in Figure 2.6, 8 out of 40 states (20%) indicated “Yes” they do use a similar section. The remaining 32 responses indicated that

To: State Bridge Engineer  
 Texas DOT  
 125 East 11<sup>th</sup> St.  
 Austin, Texas 78701

From: Charles Newhouse, PhD, PE  
 Dept. of Civil & Environmental Engineering  
 Texas Tech University  
 Box 41023 | Lubbock, Texas 79409  
 Phone: (806) 742-3523  
 Charles.Newhouse@ttu.edu

The *Texas Department of Transportation* is conducting a research project and would appreciate your help with this short survey. Please respond to the questions below and return in the envelope provided. Postage is already paid.



1. Does your state use a precast, prestressed U or Tub section similar to the Texas U40 U-Beam shown above?	Yes No
2. Do you know of any other states that use a section similar to the one shown? (Please List)  _____	Yes No
3. Does your state allow beam sections to be placed on a slope matching the slope of the roadway as shown above?	Yes No
4. Does your state use uniform height elastomeric bearing pads to support members placed on a slope matching the slope of the roadway?	Yes No
5. If there is someone in your office that is familiar with either sections similar to the Texas U40 U-Beam shown or with using uniform height elastomeric bearings to support members on a slope, please provide their contact information.  Name: _____ Phone: _____  Email: _____	

**Thank You! – A summary of the results will be mailed to you.**

Figure 2.5 – Final Questionnaire Survey

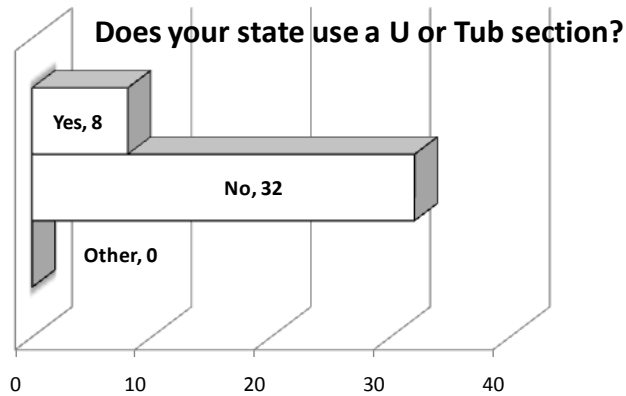


Figure 2.6 – Responses to Question No. 1

they do not use a similar section. Although California did not respond, it is known that U-sections are used in their state. However, the U-sections used in California are often made integral with the pier for seismic reasons. Therefore, California would not experience the same concerns caused by transverse slope.

### 2.2.2. Question No. 2

The second question was: “Do you know of any other states that use a section similar to the one shown (Please List)?” Seven states (17.5%) responded yes as shown in Figure 2.7. The states that were indicated were: California, Colorado, Florida, Louisiana, Oregon, and Washington. Thirty-one states (77.5%) indicated they did not know of any states that use a similar section. Two states (5%) indicated they possibly knew of a state that used a similar section. The West Virginia Department of Transportation indicated that Tennessee may have used a similar section in the 1980’s. The Wisconsin Department of Transportation indicated that it is possible that Indiana may have used a similar section at one time.

### 2.2.3. Question No. 3

The third question was: “Does your state allow beam sections to be placed on a slope matching the slope of the roadway as shown?” The responses were evenly split as shown in Figure 2.8. Twenty (50%) responded “Yes” and 19 (47.5%) responded “No”. One responded “Not applicable”. The Florida Department of Transportation indicated they do allow for sections to be placed on a slope matching the roadway, but only for slopes less than 2%. For greater

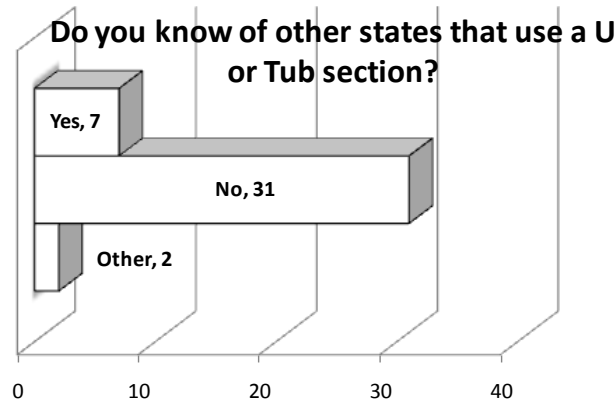


Figure 2.7 – Responses to Question No. 2



Figure 2.8 – Responses to Question No. 3

slopes, a tapered steel sole plate is used. The Montana Department of Transportation indicated that only certain sections are allowed to be placed on a slope. The South Carolina Department of Transportation indicated that they do allow U-beam sections to be placed on a matching slope. The Wyoming Department of Transportation indicated that only Precast I-sections are allowed to be placed on a matching slope.

The question was intended to address the slope of the roadway in the transverse (perpendicular to traffic) direction. The picture was provided to clarify this. Unfortunately, it is possible that some of the respondents assumed that the question asked about matching the slope in either the transverse or the longitudinal direction.

A follow-up conversation with the Florida Department of Transportation addressed the 2% limit for transverse slopes. It was indicated that the 2% limit for transverse slopes came from the rule-of-thumb 2% limit for longitudinal slopes which has historically worked well.

#### 2.2.4. Question No. 4

The fourth question was: “Does your state use uniform height elastomeric bearing pads to support members placed on a slope matching the slope of the roadway?” The response to the fourth question was identical to the response of the third question, as shown in Figure 2.9. Twenty (50%) of the states indicated “Yes”, 19 states (47.5%) indicated “No”, and one state (2.5 %) indicated not applicable. The Colorado Department of Transportation indicated that most spans were designed simple and made continuous with only a leveling pad required. The Pennsylvania Department of Transportation indicated that only prestressed concrete adjacent box beams are placed parallel to the roadway. The South Carolina Department of Transportation indicated that “Yes” was for precast deck beam units.

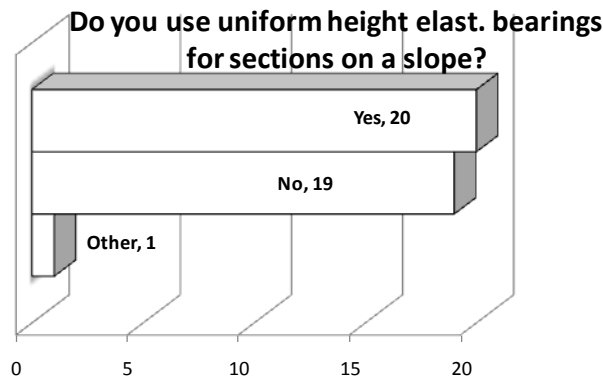


Figure 2.9 – Responses to Question No. 4

#### 2.3. Pontis Element No. 310 – Elastomeric Bearing

One of the two most commonly performed bridge inspections is the Pontis Bridge Inspection, or the Element Data inspection. Derived from the Latin word for bridge, Pontis inspections allow the bridge inspector to collect more specific data on individual members, called elements, of a bridge. Pontis inspections were first performed as early as 1989 (National Cooperative Highway Research Program 2009). Currently, the Texas DOT requires bridge inspectors to collect element level data in accordance with the TxDOT “Elements” Field Inspection and Coding Manual. (Texas Department of Transportation 2001)

Elastomeric Bearings are coded as element number 310. When an inspector performs an Elements Field Inspection (or Pontis Inspection), he or she inspects each bearing and assigns one of three condition states to the bearing. Although the FHWA provides guidelines on what

constitutes each condition state, state departments of transportation have taken the FHWA guidelines and produced more specific state guidelines in an attempt to clarify what condition state a particular element should be coded. For most elements, including element number 310 elastomeric bearings, the Texas Department of Transportation has adopted the FHWA condition states. The recommended condition states for element number 310 from eight states including Texas were investigated. Table 2.2 shows the state, the document that provides the condition states, and the web address for each document.

Table 2.3 shows the wording used for the Condition State No. 1 for each state. The basic wording provided by the FHWA is provided at the top of the table. If the wording is the same for a given state, “Basic Wording” is indicated. The Feasible Actions column shows the recommended action if the element is coded in this category. DN stands for do nothing. As can be noted from the table, some states add a significant amount of descriptive material to classify the condition of the element. Of particular importance for this study is the wording related to the allowable vertical slope and the bulging of the bearing, neither of which is captured by the basic wording.

Table 2.4 shows Condition State No. 2 and Table 2.5 shows Condition State No. 3. It appears that the wording in Condition State No. 3 for Texas is incorrect – this is why it has been lined out. Several states have adopted slope limitations for the bearings. Although these slopes are most likely intended for slope of the bearing in the longitudinal direction the information is useful for considering a slope limitation for the transverse direction. The maximum allowable slope for Condition State No. 1 is 30 degrees while the maximum allowable slope for Condition State No. 2 is 45 degrees.

Table 2.2 – List of State Element Data (Pontis) Documents

State	Document Name	Web Address
Texas	Texas DOT, "Elements" Field Inspection and Coding Manual - for the TxDOT Bridge Management System, Rev. 9-14-2001	<a href="http://onlinemanuals.txdot.gov/txdotmanuals/ins/field_inspection_manual.pdf">http://onlinemanuals.txdot.gov/txdotmanuals/ins/field_inspection_manual.pdf</a>
Colorado	Colorado DOT, "Pontis Bridge Inspection Coding Guide", Revised October 1998	<a href="http://www.dot.state.co.us/Bridge/Pontis/pontiscovers.pdf">http://www.dot.state.co.us/Bridge/Pontis/pontiscovers.pdf</a>
Idaho	Idaho Transportation Department, "Idaho Bridge Inspection Coding Guide - U.S. Customary Units", Revised Edition January 2004	<a href="http://itd.idaho.gov/bridge/inspection/BridgeInspectionCodingManual.pdf">http://itd.idaho.gov/bridge/inspection/BridgeInspectionCodingManual.pdf</a>
Michigan	Michigan DOT, "Pontis Bridge Inspection Manual", 2007	<a href="http://www.michigan.gov/documents/mdot/MDOT_PontisManual_2007_195365_7.pdf">http://www.michigan.gov/documents/mdot/MDOT_PontisManual_2007_195365_7.pdf</a>
Minnesota	Minnesota DOT, "Bridge Inspection Manual - Version 1.7", April 2008	<a href="http://www.dot.state.mn.us/bridge/manuals/inspection/Bridge%20Inspection%20Manual%20(Versions%201.7%20-%20Apr%202008).pdf">http://www.dot.state.mn.us/bridge/manuals/inspection/Bridge%20Inspection%20Manual%20(Versions%201.7%20-%20Apr%202008).pdf</a>
New Jersey	New Jersey DOT, "Pontis Coding Guide Manual", 2003	<a href="http://www.state.nj.us/transportation/eng/structeval/pdf/PontisCodingGuide.pdf">http://www.state.nj.us/transportation/eng/structeval/pdf/PontisCodingGuide.pdf</a>
Oregon	Oregon DOT, "Bridge Inspection Coding Guide", 2009	<a href="ftp://ftp.odot.state.or.us/Bridge/Coding_Guide_Chitrat/2009_Coding_Guide/ODOT_CodingGuide2009_BridgeWeb.pdf">ftp://ftp.odot.state.or.us/Bridge/Coding_Guide_Chitrat/2009_Coding_Guide/ODOT_CodingGuide2009_BridgeWeb.pdf</a>
Virginia	Virginia DOT, "Element Data Collection Manual"	<a href="http://virginiadot.org/business/resources/PONTIS_Element_Data_Collection_Manual_Modified_by_VDOT.pdf">http://virginiadot.org/business/resources/PONTIS_Element_Data_Collection_Manual_Modified_by_VDOT.pdf</a>

Table 2.3 – Condition State No. 1 for Element No. 310

DOT	Description	Feasible Actions
<i>Basic Wording</i>	<i>The element shows little or no deterioration. Shear deformations are correct for existing temperatures.</i>	N/A
Texas	Basic Wording.	None
Colorado	Basic Wording.	DN
Idaho	Basic Wording.	None
Michigan	"Good". Basic Wording	None
Minnesota	Elastomeric expansion bearing is in good condition and is functioning as intended. The bearing pad is properly positioned - deformation and orientation is appropriate for the current temperature. The elastomeric covering may have superficial deterioration (the steel reinforcement layers are not exposed). Pintle plates, restraints, or anchor bolts (if present) are sound, properly positioned, and functioning as intended. The bearing seat is in good condition (there is no loss of bearing area).	None
New Jersey	Basic Wording. *The vertical slope is equal to or less than 30 degrees. *The slope information is for guidance only.	Do Nothing.
Oregon	Basic Wording. As a rule of thumb, the maximum allowable shear deformation is 1/2 the height of the bearing pad dimension. (1/4 H each side of the vertical plane). Bulging is considered a noteworthy deficiency, and excessive bulging is considered to be more than 15% of "H".	Do Nothing.
Virginia	The element shows little or no deterioration and has minimal debris and corrosion. The coating system, if present, is sound and functioning as intended. Vertical and horizontal alignments are within limits. For elastomeric bearings the vertical slope is 0 - 30 degrees. Bearing support is sound. There is no cracking of support members. Any lubricating system is functioning properly. The supported member is stable under traffic.	None

Table 2.4 – Condition State No. 2 for Element No. 310

DOT	Description	Feasible Actions
Basic Wording	<i>Minor cracking, splitting or other deterioration may be present. Shear deformation may be slightly excessive. Strength and/or serviceability are not affected.</i>	N/A
Texas	Basic Wording.	None
Colorado	Basic Wording.	1) DN 2) Reset Bearings
Idaho	Basic Wording.	None
Michigan	"Fair". Basic Wording.	None
Minnesota	Elastomeric expansion bearing has moderate deterioration - bearing function may be slightly impaired. Bearing pad deformation may be near design limits (25% of the pad thickness), or the orientation may be inappropriate for the current temperature (resetting may be recommended). The pad may have bulged, deformed laterally, or moved slightly out of position. The elastomeric covering may have split or torn (steel reinforcement layers may be exposed). Pintle plates, restraints, or anchor bolts (if present) may have moderate deterioration, slight binding, or may be slightly out of position. The bearing seat may have moderate deterioration (there may be a slight loss of bearing area).	None
New Jersey	Basic Wording. *The vertical slope is greater than 30 degrees but less than 45 degrees. *The slope information is for guidance only.	1) Do Nothing. 2) Reset Bearings
Oregon	Basic Wording. As a rule of thumb, the maximum total allowable shear deformation is 1/2 the height of the bearing pad dimension. (1/4 H each side of the vertical plane). Bulging is considered a noteworthy deficiency, and excessive bulging is considered to be more than 15% of "H".	1) Do Nothing. 2) Reset Bearings
Virginia	Basic Wording. Strength and/or the ability of this element to function as intended are not affected (the vertical slope is 30 - 45 degrees).	None

Table 2.5 – Condition State No. 3 for Element No. 310 imminent

DOT	Description	Feasible Actions
Basic Wording	<i>Advanced deterioration. Shear deformations may be excessive. Top and bottom surfaces may no longer be parallel. Loss of bearing support is imminent.</i>	N/A
Texas	<del>Advanced corrosion of joint armor. There may be large spalls at the joint edges or adjacent to armor. Armor anchors are loose.</del>	None.
Colorado	Basic Wording.	1) DN 2) Reset Bearings 3) Replace unit & reset girders
Idaho	Basic Wording.	None.
Michigan	"Poor/Serious". Basic Wording.	Replace Element
Minnesota	Elastomeric expansion bearing has severe deterioration - resetting or replacement may be required. Bearing pad deformation may be beyond the design limits (25% of the pad thickness) - the pad may [be] severely bulged or significantly out of position. Bearing seat may have severe deterioration (there may be significant loss of bearing area) - supplemental supports or load restrictions may be warranted.	None.
New Jersey	Basic Wording. The vertical slope is greater than 45 degrees.	1) Do Nothing 2) Reset Bearings 3) Replace unit & reset girders
Oregon	Basic Wording. As a rule of thumb, the maximum total allowable shear deformation is 1/2 the height of the bearing pad dimension. (1/4 H each side of the vertical plane). Bulging is considered a noteworthy deficiency, and excessive bulging is considered to be more than 15% of "H".	1) Do Nothing 2) Reset Bearings 3) Replace unit / reset girder
Virginia	Shear deformations may be excessive. Top and bottom surfaces may no longer be parallel. Loss of bearing may be imminent. (The vertical slope is greater than 45 degrees.)	None.

### 3. AASHTO DESIGN PROVISIONS

#### 3.1. Current Design Provisions

The TxDOT LRFD Bridge Design Manual (TxDOT, LRFD Bridge Design Manual 2007) outlines TxDOT’s approach for the design of steel-reinforced elastomeric bearings in Section 2 of Chapter 5. The “Materials” section requires the use of 50-durometer neoprene, a shear modulus range of 95 to 175 psi (the least favorable value for the design check), steel shim thickness of 0.105 in., and prohibits the use of adhesives between bearings and other components. While no limitation exists on the shape factor in the AASHTO standards, TxDOT sets a target value for the shape factor between 10 and 12 in order to take advantage of the bearing’s compressive capacity.

The “Geometric Constraint” section allows for the use of tapered bearings as long as the taper does not exceed 0.055 ft/ft. Additional taper requirements are given, but these provisions are usually used for I-beam sections instead of U-beam sections. The standard drawings are also referenced in the section and reproduced in Table 3.1. These standard drawings are available on-line and are included in Appendix 3-1. (TxDOT, TxDOT Expressway British Standards (English) 2009)

Table 3.1 - Standard TxDOT U-beam Sheets

Standard Sheet Name	Description
-	Index Sheet of U-Beams
UBD	Prestressed Concrete U-Beam Details
UBEB	Elastomeric Bearing and Bearing Seat Details
UBMS	Miscellaneous Slab Details
UBND	Prestressed Concrete U-Beam (Design Data)
UBTS	Thickened Slab End Details
MEBR(U)	Minimum Erection and Bracing Requirements

The “Structural Analysis” section states that a temperature change of 70 degrees Fahrenheit should be used for a conservative estimate of thermal movement after erection (in one direction). It also indicates that shrinkage, creep, and elastic shortening should not be considered when determining maximum movement. It is indicated that infrequent slip will accommodate

these movements. The impact allowance, IM, should not be used when checking compressive stress. Appropriate shear live load distribution, modified for skew, should be used. The lightest predicted DL should be used when checking against slip. Load combination Service I should be used for all gravity loads.

The “Design Criteria” section gives the following additional criteria, reproduced verbatim from the manual:

### **Design Criteria**

Follow Design Method A in *AASHTO LRFD Bridge Design Specifications*, Article 14.7.6, with the following exceptions:

- ◆ DL compressive stress limit is the lesser of 1.20 ksi and 1.2 GS.
- ◆ Total compressive stress limit is the lesser of 1.50 ksi and 1.5 GS. This limit can be exceeded up to 15% at the engineer’s discretion.
- ◆ For rotation check, disregard *AASHTO LRFD Bridge Design Specifications*, Article 14.7.6.3.5. Rotation is acceptable if the total compressive deflection equals or exceeds  $\frac{\Theta_x(0.8xL)}{2}$ , where L is the pad length defined in *AASHTO LRFD Bridge Design Specifications*, and  $\Theta$  is the total rotation. Estimate compressive deflection using *AASHTO LRFD Bridge Design Specifications*, Figure C14.7.5.3.3-1.
- ◆ Calculate total rotation for dead and live load plus 0.005 radians for construction uncertainties as required by *AASHTO LRFD Bridge Design Specifications*, Article 14.4.2.1. Take maximum live load rotation as  $4 * \Delta / (\text{span length})$ , where  $\Delta$  is midspan LL deflection.
- ◆ Account for pad taper when checking against slip as required by *AASHTO LRFD Bridge Design Specifications*, Article 14.7.6.4, as follows:  $\Delta_s \leq (0.2 - Gr) \times DLxh_{rt} / (GxA)$  , where Gr = beam grade in ft./ft.
- ◆ You may use  $h_{rt}$  instead of total pad height when checking stability as required in *AASHTO LRFD Bridge Design Specifications*, Article 14.7.6.3.6.

In addition to the manuals and specifications listed above, the TxDOT Bridge Detailing Manual (TxDOT, Bridge Detailing Manual 2001) includes requirements for design and detailing.

Requirements for bearing seat detailing are located in Chapter 6, Section 9. TxDOT has created a “Recommended Beam Spacing Table” which provides recommended span lengths, overhangs, and beam spacings for U-40 and U-54 beams (TxDOT, Superstructure Design Information 2009). The table shows recommendations for U-40 beams to range from a span of 75 ft with an overhang of 6’-9” and a maximum spacing of 16’-7” to a span of 105 ft with an overhang of 5’-0” and a maximum spacing of 7’-6”. For U-54 beams, the table shows recommendations from a span of 75 ft with an overhang of 6’-9” and a maximum spacing of 16’-7” to a span of 120 ft with an overhang of 5’-0” and a maximum spacing of 10’-3”. A copy of this table is provided in Section 3.3 of this document.

A “Design Example for Elastomeric Bearings for Prestressed Concrete Beams” is provided on the TxDOT website (TxDOT, Texas Department of Transportation: Other Design Information 2006). This example demonstrates how the TxDOT modifications should be applied for bearing design. Since the example is pertinent to this project, it is included in Appendix 3.2.

### **3.2. Theory of the Proposed Modifications to Current Provisions**

The current design provisions as outlined in the above section do not contain specific provisions for consideration of the transverse slope. Therefore, it was necessary to develop a way to incorporate the transverse slope into the AASHTO design equations. This was complicated by the fact that some designers believe that steel-reinforced elastomeric bearings should never be allowed to resist a transverse shear, and thus, the check should never have to be made. Nonetheless, a force-equilibrium approach was used to determine the loading due to the transverse slope.

In order to incorporate the transverse slope into the AASHTO LRFD design equations, the end reaction of the U-beam was first considered in equilibrium. As shown in Figure 3.1, the end reaction  $P$  acts straight down. This reaction can be considered equal to the vector resultant of the two component vectors parallel and perpendicular to the bearing seat. For a transverse slope equal to  $\Theta$ , and assuming small angle theory where the tangent of a small angle is approximately equal to the angle (in radians), the transverse component is equal to the reaction  $P$  times the transverse slope,  $P\Theta$ . This transverse force,  $P\Theta$ , is then used to determine a transverse displacement at the top of the bearing using conventional displacement analysis. This displacement has been named  $\Delta_1$ .

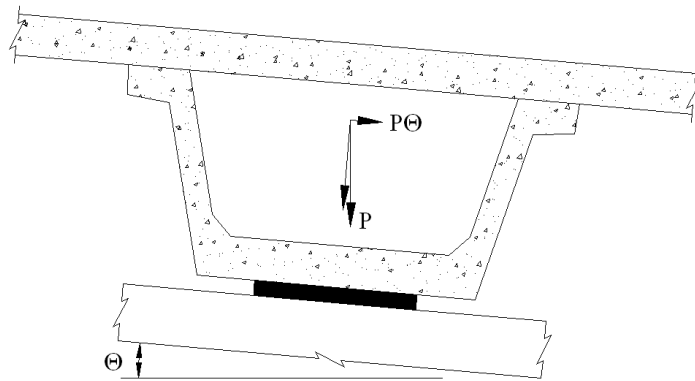


Figure 3.1 - Transverse Component  $P\Theta$  for Delta1 Displacement

Next, since the U-beam sections are so large, the geometry of the section could cause the end reaction  $P$  acting through the centroid of the combined U-beam and deck section to act off-center of the bearing. This leads to the consideration of a second displacement called Delta2. As shown in Figure 3.2, the second horizontal displacement is determined by first calculating the perpendicular distance from the bottom of the U-beam section to the centroid of the combined U-beam and slab section,  $Y_{\text{bottom}}$ . This centroid is dependent on the U-section, the 2 in. haunch, and the width of the slab. The horizontal distance, Delta2, is then determined by multiplying the  $Y_{\text{bottom}}$  by the transverse slope  $\Theta$  in radians.

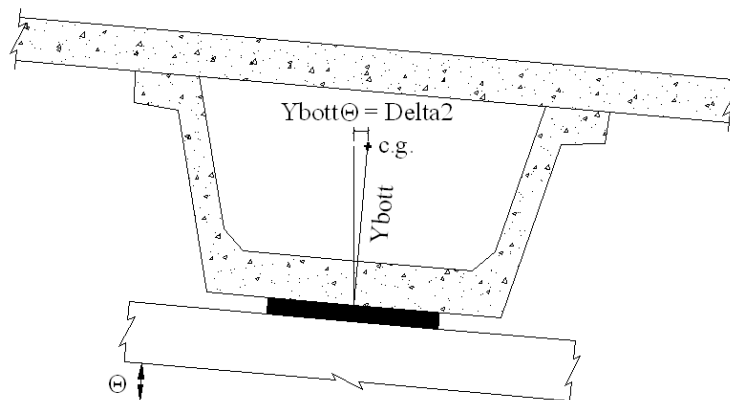


Figure 3.2 - Geometric Displacement Delta2 caused by  $Y_{\text{bott}}\Theta = \text{Delta2}$

Once the two displacements, Delta1 and Delta2, are determined a transverse moment can be calculated by multiplying the end reaction,  $P$ , by the sum of both displacements Delta1 and Delta2. In a way, this is similar to the consideration of the P-delta effect in column design.

The standard bearing arrangement (shown in Figure 3.3) for U-beams requires a single bearing on one end and two smaller bearings at the other end. The plan size of the single bearing is 2'-8" by 9" while each of the two double bearings are exactly half as big, 1'-4" by 9". Since the heights are the same, and the plan area of the single bearing is equal to the combined plan area of the two double bearings, the transverse deflection  $\Delta_1$  is theoretically the same for each.

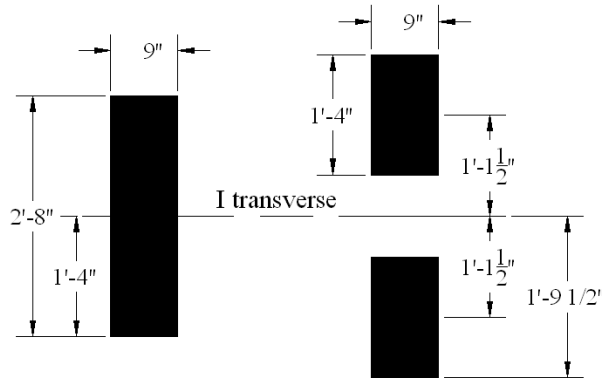


Figure 3.3 - Single and Double Bearing Plan Configurations

However, since the double bearings are spaced out with at least 11 in. between the inside edges of the bearings (as shown in Figure 3.3 for a situation with no skew), the resisting transverse moment of inertia for the double bearing configuration is higher than the resisting transverse moment of inertia for the single bearing configuration. The moment of inertia,  $I$ , for the single bearing configuration is  $24,576 \text{ in}^4$  while the moment of inertia for the double bearing configuration is  $58,632 \text{ in}^4$ . The resulting section moduli for the single and double pad configurations are  $1,536 \text{ in}^3$  and  $2,727 \text{ in}^3$ , respectively. Theoretically, since the double bearing configuration has a transverse moment of inertia approximately 2.4 times higher than the single bearing configuration and a section modulus approximately 1.8 times higher than the single bearing configuration, the double bearing should be able to resist the transverse moment better than the single bearing.

### 3.3. Limits Considered

These proposed revisions were considered for the range of span and U-beam spacings normally used in Texas. This range, shown in Table 3.2, was taken from the “Recommended

Table 3.2 - U-beam Recommended Spacings for LRFD

### U Beams, Recommended Spacings for LRFD

U40 Beam Spacings vs. Span Lengths		
Span Length	Overhang	Max. Spacing
75'	6'-9"	16'-7"
80'	6'-9"	16'-7"
	5'-0"	16'-7"
85'	6'-9"	14'-0"
	5'-0"	16'-0"
90'	6'-9"	11'-6"
	5'-0"	13'-6"
95'	5'-0"	11'-0"
100'	5'-0"	9'-3"
105'	5'-0"	7'-6" <sup>1</sup>

Approximate Structure depth = 40" beam + 8" slab + 2" haunch = 50"

U54 Beam Spacings vs. Span Lengths		
Span Length	Overhang	Max. Spacing
75'	6'-9"	16'-7"
80'	6'-9"	16'-7"
85'	6'-9"	16'-7"
90'	6'-9"	16'-7"
95'	6'-9"	16'-7"
100'	6'-9"	16'-7"
	5'-0"	16'-7"
105'	6'-9"	14'-3"
	5'-0"	16'-3"
110'	6'-9"	12'-0"
	5'-0"	14'-0"
115'	6'-9"	10'-0"
	5'-0"	11'-9"
120'	5'-0"	10'-3"

Approximate Structure depth = 54" beam + 8" slab + 2" haunch = 64"

<sup>1</sup>0.600" 270 ksi low-relaxation strand

- Interior and exterior beam design
- 0.110 klf composite dead load (1/3<sup>rd</sup> of T501 rail ~ 0.330klf)
- 65% relative humidity
- 1/2" 270 ksi low-relaxation strand, unless noted otherwise
- $f_{ci\ max} = 6500\ \text{psi}$ ,  $f_{c\ max} = 8500\ \text{psi}$ , unless noted otherwise
- 2" overlay
- Span lengths shown are CL to CL Bent with 9 1/2" distance to CL Bearing

Beam Spacing” table in the Superstructure Design Recommendation section of the TxDOT website. (TxDOT, Superstructure Design Information 2009)

### **3.4. Design Example with Proposed Modifications**

For the following example and the summary tables shown in Section 3.5, design provisions for Prestressed Concrete U-Beams (Types U40 and U54) were obtained from Section 6 of Chapter 3 of the TxDOT LRFD Bridge Design Manual (TxDOT, LRFD Bridge Design Manual 2007). Requirements to determine the distribution factor for shear, called DFV, were obtained from the TxDOT spreadsheet “LRFD Distribution Factors” located on the Superstructure Design section of the TxDOT website (TxDOT, Superstructure Design 2009).

Design live load was determined using standard HL-93 loading which consists of the sum of the HS20-44 truck and a lane load of 0.64 klf. No impact factor was used in the analysis.

Design dead loads were determined from several sources. Beam properties were taken from the standard TxDOT drawing UBD dated July 2006 (TxDOT, TxDOT Expressway British Standards (English) 2009). A self-weight of 1.021 klf was used for the example. A haunch of 0.066 klf was determined by assuming a standard 2 in. haunch over the top flange widths of 1’-3 ¼”. The minimum value for the end block (2.65 kips) was determined assuming a 1’-6” block and the maximum value (3.53 kips) was determined assuming a 2’-0” block. The minimum value for the interior diaphragm (0.88 kips) was calculated from the standard drawing and the maximum value for the interior diaphragm (2 kips) was taken from Section 6 of the TxDOT LRFD Bridge Design manual (TxDOT, LRFD Bridge Design Manual 2007). An 8 in. thick slab was assumed, which at a unit weight of 0.15 kcf, produces a slab weight of 0.1 times the beam spacing in feet. Both maximum and minimum dead loads were used in the applicable checks (i.e. minimum dead load was used in the anchorage slip check).

Properties for the standard bearings, as shown previously in Figure 3.3, were obtained from the standard U-beam bearing sheet, UBEB, dated July 2006 (TxDOT, TxDOT Expressway British Standards (English) 2009). On one end of a U-beam, a single bearing sized 32 in. wide by 9 in. long is used. On the other end of the beam, two bearings each 16 in. wide by 9 in. long are used. These bearings are located 13 ½ in. each from the longitudinal center line. The standard bearing for both types has a ¼ in. top and bottom pad thickness, 4 interior layers at 3/8 in. thick,

and five steel shims at 0.105 in. thick. The one-pad type has a shape factor,  $S$ , equal to 9.37 and the two-pad type has a shape factor equal to 7.68.

Using the above assumptions, all applicable limit states were checked using the additional moment caused by the transverse slope (the moment caused by the proposed  $\Delta_1$  and  $\Delta_2$  displacements). The only limit state that was not affected by the additional transverse moment was the Stability check. The remaining five limit states, Compressive Stress, Shear Strain, Anchorage Slip, Compressive Deflection, and Rotation were all modified to include the effect of the transverse moment. For each limit state, the ratio of the actual state to the allowable was determined. Therefore a ratio below 1.0 indicates the particular state is OK. If the ratio is above 1.0 it indicates that the check has failed.

The calculations that consider the proposed changes have been performed in both Excel and Mathcad. Since Excel calculations can be difficult to follow, a partial example follows in Mathcad. In addition to the Mathcad example, Excel tabulated results for the typical span arrangements are provided.

The following example shows the calculations for an interior U40 beam with an effective span length of 73.5 ft and a U-beam spacing of 16.5 ft. The effective span length from Centerline to Centerline of bearing of 73.5 ft was determined from Table 3.2 which shows the span length from Centerline to Centerline of bent. The spacing was rounded down 2 in. for simplicity. The example assumes a longitudinal slope of 2% and a transverse slope of 3%. The interior DFV was determined to be 1.394 using the TxDOT spreadsheet “LRFD Distribution Factors” (TxDOT, Superstructure Design 2009).

First, the dead and live loads are determined as shown in Figure 3.4. Next, the bearing pad properties for both the single and double pad configurations are calculated as shown in Figure 3.5. The third step shows the calculation of the  $\Delta_1$  and  $\Delta_2$  displacements and the resulting transverse moment,  $M_T$ , in Figure 3.6. Again, this proposed moment,  $M_T$ , is not explicitly required by LRFD design procedures. The proposed moment is based on the two displacements,  $\Delta_1$  and  $\Delta_2$ . The validity of including this moment will be discussed in later sections of this report.

Figure 3.7 shows the first four checks. All checks show the resulting ratio of the actual state divided by the allowable state. The “Compressive Stress Check” includes the moment terms for the transverse moment,  $M_T$ , for the actual stress equations,  $f_{act}$ . The “Shear Strain

Check” assumes that the U-beams will be in a four-span continuous unit. Therefore the effective length for expansion is two times a span (or half of the unit length). To account for the transverse displacement, the total effective displacement,  $\Delta_{S\text{Eff}}$ , was determined by calculating the vector resultant of the transverse and longitudinal displacements. This increases the displacement from the 0.74 in. to 0.79 in. The “Anchorage Slip Check” determines an effective slope,  $\Theta_{\text{effective}}$ , as the vector resultant of the transverse and longitudinal slopes. This increases the slope from 3.0% to 3.6%. For this case, the ratio is calculated to be 1.17. This indicates that the state has been exceeded by 17%. No modifications have been made to the “Stability Check” – it is shown merely for completeness.

Figure 3.8 shows the final two checks and the resulting maximum ratio for the single pad configuration. Equations for the two specific shape factors ( $S=9.37$  for the single pad configuration and  $S=7.68$  for the double pad configuration) were determined from Figure C14.7.5.3.3-1 in the AASHTO LRFD Bridge Design Specifications “Compressive Deflection Check” (AASHTO 2006 with Interims). This allows for the strain to be determined from a calculation using the actual stress,  $f_{\text{act}}$ . The best-fit curve equations for the two shape factors are:

$$\varepsilon_{(S=9.37)} = -0.726 * f_{\text{act}}^2 + 5.194 * f_{\text{act}} \quad \text{Eq. 3.1}$$

$$\varepsilon_{(S=7.68)} = -0.796 * f_{\text{act}}^2 + 5.728 * f_{\text{act}} \quad \text{Eq. 3.2}$$

where  $f_{\text{act}}$  is the compressive stress in units of ksi.

The transverse dead load and the transverse live load moments,  $M_{\text{TDL}}$  and  $M_{\text{TLL}}$ , are included in the “Rotation Check”. These terms decrease the stress caused by the vertical load on one side of the bearing which decreases the allowable strain. Finally, the maximum ratio for all six cases is determined to be 1.17. This ratio is the controlling ratio for the single pad configuration. The sample calculation for the double pad configuration is not shown. But, as expected, the double pad configuration performs better, with a maximum ratio of 0.88.

## Dead and Live Loads

### General Information

$$\text{span} = 73.5\text{ft} \quad \text{spa} = 16.5 \text{ ft} \quad \text{DFV} = 1.394$$

### Dead Loads

$$w_{\text{self}} = 1.021 \text{ klf} \quad w_{\text{rail}} = 0.11 \text{ klf} \quad w_{\text{bolster}} = 0.066 \text{ klf}$$

$$w_{\text{slab}} = 0.1 \frac{\text{kip}}{\text{ft}^2} \text{ spa} \quad w_{\text{slab}} = 1.65 \text{ klf}$$

$$w_{\text{overmin}} = 0 \text{ klf} \quad w_{\text{overmax}} = 0.023 \frac{\text{kip}}{\text{ft}^2} \text{ spa} \quad w_{\text{overmax}} = 0.38 \text{ klf}$$

$$P_{\text{ebmin}} = 2.65 \text{ kip} \quad P_{\text{ebmax}} = 3.53 \text{ kip}$$

$$P_{\text{intdiamin}} = 0.88 \text{ kip} \quad P_{\text{intdiamax}} = 2 \text{ kip}$$

$$R_{D\text{min}} = \left( \frac{\text{span}}{2} \right) (w_{\text{self}} + w_{\text{rail}} + w_{\text{bolster}} + w_{\text{slab}} + w_{\text{overmin}}) + P_{\text{ebmin}} + P_{\text{intdiamin}}$$

$$R_{D\text{min}} = 108.157 \text{ kip}$$

$$R_{D\text{max}} = \left( \frac{\text{span}}{2} \right) (w_{\text{self}} + w_{\text{rail}} + w_{\text{bolster}} + w_{\text{slab}} + w_{\text{overmax}}) + P_{\text{ebmax}} + P_{\text{intdiamax}}$$

$$R_{D\text{max}} = 124.104 \text{ kip}$$

### Live Loads

$$R_{L1} = 32 \text{ kip} + 32 \text{ kip} \frac{\text{span} - 14\text{ft}}{\text{span}} + 8 \text{ kip} \frac{\text{span} - 28\text{ft}}{\text{span}} \quad R_{L1} = 62.857 \text{ kip}$$

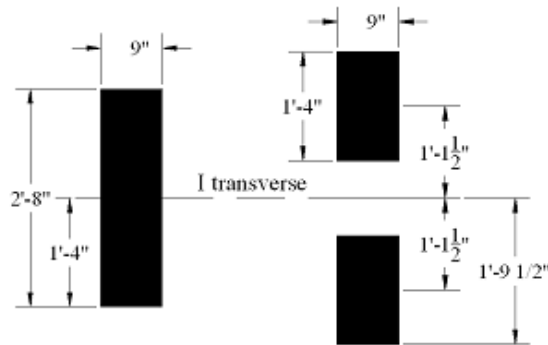
$$R_{L2} = 0.64 \text{ klf} \frac{\text{span}}{2} \quad R_{L2} = 23.52 \text{ kip}$$

$$R_{LL} = \text{DFV} (R_{L1} + R_{L2}) \quad R_{LL} = 120.41 \text{ kip}$$

Figure 3.4 - Dead and Live Loads

### Bearing Properties

$$\begin{array}{llll}
 h_s = 0.105 \text{ in} & h_{ro} = 0.25 \text{ in} & n_{ro} = 2 & h_{rto} = h_{ro} n_{ro} \\
 h_{rto} = 0.5 \text{ in} & h_{ri} = 0.375 \text{ in} & n_{ri} = 4 & h_{rti} = h_{ri} n_{ri} \\
 h_{rti} = 1.5 \text{ in} & h_{rt} = h_{rto} + h_{rti} & h_{rt} = 2 \text{ in} & T = h_{rt} + (n_{ro} + n_{ri} - 1) h_s \\
 T = 2.525 \text{ in} & d_2 = 13.5 \text{ in} & & 
 \end{array}$$



### One Pad Properties

$$\begin{array}{llll}
 W_1 = 32 \text{ in} & L_1 = 9 \text{ in} & A_1 = W_1 L_1 & A_1 = 288 \text{ in}^2 \\
 A_{1b} = (W_1 + L_1) 2 h_{ri} & A_{1b} = 30.75 \text{ in}^2 & S_1 = \frac{A_1}{A_{1b}} & S_1 = 9.366 \\
 I_{T1} = \frac{L_1 W_1^3}{12} & I_{T1} = 24576 \text{ in}^4 & S_{T1} = \frac{I_{T1}}{\frac{W_1}{2}} & S_{T1} = 1536 \text{ in}^3
 \end{array}$$

### Two Pad Properties

$$\begin{array}{llll}
 W_2 = 16 \text{ in} & L_2 = 9 \text{ in} & A_2 = W_2 L_2 & A_2 = 144 \text{ in}^2 \\
 A_{2b} = (W_2 + L_2) 2 h_{ri} & A_{2b} = 18.75 \text{ in}^2 & S_2 = \frac{A_2}{A_{2b}} & S_2 = 7.68 \\
 I_{T2} = 2 \frac{L_2 W_2^3}{12} + 2 (L_2 W_2) d_2^2 & & I_{T2} = 58632 \text{ in}^4 & \\
 & & S_{T2} = \frac{I_{T2}}{d_2 + \frac{W_2}{2}} & S_{T2} = 2727 \text{ in}^3
 \end{array}$$

Figure 3.5 - Bearing Pad Properties

## Transverse Loads

### ***Delta1 Displacement***

$$\Theta_T = 0.03 \quad \Theta_L = 0.02 \quad G_{low} = 0.095 \text{ksi} \quad G_{high} = 0.175 \text{ksi}$$

$$P_D = R_{Dmax} \quad P_D = 124.104 \text{kip} \quad P_{LL} = R_{LL} \quad P_{LL} = 120.41 \text{kip}$$

$$\text{Delta1}_D = \frac{P_D \Theta_T h_{rt}}{G_{low} A_1} \quad \text{Delta1}_D = 0.27 \text{in}$$

$$\text{Delta1}_{LL} = \frac{P_{LL} \Theta_T h_{rt}}{G_{low} A_1} \quad \text{Delta1}_{LL} = 0.26 \text{in}$$

### ***Delta2 Displacement***

$$Y_{bott} = 34.80 \text{in} \quad \text{Delta2} = Y_{bott} \Theta_T \quad \text{Delta2} = 1.044 \text{in}$$

$$M_{TDL} = \left( \text{Delta1}_D + \text{Delta2} \right) P_D \quad M_{TDL} = 163.34 \text{kip in}$$

$$M_{TLL} = \left( \text{Delta1}_{LL} + \text{Delta2} \right) P_{LL} \quad M_{TLL} = 157.503 \text{kip in}$$

$$M_T = M_{TDL} + M_{TLL} \quad M_T = 320.843 \text{kip in}$$

Figure 3.6 - Delta1 and Delta2 Displacements

## One Pad Checks

### Compressive Stress Check

$$f_{all} = \min | 1.2 \text{ksi}, 1.2 G_{low} S_1 | \quad f_{all} = 1.068 \text{ ksi}$$

$$f_{act} = \frac{P_D}{A_1} + \frac{M_{TDL}}{S_{T1}} \quad f_{act} = 0.537 \text{ ksi} \quad \text{Ratio}_1 = \frac{f_{act}}{f_{all}} \quad \text{Ratio}_1 = 0.50$$

$$f_{all} = \min | 1.5 \text{ksi}, 1.5 G_{low} S_1 | \quad f_{all} = 1.335 \text{ ksi}$$

$$f_{act} = \frac{P_D + P_{LL}}{A_1} + \frac{M_{TDL} + M_{TLL}}{S_{T1}} \quad f_{act} = 1.058 \text{ ksi} \quad \text{Ratio}_2 = \frac{f_{act}}{f_{all}} \quad \text{Ratio}_2 = 0.79$$

### Shear Strain Check

$$\alpha = 0.000006 \quad \text{DeltaT} = 70 \quad \text{Span} = 73.5 \text{ft}$$

$$\Delta_{s1} = \alpha \text{DeltaT} \text{Span} \cdot 2 \quad \Delta_{s1} = 0.741 \text{ in} \quad \text{Delta1}_D = 0.272 \text{ in}$$

$$\Delta_{sEff} = \sqrt{\Delta_{s1}^2 + \text{Delta1}_D^2} \quad \Delta_{sEff} = 0.789 \text{ in}$$

$$h_{rt} = 2 \text{ in} \quad \text{Ratio}_3 = \frac{2 \Delta_{sEff}}{h_{rt}} \quad \text{Ratio}_3 = 0.79$$

### Anchorage Slip Check

$$\gamma_p = 0.9 \quad \Theta_{effective} = \Theta_T^2 + \Theta_L^2 \cdot \frac{1}{2} \quad \Theta_{effective} = 0.036 \quad \text{Limit} = 0.2$$

$$\Delta_{s2} = \frac{\text{Limit} - \Theta_{effective} \cdot \gamma_p \cdot R_{Dmin} \cdot h_{rt}}{G_{high} A_1} \quad \Delta_{s2} = 0.633 \text{ in}$$

$$\text{Ratio}_4 = \frac{\Delta_{s1}}{\Delta_{s2}} \quad \text{Ratio}_4 = 1.17$$

### Stability Check

$$h_{rtall} = \min \left( \frac{L_1}{3}, \frac{W_1}{3} \right) \quad h_{rtall} = 3 \text{ in} \quad \text{Ratio}_5 = \frac{h_{rt}}{h_{rtall}} \quad \text{Ratio}_5 = 0.67$$

Figure 3.7 – Single Pad Configuration Checks

## One Pad Checks (Continued)

### Compressive Deflection Check

$$S_1 = 9.366 \quad f_{act} = 1.058 \text{ ksi} \quad \epsilon |f_{act}| = \frac{-0.726}{\text{ksi}^2} f_{act}^2 + \frac{5.194}{\text{ksi}} f_{act} \quad \epsilon |f_{act}| = 4.682$$

$$\text{creep} = 0.25$$

$$\delta_{act} = (1 + \text{creep}) \frac{\epsilon |f_{act}|}{100} h_{ri} \quad \delta_{act} = 0.022 \text{ in}$$

$$\delta_{all} = 0.07 h_{ri} \quad \delta_{all} = 0.026 \text{ in}$$

$$\text{Ratio}_6 = \frac{\delta_{act}}{\delta_{all}} \quad \text{Ratio}_6 = 0.836$$

### Rotation Check

$$f_{min} = \frac{P_D + P_{LL}}{A_1} - \frac{M_{TDL} + M_{TLL}}{S_{T1}} \quad f_{min} = 0.64 \text{ ksi}$$

$$\epsilon |f_{min}| = 3.027 \quad \delta_{2all} = \frac{\epsilon |f_{min}| h_{rt}}{100} \quad \delta_{2all} = 0.061 \text{ in}$$

$$\Delta_{LLest} = \frac{\text{Span}}{800} \quad \Delta_{LLest} = 1.103 \text{ in} \quad \theta_{LLest} = \frac{4 \Delta_{LLest}}{\text{span}} \quad \theta_{LLest} = 0.005$$

$$\theta_{CT} = 0.005 \quad \delta_{2act} = \frac{|\theta_{LLest} + \theta_{CT}| 0.8 L_2}{2} \quad \delta_{2act} = 0.036 \text{ in}$$

$$\text{Ratio}_7 = \frac{\delta_{2act}}{\delta_{2all}} \quad \text{Ratio}_7 = 0.595$$

$$\text{Ratio} = \begin{pmatrix} 0 \\ 0.5 \\ 0.79 \\ 0.79 \\ 1.17 \\ 0.67 \\ 0.84 \\ 0.59 \end{pmatrix}$$

$$\max(\text{Ratio}) = 1.17$$

Figure 3.8 - Single Pad Configuration Checks (Cont.)

### 3.4.1. Discussion of Design Example

Considering the proposed Delta1 and Delta2 displacements and the resulting transverse moment,  $M_T$ , resulted in a worst case ratio of 1.17 with the Anchorage Slip check as the controlling case. Eliminating the transverse slope of 3% reduces the ratio to 1.07. Eliminating both the transverse slope of 3% and the longitudinal slope of 2% reduces the ratio to 0.96, which is less than 1, indicating that all design states meet design criteria.

It was expected that the standard bearings should meet design criteria when both the transverse and longitudinal slopes are zero. In general, this was found to be the case. To illustrate the influence of the transverse slope, Excel charts were created for the typical span and spacing for both U-40 and U-54 beams. These charts are shown in the following section.

### 3.5. Summary of Design States

The six design states were considered for both U-40 and U-54 sections over the typically used ranges of span length and spacings considering the effect of the transverse superelevation. The transverse superelevation is shown for values of 0%, 2%, 4%, 6%, and 8%. The first five tables, Tables 3.4 through 3.8, show the values for the U-40 sections while the next five tables, Tables 3.9 through 3.13, show the values for the U-54 sections.

Within each table, the longitudinal and transverse slopes are kept constant (i.e. 0% for the first table) but the number of spans changes from 2 to 3 to 4. The number of spans indicates the type of span unit. It was assumed that a 2 span unit would have an effective length for expansion of 1 span, a 3 span unit would have an effective length of expansion of 1.5 spans, and a 4 span unit would have an effective length of expansion of 2 spans. The tables are presented in this manner so that the effect of span length could easily be seen.

For a given span unit, the top portion shows the highest ratio for all six of the limit states. Ratios less than or equal to 1.0 are shown in green, ratios greater than 1.0 but less than or equal to 1.25 are shown in yellow, and ratios above 1.25 are shown in red. The bottom portion shows which of the limit states controls (has the highest ratio). The limit states are shown abbreviated using the abbreviations in Table 3.3.

Table 3.3 - Design Limit State Abbreviations

Design Limit State Name	Abbreviation
Compressive Stress Check	Comp
Shear Strain Check	SS
Anchorage Slip Check	Slip
Stability Check	Stab
Compressive Deflection Check	C Def
Rotation Check	Rot

Table 3.4 - U40 with 0% Transverse Slope

Interior Beams																
Long. Slope 0 Trans. Slope 0 Spans 2																
Spacing, ft																
Span, ft	16.5	16	14.5	14	13.5	12.5	12	11.5	11	10.5	10	9.5	9	8.5	8	7.5
73.5	0.50		0.71			0.67				0.67				0.68		
78.5	0.81		0.74			0.67				0.67				0.67		
83.5		0.82		0.75			0.68				0.67				0.68	
88.5					0.76			0.69				0.67				0.70
93.5									0.69				0.67			
98.5												0.67				0.70
103.5																0.70
Interior Beams																
Long. Slope 0 Trans. Slope 0 Spans 2																
Spacing, ft																
Span, ft	16.5	16	14.5	14	13.5	12.5	12	11.5	11	10.5	10	9.5	9	8.5	8	7.5
73.5	Comp		Comp			Stab				Stab				Rot		
78.5	Comp		Comp			C Def				Stab				Stab		
83.5		Comp		Comp			C Def				Stab					Slip
88.5					Comp			C Def				Stab				Slip
93.5									C Def				Stab			
98.5												Stab				Slip
103.5																Slip
Interior Beams																
Long. Slope 0 Trans. Slope 0 Spans 3																
Spacing, ft																
Span, ft	16.5	16	14.5	14	13.5	12.5	12	11.5	11	10.5	10	9.5	9	8.5	8	7.5
73.5	0.78		0.77			0.83				0.90				0.99		
78.5	0.81		0.77			0.83				0.91				0.99		
83.5		0.82		0.79			0.85				0.93				1.02	
88.5					0.81			0.87				0.95				1.04
93.5									0.89				0.97			
98.5												0.95				1.05
103.5																1.05
Interior Beams																
Long. Slope 0 Trans. Slope 0 Spans 3																
Spacing, ft																
Span, ft	16.5	16	14.5	14	13.5	12.5	12	11.5	11	10.5	10	9.5	9	8.5	8	7.5
73.5	Comp		Slip			Slip				Slip				Slip		
78.5	Comp		Slip			Slip				Slip				Slip		
83.5		Comp		Slip			Slip				Slip					Slip
88.5					Slip			Slip				Slip				Slip
93.5									Slip				Slip			
98.5												Slip				Slip
103.5																Slip
Interior Beams																
Long. Slope 0 Trans. Slope 0 Spans 4																
Spacing, ft																
Span, ft	16.5	16	14.5	14	13.5	12.5	12	11.5	11	10.5	10	9.5	9	8.5	8	7.5
73.5	0.96		1.03			1.11				1.20				1.32		
78.5	0.96		1.03			1.11				1.21				1.32		
83.5		0.98		1.05			1.14				1.24				1.36	
88.5					1.07			1.16				1.27				1.39
93.5									1.19				1.30			
98.5												1.27				1.40
103.5																1.40
Interior Beams																
Long. Slope 0 Trans. Slope 0 Spans 4																
Spacing, ft																
Span, ft	16.5	16	14.5	14	13.5	12.5	12	11.5	11	10.5	10	9.5	9	8.5	8	7.5
73.5	Slip		Slip			Slip				Slip				Slip		
78.5	Slip		Slip			Slip				Slip				Slip		
83.5		Slip		Slip			Slip				Slip					Slip
88.5					Slip			Slip				Slip				Slip
93.5									Slip				Slip			
98.5												Slip				Slip
103.5																Slip

Table 3.5 - U40 with 2% Transverse Superelevation

Interior Beams																			
				Long. Slope				0				Trans. Slope				0.02	Spans		2
Spacing, ft																			
Span, ft	16.5	16	14.5	14	13.5	12.5	12	11.5	11	10.5	10	9.5	9	8.5	8	7.5			
73.5	0.85		0.77			0.70				0.70				0.78					
78.5	0.88		0.81			0.73				0.67				0.75					
83.5		0.90		0.82			0.74				0.69				0.75				
88.5					0.83			0.74				0.70				0.77			
93.5									0.75				0.72						
98.5												0.71				0.78			
103.5																0.78			
Interior Beams																			
				Long. Slope				0				Trans. Slope				0.02	Spans		2
Spacing, ft																			
Span, ft	16.5	16	14.5	14	13.5	12.5	12	11.5	11	10.5	10	9.5	9	8.5	8	7.5			
73.5	Comp		Comp			C Def				Rot				Rot					
78.5	Comp		Comp			Com				Rot				Rot					
83.5		Comp		Comp			Com				Slip				Slip				
88.5					Comp			Comp				Slip				Slip			
93.5									Comp				Slip						
98.5												Comp				Slip			
103.5																Slip			
Interior Beams																			
				Long. Slope				0				Trans. Slope				0.02	Spans		3
Spacing, ft																			
Span, ft	16.5	16	14.5	14	13.5	12.5	12	11.5	11	10.5	10	9.5	9	8.5	8	7.5			
73.5	0.85		0.86			0.92				1.00				1.10					
78.5	0.88		0.86			0.93				1.01				1.10					
83.5		0.90		0.88			0.95				1.03				1.13				
88.5					0.90			0.97				1.06				1.16			
93.5									0.99				1.08						
98.5												1.06				1.17			
103.5																1.17			
Interior Beams																			
				Long. Slope				0				Trans. Slope				0.02	Spans		3
Spacing, ft																			
Span, ft	16.5	16	14.5	14	13.5	12.5	12	11.5	11	10.5	10	9.5	9	8.5	8	7.5			
73.5	Comp		Slip			Slip				Slip				Slip					
78.5	Comp		Slip			Slip				Slip				Slip					
83.5		Comp		Slip			Slip				Slip				Slip				
88.5					Slip			Slip				Slip				Slip			
93.5									Slip				Slip						
98.5												Slip				Slip			
103.5																Slip			
Interior Beams																			
				Long. Slope				0				Trans. Slope				0.02	Spans		4
Spacing, ft																			
Span, ft	16.5	16	14.5	14	13.5	12.5	12	11.5	11	10.5	10	9.5	9	8.5	8	7.5			
73.5	1.07		1.14			1.23				1.34				1.46					
78.5	1.07		1.15			1.24				1.34				1.47					
83.5		1.09		1.17			1.26				1.37				1.51				
88.5					1.19			1.29				1.41				1.55			
93.5									1.32				1.44						
98.5												1.41				1.55			
103.5																1.56			
Interior Beams																			
				Long. Slope				0				Trans. Slope				0.02	Spans		4
Spacing, ft																			
Span, ft	16.5	16	14.5	14	13.5	12.5	12	11.5	11	10.5	10	9.5	9	8.5	8	7.5			
73.5	Slip		Slip			Slip				Slip				Slip					
78.5	Slip		Slip			Slip				Slip				Slip					
83.5		Slip		Slip			Slip				Slip				Slip				
88.5					Slip			Slip				Slip				Slip			
93.5									Slip				Slip						
98.5												Slip				Slip			
103.5																Slip			

Table 3.6 - U40 with 4% Transverse Superelevation

Interior Beams																			
				Long. Slope				0				Trans. Slope				0.04	Spans		2
Spacing, ft																			
Span, ft	16.5	16	14.5	14	13.5	12.5	12	11.5	11	10.5	10	9.5	9	8.5	8	7.5			
73.5	0.92		0.84			0.76				0.83				0.91					
78.5	0.96		0.87			0.78				0.80				0.88					
83.5		0.98		0.89			0.79				0.79				0.87				
88.5					0.90			0.80				0.79				0.87			
93.5									0.81				0.81						
98.5												0.80				0.87			
103.5																0.88			
Interior Beams																			
				Long. Slope				0				Trans. Slope				0.04	Spans		2
Spacing, ft																			
Span, ft	16.5	16	14.5	14	13.5	12.5	12	11.5	11	10.5	10	9.5	9	8.5	8	7.5			
73.5	Comp		Comp			Rot				Rot				Rot					
78.5	Comp		Comp			Comp				Rot				Rot					
83.5		Comp		Comp			Comp				Rot				Rot				
88.5					Comp			Comp				Slip				Slip			
93.5									Comp				Slip						
98.5												Slip				Slip			
103.5																Slip			
Interior Beams																			
				Long. Slope				0				Trans. Slope				0.04	Spans		3
Spacing, ft																			
Span, ft	16.5	16	14.5	14	13.5	12.5	12	11.5	11	10.5	10	9.5	9	8.5	8	7.5			
73.5	0.92		0.96			1.04				1.13				1.23					
78.5	0.96		0.97			1.04				1.13				1.24					
83.5		0.98		0.99			1.07				1.16				1.27				
88.5					1.01			1.09				1.19				1.31			
93.5									1.12				1.22						
98.5												1.19				1.31			
103.5																1.31			
Interior Beams																			
				Long. Slope				0				Trans. Slope				0.04	Spans		3
Spacing, ft																			
Span, ft	16.5	16	14.5	14	13.5	12.5	12	11.5	11	10.5	10	9.5	9	8.5	8	7.5			
73.5	Comp		Slip			Slip				Slip				Slip					
78.5	Comp		Slip			Slip				Slip				Slip					
83.5		Comp		Slip			Slip				Slip				Slip				
88.5					Slip			Slip				Slip				Slip			
93.5									Slip				Slip						
98.5												Slip				Slip			
103.5																Slip			
Interior Beams																			
				Long. Slope				0				Trans. Slope				0.04	Spans		4
Spacing, ft																			
Span, ft	16.5	16	14.5	14	13.5	12.5	12	11.5	11	10.5	10	9.5	9	8.5	8	7.5			
73.5	1.20		1.29			1.39				1.51				1.65					
78.5	1.20		1.29			1.39				1.51				1.65					
83.5		1.22		1.32			1.42				1.55				1.69				
88.5					1.34			1.45				1.58				1.74			
93.5									1.49				1.62						
98.5												1.59				1.75			
103.5																1.75			
Interior Beams																			
				Long. Slope				0				Trans. Slope				0.04	Spans		4
Spacing, ft																			
Span, ft	16.5	16	14.5	14	13.5	12.5	12	11.5	11	10.5	10	9.5	9	8.5	8	7.5			
73.5	Slip		Slip			Slip				Slip				Slip					
78.5	Slip		Slip			Slip				Slip				Slip					
83.5		Slip		Slip			Slip				Slip				Slip				
88.5					Slip			Slip				Slip				Slip			
93.5									Slip				Slip						
98.5												Slip				Slip			
103.5																Slip			

Table 3.7 - U40 with 6% Transverse Superelevation

Interior Beams																
Long. Slope 0 Trans. Slope 0.06 Spans 2																
Spacing, ft																
Span, ft	16.5	16	14.5	14	13.5	12.5	12	11.5	11	10.5	10	9.5	9	8.5	8	7.5
73.5	0.99		0.90			0.95				1.02				1.11		
78.5	1.03		0.94			0.92				0.99				1.07		
83.5		1.05		0.95			0.91				0.97				1.06	
88.5					0.97			0.90				0.96				1.05
93.5									0.89				0.95			
98.5												0.91				1.00
103.5																1.00

Interior Beams																
Long. Slope 0 Trans. Slope 0.06 Spans 2																
Spacing, ft																
Span, ft	16.5	16	14.5	14	13.5	12.5	12	11.5	11	10.5	10	9.5	9	8.5	8	7.5
73.5	Comp		Rot			Rot				Rot				Rot		
78.5	Comp		Comp			Rot				Rot				Rot		
83.5		Comp		Comp			Rot				Rot				Rot	
88.5					Comp			Rot				Rot				Rot
93.5									Rot				Rot			
98.5												Rot				Slip
103.5																Slip

Interior Beams																
Long. Slope 0 Trans. Slope 0.06 Spans 3																
Spacing, ft																
Span, ft	16.5	16	14.5	14	13.5	12.5	12	11.5	11	10.5	10	9.5	9	8.5	8	7.5
73.5	1.03		1.10			1.19				1.29				1.41		
78.5	1.03		1.10			1.19				1.29				1.42		
83.5		1.05		1.13			1.22				1.33				1.45	
88.5					1.15			1.25				1.36				1.49
93.5								1.27					1.39			
98.5												1.36				1.50
103.5																1.50

Interior Beams																
Long. Slope 0 Trans. Slope 0.06 Spans 3																
Spacing, ft																
Span, ft	16.5	16	14.5	14	13.5	12.5	12	11.5	11	10.5	10	9.5	9	8.5	8	7.5
73.5	Slip		Slip			Slip				Slip				Slip		
78.5	Comp		Slip			Slip				Slip				Slip		
83.5		Comp		Slip			Slip				Slip				Slip	
88.5					Slip			Slip				Slip				Slip
93.5									Slip				Slip			
98.5												Slip				Slip
103.5																Slip

Interior Beams																
Long. Slope 0 Trans. Slope 0.06 Spans 4																
Spacing, ft																
Span, ft	16.5	16	14.5	14	13.5	12.5	12	11.5	11	10.5	10	9.5	9	8.5	8	7.5
73.5	1.37		1.47			1.59				1.72				1.88		
78.5	1.37		1.47			1.59				1.73				1.89		
83.5		1.40		1.50			1.62				1.77				1.94	
88.5					1.53			1.66				1.81				1.99
93.5									1.70				1.86			
98.5												1.82				2.00
103.5																2.00

Interior Beams																
Long. Slope 0 Trans. Slope 0.06 Spans 4																
Spacing, ft																
Span, ft	16.5	16	14.5	14	13.5	12.5	12	11.5	11	10.5	10	9.5	9	8.5	8	7.5
73.5	Slip		Slip			Slip				Slip				Slip		
78.5	Slip		Slip			Slip				Slip				Slip		
83.5		Slip		Slip			Slip				Slip				Slip	
88.5					Slip			Slip				Slip				Slip
93.5									Slip				Slip			
98.5												Slip				Slip
103.5																Slip

Table 3.8 - U40 with 8% Transverse Superelevation

Interior Beams																			
		Long. Slope					0	Trans. Slope					0.08	Spans					2
		Spacing, ft																	
Span, ft	16.5	16	14.5	14	13.5	12.5	12	11.5	11	10.5	10	9.5	9	8.5	8	7.5			
73.5	1.24		1.26			1.30				1.35				1.42					
78.5	1.21		1.23			1.26				1.31				1.37					
83.5		1.19		1.21			1.24				1.29				1.35				
88.5					1.19			1.22				1.27				1.34			
93.5									1.20				1.25						
98.5												1.21				1.27			
103.5																1.24			
Interior Beams																			
		Long. Slope					0	Trans. Slope					0.08	Spans					2
		Spacing, ft																	
Span, ft	16.5	16	14.5	14	13.5	12.5	12	11.5	11	10.5	10	9.5	9	8.5	8	7.5			
73.5	Rot		Rot			Rot				Rot				Rot					
78.5	Rot		Rot			Rot				Rot				Rot					
83.5		Rot		Rot			Rot				Rot				Rot				
88.5					Rot			Rot				Rot				Rot			
93.5									Rot				Rot						
98.5												Rot				Rot			
103.5																Rot			
Interior Beams																			
		Long. Slope					0	Trans. Slope					0.08	Spans					3
		Spacing, ft																	
Span, ft	16.5	16	14.5	14	13.5	12.5	12	11.5	11	10.5	10	9.5	9	8.5	8	7.5			
73.5	1.24		1.29			1.39				1.51				1.65					
78.5	1.21		1.29			1.39				1.51				1.65					
83.5		1.22		1.32			1.42				1.55				1.69				
88.5					1.34			1.45				1.58				1.74			
93.5									1.49				1.62						
98.5												1.59				1.75			
103.5																1.75			
Interior Beams																			
		Long. Slope					0	Trans. Slope					0.08	Spans					3
		Spacing, ft																	
Span, ft	16.5	16	14.5	14	13.5	12.5	12	11.5	11	10.5	10	9.5	9	8.5	8	7.5			
73.5	Rot		Slip			Slip				Slip				Slip					
78.5	Rot		Slip			Slip				Slip				Slip					
83.5		Slip		Slip			Slip				Slip				Slip				
88.5					Slip			Slip				Slip				Slip			
93.5									Slip				Slip						
98.5												Slip				Slip			
103.5																Slip			
Interior Beams																			
		Long. Slope					0	Trans. Slope					0.08	Spans					4
		Spacing, ft																	
Span, ft	16.5	16	14.5	14	13.5	12.5	12	11.5	11	10.5	10	9.5	9	8.5	8	7.5			
73.5	1.60		1.71			1.85				2.01				2.19					
78.5	1.60		1.72			1.85				2.01				2.20					
83.5		1.63		1.75			1.90				2.06				2.26				
88.5					1.79			1.94				2.11				2.32			
93.5									1.98				2.17						
98.5												2.12				2.33			
103.5																2.33			
Interior Beams																			
		Long. Slope					0	Trans. Slope					0.08	Spans					4
		Spacing, ft																	
Span, ft	16.5	16	14.5	14	13.5	12.5	12	11.5	11	10.5	10	9.5	9	8.5	8	7.5			
73.5	Slip		Slip			Slip				Slip				Slip					
78.5	Slip		Slip			Slip				Slip				Slip					
83.5		Slip		Slip			Slip				Slip				Slip				
88.5					Slip			Slip				Slip				Slip			
93.5									Slip				Slip						
98.5												Slip				Slip			
103.5																Slip			

Table 3.9 - U54 with 0% Transverse Slope

Interior Beams														Long. Slope	0	Trans. Slope	0	Spans		2			
														Spacing, ft									
Span, ft	16.5	16	14.5	14	13.5	12.5	12	11.5	11	10.5	10	9.5	9	8.5									
73.5	0.81		0.75			0.77				0.83				0.90									
78.5	0.85		0.78			0.78				0.84				0.91									
83.5	0.88		0.81			0.78				0.84				0.91									
88.5	0.91		0.84			0.78				0.84				0.91									
93.5	0.95		0.87			0.79				0.84				0.92									
98.5	0.98		0.90			0.82				0.85				0.92									
103.5				0.91			0.83				0.86												
108.5							0.85				0.87												
113.5											0.87												
118.5											0.90												
Interior Beams														Long. Slope	0	Trans. Slope	0	Spans		2			
														Spacing, ft									
Span, ft	16.5	16	14.5	14	13.5	12.5	12	11.5	11	10.5	10	9.5	9	8.5									
73.5	Comp		Comp			Slip				Slip				Slip									
78.5	Comp		Comp			Slip				Slip				Slip									
83.5	Comp		Comp			Slip				Slip				Slip									
88.5	Comp		Comp			Slip				Slip				Slip									
93.5	Comp		Comp			Comp				Slip				Slip									
98.5	Comp		Comp			Comp				Slip				Slip									
103.5				Comp			Comp				Slip												
108.5							Comp				Slip												
113.5											Slip												
118.5											SS												
Interior Beams														Long. Slope	0	Trans. Slope	0	Spans		3			
														Spacing, ft									
Span, ft	16.5	16	14.5	14	13.5	12.5	12	11.5	11	10.5	10	9.5	9	8.5									
73.5	0.81		0.75			0.77				0.83				0.90									
78.5	0.85		0.78			0.78				0.84				0.91									
83.5	0.88		0.81			0.78				0.84				0.91									
88.5	0.91		0.84			0.78				0.84				0.91									
93.5	0.95		0.87			0.79				0.84				0.92									
98.5	0.98		0.90			0.82				0.85				0.92									
103.5				0.91			0.83				0.86												
108.5							0.85				0.87												
113.5											0.87												
118.5											0.90												
Interior Beams														Long. Slope	0	Trans. Slope	0	Spans		3			
														Spacing, ft									
Span, ft	16.5	16	14.5	14	13.5	12.5	12	11.5	11	10.5	10	9.5	9	8.5									
73.5	Comp		Comp			Slip				Slip				Slip									
78.5	Comp		Comp			Slip				Slip				Slip									
83.5	Comp		Comp			Slip				Slip				Slip									
88.5	Comp		Comp			Slip				Slip				Slip									
93.5	Comp		Comp			Comp				Slip				Slip									
98.5	Comp		Comp			Comp				Slip				Slip									
103.5				Comp			Comp				Slip												
108.5							Comp				Slip												
113.5											Slip												
118.5											SS												

Interior Beams		Long. Slope					0	Trans. Slope					0	Spans				4
		Spacing, ft																
Span, ft	16.5	16	14.5	14	13.5	12.5	12	11.5	11	10.5	10	9.5	9	8.5				
73.5	0.90		0.96			1.03				1.11				1.21				
78.5	0.90		0.96			1.03				1.12				1.21				
83.5	0.90		0.97			1.04				1.12				1.22				
88.5	0.91		0.97			1.04				1.12				1.22				
93.5	0.95		0.97			1.04				1.13				1.22				
98.5	0.99		0.99			1.04				1.13				1.23				
103.5				1.04			1.07				1.15							
108.5							1.09				1.16							
113.5											1.16							
118.5											1.19							

Interior Beams		Long. Slope					0	Trans. Slope					0	Spans				4
		Spacing, ft																
Span, ft	16.5	16	14.5	14	13.5	12.5	12	11.5	11	10.5	10	9.5	9	8.5				
73.5	Slip		Slip			Slip				Slip				Slip				
78.5	Slip		Slip			Slip				Slip				Slip				
83.5	Slip		Slip			Slip				Slip				Slip				
88.5	Comp		Slip			Slip				Slip				Slip				
93.5	Comp		Slip			Slip				Slip				Slip				
98.5	SS		SS			Slip				Slip				Slip				
103.5				SS			Slip				Slip							
108.5							SS				Slip							
113.5											Slip							
118.5											SS							

Table 3.10 - U54 with 2% Transverse Superelevation

Interior Beams		Long. Slope					0	Trans. Slope			0.02	Spans				2
		Spacing, ft														
Span, ft	16.5	16	14.5	14	13.5	12.5	12	11.5	11	10.5	10	9.5	9	8.5		
73.5	0.91		0.83			0.86				0.93				1.01		
78.5	0.95		0.86			0.86				0.93				1.01		
83.5	0.98		0.90			0.86				0.93				1.01		
88.5	1.02		0.93			0.87				0.94				1.02		
93.5	1.06		0.97			0.88				0.94				1.02		
98.5	1.10		1.00			0.91				0.94				1.02		
103.5				1.01			0.92				0.96					
108.5							0.95				0.96					
113.5											0.96					
118.5											0.97					

Interior Beams		Long. Slope					0	Trans. Slope			0.02	Spans				2
		Spacing, ft														
Span, ft	16.5	16	14.5	14	13.5	12.5	12	11.5	11	10.5	10	9.5	9	8.5		
73.5	Comp		Comp			Slip				Slip				Slip		
78.5	Comp		Comp			Slip				Slip				Slip		
83.5	Comp		Comp			Slip				Slip				Slip		
88.5	Comp		Comp			Slip				Slip				Slip		
93.5	Comp		Comp			Comp				Slip				Slip		
98.5	Comp		Comp			Comp				Slip				Slip		
103.5				Comp			Comp				Slip					
108.5							Comp				Slip					
113.5											Slip					
118.5											Slip					

Interior Beams		Long. Slope					0	Trans. Slope			0.02	Spans				3
		Spacing, ft														
Span, ft	16.5	16	14.5	14	13.5	12.5	12	11.5	11	10.5	10	9.5	9	8.5		
73.5	0.91		0.83			0.86				0.93				1.01		
78.5	0.95		0.86			0.86				0.93				1.01		
83.5	0.98		0.90			0.86				0.93				1.01		
88.5	1.02		0.93			0.87				0.94				1.02		
93.5	1.06		0.97			0.88				0.94				1.02		
98.5	1.10		1.00			0.91				0.94				1.02		
103.5				1.01			0.92				0.96					
108.5							0.95				0.96					
113.5											0.96					
118.5											0.97					

Interior Beams		Long. Slope					0	Trans. Slope			0.02	Spans				3
		Spacing, ft														
Span, ft	16.5	16	14.5	14	13.5	12.5	12	11.5	11	10.5	10	9.5	9	8.5		
73.5	Comp		Comp			Slip				Slip				Slip		
78.5	Comp		Comp			Slip				Slip				Slip		
83.5	Comp		Comp			Slip				Slip				Slip		
88.5	Comp		Comp			Slip				Slip				Slip		
93.5	Comp		Comp			Comp				Slip				Slip		
98.5	Comp		Comp			Comp				Slip				Slip		
103.5				Comp			Comp				Slip					
108.5							Comp				Slip					
113.5											Slip					
118.5											Slip					

Interior Beams		Long. Slope					0	Trans. Slope			0.02	Spans				4
Span, ft	Spacing, ft															
	16.5	16	14.5	14	13.5	12.5	12	11.5	11	10.5	10	9.5	9	8.5		
73.5	1.00		1.07			1.14				1.23				1.34		
78.5	1.00		1.07			1.15				1.24				1.35		
83.5	1.00		1.07			1.15				1.24				1.35		
88.5	1.02		1.08			1.15				1.25				1.35		
93.5	1.06		1.08			1.16				1.25				1.36		
98.5	1.10		1.08			1.16				1.25				1.36		
103.5				1.10			1.18				1.28					
108.5							1.19				1.28					
113.5											1.29					
118.5											1.29					

Interior Beams		Long. Slope					0	Trans. Slope			0.02	Spans				4
Span, ft	Spacing, ft															
	16.5	16	14.5	14	13.5	12.5	12	11.5	11	10.5	10	9.5	9	8.5		
73.5	Slip		Slip			Slip				Slip				Slip		
78.5	Slip		Slip			Slip				Slip				Slip		
83.5	Slip		Slip			Slip				Slip				Slip		
88.5	Comp		Slip			Slip				Slip				Slip		
93.5	Comp		Slip			Slip				Slip				Slip		
98.5	Comp		Slip			Slip				Slip				Slip		
103.5				Slip			Slip				Slip					
108.5							Slip				Slip					
113.5											Slip					
118.5											Slip					

Table 3.11 - U54 with 4% Transverse Superelevation

Interior Beams														Long. Slope	0	Trans. Slope	0.04	Spans		2
														Spacing, ft						
Span, ft	16.5	16	14.5	14	13.5	12.5	12	11.5	11	10.5	10	9.5	9	8.5						
73.5	1.00		0.91			0.97				1.04				1.13						
78.5	1.04		0.95			0.97				1.05				1.14						
83.5	1.09		0.99			0.97				1.05				1.14						
88.5	1.13		1.03			0.97				1.05				1.14						
93.5	1.17		1.07			0.98				1.05				1.15						
98.5	1.21		1.11			1.00				1.06				1.15						
103.5				1.12			1.01				1.08									
108.5							1.04				1.08									
113.5											1.09									
118.5											1.09									

Interior Beams														Long. Slope	0	Trans. Slope	0.04	Spans		2
														Spacing, ft						
Span, ft	16.5	16	14.5	14	13.5	12.5	12	11.5	11	10.5	10	9.5	9	8.5						
73.5	Comp		Comp			Slip				Slip				Slip						
78.5	Comp		Comp			Slip				Slip				Slip						
83.5	Comp		Comp			Slip				Slip				Slip						
88.5	Comp		Comp			Slip				Slip				Slip						
93.5	Comp		Comp			Slip				Slip				Slip						
98.5	Comp		Comp			Comp				Slip				Slip						
103.5				Comp			Comp				Slip									
108.5							Comp				Slip									
113.5											Slip									
118.5											Slip									

Interior Beams														Long. Slope	0	Trans. Slope	0.04	Spans		3
														Spacing, ft						
Span, ft	16.5	16	14.5	14	13.5	12.5	12	11.5	11	10.5	10	9.5	9	8.5						
73.5	1.00		0.91			0.97				1.04				1.13						
78.5	1.04		0.95			0.97				1.05				1.14						
83.5	1.09		0.99			0.97				1.05				1.14						
88.5	1.13		1.03			0.97				1.05				1.14						
93.5	1.17		1.07			0.98				1.05				1.15						
98.5	1.21		1.11			1.00				1.06				1.15						
103.5				1.12			1.01				1.08									
108.5							1.04				1.08									
113.5											1.09									
118.5											1.09									

Interior Beams														Long. Slope	0	Trans. Slope	0.04	Spans		3
														Spacing, ft						
Span, ft	16.5	16	14.5	14	13.5	12.5	12	11.5	11	10.5	10	9.5	9	8.5						
73.5	Comp		Comp			Slip				Slip				Slip						
78.5	Comp		Comp			Slip				Slip				Slip						
83.5	Comp		Comp			Slip				Slip				Slip						
88.5	Comp		Comp			Slip				Slip				Slip						
93.5	Comp		Comp			Slip				Slip				Slip						
98.5	Comp		Comp			Comp				Slip				Slip						
103.5				Comp			Comp				Slip									
108.5							Comp				Slip									
113.5											Slip									
118.5											Slip									

Interior Beams															
	Long. Slope					0	Trans. Slope				0.04	Spans			4
	Spacing, ft														
Span, ft	16.5	16	14.5	14	13.5	12.5	12	11.5	11	10.5	10	9.5	9	8.5	
73.5	1.12		1.20			1.29				1.39				1.51	
78.5	1.13		1.20			1.29				1.39				1.51	
83.5	1.13		1.21			1.30				1.40				1.52	
88.5	1.13		1.21			1.30				1.40				1.52	
93.5	1.17		1.21			1.30				1.41				1.53	
98.5	1.21		1.22			1.31				1.41				1.53	
103.5				1.24			1.33				1.44				
108.5							1.33				1.44				
113.5											1.45				
118.5											1.45				

Interior Beams															
	Long. Slope					0	Trans. Slope				0.04	Spans			4
	Spacing, ft														
Span, ft	16.5	16	14.5	14	13.5	12.5	12	11.5	11	10.5	10	9.5	9	8.5	
73.5	Slip		Slip			Slip				Slip				Slip	
78.5	Slip		Slip			Slip				Slip				Slip	
83.5	Slip		Slip			Slip				Slip				Slip	
88.5	Slip		Slip			Slip				Slip				Slip	
93.5	Comp		Slip			Slip				Slip				Slip	
98.5	Comp		Slip			Slip				Slip				Slip	
103.5				Slip			Slip				Slip				
108.5							Slip				Slip				
113.5											Slip				
118.5											Slip				

Table 3.12 - U54 with 6% Transverse Superelevation

Interior Beams														
Long. Slope					0					Trans. Slope				
					0.06					Spans				
2														
Spacing, ft														
Span, ft	16.5	16	14.5	14	13.5	12.5	12	11.5	11	10.5	10	9.5	9	8.5
73.5	1.09		1.08			1.12				1.19				1.29
78.5	1.14		1.05			1.11				1.19				1.30
83.5	1.19		1.08			1.11				1.20				1.30
88.5	1.24		1.12			1.11				1.20				1.31
93.5	1.28		1.17			1.12				1.21				1.31
98.5	1.33		1.21			1.12				1.21				1.31
103.5				1.22			1.14				1.24			
108.5							1.14				1.24			
113.5											1.24			
118.5											1.24			

Interior Beams														
Long. Slope					0					Trans. Slope				
					0.06					Spans				
2														
Spacing, ft														
Span, ft	16.5	16	14.5	14	13.5	12.5	12	11.5	11	10.5	10	9.5	9	8.5
73.5	Comp		Rot			Rot				Slip				Slip
78.5	Comp		Rot			Slip				Slip				Slip
83.5	Comp		Comp			Slip				Slip				Slip
88.5	Comp		Comp			Slip				Slip				Slip
93.5	Comp		Comp			Slip				Slip				Slip
98.5	Comp		Comp			Slip				Slip				Slip
103.5				Comp			Slip				Slip			
108.5							Slip				Slip			
113.5											Slip			
118.5											Slip			

Interior Beams														
Long. Slope					0					Trans. Slope				
					0.06					Spans				
3														
Spacing, ft														
Span, ft	16.5	16	14.5	14	13.5	12.5	12	11.5	11	10.5	10	9.5	9	8.5
73.5	1.09		1.08			1.12				1.19				1.29
78.5	1.14		1.05			1.11				1.19				1.30
83.5	1.19		1.08			1.11				1.20				1.30
88.5	1.24		1.12			1.11				1.20				1.31
93.5	1.28		1.17			1.12				1.21				1.31
98.5	1.33		1.21			1.12				1.21				1.31
103.5				1.22			1.14				1.24			
108.5							1.14				1.24			
113.5											1.24			
118.5											1.24			

Interior Beams														
Long. Slope					0					Trans. Slope				
					0.06					Spans				
3														
Spacing, ft														
Span, ft	16.5	16	14.5	14	13.5	12.5	12	11.5	11	10.5	10	9.5	9	8.5
73.5	Comp		Rot			Rot				Slip				Slip
78.5	Comp		Rot			Slip				Slip				Slip
83.5	Comp		Comp			Slip				Slip				Slip
88.5	Comp		Comp			Slip				Slip				Slip
93.5	Comp		Comp			Slip				Slip				Slip
98.5	Comp		Comp			Slip				Slip				Slip
103.5				Comp			Slip				Slip			
108.5							Slip				Slip			
113.5											Slip			
118.5											Slip			

Interior Beams														
	Long. Slope						0	Trans. Slope			0.06	Spans		4
	Spacing, ft													
Span, ft	16.5	16	14.5	14	13.5	12.5	12	11.5	11	10.5	10	9.5	9	8.5
73.5	1.28		1.37			1.47				1.59				1.72
78.5	1.29		1.38			1.48				1.59				1.73
83.5	1.29		1.38			1.48				1.60				1.74
88.5	1.29		1.38			1.48				1.60				1.74
93.5	1.30		1.39			1.49				1.61				1.75
98.5	1.33		1.39			1.49				1.61				1.75
103.5				1.42			1.52				1.65			
108.5							1.53				1.65			
113.5											1.65			
118.5											1.66			

Interior Beams														
	Long. Slope						0	Trans. Slope			0.06	Spans		4
	Spacing, ft													
Span, ft	16.5	16	14.5	14	13.5	12.5	12	11.5	11	10.5	10	9.5	9	8.5
73.5	Slip		Slip			Slip				Slip				Slip
78.5	Slip		Slip			Slip				Slip				Slip
83.5	Slip		Slip			Slip				Slip				Slip
88.5	Slip		Slip			Slip				Slip				Slip
93.5	Slip		Slip			Slip				Slip				Slip
98.5	Comp		Slip			Slip				Slip				Slip
103.5				Slip			Slip				Slip			
108.5							Slip				Slip			
113.5											Slip			
118.5											Slip			

Table 3.13 - U54 with 8% Transverse Superelevation

Interior Beams														Long. Slope	0	Trans. Slope	0.08	Spans		2							
														Spacing, ft													
Span, ft	16.5	16	14.5	14	13.5	12.5	12	11.5	11	10.5	10	9.5	9	8.5													
73.5	2.10		1.99			1.92				1.88				1.87													
78.5	2.09		1.97			1.88				1.84				1.82													
83.5	2.08		1.95			1.85				1.80				1.78													
88.5	2.08		1.93			1.83				1.76				1.74													
93.5	2.08		1.92			1.81				1.74				1.70													
98.5	2.09		1.91			1.79				1.71				1.67													
103.5				1.87			1.75				1.67																
108.5							1.74				1.65																
113.5											1.64																
118.5											1.62																

Interior Beams														Long. Slope	0	Trans. Slope	0.08	Spans		2							
														Spacing, ft													
Span, ft	16.5	16	14.5	14	13.5	12.5	12	11.5	11	10.5	10	9.5	9	8.5													
73.5	Rot		Rot			Rot				Rot				Rot													
78.5	Rot		Rot			Rot				Rot				Rot													
83.5	Rot		Rot			Rot				Rot				Rot													
88.5	Rot		Rot			Rot				Rot				Rot													
93.5	Rot		Rot			Rot				Rot				Rot													
98.5	Rot		Rot			Rot				Rot				Rot													
103.5				Rot			Rot				Rot																
108.5							Rot				Rot																
113.5											Rot																
118.5											Rot																

Interior Beams														Long. Slope	0	Trans. Slope	0.08	Spans		3							
														Spacing, ft													
Span, ft	16.5	16	14.5	14	13.5	12.5	12	11.5	11	10.5	10	9.5	9	8.5													
73.5	2.10		1.99			1.92				1.88				1.87													
78.5	2.09		1.97			1.88				1.84				1.82													
83.5	2.08		1.95			1.85				1.80				1.78													
88.5	2.08		1.93			1.83				1.76				1.74													
93.5	2.08		1.92			1.81				1.74				1.70													
98.5	2.09		1.91			1.79				1.71				1.67													
103.5				1.87			1.75				1.67																
108.5							1.74				1.65																
113.5											1.64																
118.5											1.62																

Interior Beams														Long. Slope	0	Trans. Slope	0.08	Spans		3							
														Spacing, ft													
Span, ft	16.5	16	14.5	14	13.5	12.5	12	11.5	11	10.5	10	9.5	9	8.5													
73.5	Rot		Rot			Rot				Rot				Rot													
78.5	Rot		Rot			Rot				Rot				Rot													
83.5	Rot		Rot			Rot				Rot				Rot													
88.5	Rot		Rot			Rot				Rot				Rot													
93.5	Rot		Rot			Rot				Rot				Rot													
98.5	Rot		Rot			Rot				Rot				Rot													
103.5				Rot			Rot				Rot																
108.5							Rot				Rot																
113.5											Rot																
118.5											Rot																

Interior Beams		Long. Slope					0	Trans. Slope			0.08	Spans				4
		Spacing, ft														
Span, ft	16.5	16	14.5	14	13.5	12.5	12	11.5	11	10.5	10	9.5	9	8.5		
73.5	2.10		1.99			1.92				1.88				2.01		
78.5	2.09		1.97			1.88				1.86				2.02		
83.5	2.08		1.95			1.85				1.86				2.03		
88.5	2.08		1.93			1.83				1.87				2.03		
93.5	2.08		1.92			1.81				1.88				2.04		
98.5	2.09		1.91			1.79				1.88				2.04		
103.5				1.87			1.78				1.92					
108.5							1.78				1.93					
113.5											1.93					
118.5											1.93					

Interior Beams		Long. Slope					0	Trans. Slope			0.08	Spans				4
		Spacing, ft														
Span, ft	16.5	16	14.5	14	13.5	12.5	12	11.5	11	10.5	10	9.5	9	8.5		
73.5	Rot		Rot			Rot				Rot				Slip		
78.5	Rot		Rot			Rot				Slip				Slip		
83.5	Rot		Rot			Rot				Slip				Slip		
88.5	Rot		Rot			Rot				Slip				Slip		
93.5	Rot		Rot			Rot				Slip				Slip		
98.5	Rot		Rot			Rot				Slip				Slip		
103.5				Rot			Slip				Slip					
108.5							Slip				Slip					
113.5											Slip					
118.5											Slip					

### 3.5.1. Discussion of Summarized Design States

Tables 3.4 and 3.9 show that for longitudinal and transverse slopes of 0% and 2-span units that all limit states are OK for the current TxDOT modified LRFD provisions for the standard bearing for both the U-40 and U-54 members. This indicates that the standard bearing is appropriate for this type of condition. In these two tables, as the number of spans in the unit increases from 2 to 3 to 4, some limit states begin to produce ratios greater than 1.0. For both the U-40 and U-54 members, the Anchorage Slip and Shear Strain checks produce limit state ratios above 1.0.

Table 3.6 shows the results for the U-40 specimens with a transverse slope of 4%. For this condition, all of the limit states are green for the 2-span units. For the 3-span units, only four of the 24 limit states are red. For the 4-span units, 21 of the 24 limit states are red. Increasing the transverse slope to 6%, as shown in Table 3.7, causes 8 out of the 24 limit states for the 2 span units to change from green to yellow. For the 3-span units, the number of red limit states increases from four to 13. For the 4-span units, all 24 limit states become red. An overview of the tables suggests that as the transverse slope increases from 4% to 6% causes a majority of the limit states to begin to exceed 1.0.

Likewise, for the U-54 specimens, as the transverse slope increases above 4%, a majority of the limit states begin to go above 1.0. At 2% transverse slope in Table 3.10, considering all span arrangements (2-span, 3-span, and 4-span units) only 12 out of 111 states are red. Increasing to 4% transverse slope in Table 3.11 causes the number of red limit states to increase from 12 to 24. A further increase to 6% transverse slope as shown in Table 3.12 cause the number of red limit states to increase from 24 to 53.

For an 8% transverse slope, Table 3.8 shows that for the U-40 beams, all span unit arrangements, all 72 limit states are either yellow or red. Fifty-seven of the 72 total limit states are red, the remaining 15 are yellow. For the U-54 beams at an 8% transverse slope, all 111 of the limit states are red. This suggests that for both U-40 and U-54 beams, an 8% transverse slope should not be considered.

## **4. OBSERVATIONS AND TESTING**

After inspecting both bridge systems in Wichita Falls and Lubbock, Texas, TechMRT designed an experiment to investigate the effects of transverse superelevation on a uniform-height steel-reinforced elastomeric bearing. The tests allowed for loads to be applied in vertical, longitudinal, and transverse directions. This section details the tests performed, the procedures used, and the results of the experiments.

### **4.1. Overview of Tests Performed**

Two separate field test series, one laboratory test series, and one analytical test series were performed to observe and confirm the effect transverse superelevation has on the performance of the standard design steel-reinforced elastomeric bearings. First, select bearings on two bridges with U-beams on a transverse superelevation in Wichita Falls, Texas were inspected and documented. This successful Wichita Falls test series led to an additional field test in Lubbock, Texas. The Lubbock field test included instrumentation of bearings prior to construction in an end span of the US 82 BOS-W Ramp Overpass at E-4<sup>th</sup> Ramp. Finally, both single and double bearing configurations were tested in the Structures Laboratory at Texas Tech University. The laboratory results were compared to a finite element analysis developed to aid in the research.

### **4.2. Wichita Falls Bridge Inspection**

The purpose of this inspection was to inspect the bearings on two bridges with significant transverse superelevations (5.3% and 6.0%). The bridges chosen were at the intersection of US Highway 281/287 and US Highway 82 in Wichita Falls, Texas. Specifically, bearings were inspected under the southbound *Mainlanes* of US Highway 281/287 (NBI No. 03243004309130) and *Alignment "C"* connecting US 281/287 South to US 82 West (NBI No. 032430004401132). The bridges were inspected on February 28, 2008. Additional information regarding the inspection is documented in a memorandum sent to John Holt dated April 17, 2008, and is included as Appendix 4-1 in this report.

#### 4.2.1. Documentation of the Inspection

Table 4.1 provides a summary of the bearings inspected. The first column shows the bearing names. The second column indicates whether the bearing was a single 32 in. by 9 in.

Table 4.1 – Location of Bearings Inspected

Bearing Name	Bearing Configuration	Bridge	Bent	Span	Beam	Station Direction	Notes
A	Single	Elevated Mainlanes	A3	2	1	Up	-
B	Single	Elevated Mainlanes	A4	3	2	Up	-
C	Single	Elevated Mainlanes	A4	3	4	Up	-
D1	Double	Elevated Mainlanes	A4	4	4	Back	To Left
D2	Double	Elevated Mainlanes	A4	4	4	Back	To Right
E	Single	Alignment 'C'	10	9	1	Up	-
F	Single	Alignment 'C'	10	9	2	Up	-
G	Double	Alignment 'C'	9	9	1	Back	To Left
H	Double	Alignment 'C'	9	9	1	Back	To Right
I	Double	Alignment 'C'	9	9	2	Back	To Left
J	Double	Alignment 'C'	9	9	2	Back	To Right
K	Single	Alignment 'C'	9	8	1	Up	-
L	Double	Alignment 'C'	8	8	1	Back	To Left
M	Double	Alignment 'C'	8	8	1	Back	To Right
N	Double	Alignment 'C'	7	7	1	Back	To Right
O	Double	Alignment 'C'	7	7	1	Back	To Left

bearing or a double 16 in. by 9 in. bearing. The third column shows where the bearings were located; bearings A through D were located on the *Mainlanes* bridge while bearings E through O were located on the *Alignment "C"* bridge. The fourth, fifth, and sixth columns show the bent, span, and beam respectively. The seventh column shows whether the inspection was looking up or back station. Finally, the last column distinguishes the double bearings.

Table 4.2 provides a summary of the data recorded for each bearing inspected. The third column "Trans. Slope" shows the measured transverse slope as a percent of the U-beam using a digital level. The fourth column "Down Side" indicates which side of the bearing is lower. The fifth and sixth columns "Trans. Angle" show the measured obtuse angle in degrees minus 90 degrees. The angles were measured using a clear plastic protractor with a radius of approximately 2 in. (see Figure 4.1). The seventh and eighth columns show the approximate height of the bearing at its left and right edges, respectively. The height shown is the "X" value

in the formula  $2+X/32$  in. Therefore, a value of 16 would indicate a bearing height of  $2 \frac{16}{32}$  in., or 2.5 in. The final column indicates whether or not there was lift-off noticed.

Table 4.2 – Summary Wichita Falls Inspection Data

Bearing	Bearing Config.	Trans. Slope, %	Down side	Left Trans. Angle, Degrees	Right Trans. Angle, Degrees	Left Height (2+x/32 inches)	Right Height (2+x/32 inches)	Lift Off Visible
A	Single	5.8	Left	18	14	15	16	Y
B	Single	3.7	Left	12	9	13	16	N
C	Single	3	Left	20	20	17	12	Y
D1	Double	1	Right	10	10	12	12	N
D2	Double	1	Right	10	10	16	14	N
E	Single	6.1	Left	15	10	14	18	N
F	Single	5.2	Left	15	14	17	18	Y
G	Double	6.4	Right	10	10	19	14	Y
H	Double	6.4	Right	13	15	16	14	Y
I	Double	5.3	Right	18	20	17	15	Y
J	Double	5.3	Right	15	15	14	15	Y
K	Single	6.6	Left	15	10	13	15	Y
L	Double	6.2	Right	9	10	17	18	Y
M	Double	6.2	Right	10	10	17	18	Y
N	Double	5.3	Right	7	6	15	14	N
O	Double	5.3	Right	6	9	16	18	N

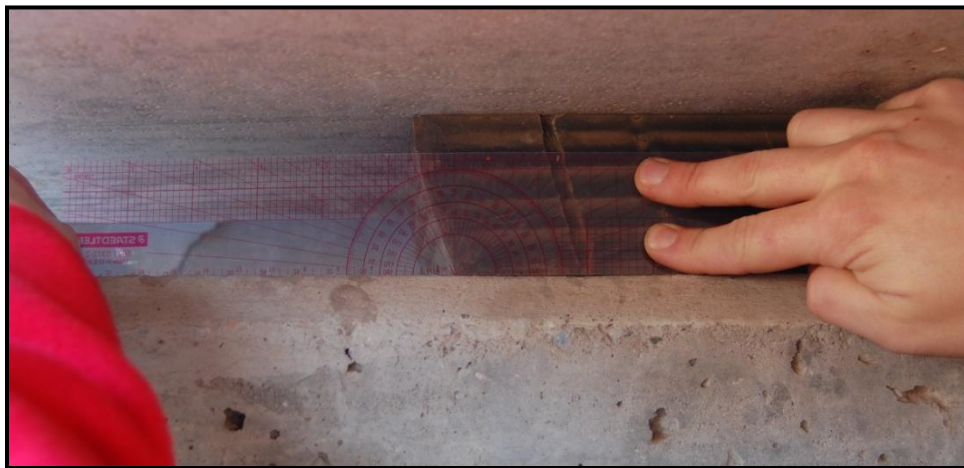


Figure 4.1 – Protractor used to Measure Transverse Angles

Figure 4.2 shows an elevation view of a typical bearing, “Bearing A”, the first bearing in Tables 1 and 2. Note the angled slope to the left and right ends of approximately 18 and 14

degrees, respectively. Figure 4.3 shows a close-up of the left side of “Bearing C” which displays a measured transverse angle of 20 degrees. Note how the edge does display a double curvature



Figure 4.2 – Elevation of Bearing A



Figure 4.3 – Close-up of Bearing C

caused by the friction between the bearing surface and the U-beam to the top and the pier cap to the bottom.

In order to prevent the superstructure from translating downhill due to the superelevation, the *Alignment 'C'* bridge had shear keys detailed as shown in Figure 4.4. This detail was taken from sheet 420 of the plans. On the up-slope side of the detail, the U-beam had pressed against the shear key and had caused minor spalling on the key in some locations. On the down-slope

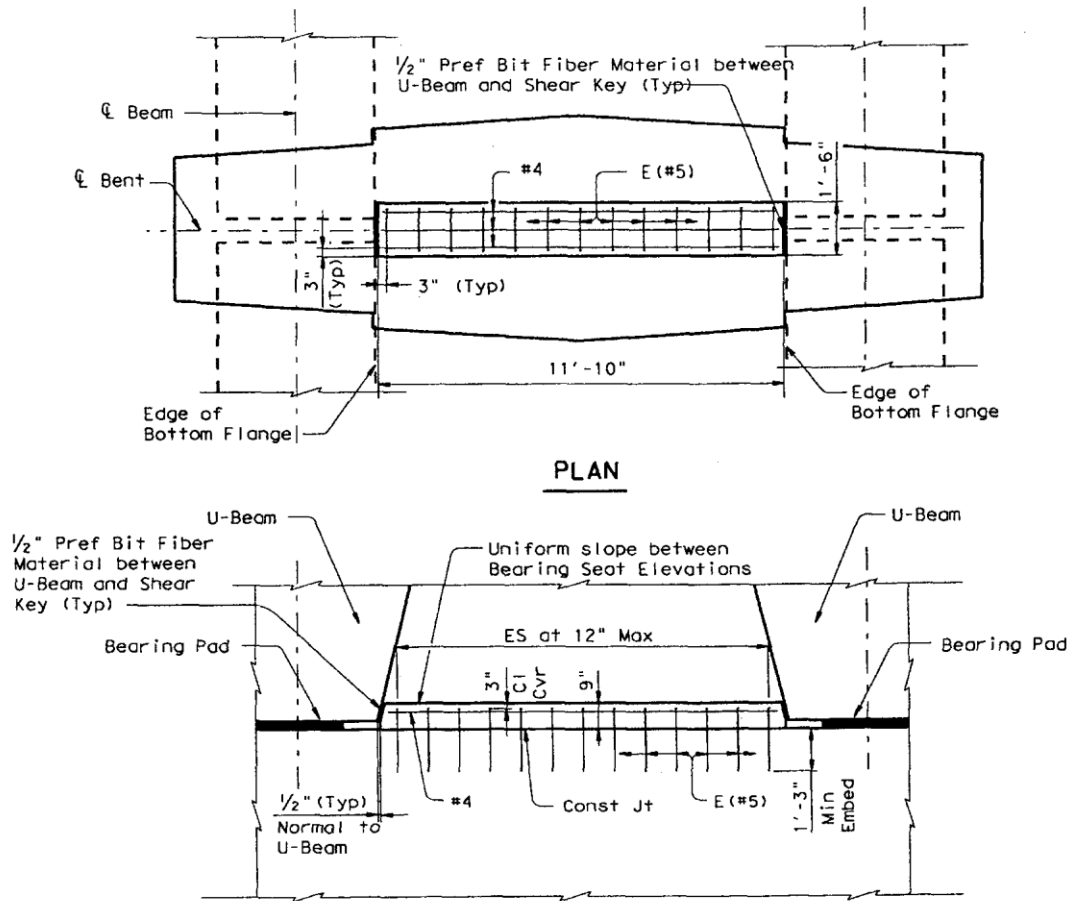


Figure 4.4 – Section thru Shear Key for Alignment 'C'

side of the detail, a slight gap was noticed in some places, indicating that the superstructure had moved in the down-slope direction.

It was also noted that the entire superstructure was pivoting about the upslope edge of the shear key in places. As large vehicles passed overhead, the superstructure would pivot about the upslope edge of the shear key, causing the down-slope bearing to compress up and down. The bearing could be heard to “squeak” as the traffic went overhead. The magnitude of the compression was enough to notice the sound even from the ground level.

#### 4.2.2. Comparison to Predicted Values

Table 4.3 shows predicted transverse angles in degrees for randomly selected locations throughout the two bridges. The predicted angles were determined for both a design minimum and maximum dead load using the provisions outlined in sections 3.2 through 3.4. Since full

Table 4.3 – Predicted Transverse Deflections for Select Locations

Bridge	Bent	Span	Beam	Long. Slope	Trans. Slope	Beam	Min Delta, Degrees	Max Delta, Degrees
Elevated Mainlanes	A3	2	1	0.69%	5.3%	Interior	12.6	14.1
Elevated Mainlanes	A3	2	2	0.69%	5.3%	Exterior	11.2	12.4
Elevated Mainlanes	A4	3	4	0.69%	5.3%	Interior	11.4	12.6
Elevated Mainlanes	A4	3	4	0.69%	5.3%	Exterior	11.0	12.1
Alignment 'C'	7,8,9	8,9	1	0.62%	6.0%	Exterior	12.1	13.6

plans were not available, TechMRT had to estimate some input values. The inverse tangent of the deflection was used to determine the angle resulting from the transverse deflection.

As shown in Table 4.3 and Table 4.2, the predicted values were similar in magnitude to the observed values. Some of the single bearings inspected displayed transverse angles greater than the angles predicted while some of the double bearings inspected displayed angles less than the angles predicted. The average transverse angle for all single bearings was 14.3 degrees and the average transverse angle for all the single bearings was 11.3 degrees. Theoretically, the transverse deflection produced by a load at the top of the bearing would be the same for either a standard single or double bearing configuration if the effect of the transverse moment is ignored. This is true since half of the transverse loading to a single bearing would be divided between each of the two double bearings and each of the double bearings is half the size of the single bearing. However, since the double bearing configuration has a higher moment of inertia it should be able to better resist the effect of the transverse moment.

#### 4.2.3. Summary of the Wichita Falls Inspection

Overall, the inspection confirmed the fact that U-beams placed on significant transverse superelevations (5.3% and 6.0%) with standard uniform-height elastomeric bearings do cause the bearings to shear significantly in the transverse direction. Specific observations include:

1. The average transverse slope for the single bearings was 14.3° and the average transverse slope for the double bearings was 11.3°, both in the down-slope direction.
2. All bearings inspected under U-beams with a significant transverse superelevation displayed a transverse displacement. This supports the presence of the proposed “Delta1” displacement.
3. Some bearings inspected under U-beams with a significant transverse superelevation displayed evidence of a transverse moment, with uplift on the upslope side. This supports the presence of the proposed “Delta2” displacement.
4. Using a protractor cut to a 2 in. height worked well for measuring transverse slopes of the bearings. The transverse slopes were generally not straight lines; however, the angle at the top of the protractor where the measurement was made was usually in a straight line portion of the profile.
5. Measuring the height of a bearing proved to be difficult because of the intentional roughness of the bearing seats.
6. The presence of the shear key detail did not prevent the transverse displacement of the top of the bearings. Also, damage did occur where the U-beams rested against the shear keys. The unusual phenomena of the bridge superstructure pivoting about the shear key could lead to premature damage to the bearing pads.

#### **4.3. US 82 Bos-W Ramp Overpass at East 4th Street in Lubbock, Texas Field Test**

The purpose of this field test was twofold : (1) to visually confirm the effect of transverse superelevation on standard bearings and (2) to test the ability to perform long-term monitoring of strains using strain gages. To accomplish these objectives, TechMRT, with the assistance of personnel from TxDOT and Granite Construction, located a bridge that would be constructed during the duration of the research project to observe the response of the bearings to transverse superelevation throughout the construction process. TechMRT was given permission to place strain gages on three bearings prior to the placement of the U-beams and was granted periodic access to visually inspect and electronically monitor the change in strain in the bearings. In the following section, data are presented from prior to placing the U-beams until after the placement of the deck.

#### 4.3.1. Testing Program Overview

The US 82 Bos-W Ramp Overpass at E-4th Ramp at the location investigated was constructed of three U-54 beams placed at a 3.8% transverse superelevation supporting a 38 foot wide deck. The three bearings for the 87.59 ft long beam marked U54-1 in Span 1 were gaged. Figure 4.5 and Figure 4.6 show details of the bridge. Beam U54-1 was in Span 1 which connected Bent 2 to Abutment 1 as traffic flowed over the bridge east to west. The Abutment 1 end of the beam (west side) was supported by two 9-in. by 16-in. elastomeric bearings and the bottom of the U54 Section rested on the bearings. The Bent 2 end of the beam (east side) was supported by a single 9-in. by 32-in. elastomeric bearing. The nominal thickness of the bearings was 2 ½ in. The bearings were tapered to account for the beam's longitudinal slope. The upslope side of the bearing was 2 ¾ in. thick while the down slope side of the bearing was 2 3/8 in. thick. The U-beam was dapped at the east end in order to allow the bottom of the U54 section to lie at the same elevation as the bottom of the bent cap. This dapped end detail made inspection of the single bearing difficult.

Prior to placement of the U-beams, TechMRT obtained the three bearings for beam U54-1 and placed a total of 14 rectangular rosette gages (42 individual gages) on the exterior front and rear faces of the bearings; see Figure 4.7 and Figure 4.8. On the smaller bearings, a strain rosette was placed near the corners of each bearing pad on both the front and rear faces. For the large bearing pad, six gages were placed on the bearing, one at each of the 4 corners and one near the center of the front and rear face of the bearing pad. See Appendix 4-2 for specific information regarding the installation and location of the strain gages.

Since large strains were expected, a high-elongation polyimide backing was chosen for the strain gages. The gages were also applied with an epoxy capable of withstanding high strains. A bondable terminal was applied in order that 26 AWG 3-conductor cable could be attached to each gage individually. An RJ45 connector was attached to the end of each conductor cable. Each rosette was applied so that the number 1 gage was in the horizontal direction, the number 2 gage was at a 45 degree angle, and the number 3 gage was in the vertical direction. An electrically-neutral protective coating was applied to the gages for protection. The coating system consisted of Vishay Micro-Measurements M-coat F-kit and an additional protective rubber pad for physical protection. The RJ45 connectors were also protected by placing them in a plastic bag.





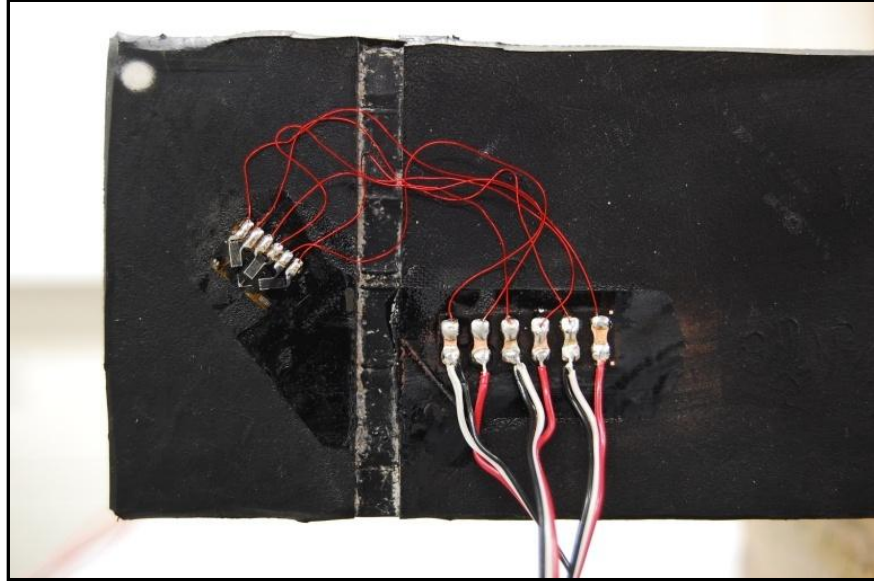


Figure 4.7 – Rosette Strain Gage (left) and Bondable Terminal (right)

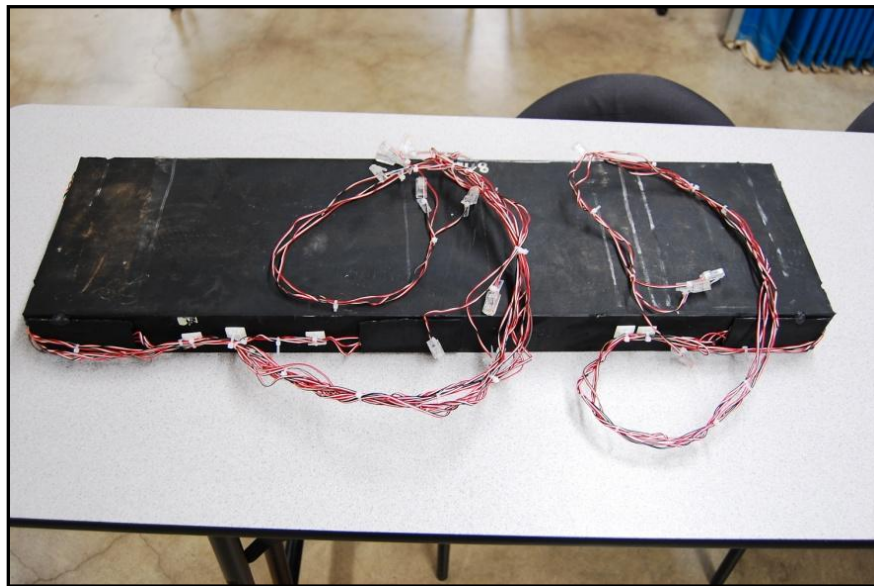


Figure 4.8 – Fully Gaged Single Bearing

The strains were recorded with a Vishay P3 Strain Indicator and Recorder capable of reading strains with an accuracy of 1 microstrain. The P3 has a range of +/- 30,000 microstrains (or 3% strain) for the gage factor of 2.06 used. The P3 has four channels, three of which were used for the three gages in each rosette. The fourth channel was used to record a precision resistor wired so that it could be read as a quarter bridge, similar to the strain gages. The

automatic balance on all four channels was turned off allowing actual strain readings. Any change in the precision resistor over time would indicate that drift had occurred.

#### 4.3.2. Testing Performed

On May 22, 2008, initial readings were taken for the three bearings in an unloaded state. To accomplish this, TechMRT placed the three bearings on a slope matching the slope in the field and recorded the three gages for each rosette and the precision resistor for each rosette. The bearings were returned to the contractor for installation. The U-beam was placed on the bearing the following day, May 23, 2008. The first set of data was recorded at approximately 10:00 AM. All gages A through H were recorded for the double bearings; however, due to the dapped end detail and the fact that a lift was not available, only gages L and O were recorded for the single bearing. A visual inspection took place for the double bearings.

Five days later, on May 28, 2008, readings were recorded for all gages. Of the 42 individual gages installed, readings were obtained for 41 of the gages, an over 97% survival rate. Additional readings were obtained as shown in Table 4.4.

Table 4.4 – Tests Performed for US 82 BOS-W Ramp Overpass

Description of Test	Test No.	Date	Days under loading, days
Zero Readings	0	Thursday, May 22, 2008	0
After Setting Beams	1	Friday, May 23, 2008	1
After Setting Beams	2	Wednesday, May 28, 2008	6
After Setting Beams	3	Friday, July 25, 2008	64
After Setting Beams	4	Tuesday, September 09, 2008	110
After Setting Beams and Deck	5	Thursday, September 25, 2009	126
After Setting Beams and Deck	6	Tuesday, October 28, 2008	159

#### 4.3.3. Results - Visual Observations

The procedure for the visual inspections of the bearings was similar to that used for the Wichita Falls Inspection previously detailed. The initial inspection, Test No. 1, which took place immediately after setting the U-beams, revealed transverse angles of 5, 5, 4, and 5 degrees for the four sides of the double bearings. Using the proposed modified equations presented in Section 3 that include the Delta1 and Delta2 effects, the predicted transverse angle was 4.39

degrees. Therefore, the observed matched the predicted well. The calculations for the predicted transverse angle are provided in Appendix 4-2 of this report.

#### 4.3.4. Results - Strain Gage Readings

Even though a great deal of precaution was taken to ensure reliable readings, the long-term strain data provided inconclusive results at best. A checklist was used to ensure that the settings on the P3 strain indicator were set properly prior to each set of readings. Also, the precision resistor was recorded on the fourth channel each time the three gages at each location were recorded. For tests up to test number six which occurred at an age of 160 days, the precision resistor varied only 17 microstrains, -6 to +11 microstrains. See Figure 4.9 for the change in strain readings for the precision resistor for the double bearings. The results for the single bearing were similar.

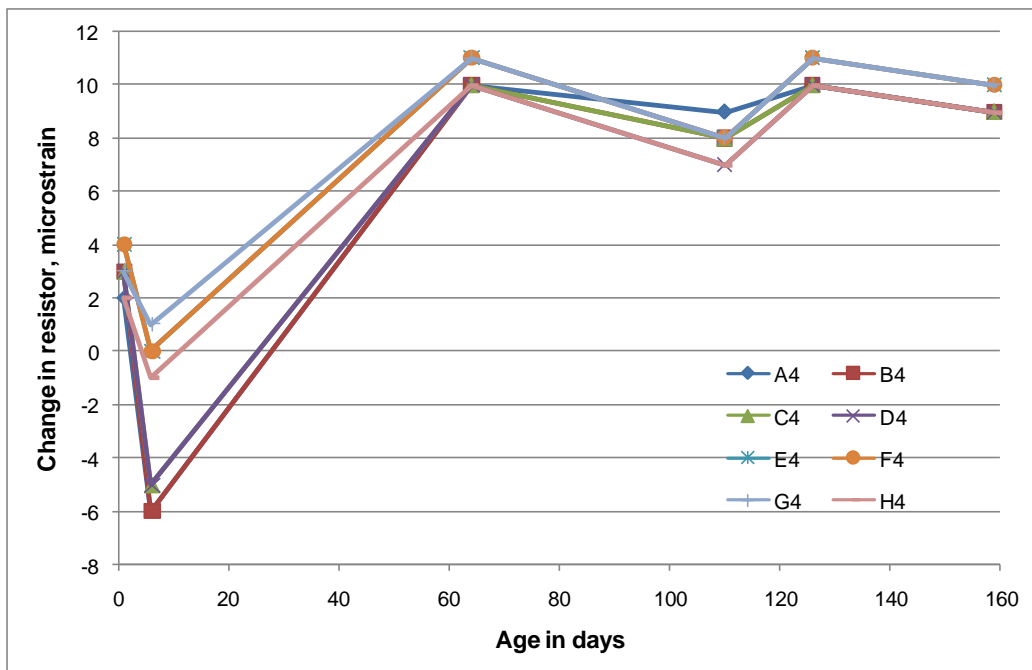


Figure 4.9 – Change in Strain for the Precision Resistor

A review of the change in strain for the vertical gages (the number 3 gages) shown in Figure 4.10 is not easy to interpret. For the tests performed immediately after setting the beams at days 1 and 6, some gages showed compressive strains (negative) while others showed tensile strains (positive). This could be explained by the fact that transverse slope does cause the

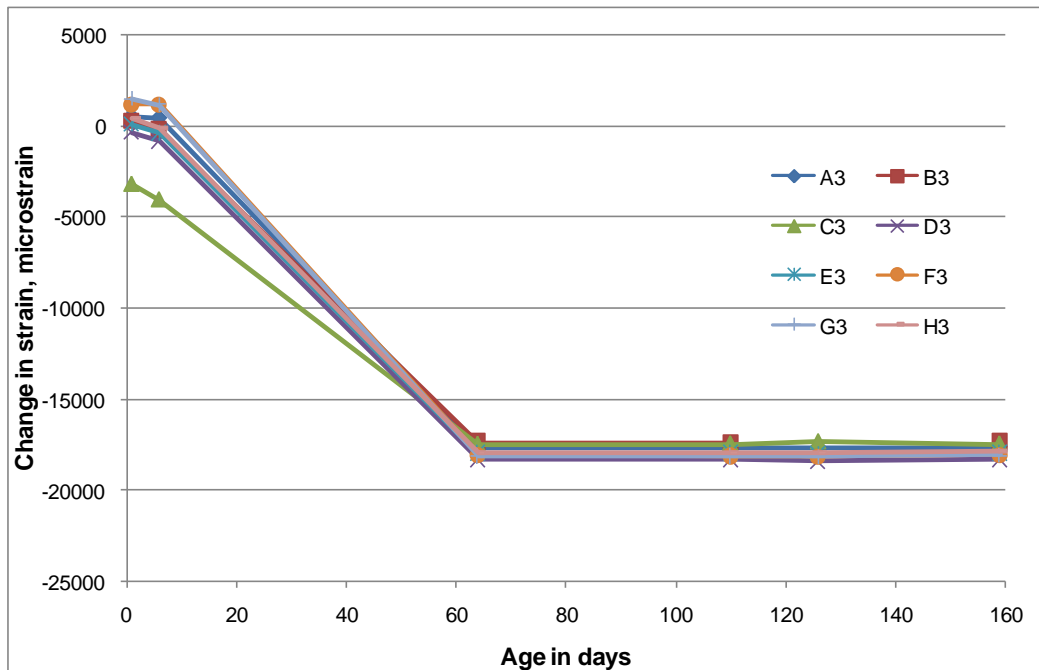


Figure 4.10 – Change in Strain for Vertical Gages on Double Bearings

centroid of the U-beams to shift and cause a transverse moment to be induced. However, it was anticipated that the combination of the transverse moment and the vertical compressive load would cause all of the gages to go into compression, with the down-slope gages in more compression than the up-slope gages.

Between the day 6 and day 64 readings, all gages began to display significant compressive strains. The behavior observed on the day 64 readings was closer to the originally anticipated behavior. But, explaining why the readings changed so significantly during the time between readings is difficult. If an error occurred in a setting on the P3, the error should have been recorded in the resistor readings. Yet, the change in resistor values remained small.

As shown in Figure 4.11, the horizontal gages (the number 1 gages) acted similarly to the vertical gages. Another interesting phenomenon took place when the deck was placed. As shown in Figure 4.9, Figure 4.10, Figure 4.11, the recorded changes in the resistor and the changes in strain did not change much due to the placement of the deck. The deck was placed between days 126 and 159. As shown in Figure 4.9, the resistors varied a maximum of only 4 microstrains from day 126 to 159. Likewise, the change in the gage readings for both the vertical and the horizontal gages varied little from day 126 to 159.

#### 4.3.5. Summary of US 82 Bos-W Ramp Overpass Tests

The visual observations helped to confirm that it is appropriate to use the proposed method outlined in Section 3 to predict transverse displacements.

The change in strain gage readings over time can most likely be attributed to the localized behavior of the outer layer of the elastomer. It is possible that, over time, creep and bulging effects caused the outer layer to bulge between the shim layers. A gage placed on the outer point of the bulge should theoretically read tension while a gage placed on the inner point of the bulge

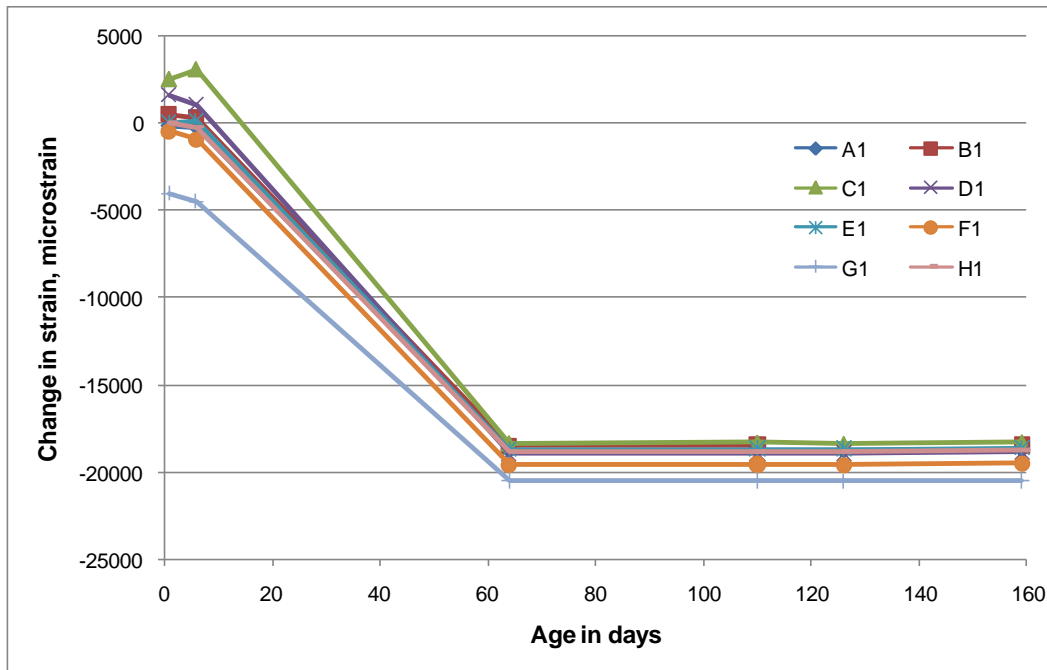


Figure 4.11 – Change in Strain for Horizontal Gages on Double Bearings

should theoretically read compression. This could help explain the behavior at later days. When the U-beams were initially set, it is possible that the center portion of the bearings carried the load and the edges were essentially unloaded for a time until creep effects allowed load redistribution.

It is also possible that the data are bad. Either the gages failed or the P3 Strain Indicator was set incorrectly. Failed gages typically provide “offscale” readings or readings that vary greatly (drift). Compared to each other, the readings were consistent and do not appear to result from failed gages. A failed P3 strain indicator would have given different readings for the precision resistor. But the resistor readings remained consistent throughout the testing with little variability.

## **4.4. Laboratory Testing**

### **4.4.1. Testing Program**

The following section provides details on the designed tests, the equipment used to conduct the experiments, the test matrix developed to simulate varying conditions, and an overview of the testing procedure. Discussion of the results follows in Chapter 5 of this report.

#### *4.4.1.1. Design of Experimental Apparatus*

The goal of the laboratory testing was to determine the significance of transverse superelevation on the performance of uniform-height steel-reinforced elastomeric bearings. U-beams are heavier than typical I-beam sections on a per-foot basis. This causes the transverse component of the end reaction to have the potential to adversely affect the standard bearings either by itself or in combination with vertical and longitudinal actions. TechMRT designed and constructed a test frame that would allow the bearings to be loaded in the vertical, transverse, and longitudinal directions simultaneously. The test frame allowed for the testing of bearings with a vertical load up to 390 kips combined with a transverse load to model superelevation varying from zero to eight percent and a longitudinal load to model design thermal expansion/contraction for the maximum span lengths anticipated.

#### *4.4.1.2. Test Frame*

The test frame was composed of three separate smaller frames as shown in Figure 4.12 on the following page, allowing for the bearing to be loaded in three directions simultaneously. The vertical load was applied by the larger orange RAM shown. The longitudinal forces were applied through the use of the smaller, yellow RAMS visible in Figure 4.13. The transverse force in the other principle direction was applied with a RAM identical to the horizontal RAMS shown in Figure 4.14. All parts of the framing system were anchored to the floor using 2.5-inch diameter anchor bolts at each corner of their respective base plates.

#### *4.4.1.3. Concrete Blocks*

The triaxial loading was applied to the test bearings using a system of three concrete blocks. The concrete blocks had dimensions of 48 in. by 28 in. by 24 in. and are displayed in Figure 4.12 and Figure 4.13. The vertical force, simulating the vertical component of the gravity



Figure 4.12 – Elevation View of Testing Frame



Figure 4.13 – Elevation View of Longitudinal Rams

loads, was applied downward to the top block, while the transverse and longitudinal forces were applied in their respective directions to the center blocks. The transverse force simulated the horizontal force resulting from the transverse superelevation while the longitudinal force simulated the temperature effects of expansion/contraction of the U-beam. Bearings placed between the top block and the center block were the test bearings while the bearings placed between the center block and the bottom block were a dummy set of bearings used to allow the



Figure 4.14 – Application of Transverse Load

center block to move freely. Identical bearings were used as the dummy bearings to allow for a symmetric loading condition.

It is important to realize that only the center block was free to move. The bottom block did not move due to friction between the block and concrete floor. The top block was held in place by three angle members preventing it from moving in the longitudinal direction. Wood blocks prevented transverse displacement of the concrete blocks.

#### 4.4.1.4. Hydraulic Cylinders

Four hydraulic cylinders were used to apply the loads to the concrete blocks and subsequently to the bearings. The vertical cylinder was a Power Team RD 500 Series Model B hydraulic cylinder. The Power Team cylinder could produce a maximum load of 1,000 kips and was loaded using a Power Team No. 9504 air compressor. The compressive RAM is shown in Figure 4.12 (large, vertically oriented cylinder). The other three cylinders were EnerPac RCH-603 hydraulic cylinders. A single EnerPac cylinder is capable of producing a maximum load of 120 kips. One cylinder was used to apply the transverse force (see Figure 4.14), while two cylinders were used to supply the longitudinal force as shown in Figure 4.13. These three cylinders were loaded using two EnerPac P-80 hand pumps, one for the transverse RAM and one that controlled both of the longitudinal RAMS. Each load was applied sequentially and

individually. First, the vertical force was applied, followed by the transverse force and then the longitudinal force.

#### 4.4.1.5. Bearings

The elastomeric bearings used in this test were supplied by Dynamic Rubber. The bearings were fabricated as standard bearings from TxDOT Sheet “UBEB – Elastomeric Bearing and Bearing Seat Details – Prestr Conc U-Beams” dated July 2006 and provided in Appendix 3-1. Figure 4.15 shows both the smaller double bearings (16-in. by 9-in. by 2.5-in.) and the larger



Figure 4.15 – Standard Single and Double Bearings

single bearings (32-in. by 9-in. by 2.5-in.). All bearings were placed in the recommended positions per TxDOT sheet UBEB. All bearings were reinforced with five layers of 0.105-in. thick steel shims.

#### 4.4.1.6. Strain Gages

One double bearings and each single bearing used for each test were fitted with ten rectangular rosette strain gages (Vishay Micro-Measurement EP-08-125RA-120). These strain gages were chosen because they had the capability of reading the largest strain values (+/- 10%) in addition to the reasons explained in section 4.3.1 of this report. The gages were affixed to the bearings according to manufacturer specifications using a high-elongation epoxy. The placement of the gages on each bearing is shown in Figure 4.16 through Figure 4.18 for the single bearing

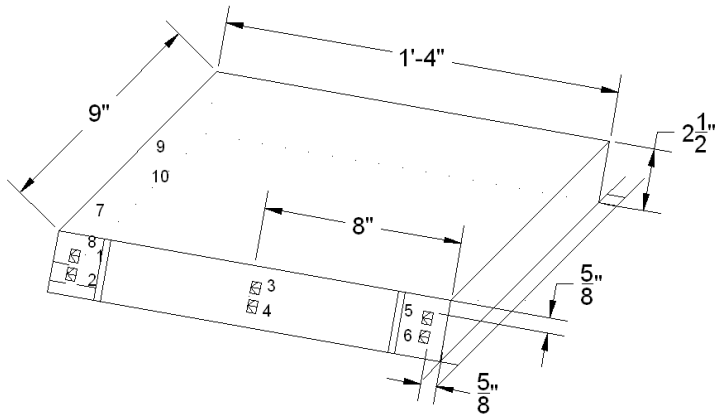


Figure 4.16 – Double Bearing Strain Gage Placement

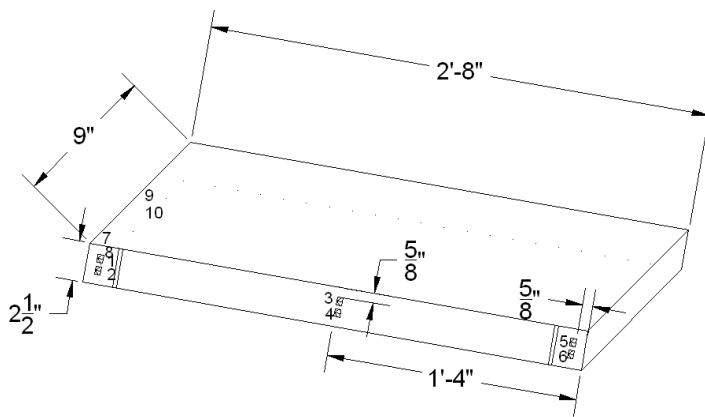


Figure 4.17 – Single Bearing Strain Gage Placement

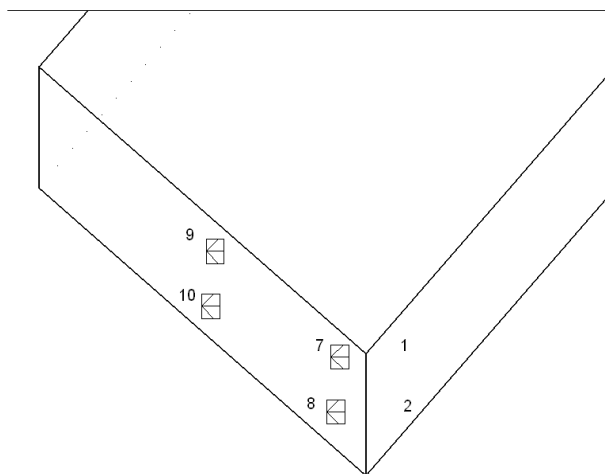


Figure 4.18 – Strain Gage Placement on Transverse Faces

and double bearing configurations, respectively. Figure 4.19 shows the gages installed on the smaller bearing. Note that each of the three individual gages in the rosette was attached to a bondable terminal with a 34 gage red wire.



Figure 4.19 – Strain Gage Installed, 32-in. by 9-in. Bearing

The strain gage data was recorded with the aid of a Vishay Micro-Measurements System 5000. The strain gages were attached to the bearings in order to get an idea of the strain profile across the faces of the bearing. Originally, strain gages 7-10 in Figure 4.18 were placed on the opposite face of the bearing for the first test (Test Series D2A); however, the location was changed since most of these gages detached due to excessive bulging on the face of the bearing.

#### 4.4.1.7. Pressure Gages

All forces were applied to the center concrete block in the transverse and longitudinal directions via RAMS as indicated in Section 0. The force was obtained by converting the pressure applied to the RAM (in psi) into its corresponding force (in kips) by multiplying the pressure by the effective cylinder area. The pressures at each RAM were obtained through two separate methods. The first was an Enerpac pressure gage connected to the hydraulic line immediately after the hand pump and the second was a Stellar Technology (ST-7500G-111) pressure transducer connected to the hydraulic line shortly after the connection for the pressure gage. Both the gage and the pressure transducer gave consistent readings before the first test was

conducted so the transducer was used as the primary indicator of the pressure in the hydraulic lines. The Enerpac pressure gages were used as a backup device in the event of a transducer failure. Periodically throughout the experiment, simple checks were completed to ensure that the transducers and pressure gages were reading the same and no disparities were noticed.

#### 4.4.1.8. *Linear Displacement Gages*

Linear displacement of the center block in the longitudinal and transverse directions was monitored via three Vishay Micro-Measurements cable extension displacement sensors, Model CDS-10, see Figure 4.20 and Figure 4.21. One sensor was used to measure the transverse displacement of the center block while two sensors were used to measure the longitudinal displacement of the center block at the center point of the double bearings.

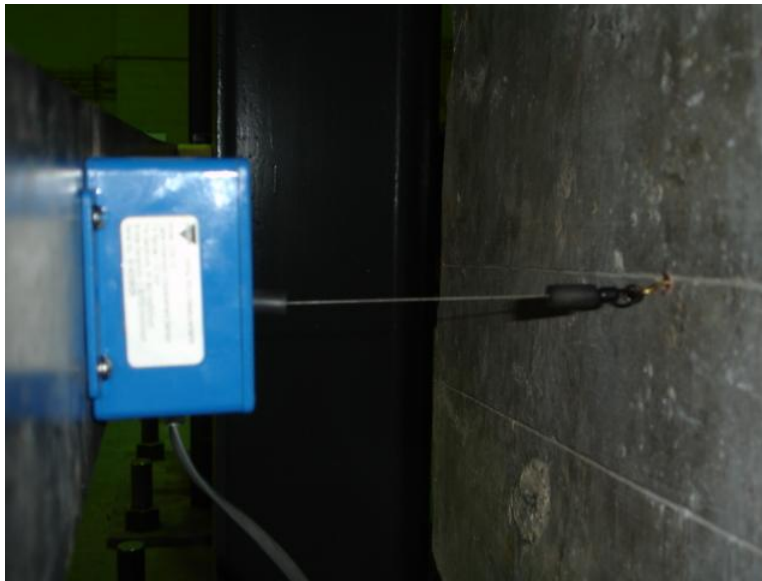


Figure 4.20 – Cable Extension Displacement Sensor – Transverse Direction

#### 4.4.1.9. *Vishay Micro-Measurements System 5000 Data Recorder*

All of the data from the linear displacement gages, strain gages, and pressure transducers was recorded using the Vishay Micro-Measurements System 5000 Data Recorder shown in Figure 4.22. Each strain gage and linear displacement gage was attached to the System 5000 through a quarter bridge connection with a strain gage card while the pressure transducers were attached to the System 5000 via a full bridge connection across a high level card. These connections are illustrated in Figure 4.23. The accompanying Strain Smart software allowed for



Figure 4.21 – Cable Extension Displacement Sensors – Longitudinal Direction

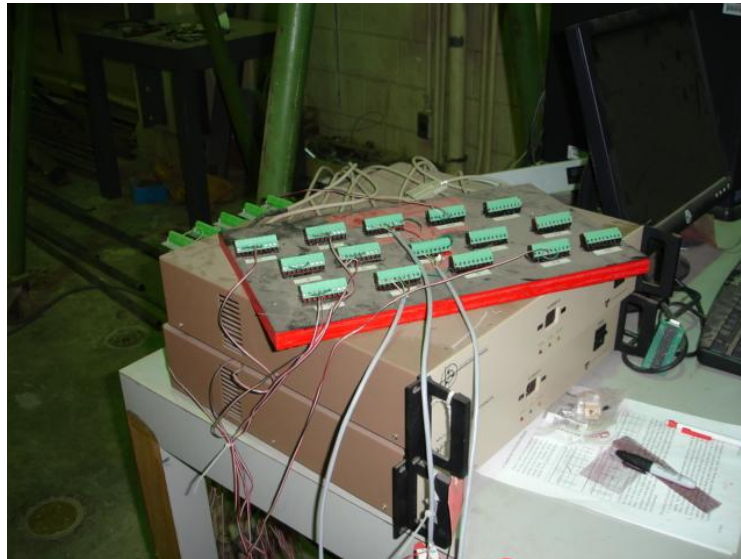


Figure 4.22 – Vishay Model 5000

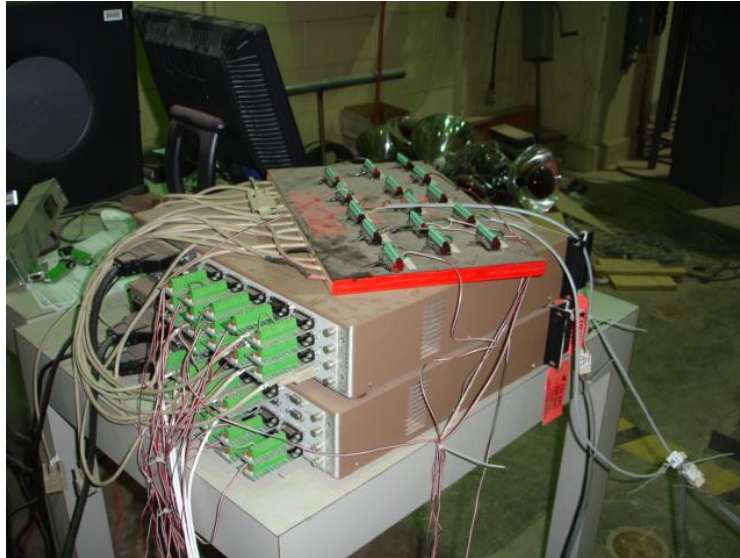


Figure 4.23 – Wiring for Vishay Model 5000

easy display and instantaneous recording of the data during each test as well as facilitating the exportation of the time history of the data for further analysis.

#### *4.4.1.10. Test Matrix and Procedure*

TechMRT originally intended to test each bearing under the worst case vertical load scenario based on a U-54 beam with maximum span length and maximum beam spacing. This vertical load was determined to be 390 kips. The thought was that this load case would produce the largest transverse force with varying superelevations and was thus the design case for the bearings. However, after analyzing the effects of the first test series, D2A, TechMRT decided that smaller loads associated with shorter span lengths, the U-40 beam, or smaller beam spacing may need to be investigated. Thus, a single test for each bearing configuration with vertical loads of 150 kips, 210 kips, 270 kips, and 330 kips were run. The entire test matrix is shown in Table 4.5. The first three columns of this table provide information about the test series including the assigned test series name, bearing pad configuration and superelevation. The fourth column shows the order in which the individual test series were run. The last columns show the number of test runs performed at each vertical load increment within the test series.

Table 4.5 – Laboratory Test Matrix

Test Series	Bearing Configuration	Superelevation, percentage	Order of Completion	Compressive Load in Kips Applied by Test Number				
				1-10	11	12	13	14
D0A	Double	0	4	390	330	270	210	150
D2A	Double	2	1	390	330	270	210	150
D4A	Double	4	2	390	330	270	210	150
D6A	Double	6	3	390	330	270	210	150
D8A	Double	8	5	390	330	270	210	150
S0A	Single	0	10	390	330	270	210	150
S2A	Single	2	9	390	330	270	210	150
S4A	Single	4	8	390	330	270	210	150
S6A	Single	6	7	390	330	270	210	150
S8A	Single	8	6	390	330	270	210	150

Tests were conducted on both the single bearing and double bearing configurations with vertical loads ranging from 150 kips to 390 kips and superelevations of 0%, 2%, 4%, 6%, and 8%. Ten tests were performed with a vertical load of 390 kips to show that the procedure and subsequent results were repeatable. The 390 kip vertical load tests are designated test cycles one through ten while the 330 kip, 270 kip, 210 kip, and 150 kip vertical load tests are designated test cycles eleven, twelve, thirteen, and fourteen, respectively. Since TechMRT observed evidence of serviceability failures of the bearings with superelevations of 6% and 8% after a few tests at the 390 kip load, the tests at this level were halted after 4 cycles in each of these cases. This will be explained in greater detail in the Chapter 5 of this report.

#### 4.4.1.11. Simulation of Forces

The testing procedure is shown in Table 4.6. Three forces were simultaneously applied to the bearings in order to conduct the designed experiment. First, a vertical force was applied to induce the vertical load on the bearing. While the vertical force remained, a transverse force simulating the horizontal force caused by the superelevation was applied. Next, while both the vertical and the transverse loads were maintained, a longitudinal force simulating the effect of the temperature (expansion/contraction) of the beam was applied.

Table 4.6 – Summary of Testing Procedure

Step	Action	Manual Data Recorded
1	Turn On System 5000	
2	Start Recording Using Strain Smart	
3	Apply Vertical Load to desired amount (1000 psi = 100 kips)	
4	Measure Initial Bearing Angles	Transverse and Longitudinal Angles
5	Measure Initial Slip based on Reference Lines	Measure transverse and longitudinal slip versus reference lines
6	Apply Transverse Load	Measure Transverse Force and slip at pre-determined deflection points
7	Measure Bearing Angles	Transverse and Longitudinal Angles
8	Measure Slip based on Reference Lines	Measure transverse and longitudinal slip versus reference lines
9	Apply Longitudinal Loads	Measure Longitudinal Force and slip at pre-determined deflection points
10	Measure Bearing Angles	Transverse and Longitudinal Angles
11	Measure Slip based on Reference Lines	Measure transverse and longitudinal slip versus reference lines
12	Release Longitudinal Load	
13	Measure Bearing Angles	Transverse and Longitudinal Angles
14	Measure Slip based on Reference Lines	Measure transverse and longitudinal slip versus reference lines
15	Release Transverse Load	
16	Measure Bearing Angles	Transverse and Longitudinal Angles
17	Measure Slip based on Reference Lines	Measure transverse and longitudinal slip versus reference lines
18	Release Vertical Load	
19	Measure Bearing Angles	Transverse and Longitudinal Angles
20	Measure Slip based on Reference Lines	Measure transverse and longitudinal slip versus reference lines

To apply the transverse force, the idea of superelevating the concrete blocks was investigated. However, TechMRT determined that this idea was not cost effective. Instead of inclining the blocks, the expected deflection at the top corner of the bearing was calculated and the center block was moved this distance to simulate the transverse movement resulting from the superelevation of the bearing.

The same method was applied with the application of the longitudinal force to the bearings. TechMRT determined that the maximum displacement would be 1.20 in. for the maximum span length, so the center block was pushed in the longitudinal direction until it had moved 1.20 in.

#### 4.4.1.12. Data Recorded

The goal of the laboratory tests was to systematically apply the three forces to the test bearings while recording pertinent information about the behavior of the bearing as the test runs were conducted. The time history of the applied forces versus the displacement of the bearing and the corresponding strains were measured continuously at one second intervals via the Vishay System 5000. Other data was recorded manually during the experiment. An example of the data sheet used to manually record additional data is shown in Figure 4.24 (for the 2% simulation). This is illustrated by the fact that the transverse forces were recorded when the transverse delta reached 0, 0.15, 0.3, and 0.45 inches. The transverse delta increments varied with the superelevation; however, data was recorded in the same manner. First, the incremental forces required to cause fixed displacements were obtained as the transverse and longitudinal forces

were applied. Second, the transverse and longitudinal angles of the displaced bearings were obtained. Finally, the bearings were inspected for damage or other noticeable conditions once the full vertical, transverse, and longitudinal loads were applied.

#### 4.4.2. **Single Pad Test Results**

As indicated in section 4.4.1, TechMRT recorded a large amount of data for each test run conducted. Data recorded included the transverse and longitudinal shear displacements, slip of the bearing, lift-off, forces required to simulate the transverse and longitudinal loads, and any damage noted while inspecting the bearings. Table 4.7 and Table 4.8 summarize the displacement for each test run. The first three columns of these tables identify the test series, superelevation, and test run of the experiment. Columns four through seven provide the transverse and longitudinal angles recorded once the full tri-axial loading state was reached. Columns eight through ten list the bearing slip measured. Columns 11 through 14 show the bearing lift-off recorded while the last column lists any damage noted for each test run. Table 4.9 and Table 4.10 summarize the forces required to simulate the loading conditions for each test run of the single pad configuration. The first column provides the test series while the second and third columns provide the test run number and corresponding compressive force applied. The fourth column lists the measured transverse force applied to achieve the simulated superelevation while the last two columns provide the measured longitudinal forces applied to the center block.

LABORATORY BEARING HARD COPY DATA INFORMATION

Configuration:                      Double                      Single                      2%                      4%                      6%                      8%                      10%

Transverse Slope:                      0%

Date:                      Time:

Test Sequence:

Scan #:

Vertical Pressure:                      psi

**Transverse Data Information**

Initial Transverse Angle:                      L (Degrees)                      R (degrees)

Initial Transverse Delta:                      Inches

**Longitudinal Data Information**

Initial Longitudinal Angle (No Transverse):                      F (Degrees)                      B (degrees)

Initial Longitudinal Angle With Transverse:

Delta (in)	Transverse		Transverse Slip		Longitudinal		Longitudinal		Longitudinal	
	Pressure (psi)	Slip Left (in)	Slip Right (in)	Right (in)	Slip (in)	Pressure East (psi)	Pressure West (psi)	Pressure Pump (psi)	Slip Left (in)	Slip Right (in)
0.00										
0.15										
0.30										
0.45										
Inches Lutoff T-Top (transverse only)										

Evidence of Lutoff or Damage (Remark and Note Distance):

FI Transverse Angle (No Longitudinal): Transverse Angle With Longitudinal Force:	L (Degrees)	R (degrees)	F (Degrees)	B (degrees)
Transverse Angle After Release of Long Force: Transverse Angle After Release of Transverse:				
			Final Longitudinal Angle With Transverse (Degrees):	
			Final Longitudinal Angle After release of Long (Degrees):	
			Final Longitudinal Angle After Release of Transverse (Deg):	

Figure 4.24 – Example of Manual Data Recording Sheet

Table 4.7—Single Pad Displacement and Damage Recorded: 0% and 2% Slopes

Test Series	Transverse Slope (%)	Test Run	Transverse Angles (Degrees)		Longitudinal Angle (Degrees)		Slip (inches)				Lift - Off (inches)				Damage Noted
			Left	Right	Front	Back	Transverse		Longitudinal	Transverse		Longitudinal			
							Front	Back		Top	Bottom		Top	Bottom	
S0A	0	1	0	0	14	14	0	0	0	0	0	1.8	0.4	None	
S0A	0	2	0	0	15	15	0	0	0	0	0	1.7	0.4	None	
S0A	0	3	0	0	15	14	0	0	0	0	0	1.8	0.5	None	
S0A	0	4	0	0	15	14	0	0	0	0	0	1.9	0.4	Hairline Cracking	
S0A	0	5	0	0	16	15	0	0	0	0	0	1.9	0.4	Hairline Cracking	
S0A	0	6	0	0	16	15	0	0	0	0	0	1.9	0.4	Hairline Cracking	
S0A	0	7	0	0	16	15	0	0	0	0	0	1.9	0.4	Hairline Cracking	
S0A	0	8	0	0	17	16	0	0	0	0	0	1.9	0.4	Hairline Cracking	
S0A	0	9	0	0	16	15	0	0	0	0	0	1.7	0.4	Hairline Cracking	
S0A	0	10	0	0	16	16	0	0	0	0	0	1.8	0.4	Hairline Cracking	
S0A	0	11	0	0	5	5	0	0	0	0	0	2.5	1	Hairline Cracking	
S0A	0	12	0	0	10	10	0	0	0	0	0	2.3	0.5	Hairline Cracking	
S0A	0	13	0	0	12	14	0	0	0	0	0	2	0.5	Hairline Cracking	
S0A	0	14	0	0	13	13	0	0	0	0	0	1.8	0.4	Hairline Cracking	
S2A	2	1	5	5	13	12	0	0	0	0	0	0	0.5	None	
S2A	2	2	4	5	13	12	0	0	0	0	0	0	0	None	
S2A	2	3	4	5	13	12	0	0	0	0	0.3	0	0.7	None	
S2A	2	4	5	5	13	12	0	0	0	0	0.3	0	0.7	None	
S2A	2	5	5	5	13	12	0	0	0	0	0.3	0	0.6	None	
S2A	2	6	5	5	15	13	0	0	0	0	0.3	0	0.7	Hairline Cracking	
S2A	2	7	5	4	15	13	0	0	0	0	0.3	0	0.6	Hairline Cracking	
S2A	2	8	5	5	15	12	0	0	0	0	0.3	0	0.6	Hairline Cracking	
S2A	2	9	5	5	12	8	0	0	0	0	0.3	0	0.6	Hairline Cracking	
S2A	2	10	4	4	12	10	0	0	0	0	0.3	0	0.6	Hairline Cracking	
S2A	2	11	3	3	10	9	0	0	0	0	0.5	0	1	Hairline Cracking	
S2A	2	12	3	4	10	10	0	0	0	0	0.4	0	0.9	Hairline Cracking	
S2A	2	13	5	5	10	11	0	0	0	0	0.3	0	1	Hairline Cracking	
S2A	2	14	4	5	10	11	0	0	0	0	0.3	0	0.7	Hairline Cracking	

Table 4.8—Single Pad Displacement and Damage Recorded: 4%, 6% and 8% Slopes

Test Series	Transverse Slope (%)	Test Run	Transverse Angles (Degrees)		Longitudinal Angle (Degrees)		Slip (inches)				Lift - Off (inches)				Damage Noted
			Left	Right	Front	Back	Transverse		Longitudinal	Transverse		Longitudinal			
							Front	Back		Top	Bottom	Top	Bottom		
S4A	4	1	10	8	12	14	0	0	0	1.2	0.5	0	0.6	None	
S4A	4	2	8	8	13	13	0	0	0	0.9	0.5	0	0.6	None	
S4A	4	3	8	8	14	13	0	0	0	0.9	0.4	0	0.5	Hairline Cracking	
S4A	4	4	10	10	12	12	0	0	0	0.9	0.5	0	0.4	Hairline Cracking	
S4A	4	5	9	8	13	11	0	0	0	0.8	0.5	0	0.5	Hairline Cracking	
S4A	4	6	8	8	15	12	0	0	0	1	0.5	0	0.6	Hairline Cracking	
S4A	4	7	8	7	12	10	0	0	0	0.7	0.4	0	0.4	Hairline Cracking	
S4A	4	8	8	10	16	15	0	0	0	0.7	0.4	0	0.6	Heavy Cracking	
S4A	4	9	10	11	18	16	0	0	0	0.7	0.4	0	0.6	Heavy Cracking	
S4A	4	10	10	10	18	17	0	0	0	0.8	0.4	0	0.5	Heavy Cracking	
S4A	4	11	5	5	10	10	0	0	0	1.2	0.5	0	0.9	Heavy Cracking	
S4A	4	12	6	5	11	10	0	0	0	1	0.5	0	0.9	Heavy Cracking	
S4A	4	13	7	5	10	12	0	0	0	0.8	0.5	0	0.6	Heavy Cracking	
S4A	4	14	9	7	12	12	0	0	0	0.7	0.4	0	0.4	Heavy Cracking	
S6A	6	1	14	14	14	17	0	0	0.2	0.6	0.4	0	0	Hairline Cracking	
S6A	6	2	15	12	14	18	0.9	0.7	0.4	0.3	0.4	0.4	0	Hairline Cracking	
S6A	6	3	15	13	15	18	0.4	0.5	0.3	1	0.3	0	0	Heavy Cracking	
S6A	6	4	15	13	15	17	0.3	0.3	0.2	0.7	0.4	1	0	Heavy Cracking	
S6A	6	11	7	5	14	13	0.4	0.3	0.2	1.6	0.4	1	0	Heavy Cracking	
S6A	6	12	13	10	18	16	0.2	0.2	0.2	1	0.5	0.7	0	Heavy Cracking	
S6A	6	13	14	10	18	18	0.3	0.2	0.3	1	0.4	1.2	0	Tension Debonding	
S6A	6	14	15	13	18	17	0.1	0.2	0.3	0.6	0.4	0.9	0	Tension Debonding	
S8A	8	1	22	21	15	21	0.6	0.7	N/A	N/A	N/A	N/A	N/A	N/A	
S8A	8	2	21	20	15	21	1.3	1.3	0.6	0.3	0.5	0	0	Heavy Cracking	
S8A	8	3	25	23	15	24	1.3	1.3	0.5	0.2	0.4	0.5	0	Tension Debonding	
S8A	8	4	25	24	15	23	0.8	0.8	0.2	0.3	0.5	0.5	0	Tension Debonding	
S8A	8	11	5	8	14	14	1	1.1	0.3	1	0.3	0.5	0	Tension Debonding	
S8A	8	12	14	12	15	16	1	1.1	0.1	1	0.4	0.5	0	Tension Debonding	
S8A	8	13	16	14	15	16	1	1	0.3	0.4	0.5	0.5	0	Tension Debonding	
S8A	8	14	20	18	15	18	1.1	1.1	0.2	0.4	0.4	0.5	0	Delamination	

Table 4.9—Single Pad Displacement Forces Applied: 0% and 2% Slopes

Test Series	Test Run	Compressive Force (Kips)	Transverse Force (Kips)	Longitudinal Force (Kips)	
				East Ram	West Ram
S0A	1	390	0.0	14.7	14.8
S0A	2	390	0.0	14.9	14.9
S0A	3	390	0.0	14.6	14.7
S0A	4	390	0.0	14.7	14.3
S0A	5	390	0.0	14.3	14.7
S0A	6	390	0.0	15.3	15.3
S0A	7	390	0.0	14.6	14.7
S0A	8	390	0.0	14.2	14.7
S0A	9	390	0.0	14.1	14.4
S0A	10	390	0.0	14.6	14.5
S0A	11	150	0.0	12.5	12.6
S0A	12	210	0.0	14.3	14.5
S0A	13	270	0.0	15.2	15.0
S0A	14	330	0.0	14.8	14.9
S2A	1	390	18.1	14.5	14.4
S2A	2	390	17.4	14.0	14.4
S2A	3	390	17.0	13.7	13.9
S2A	4	390	17.4	14.0	14.1
S2A	5	390	17.3	14.2	14.4
S2A	6	390	17.6	14.7	14.4
S2A	7	390	17.3	14.3	14.4
S2A	8	390	19.0	14.8	14.8
S2A	9	390	17.9	13.8	13.8
S2A	10	390	17.8	13.3	13.5
S2A	11	150	16.9	13.0	13.2
S2A	12	210	16.9	14.2	14.2
S2A	13	270	17.1	14.3	14.3
S2A	14	330	17.4	14.0	14.2

Table 4.10—Single Pad Displacement Forces Applied: 4%, 6% and 8% Slopes

Test Series	Test Run	Compressive Force (Kips)	Transverse Force (Kips)	Longitudinal Force (Kips)	
				East Ram	West Ram
S4A	1	390	29.2	14.5	14.3
S4A	2	390	30.0	14.1	14.3
S4A	3	390	29.7	14.7	14.7
S4A	4	390	31.6	13.9	14.0
S4A	5	390	30.6	13.7	13.7
S4A	6	390	31.7	13.9	14.1
S4A	7	390	31.2	13.6	13.5
S4A	8	390	29.9	14.8	14.8
S4A	9	390	29.6	15.1	15.2
S4A	10	390	30.1	15.0	15.1
S4A	11	150	27.7	14.0	14.0
S4A	12	210	29.2	15.0	14.9
S4A	13	270	28.5	15.0	14.9
S4A	14	330	29.8	14.8	14.8
S6A	1	390	33.3	16.3	16.1
S6A	2	390	32.1	15.6	15.5
S6A	3	390	33.7	16.8	16.6
S6A	4	390	35.3	16.8	16.7
S6A	11	150	29.8	15.6	15.5
S6A	12	210	30.3	17.3	17.1
S6A	13	270	32.2	16.4	16.5
S6A	14	330	33.5	16.0	14.3
S8A	1	390	55.6	17.7	17.8
S8A	2	390	53.1	17.4	17.5
S8A	3	390	53.5	18.2	18.1
S8A	4	390	55.2	18.0	17.9
S8A	11	150	41.4	15.1	15.2
S8A	12	210	45.1	15.9	15.8
S8A	13	270	49.5	17.0	17.2
S8A	14	330	53.7	18.6	18.3

#### 4.4.3. Dual Pad Test Results

The same information was recorded for the double pad configuration as with the single pad configuration. . Table 4.11 and Table 4.12 summarize the displacements observed during each test run in the same format indicated in section 4.4.2. Table 4.13 and Table 4.14 summarize the forces required to simulate the loading conditions for each test run of the single pad configuration similar to the organization of Table 4.9 and Table 4.10.

#### 4.4.4. Summary of Observations

Detailed analysis of the data is explained in Chapter 5 of the report, but a few trends are discussed here. In general, an increased superelevation for both pad configurations resulted in higher transverse forces applied to the bearing. A trend appears to exist that shows the lighter vertical load applied required less transverse force to produce the desired transverse deflection. The amount of damage observed appears to increase as well as the severity of the damage observed as the superelevation increased. Additionally, transverse slip increased with increased superelevation.

Table 4.15 compares the transverse angles observed at Wichita Falls versus those observed in the lab. The first four columns of this table provide identification and summary information for the bearings. The next two columns provide the transverse angles observed for each inspected bearing. Columns seven and eight provide the average angle observed in the laboratory testing for the given superelevation listed in column three. The average angles were interpolated from the average angles for each superelevation and bearing pad configuration tested in the laboratory. The final two columns provide the minimum angle and maximum angle seen at the respective superelevations. For these angles, interpolation between lab tested superelevations did not seem appropriate. As such, TechMRT provided the maximum and minimum transverse angles for the laboratory data closest to the actual superelevation observed in the field. The lab predicted angles are presented a little differently here. In this case, rather than saying left or right transverse angles, the columns are titled uphill and downhill angles to avoid confusion when comparing the numbers. The downhill angle of the Wichita Falls bearings can be determined by looking at the fourth column of Table 4.15. Table 4.16 provides the same comparison for the Lubbock bridge inspection to the laboratory data.

The laboratory data tends to mirror the results observed in the field at Wichita Falls, Texas. The average lab angles seem to agree with the numbers observed in the field. For the laboratory data, 9 out of 16 field observations are very similar to the results of the lab data. The laboratory data provided in columns seven and eight are averages so they may not be exact matches. In general, the field angles tend to fall within the maximum and minimum ranges of the angles seen in the laboratory experiment. This is true for 15 of the 16 Wichita Falls field measurements.

The Lubbock bridge data does not provide as good a fit. The observed angles on the US82 overpass are lower than those observed in the lab. A plausible explanation may be that the data from the Lubbock bridge was recorded shortly after the bridge deck was constructed. Therefore, there was insufficient time for the effect of creep to fully occur.

Table 4.11—Double Pad Displacement and Damage Recorded: 0% and 2% Slopes

Test Series	Transverse Slope (%)	Test Run	Transverse Angles (Degrees)		Longitudinal Angle (Degrees)		Slip (inches)				Lift - Off (inches)				Damage Noted
			Left	Right	Front	Back	Transverse		Longitudinal	Transverse		Longitudinal			
							Front	Back		Top	Bottom	Top	Bottom		
D0A	0	1	-2	-1	19	17	0	0	0.1	0	0	0	0	None	
D0A	0	2	3	0	22	18	0	0	0.2	0	0	0	0	Hairline Cracking	
D0A	0	3	3	0	22	18	0	0	0.2	0	0	0	0	Hairline Cracking	
D0A	0	4	3	0	22	18	0	0	0.2	0	0	0	0	Hairline Cracking	
D0A	0	5	2	1	22	19	0	0	0.2	0	0	0	0	Hairline Cracking	
D0A	0	6	4	0	21	17	0	0	0.2	0	0	0	0	Hairline Cracking	
D0A	0	7	0	3	19	17	0	0	0.2	0	0	0	0	Hairline Cracking	
D0A	0	8	3	1	22	18	0	0	0.3	0	0	0	0	Hairline Cracking	
D0A	0	9	3	2	21	18	0	0	0.2	0	0	0	0	Hairline Cracking	
D0A	0	10	4	2	21	19	0	0	0.2	0	0	0	0	Hairline Cracking	
D0A	0	14	4	0	21	18	0	0.1	0.3	0	0	0	0	None	
D0A	0	13	5	2	21	18	0	0	0.4	0	0	0	0	None	
D0A	0	12	3	-1	21	18	0	0	0.2	0	0	0	0	None	
D0A	0	11	1	0	22	20	0	0	0.2	0	0	0	0	None	
D2A	2	1	12	--	25	--	0	0.1	0.2	0	0	0	0	Hairline Cracking	
D2A	2	2	11	--	22	--	0.1	0.1	0.2	0	0	0	0	Hairline Cracking	
D2A	2	3	10	9	19	20	0.1	0.1	0.2	0	0	0	0	Hairline Cracking	
D2A	2	4	9	12	19	17	0	0	0.1	0	0	0	0	Hairline Cracking	
D2A	2	5	9	11	20	20	0.1	0.1	0.1	0	0	0	0	Hairline Cracking	
D2A	2	6	6	6	20	23	0	0.1	0.1	0	0	0	0	Hairline Cracking	
D2A	2	7	6	7	21	22	0	0.1	0.1	0	0	0	0	Hairline Cracking	
D2A	2	8	6	6	20	22	0.1	0	0.1	0	0	0	0	Hairline Cracking	
D2A	2	9	6	6	22	25	0	0	0.1	0	0	0	0	Hairline Cracking	
D2A	2	10	6	6	20	25	0	0.1	0	0	0	0	0	Hairline Cracking	
D2A	2	14	9	8	18	19	0.1	0.1	0.3	0	0	0	0	None	
D2A	2	13	7	8	14	14	0.1	0.1	0.3	0	0	0	0	None	
D2A	2	12	5	6	18	15	0.1	0.1	0.2	0	0	0	0	None	
D2A	2	11	5	6	22	14	0.1	0.1	0.2	0	0	0	0	None	

Table 4.12—Double Pad Displacement and Damage Recorded: 4%, 6% and 8% Slopes

Test Series	Transverse Slope (%)	Test Run	Transverse Angles (Degrees)		Longitudinal Angle (Degrees)		Slip (inches)			Lift - Off (inches)				Damage Noted
			Left	Right	Front	Back	Transverse	Longitudinal	Top	Bottom	Top	Bottom		
D4A	4	1	14	16	16	19	0.2	0.2	0.1	0	0	0	0	Hairline Cracking
D4A	4	2	15	16	18	16	0.1	0.1	0	0	0	0	0	Hairline Cracking
D4A	4	3	15	16	19	18	0.2	0.2	0.1	0	0	0	0	Hairline Cracking
D4A	4	4	15	16	20	21	0.2	0.2	0.2	0	0	0	0	Hairline Cracking
D4A	4	5	15	16	17	17	0.2	0.2	0.2	0	0	0	0	Hairline Cracking
D4A	4	6	17	19	19	23	0.2	0.2	0.1	0	0	0	0	Hairline Cracking
D4A	4	7	15	15	20	22	0.2	0.3	0.1	0	0	0	0	Hairline Cracking
D4A	4	8	16	15	20	21	0.2	0.2	0.3	0	0	0	0	Delamination
D4A	4	9	15	15	19	19	0.2	0.3	0.2	0	0	0	0	Delamination
D4A	4	10	15	15	19	21	0.2	0.3	0.1	0	0	0	0	Delamination
D4A	4	14	14	13	21	19	0.2	0.3	0.2	0	0	0	0	None
D4A	4	13	14	13	16	16	0.1	0.2	0.2	0	0	0	0	None
D4A	4	12	13	14	16	16	0.2	0.2	0.1	0	0	0	0	None
D4A	4	11	14	13	16	18	0.2	0.2	0.1	0	0	0	0	Hairline Cracking
D6A	6	1	15	12	17	14	0.3	0.3	0.2	0.2	0	0	0	Hairline Cracking
D6A	6	2	12	10	16	14	0.3	0.3	0.1	0.3	0	0	0	Heavy Cracking
D6A	6	3	15	12	16	14	0.4	0.3	0.1	0.3	0	0	0	Heavy Cracking
D6A	6	4	14	12	18	17	0.3	0.3	0	0.3	0	0	0	Delamination
D6A	6	14	15	18	17	12	0.3	0.3	0.2	0.2	0	0	0	None
D6A	6	13	16	15	18	15	0.3	0.3	0.2	0.2	0	0	0	None
D6A	6	12	12	13	18	14	0.3	0.3	0.2	0.2	0	0	0	None
D6A	6	11	14	13	16	14	0.3	0.3	0.1	0.4	0	0	0	Hairline Cracking
D8A	8	1	--	--	--	--	0.4	0.4	0.1	0.5	0	0	0	Delamination
D8A	8	2	11	9	15	14	0.4	0.5	0.1	0.5	0	0	0	Delamination
D8A	8	3	11	10	10	16	0.3	0.4	0.1	0.6	0	0	0	Delamination
D8A	8	4	15	15	18	19	0.5	0.4	0.1	0.5	0	0	0	Delamination
D8A	8	14	11	10	15	13	0.4	0.4	0.1	0.1	0	0	0	None
D8A	8	13	13	14	12	11	0.4	0.5	0.1	0.2	0.3	0	0	None
D8A	8	12	13	13	12	12	0.3	0.3	0.1	0.3	0	0	0	Tension Debonding
D8A	8	11	9	9	12	11	0.1	0.1	0.1	0.5	0	0	0	Tension Debonding

Table 4.13—Double Pad Displacement Forces Applied: 0% and 2% Slopes

Test Series	Test Run	Compressive Force (Kips)	Transverse Force (Kips)	Longitudinal Force (Kips)	
				East Ram	West Ram
D0A	1	390	0.0	0.0	0.0
D0A	2	390	0.0	0.0	0.0
D0A	3	390	0.0	0.0	0.0
D0A	4	390	0.0	0.0	0.0
D0A	5	390	0.0	0.0	0.0
D0A	6	390	0.0	0.0	0.0
D0A	7	390	0.0	0.0	0.0
D0A	8	390	0.0	0.0	0.0
D0A	9	390	0.0	0.0	0.0
D0A	10	390	0.0	0.0	0.0
D0A	11	150	0.0	0.0	0.0
D0A	12	210	0.0	0.0	0.0
D0A	13	270	0.0	0.0	0.0
D0A	14	330	0.0	0.0	0.0
D2A	1	390	0.0	0.0	0.0
D2A	2	390	23.9	0.0	0.0
D2A	3	390	0.0	0.0	0.0
D2A	4	390	21.9	0.0	0.0
D2A	5	390	21.9	0.0	0.0
D2A	6	390	0.0	0.0	0.0
D2A	7	390	20.9	0.0	0.0
D2A	8	390	20.9	0.0	0.0
D2A	9	390	20.9	0.0	0.0
D2A	10	390	20.9	0.0	0.0
D2A	11	150	0.0	0.0	0.0
D2A	12	210	0.0	0.0	0.0
D2A	13	270	0.0	0.0	0.0
D2A	14	330	0.0	0.0	0.0

Table 4.14—Double Pad Displacement Forces Applied: 4%, 6% and 8% Slopes

Test Series	Test Run	Compressive Force (Kips)	Transverse Force (Kips)	Longitudinal Force (Kips)	
				East Ram	West Ram
D4A	1	390	38.7	19.5	19.6
D4A	2	390	36.3	18.6	18.7
D4A	3	390	39.1	19.1	19.2
D4A	4	390	39.2	19.1	19.1
D4A	5	390	39.7	19.0	19.2
D4A	6	390	40.3	19.2	19.5
D4A	7	390	38.9	19.6	19.6
D4A	8	390	39.8	19.0	19.1
D4A	9	390	39.0	19.5	19.5
D4A	10	390	40.7	19.4	19.5
D4A	11	150	34.8	18.5	18.5
D4A	12	210	34.9	17.7	17.7
D4A	13	270	34.9	18.2	18.4
D4A	14	330	35.6	18.5	18.5
D6A	1	390	44.8	18.2	18.2
D6A	2	390	41.9	18.2	18.3
D6A	3	390	44.6	19.2	19.3
D6A	4	390	44.2	18.1	18.1
D6A	11	150	44.9	19.0	18.9
D6A	12	210	43.0	18.3	18.3
D6A	13	270	41.6	17.2	17.2
D6A	14	330	40.2	16.3	16.1
D8A	1	390	48.2	0*	0*
D8A	2	390	59.6	17.9	18.2
D8A	3	390	53.8	16.3	16.4
D8A	4	390	56.3	17.3	17.3
D8A	11	150	42.6	15.4	15.5
D8A	12	210	48.6	16.1	16.1
D8A	13	270	66.3	15.5	15.5
D8A	14	330	46.5	16.4	16.4

\*Note Longitudinal Force Not Applied Due to Equipment Problems

Table 4.15—Comparison of Wichita Falls Bridge Data to Laboratory Data

Bearing	Bearing Configuration	Trans. Slope, Percent	Down side	Observed Angles		Lab Observed Angles			
				Left Trans. Angle, Degrees	Right Trans. Angle, Degrees	Avg Downhill Angle (Degrees)	Avg Uphill Angle (Degrees)	Max Angle Observed (Degrees)	Min Angle Observed (Degrees)
A	Single	5.8	Left	18	14	14.2	12.6	15	5
B	Single	3.7	Left	12	9	8.3	8.2	11	5
C	Single	3	Left	20	20	4.5	4.4	11	5
D1	Double	1	Right	10	10	5.2	4.3	12	5
D2	Double	1	Right	10	10	5.2	4.3	12	5
E	Single	6.1	Left	15	10	15.2	13.5	18	15
F	Single	5.2	Left	15	14	12.4	11.3	15	5
G	Double	6.4	Right	10	10	13.6	12.6	15	5
H	Double	6.4	Right	13	15	13.6	12.6	18	9
I	Double	5.3	Right	18	20	2.1	2.0	18	9
J	Double	5.3	Right	15	15	2.1	2.0	18	9
K	Single	6.6	Left	15	10	17.3	15.7	15	5
L	Double	6.2	Right	9	10	13.8	12.8	18	9
M	Double	6.2	Right	10	10	13.8	12.8	18	9
N	Double	5.3	Right	7	6	14.4	14.0	18	9
O	Double	5.3	Right	6	9	14.4	14.0	18	9

Table 4.16—Comparison of Lubbock Bridge Data to Laboratory Data

Bearing Configuration	Trans. Slope, Percent	Down side	Observed Angles		Lab Observed Angles			
			Left Trans. Angle, Degrees	Right Trans. Angle, Degrees	Avg Downhill Angle (Degrees)	Avg Uphill Angle (Degrees)	Max Angle Observed (Degrees)	Min Angle Observed (Degrees)
Double	3.8	Left	8	9	14.5	15.1	19	13
Double	3.8	Left	9	8	14.5	15.1	19	13

## 4.5. Finite Element Modeling

TechMRT also developed a finite element model (FEM) for both the single and double bearing pad configurations described earlier in this chapter. These models were used to run a series of finite element analyses with conditions matching several of the experimental tests conditions so that comparisons could be made in an attempt to validate the FEMs, allowing for the possibility of future parametric studies to be conducted, if warranted.

### 4.5.1. Description of the Finite Element Model

The bearing pads were modeled using the finite element software, ANSYS, using one of its standard elements, “SOLID186.” The SOLID186 element is a 3-dimensional, 20-node, solid brick element that exhibits quadratic displacement behavior as shown in Figure 4.25. Each node



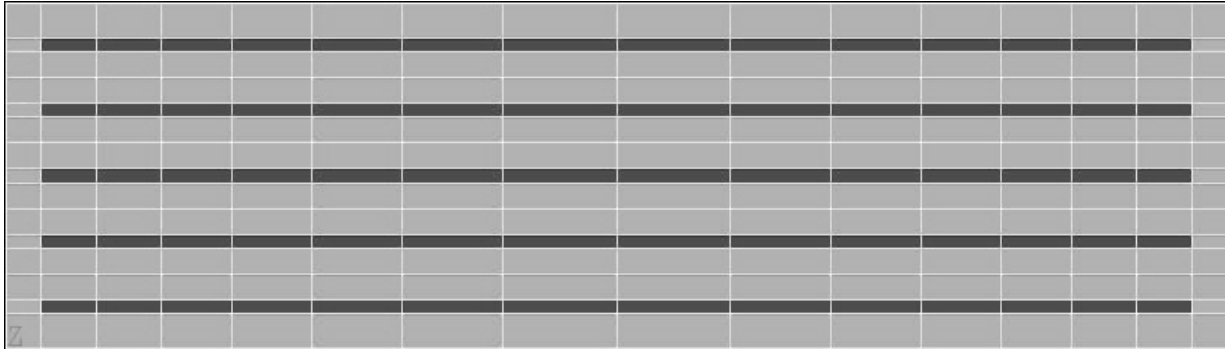


Figure 4.26—ANSYS Model of Bearing, Transverse Face

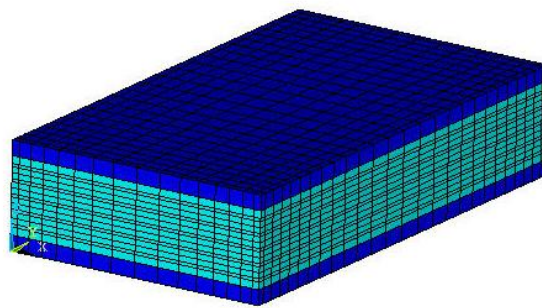


Figure 4.27--Pad Model with Rigid Extreme Layers

Ten FE analyses are compared to experimental results in the next section. The FE analyses consider only the maximum vertical load on the pad of 390 kips and the five transverse slopes (values of slope set to 0, 2, 4, 6, and 8%) for both the single and double bearing pad configurations, totaling ten FE analyses. Loads were not applied in step one but were applied in a stepwise fashion from zero to their maximum in the order of vertical load, followed by transverse load, and finally the longitudinal load. Only the analytical results from the fully loaded pads are reported. The non-linear geometry function of ANSYS was utilized during the FE analyses associated with this project.

#### 4.5.2. Comparison of FEA to Laboratory Testing

Magnitudes of angular deformation from a vertical axis were measured and calculated in degrees in the transverse and longitudinal directions of the pads at the maximum specified loading. Due to the non-linearity of the shear deformations in the pads, the angular deformations vary through the depth of the pad and along the length of the pad in each direction. Therefore,

maximum and minimum values of angular deformations were determined in each of the transverse and longitudinal directions of the pads and are used for comparison of the FEA results to the laboratory results. Table 4.17 summarizes the angular deformations (maximum and minimum values) that occur in the ten load cases for both FEA and experimental results.

Table 4.17– Angular Deformations in Pads at 390 kip Vertical Load

Bearing Configuration	Transverse Slope	Max / Min Transverse Angle Experimental (Degrees)	Max / Min Transverse Angle FEA (Degrees)	Max / Min Longitudinal Angle Experimental (Degrees)	Max / Min Longitudinal Angle FEA (Degrees)
Single	0%	0 / 0	0 / 0	17 / 14	18 / 12
Single	2%	5 / 4	11 / 8	15 / 8	16 / 11
Single	4%	11 / 7	17 / 12	18 / 10	16 / 11
Single	6%	15 / 12	20 / 13	18 / 14	18 / 12
Single	8%	25 / 20	26 / 22	24 / 15	19 / 14
Double	0%	4 / -2	0 / 0	22 / 17	21 / 18
Double	2%	12 / 6	16 / 10	25 / 17	15 / 11
Double	4%	19 / 14	20 / 18	23 / 16	20 / 14
Double	6%	15 / 10	24 / 16	18 / 14	22 / 14
Double	8%	15 / 9	27 / 20	19 / 10	20 / 12

The finite element analysis displayed the same trend as the laboratory results shown by the strain profiles in Figure 4.28 through Figure 4.31. Figure 4.28 through Figure 4.31 show the strain profile for the double pad configuration at 6% superelevation. Note that the bearing is in compression with respect to the vertical direction except for localized areas of tension along the shims. As will be discussed in section 5.4 of this report, a larger superelevation results in a larger area of localized tension and tends to mirror the damage results analyzed. As the value of the tensile strain increases, debonding and delamination occur when the stress in the localized area exceeds that of the bond between the elastomer and the steel reinforcement.

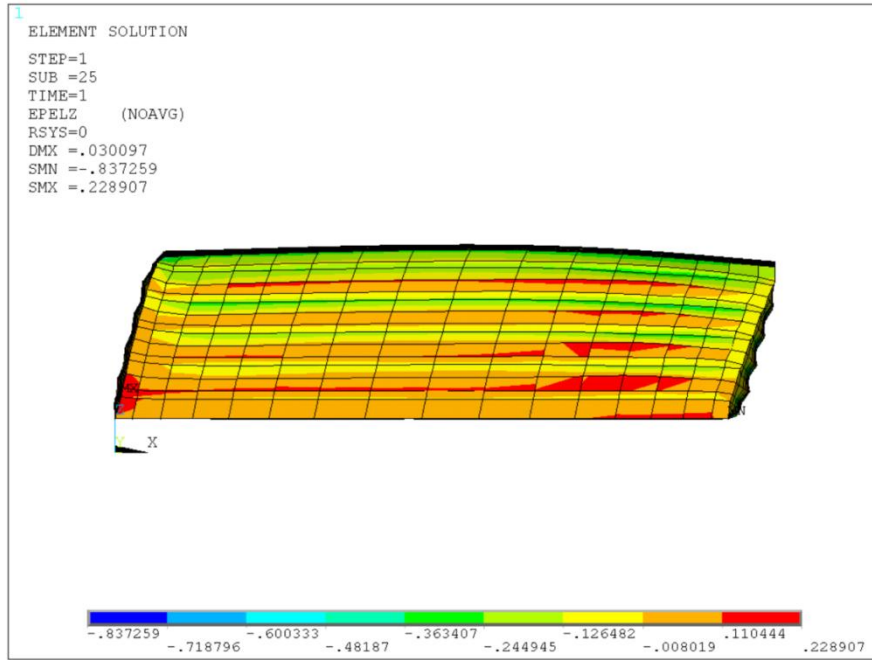


Figure 4.28--Strain Profile in z-direction, Rear Transverse Face, 6% Superelevation Double Pad Configuration

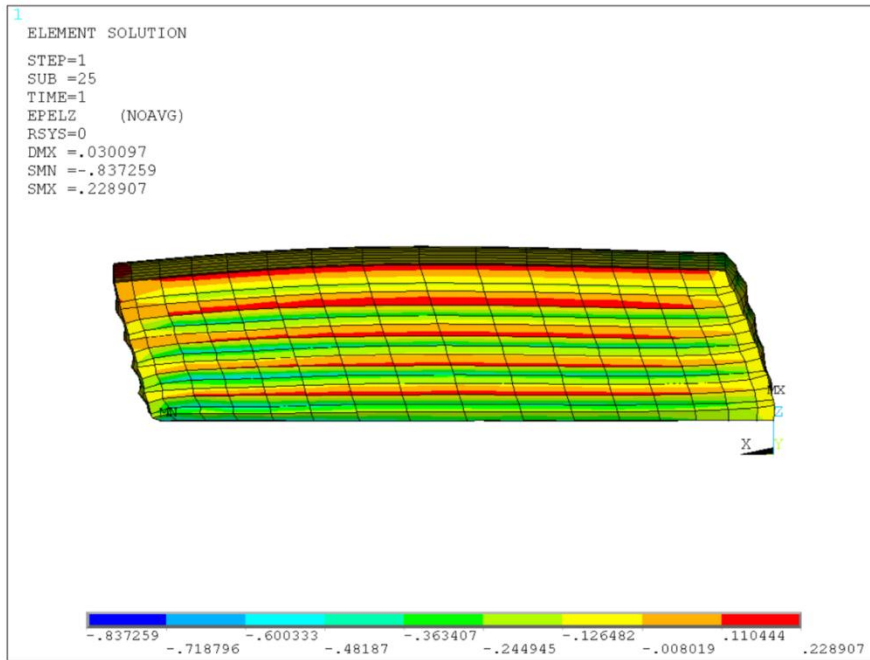


Figure 4.29-- Strain Profile in z-direction, Front Transverse Face, 6% Superelevation Double Pad Configuration

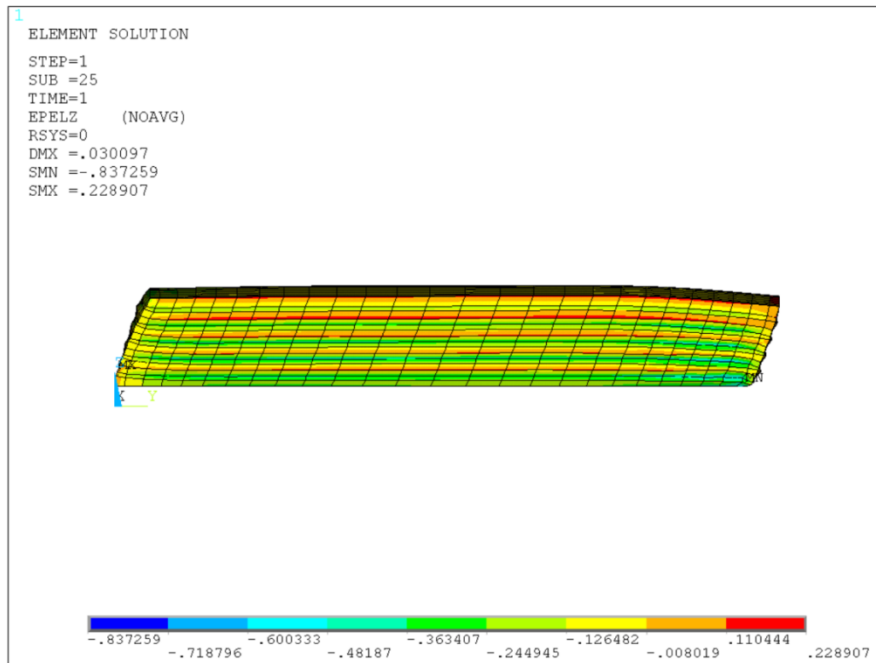


Figure 4.30-- Strain Profile in z-direction, Front Longitudinal Face, 6% Superelevation Double Pad Configuration

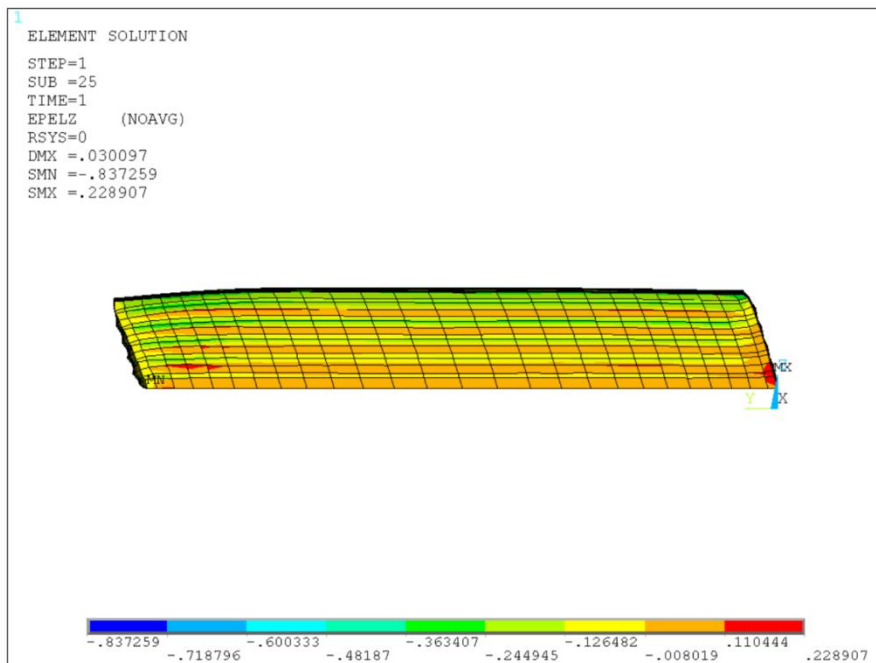


Figure 4.31-- Strain Profile in z-direction, Rear Transverse Face, 6% Superelevation Double Pad Configuration

#### 4.5.3. Summary of Observations

By comparing the measured and calculated values of the transverse and longitudinal angular deformations shown in Table 4.17 for the various load conditions, reasonable correlation is seen between similar conditions. Approximately half of the conditions have values that are within 25% of each other and approximately three out of four of the conditions have experimental and analytical results that are within 50% of each other. If the average value of the maximum and minimum values are considered, again over half of the FEA results are within 25% of the experimental values. Given the roughness of the measured experimental numbers and the roughness of the FE model, there is reasonable correlation between the experimental values and FEA values, indicating there is potential in the use of FE modeling for this application.

## 5. COMPARISON OF TESTING/OBSERVATIONS TO MODIFIED DESIGN PROVISIONS

This chapter provides an analysis of the transverse and longitudinal displacements, bearing slip, uplift data, damage prediction, and finite element analysis. The first research objective was to determine if there was a need to consider the transverse superelevation in bearing design, and if so, how it should be considered. Specifically, TechMRT attempted to determine what level of transverse superelevation of the bearings was detrimental to the serviceability of the bearing.

### 5.1. Combination of Transverse and Longitudinal Displacement

The horizontal loads were applied using displacement control. The pressure in the ram required to push the bearing the given displacement horizontally was recorded and multiplied by the ram area to give the load in kips required to push the bearing the given displacement. After the full horizontal displacement was reached, the longitudinal displacement was induced. Likewise, the pressure in the ram required to push the bearing the given displacement was recorded and converted to a load by multiplying by the area of the ram.

The theoretical load required to push the bearing the given displacement was then calculated and compared to the actual load observed. The equation governing the displacement of the elastomeric material was:

$$\Delta = \frac{F h_{rt}}{GA} \quad \text{Equation 5.1}$$

where  $\Delta$  is the displacement (either transverse or longitudinal),  $F$  is the force applied to the bearing,  $h_{rt}$  is the total height of the elastomer,  $G$  is the shear modulus, and  $A$  is the plan area of the elastomeric bearing. For the following results, an average shear modulus value of 0.115 ksi was used. The plan area for the standard single bearing is 288 in<sup>2</sup> and the plan area for each of the double bearings is exactly half, 144 in<sup>2</sup>.

The results for the single bearing tests with a modeled 4% transverse slope are presented as an example. Figure 5.1 shows the load in kips on the vertical axis plotted versus the increasing displacement on the horizontal axis for the first load cycle. The “predicted” line is the

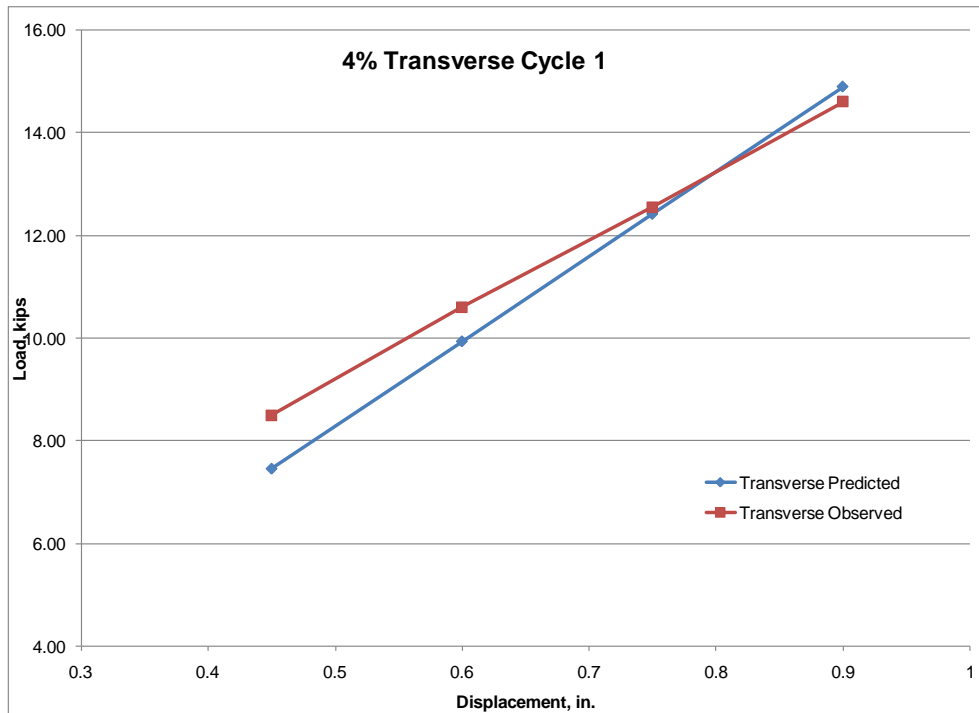


Figure 5.1 – Cycle 1 Transverse Results for 4% Test

load predicted using the deflection equation with the assumptions noted above. The “observed” line is the actual load observed that was required to push the bearing the given displacement. As Figure 5.1 shows, there is good agreement between the two.

For low displacements, the observed loads were slightly higher than the predicted loads. Figure 5.2 shows the same two “predicted” versus “observed” loads for the longitudinal displacement for the first cycle. The longitudinal displacement was induced after the transverse displacement was induced and held in place. As shown in the figure, the deflection equation predicted the displacement well for the low longitudinal displacements but predicted that a higher load than observed would be required for the higher displacements.

To incorporate the data for all cycles in one chart, the ratio of the observed to the predicted value was determined as:

$$Ratio = \frac{\text{Observed load for the given displacement}}{\text{Predicted load for the given displacement}} \quad \text{Equation 5.2}$$

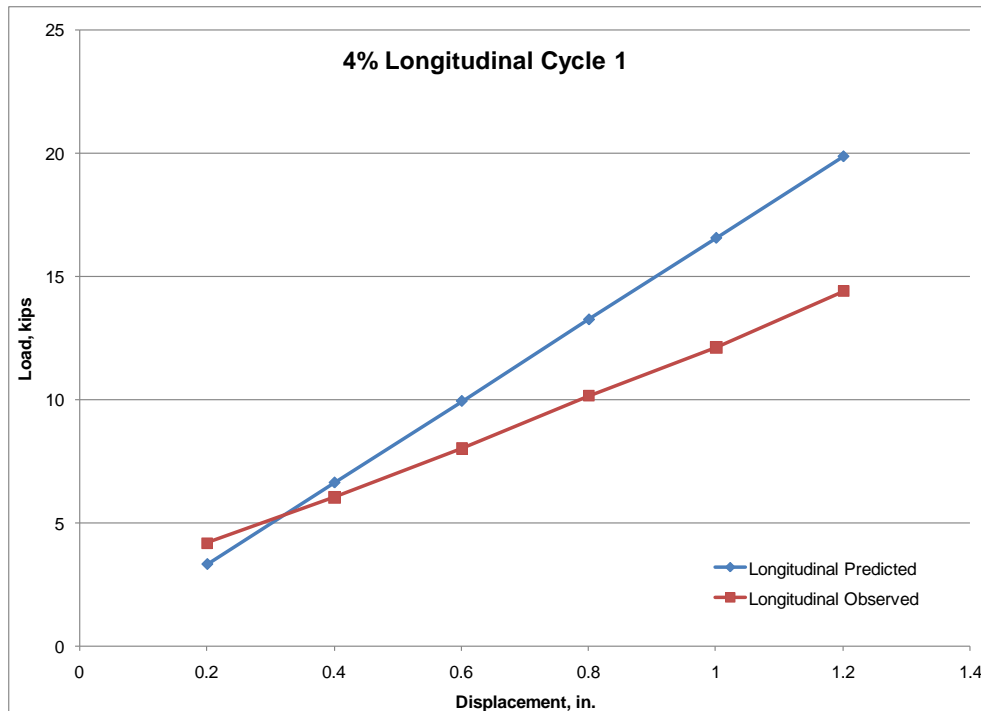


Figure 5.2 – Cycle 1 Longitudinal Results for 4% Test

This ratio is plotted for all 14 test cycles in Figure 5.3. The cycles with the full 390 kip vertical load are shown with solid lines and the cycles with the reduced vertical loading are shown with dashed lines. In general, the ratios are above 1.0 for most cycles and transverse displacements.

Since the ratio is over the predicted load required for the given displacement, a ratio greater than 1.0 indicates that more force was required to deflect the bearing than predicted by the deflection equation. This can be thought of as a conservative condition. When the ratio drops below 1.0, the condition can be considered speculative. More deflection will occur for a given load.

Figure 5.4 shows the ratios for the longitudinal displacements. In general, the ratios start above 1.0 for low displacements, then drop below 1.0 as the longitudinal displacements go above 0.3 in.

Ten tests were performed with the total compressive vertical load of 390 kips, followed by four tests with less vertical load. Figure 5.5 shows the ratio plotted versus the test number for all 14 of the transverse tests. This figure shows the results for the single pad configuration with

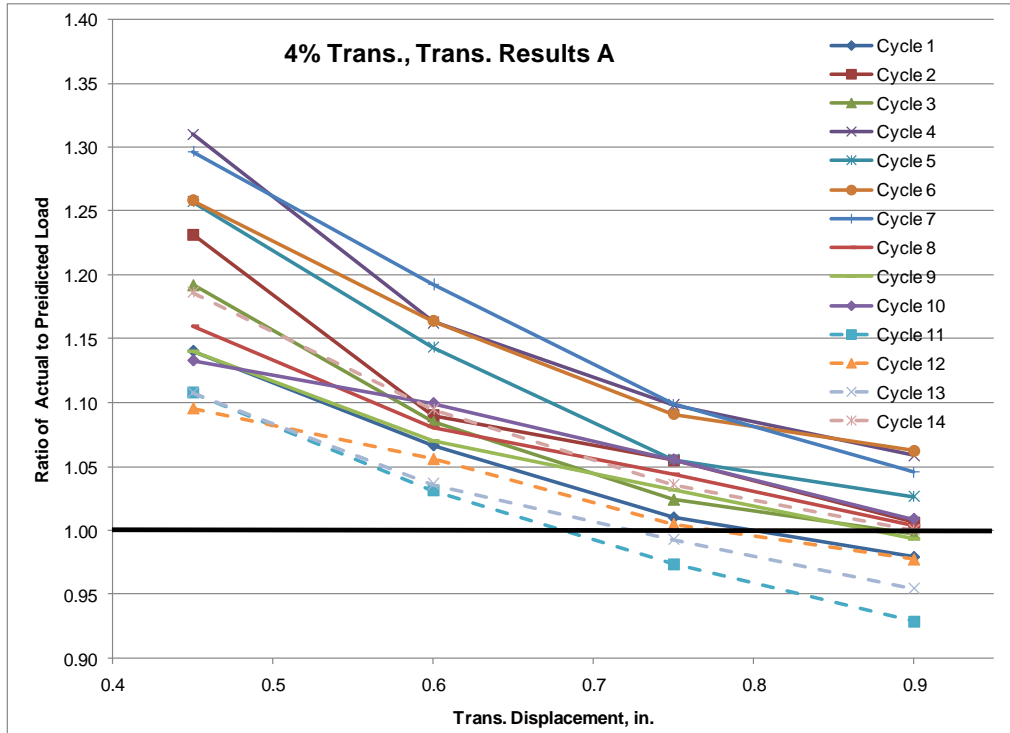


Figure 5.3 – Transverse Results for all 14 Cycles

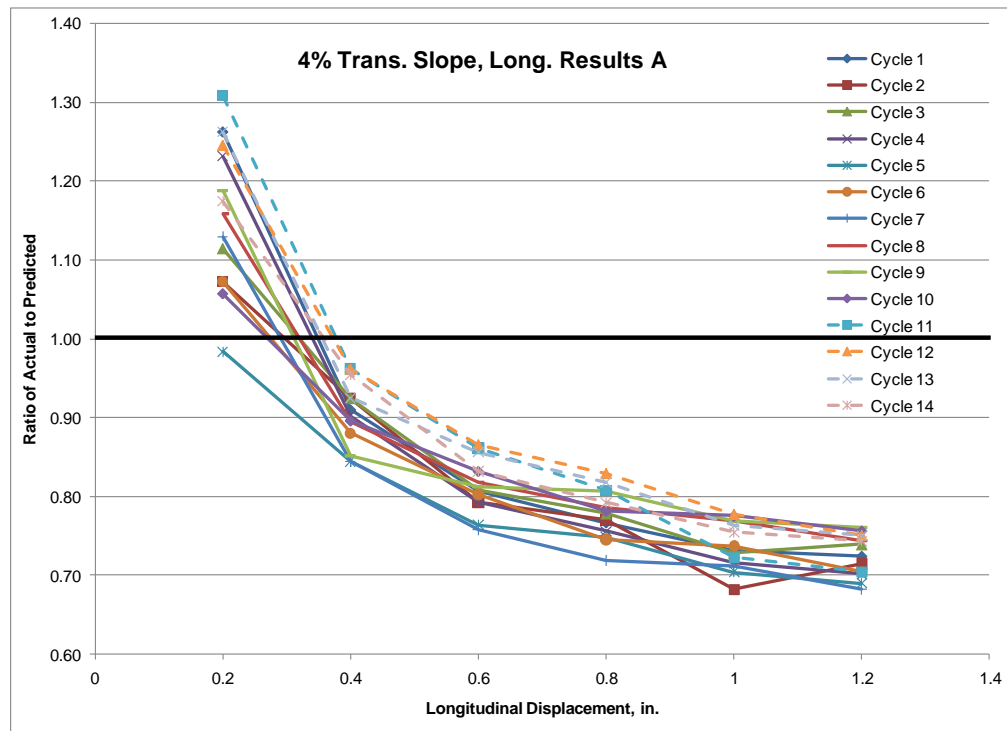


Figure 5.4 – Longitudinal Results for all 14 Cycles

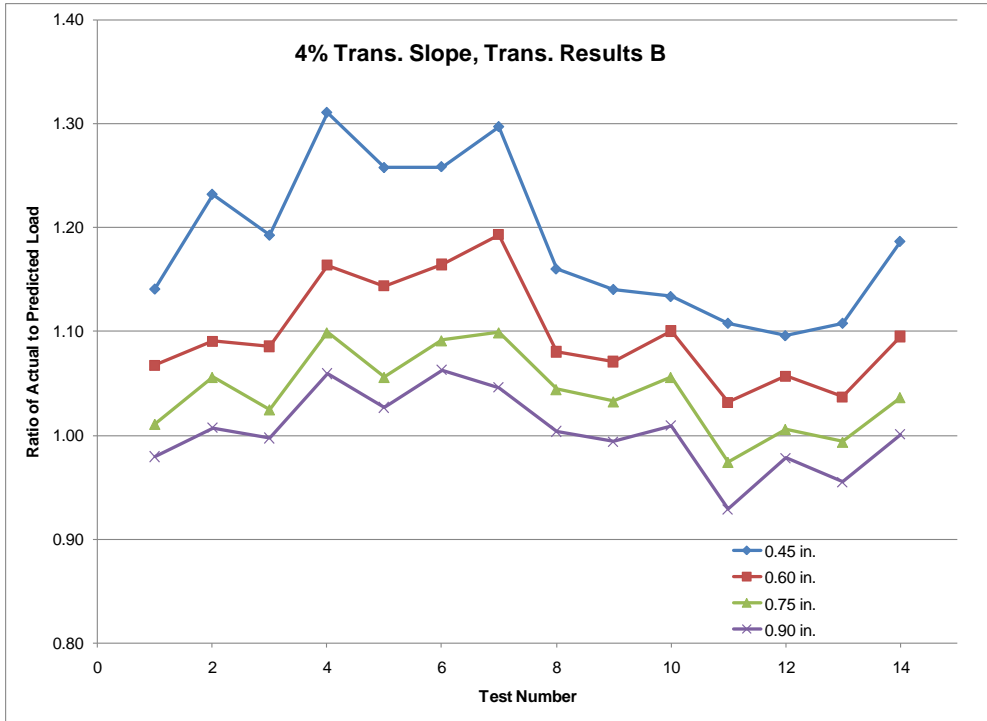


Figure 5.5 – Transverse Ratios versus Cycles

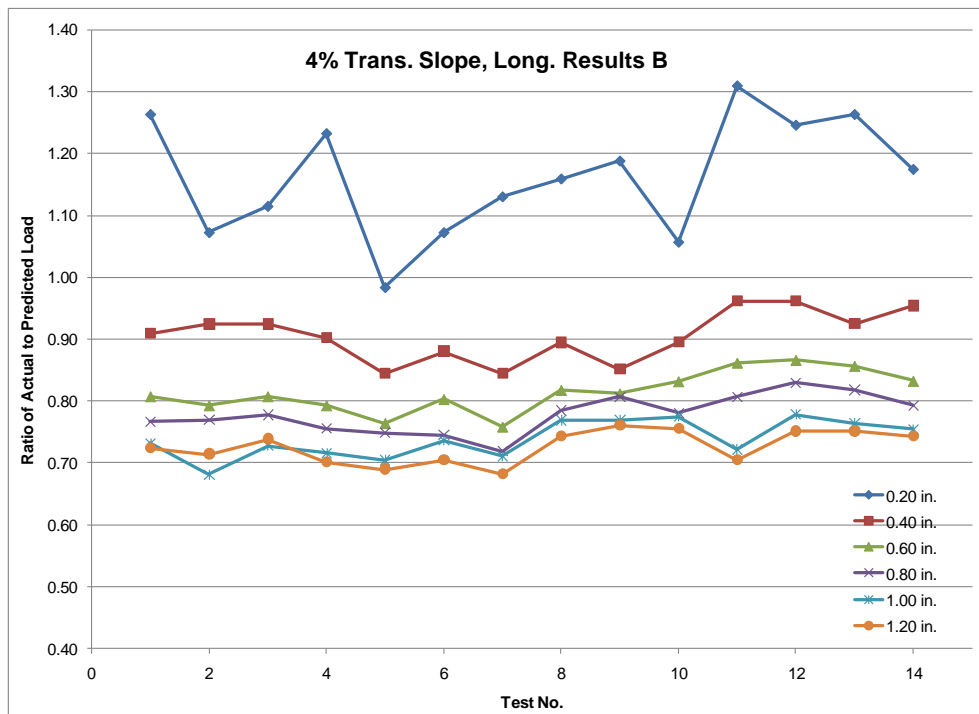


Figure 5.6 – Longitudinal Ratios versus Cycles

4% superelevation. No definite trend was noticed in this limited number of tests. Figure 5.6 shows the same results for the longitudinal tests. Again, no definite trend was noticed.

Figure 5.7 through Figure 5.24 show the ratio plotted versus the test number for all 14 of the tests performed. Each figure provides the ratios versus the transverse or longitudinal displacements for each bearing pad configuration and superelevation tested.

The results for the single pad tests are shown first. For only transverse loading, the ratios stay conservative (above 1.0) for transverse slopes of approximately 4.0% or less. However, when the longitudinal loading is applied in conjunction with the transverse loading, the ratios drop below 1.0 for longitudinal displacements as low as approximately 0.35 in. This indicates that single pads that experience both a transverse and longitudinal force exert more force to the superstructure than predicted with the conventional equations when the longitudinal displacement exceeds approximately 0.35 in.

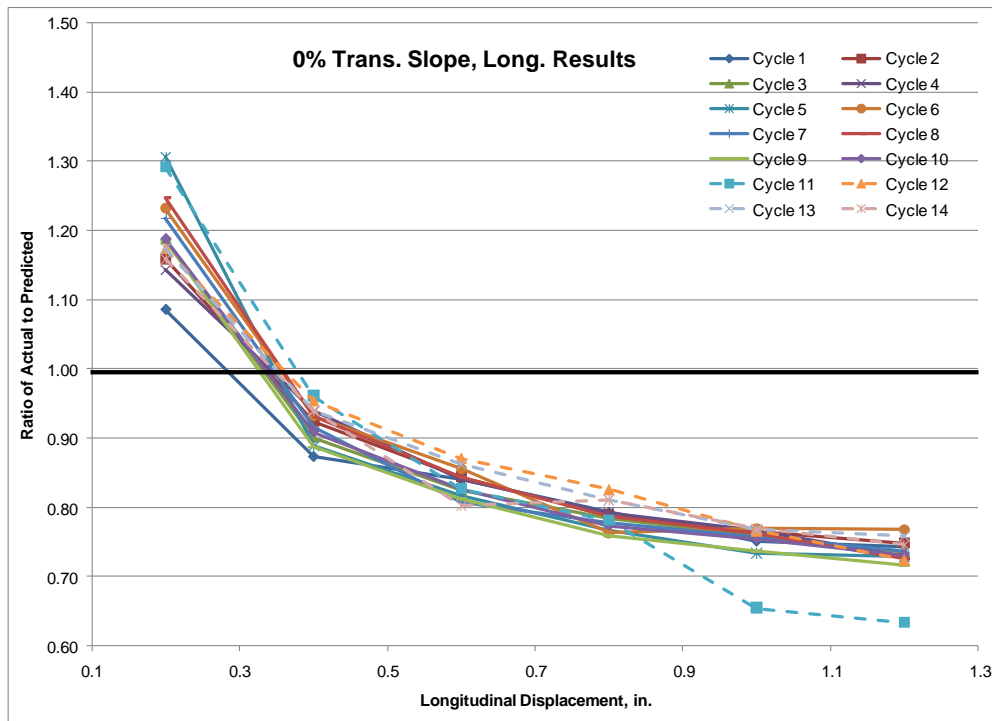


Figure 5.7 – Single Pad Long. Results for 0% Test

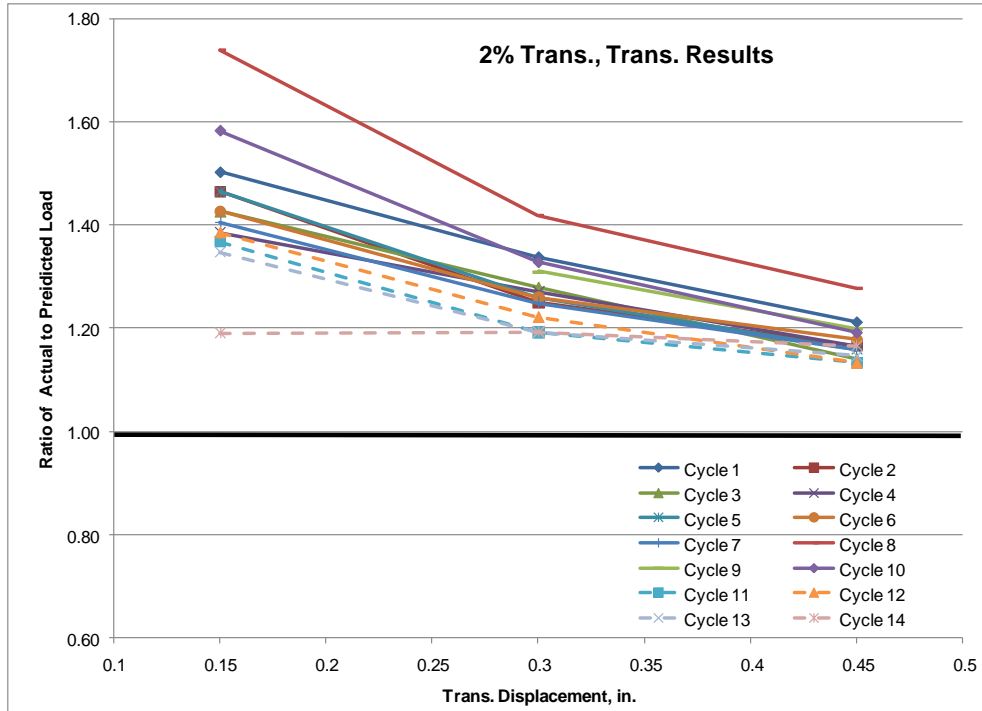


Figure 5.8 – Single Pad Transverse Results for 2% Test

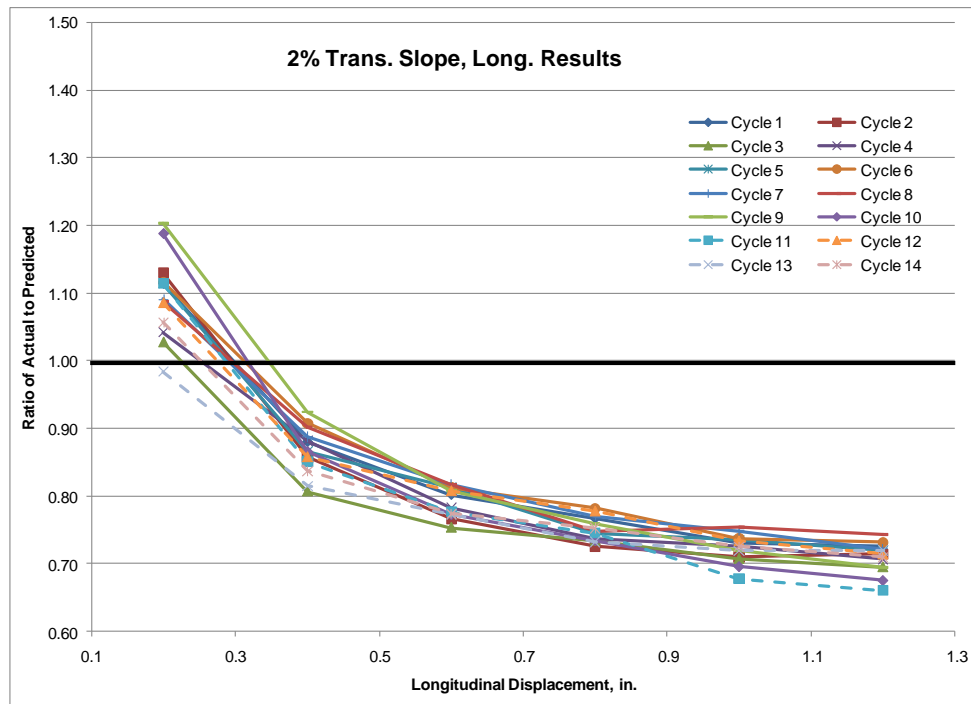


Figure 5.9 – Single Pad Long. Results for 2% Test

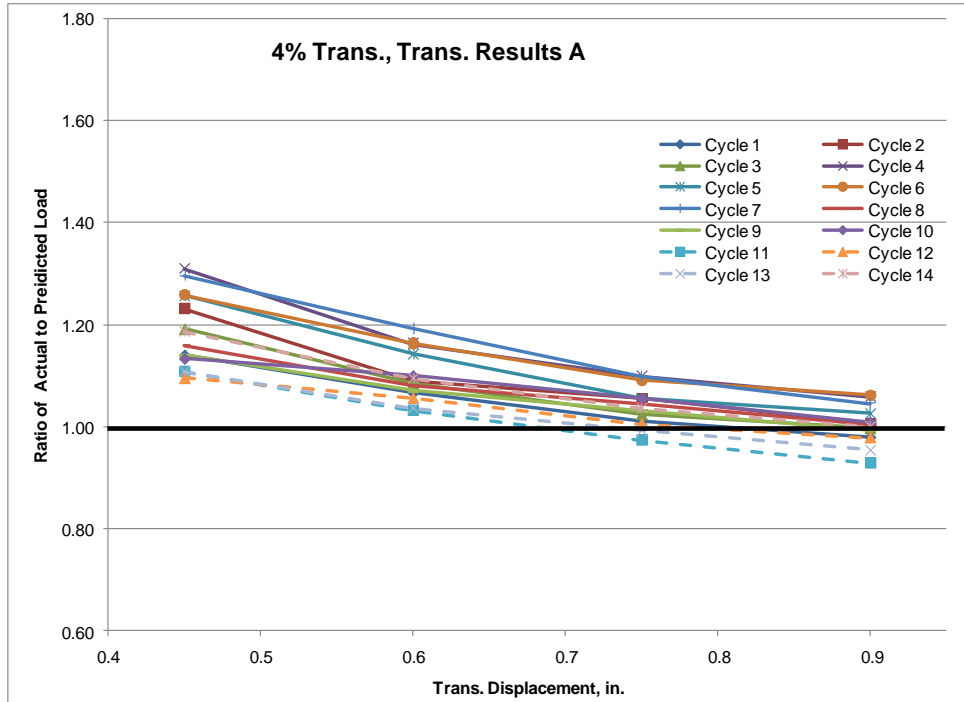


Figure 5.10 – Single Pad Trans. Results for 4% Test

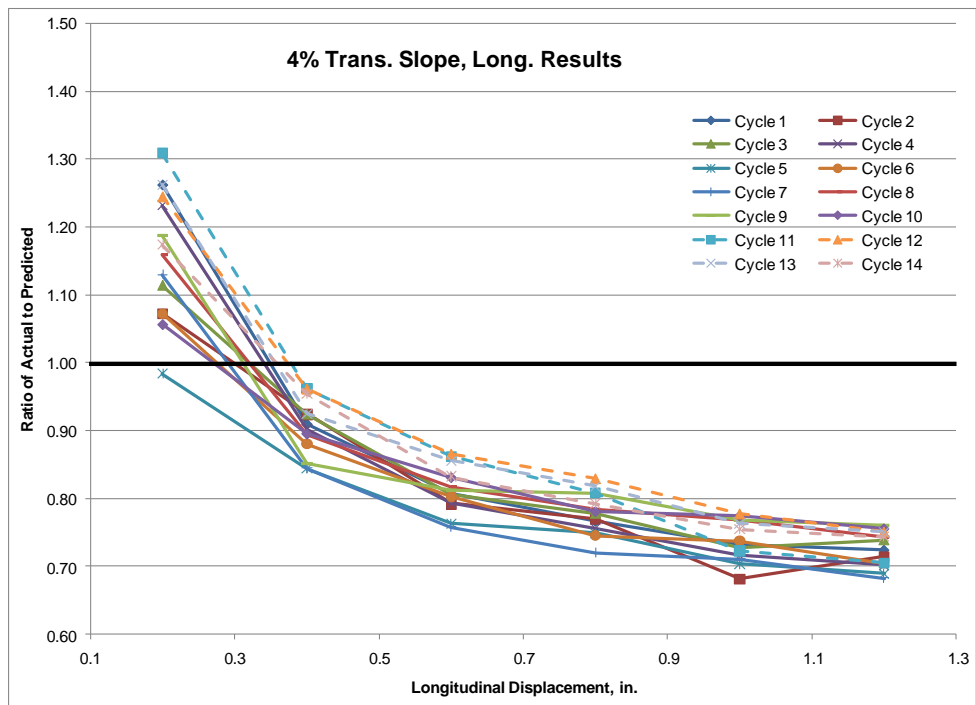


Figure 5.11- Single Pad Long. Results for 4% Test

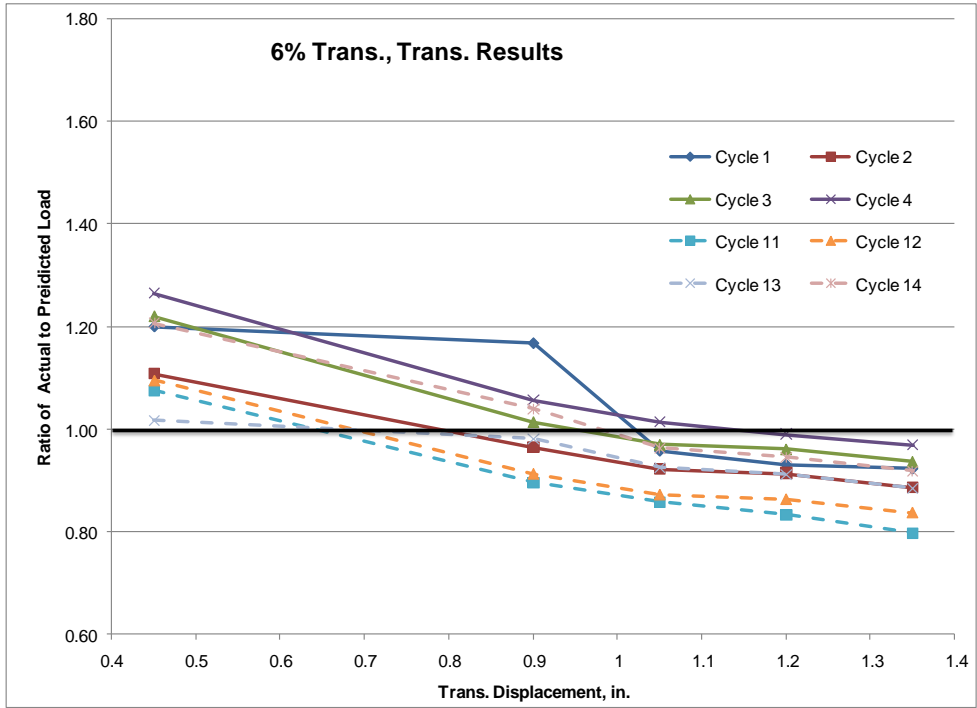


Figure 5.12 – Single Pad Trans. Results for 6% Test

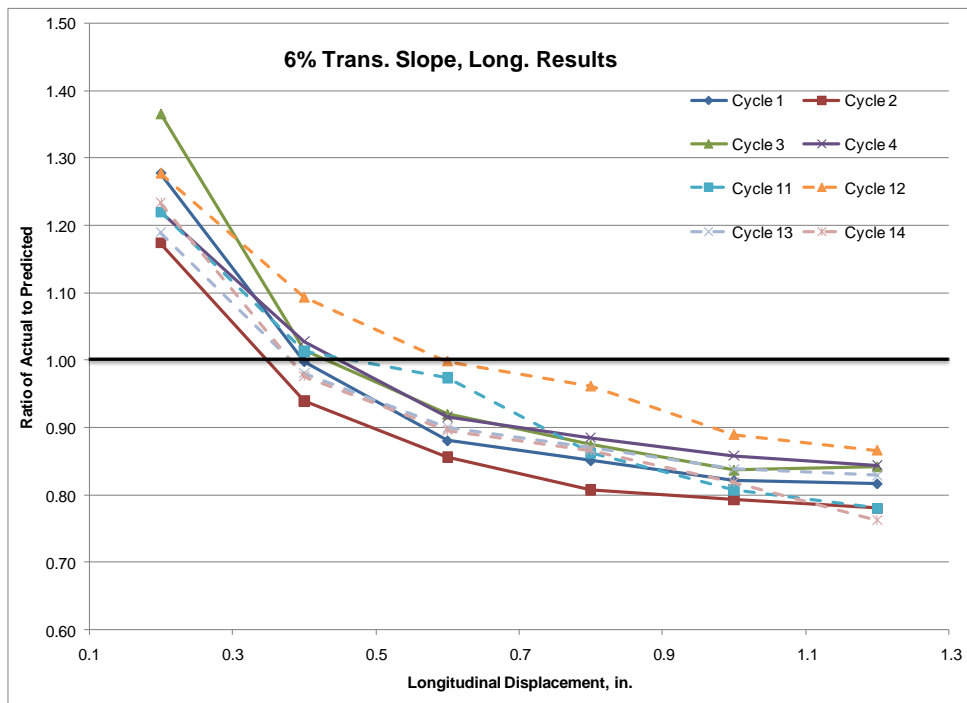


Figure 5.13 – Single Pad Long. Results for 6% Test

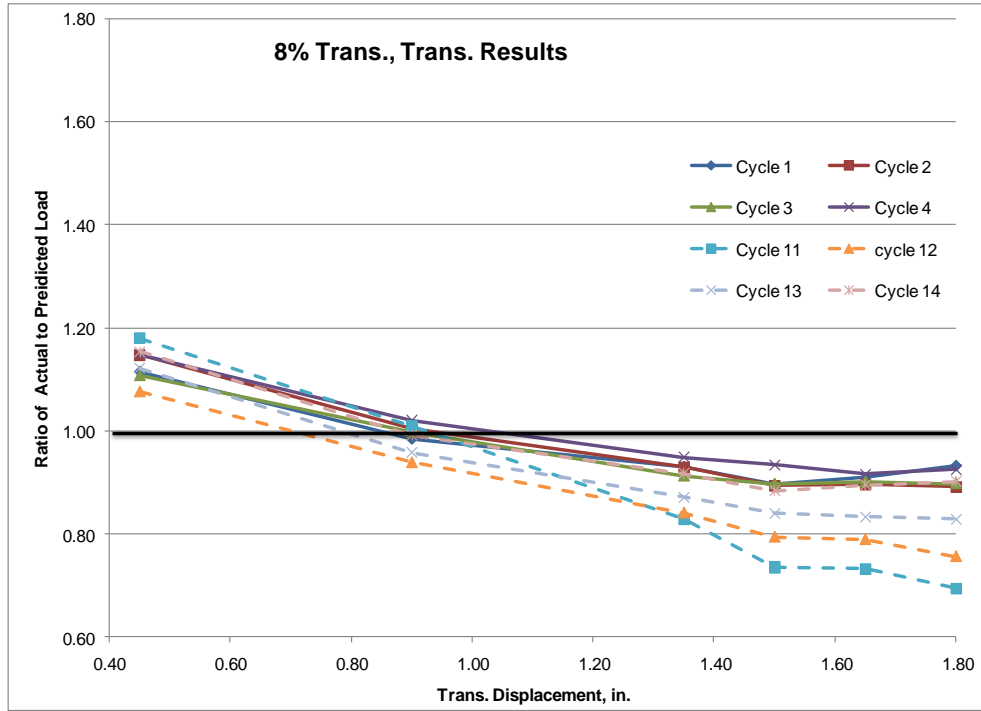


Figure 5.14 – Single Pad Trans. Results for 8% Test

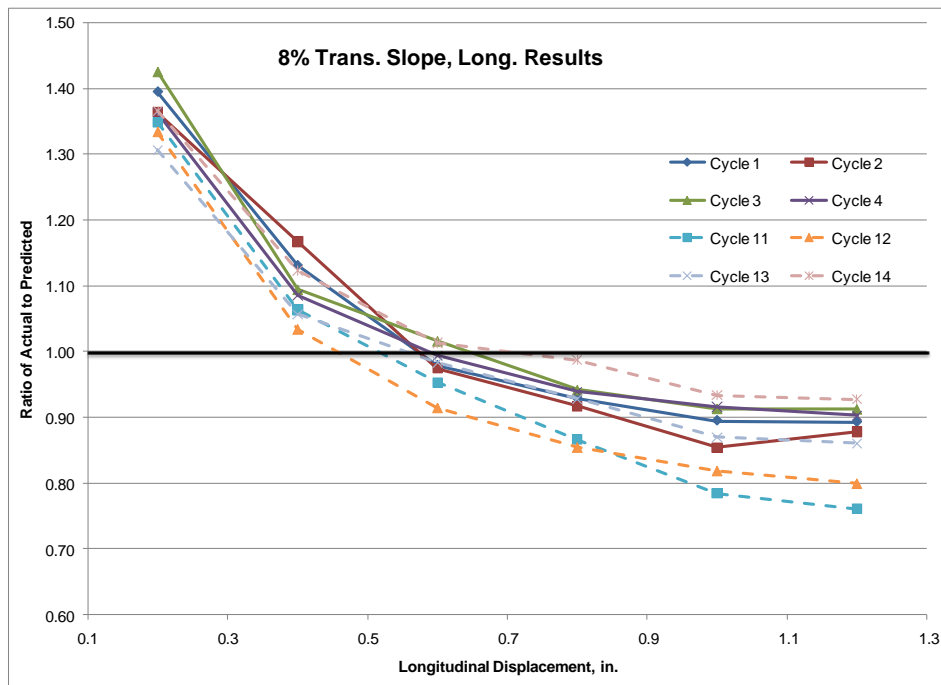


Figure 5.15 – Single Pad Long. Results for 8% Test

Results for the double pad tests are shown next. For only transverse loading, the ratios stay conservative (above 1.0) for transverse slopes of approximately 6.0% or less. This is slightly better than the single pad results. Since the double pads have a higher resistance to bending in the transverse direction, this was not unexpected. When the longitudinal loading is applied in conjunction with the transverse loading, the ratios drop below 1.0 for longitudinal displacements of approximately 0.70 in. (approximately twice the limit for the single pads) This indicates that double pads that experience both a transverse and longitudinal force exert more force to the superstructure than predicted with the conventional equations when the longitudinal displacement exceeds approximately 0.70 in.

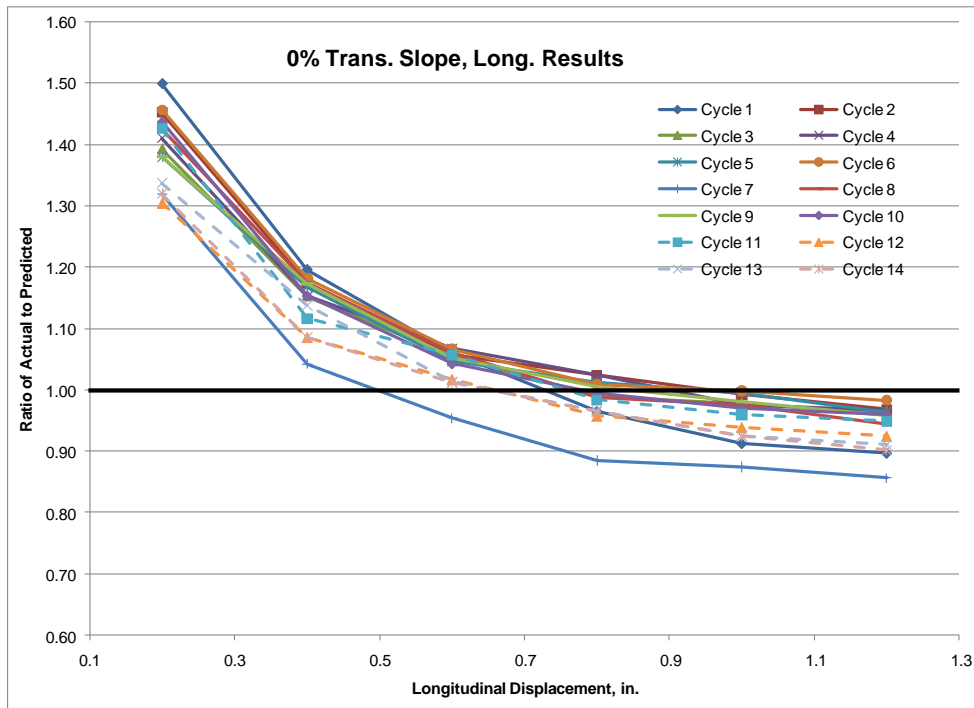


Figure 5.16 – Double Pad Long. Results for 0% Test

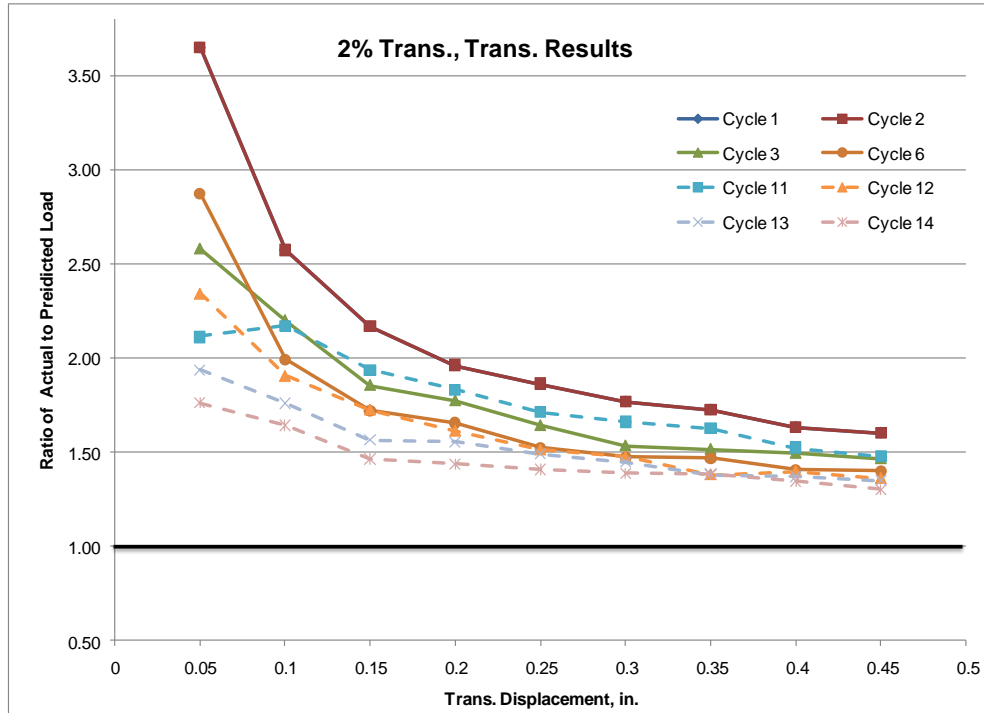


Figure 5.17 – Double Pad Trans. Results for 2% Test

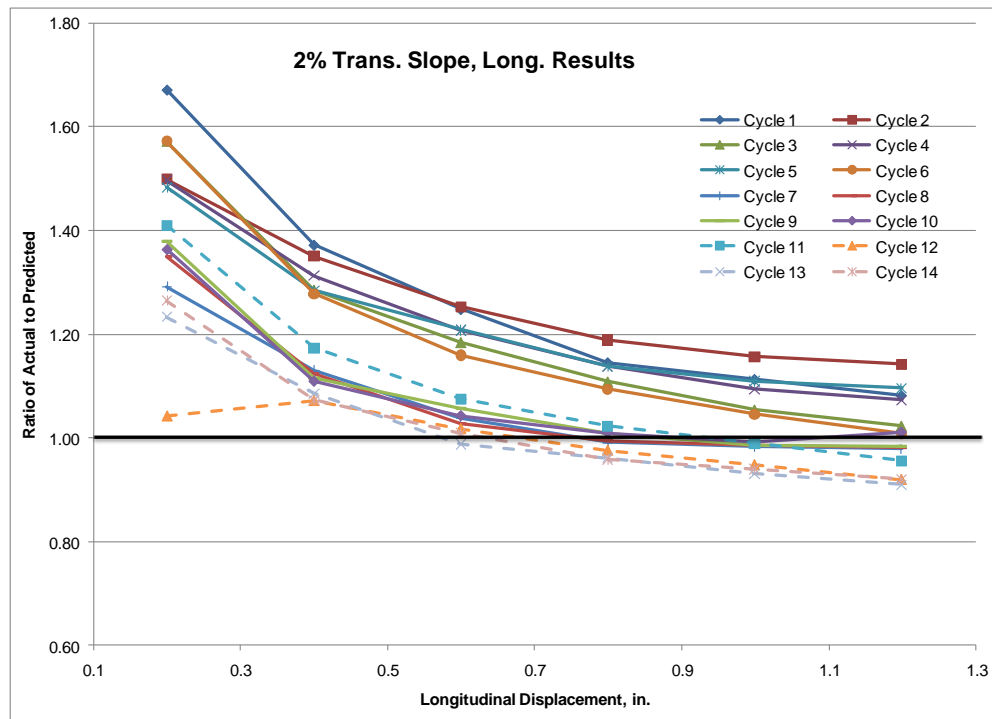


Figure 5.18 – Double Pad Long. Results for 2% Test

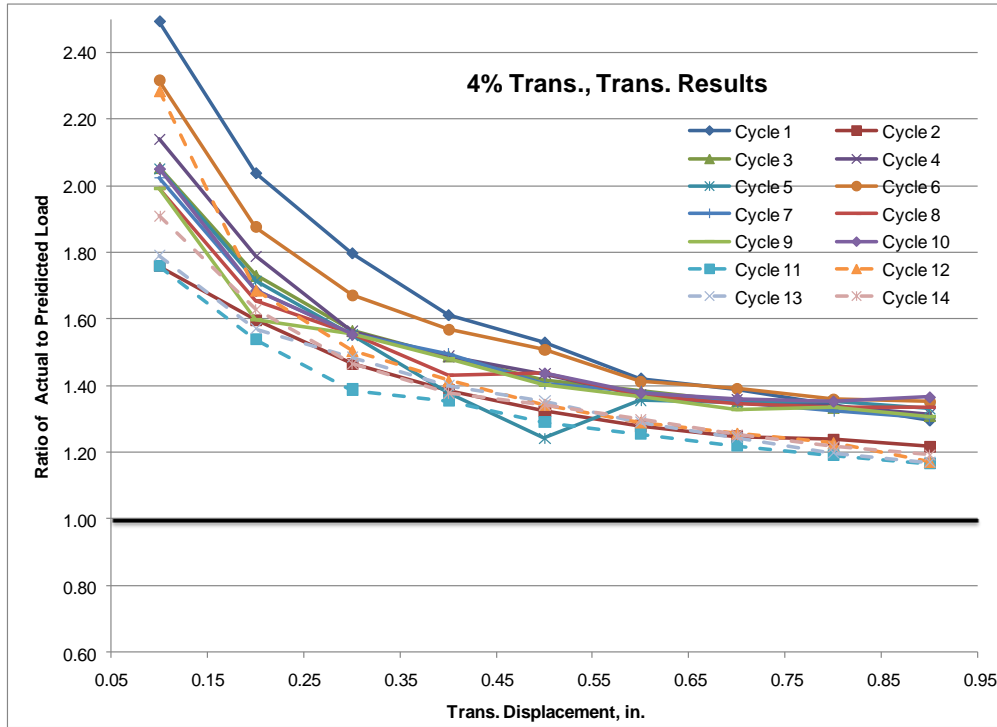


Figure 5.19 – Double Pad Trans. Results for 4% Test

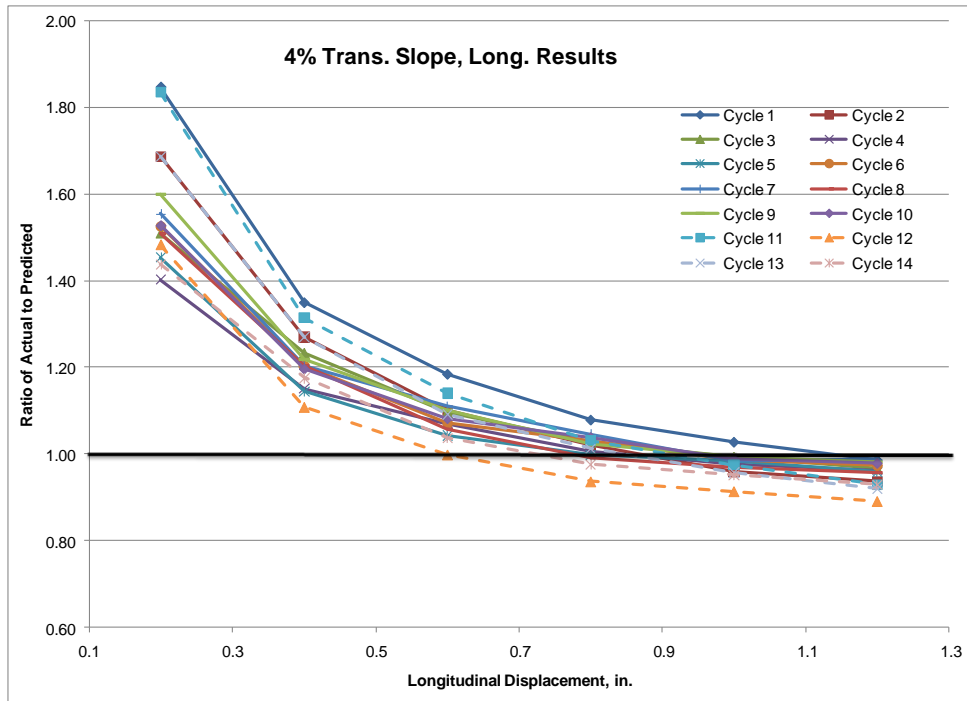


Figure 5.20 – Double Pad Long. Results for 4% Test

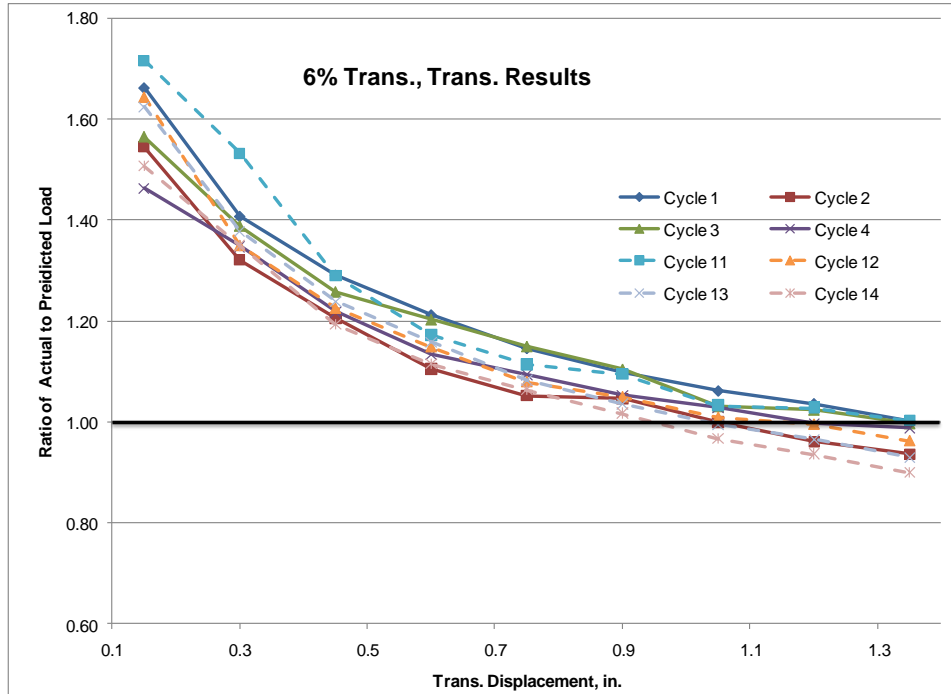


Figure 5.21 – Double Pad Trans. Results for 6% Test

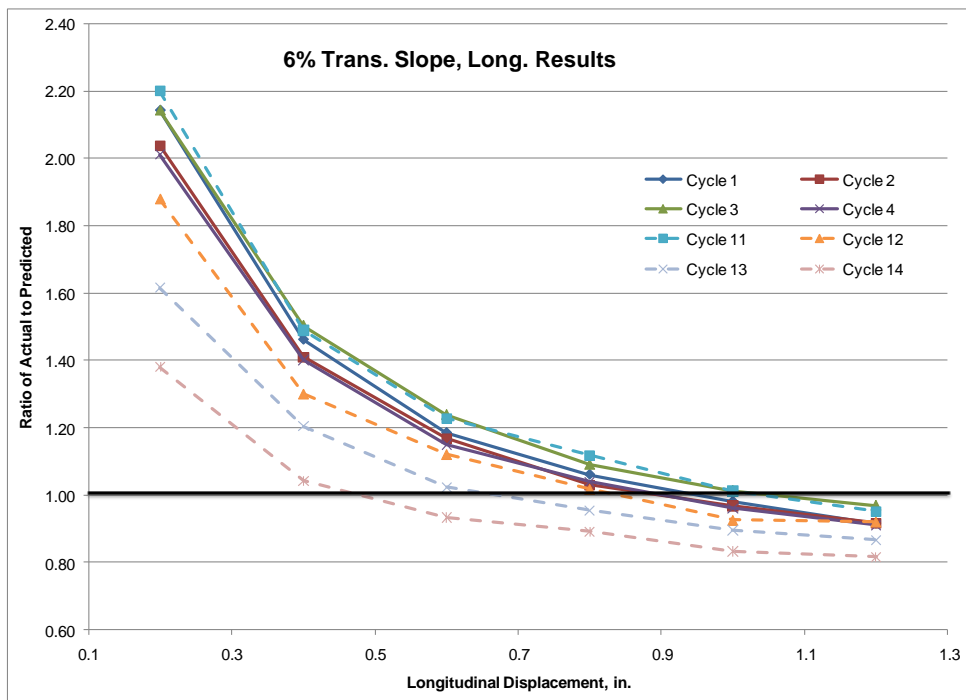


Figure 5.22 – Double Pad Long. Results for 6% Test

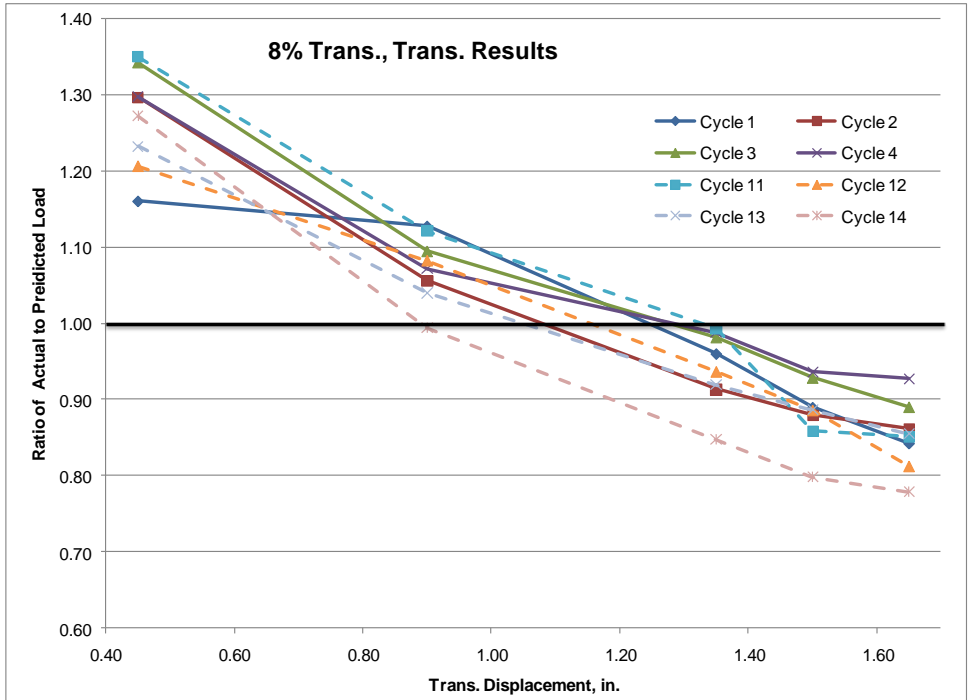


Figure 5.23 – Double Pad Results for 8% Test

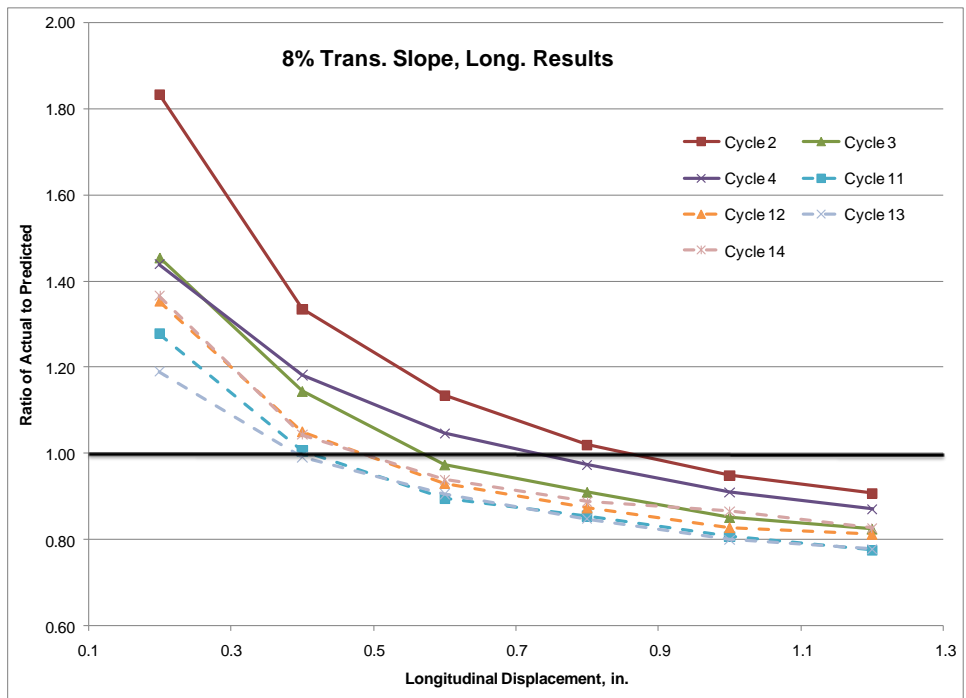


Figure 5.24 – Double Pad Long. Results for 8% Test

## 5.2. Prediction of Transverse and Longitudinal Deflections

The analysis of transverse and longitudinal deflections in section 5.1 focused mainly on the forces required to cause the deflections. This section will present a discussion of the observed shear strains in the longitudinal and transverse directions and a prediction of the shear strains in their respective direction. This analysis was based on the laboratory observation of the displaced angles in the transverse and longitudinal directions. The raw data upon which the analyses are based is provided in Section 4.4. TechMRT used Statistical Analysis Software (SAS<sup>®</sup>), Version 9.2, to aid in the regression calculations.

### 5.2.1. Analysis of Transverse Angles Observed

The first observation with respect to the transverse displacement is that the average transverse angle witnessed increased with an increase in superelevation. These trends are illustrated in Figure 5.25 and Figure 5.26. In addition to the average displacements, a prediction line resulting from linear regression analysis appears in each figure that will be discussed later in this section.

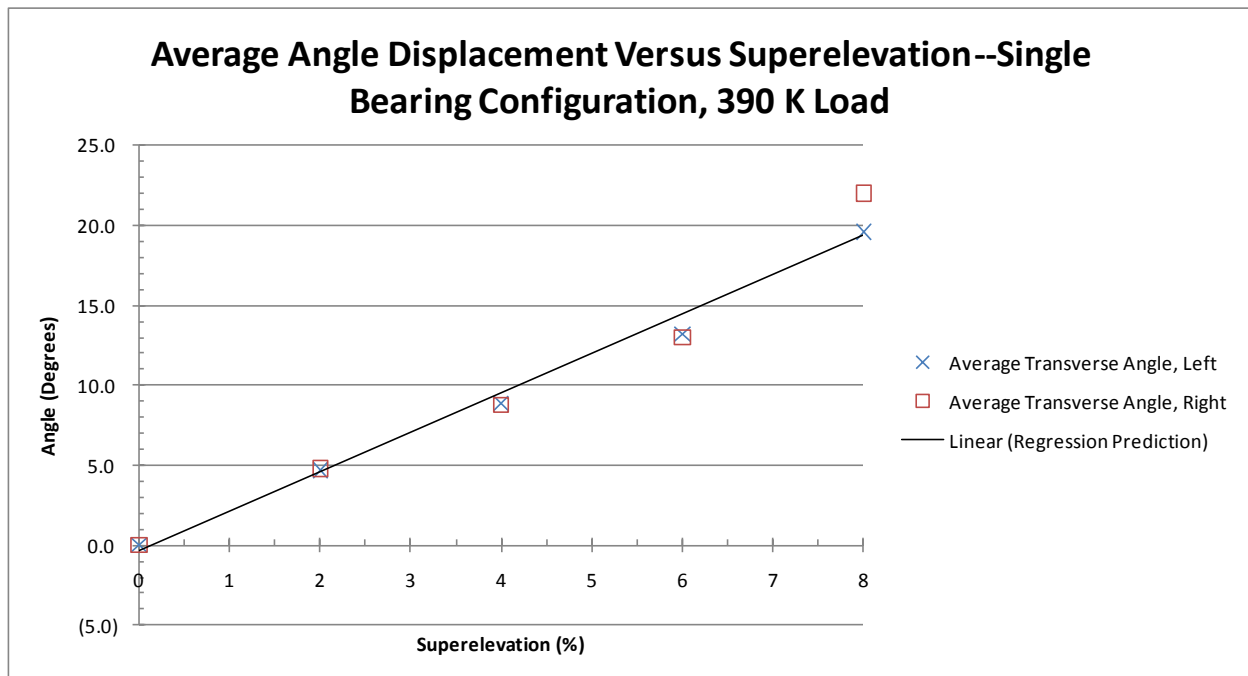


Figure 5.25—Summary of Transverse Displacement, Single Bearing Configuration

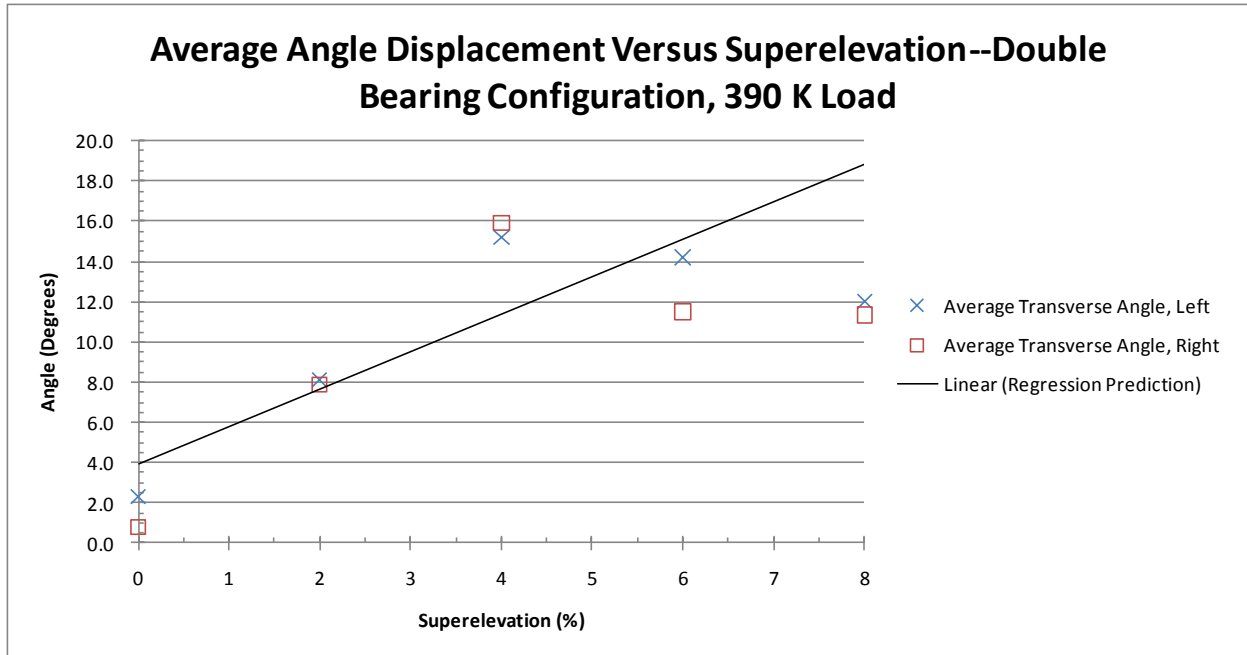


Figure 5.26—Summary of Transverse Displacement, Double Bearing Configuration

This pattern makes sense in that for an increased superelevation, one would expect an increase in the transverse angle observed. This increase continued throughout for each incremental increase in superelevation for the single pad configuration. The increase in the resulting transverse angle with an incremental increase in superelevation is not as apparent with the double pad configuration, but it does exist. The incremental increase in the transverse with an increase in superelevation appears to reach a point of diminishing returns for the double bearing configuration. This trend will be explained later in this section when discussing the regression analysis.

Figure 5.27 through Figure 5.30 show the observed change in transverse angle after the application of all the forces to the bearing pads for each test run of the single pad configuration at each respective superelevation. Test runs one through ten use a total vertical load of 390 kips, while test runs 11 through 14 use a total vertical load of 150 kips, 210 kips, 270 kips, and 330 kips, respectively. From the patterns illustrated in Figure 5.27 through Figure 5.30, the vertical load applied also appears to effect the resulting transverse displacement. Thus for the single pad configuration, there appears to be an increase in the transverse angle observed with an increase in the total vertical load applied.

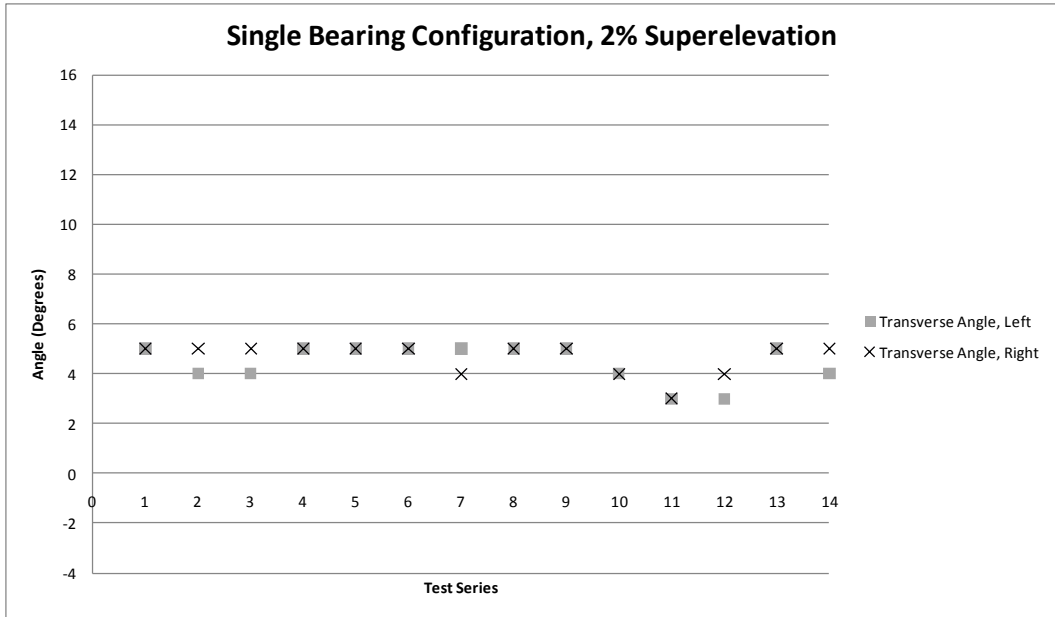


Figure 5.27--Summary of Transverse Displacement, 2% Single Pad Configuration

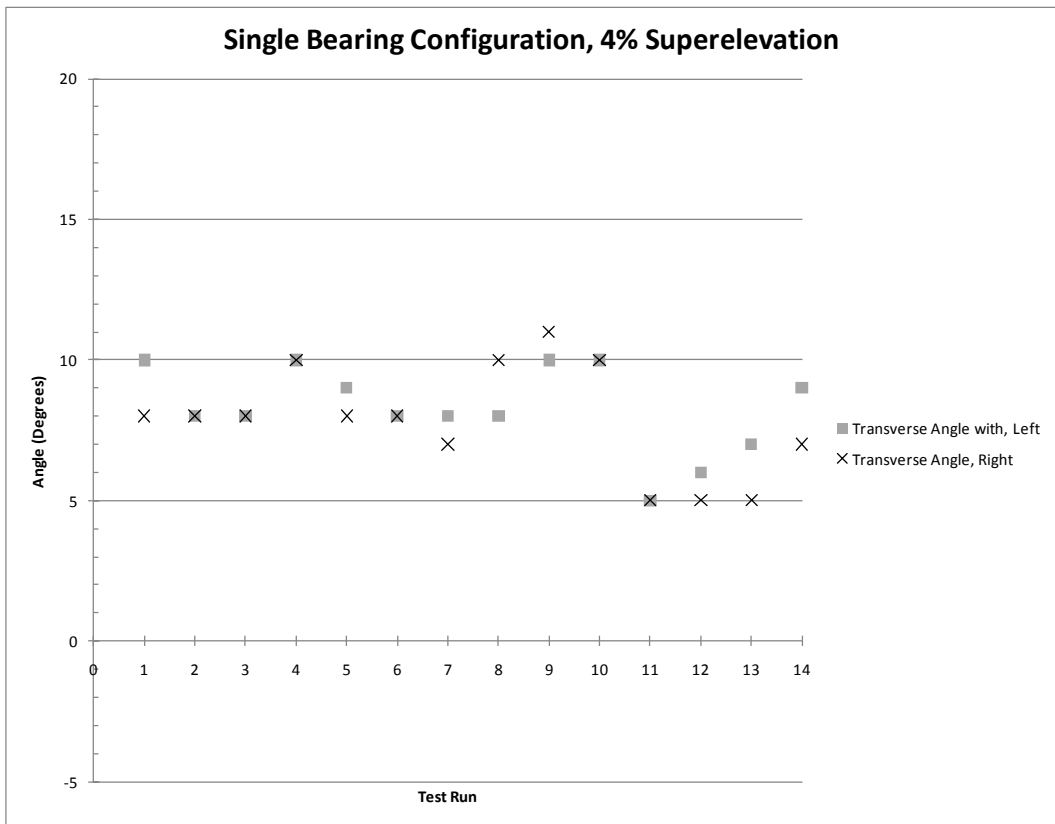


Figure 5.28--Summary of Transverse Displacement, 4% Single Pad Configuration

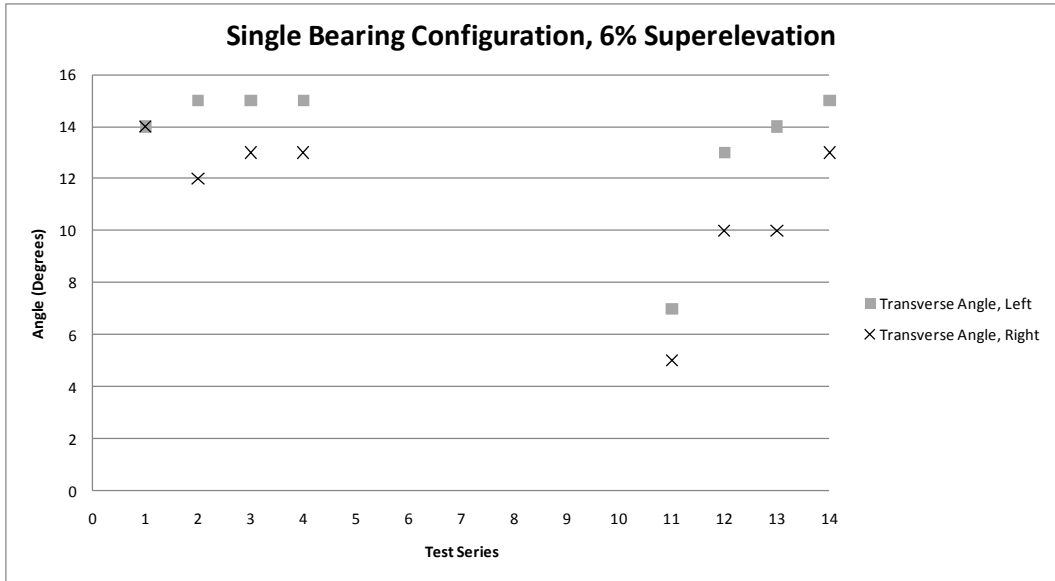


Figure 5.29--Summary of Transverse Displacement, 6% Single Pad Configuration

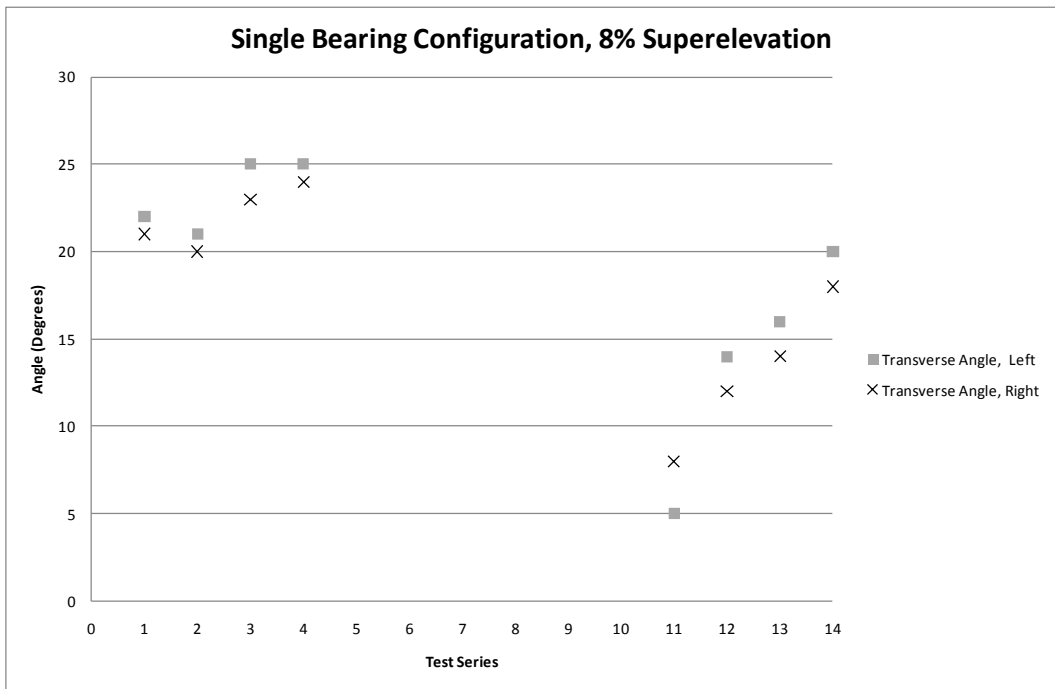


Figure 5.30--Summary of Transverse Displacement, 8% Single Pad Configuration

Figure 5.31 through Figure 5.34 show the observed change in transverse angle after the application of all forces to the double bearing pads for each test run at each respective superelevation. The vertical loads for each test run match those of the single pad configuration discussed earlier. The trend for the effect of the vertical load on the observed transverse angle is

not as visible for the double pad configuration as it was with the single pad configuration. A trend is believed to exist but is not visually apparent, and will be discussed in section 5.2.3 of this chapter.

### **5.2.2. Analysis of Longitudinal Angles Observed**

Figure 5.35 and Figure 5.36 display the average change in the longitudinal angle observed after the application of all forces to the bearing pads. In addition to the average change in angles, a prediction line resulting from linear regression analysis appears in each figure that will be discussed in the regression section of this chapter. An interesting trend develops for the longitudinal angles in that the longitudinal angle increases with an increase in superelevation for the single pad, yet decreases for an increase in superelevation for the double pad configuration.

Figure 5.37 through Figure 5.41 show the observed change in the longitudinal angle after the application of the all the forces to the bearing pads for each single pad test run at each respective superelevation. Test runs one through ten use a total vertical load of 390 kips while test runs 11 through 14 use a total vertical load of 150 kips, 210 kips, 270 kips, and 330 kips, respectively. As with the transverse angles observed, there appears to be a trend for the longitudinal angle observed with a respective increase in the vertical load applied. The trend does not appear to be as strong for the longitudinal angle as it did with the transverse angles.

Figure 5.42 through Figure 5.46 show the observed change in the longitudinal angle after the application of all forces to the double bearing pads for each test run at each respective superelevation. The vertical loads for each test run match those of the single pad configuration discussed earlier. Similar to that of the transverse angle case, no significant trend appears for the longitudinal angles observed for the double pad configuration within each superelevation.

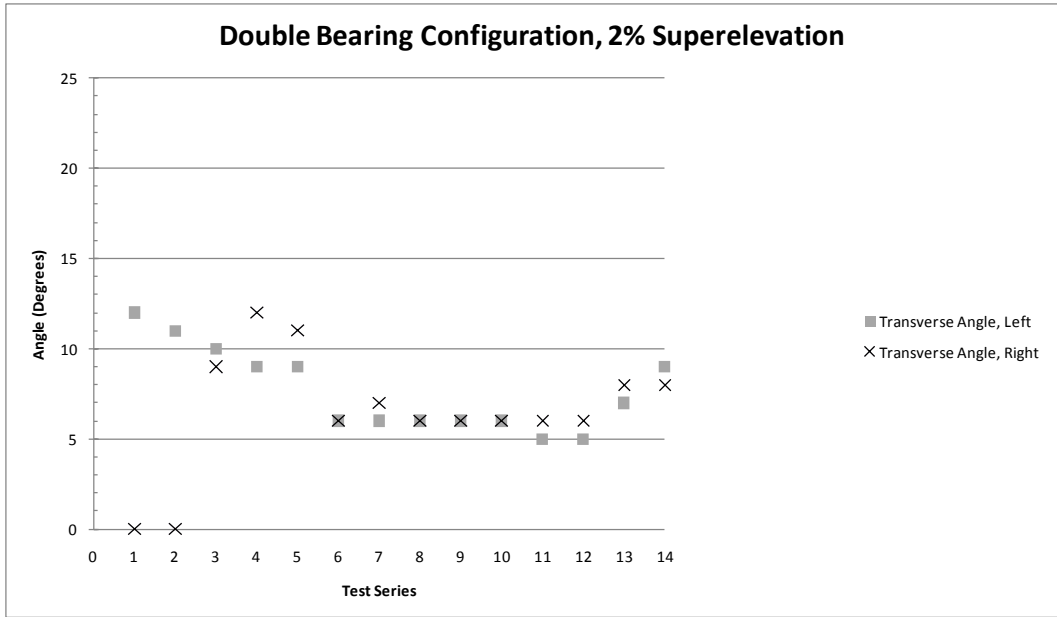


Figure 5.31--Summary of Transverse Displacement, 2% Double Pad Configuration

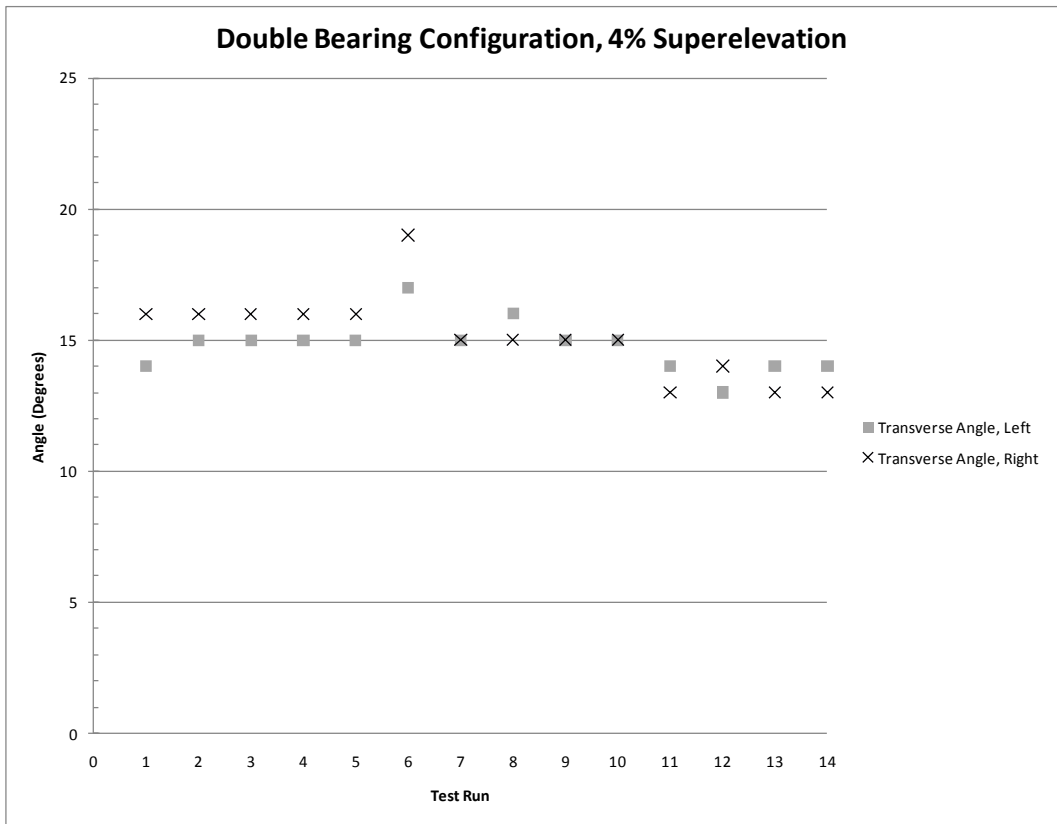


Figure 5.32--Summary of Transverse Displacement, 4% Double Pad Configuration

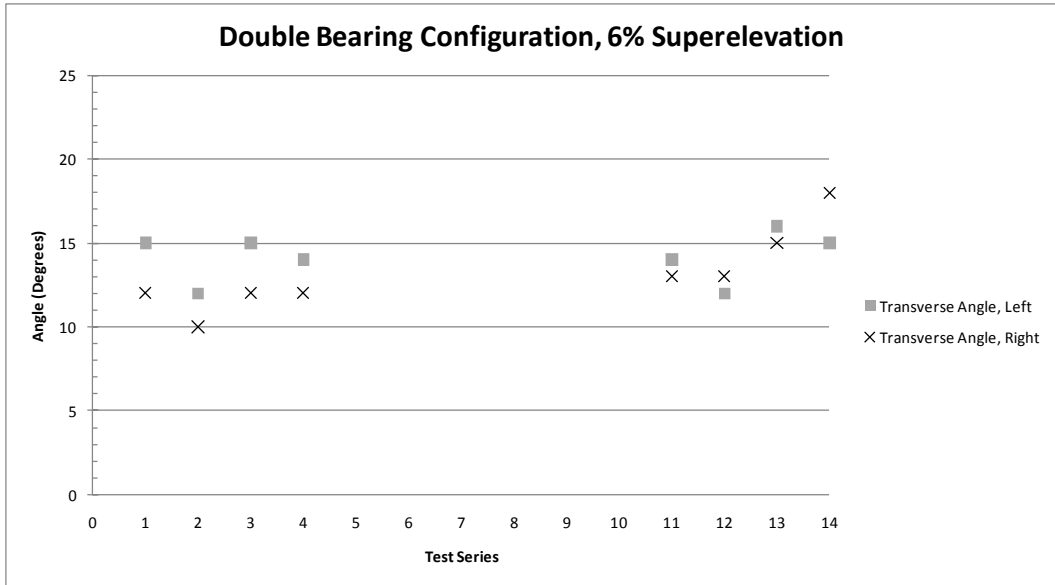


Figure 5.33--Summary of Transverse Displacement, 6% Double Pad Configuration

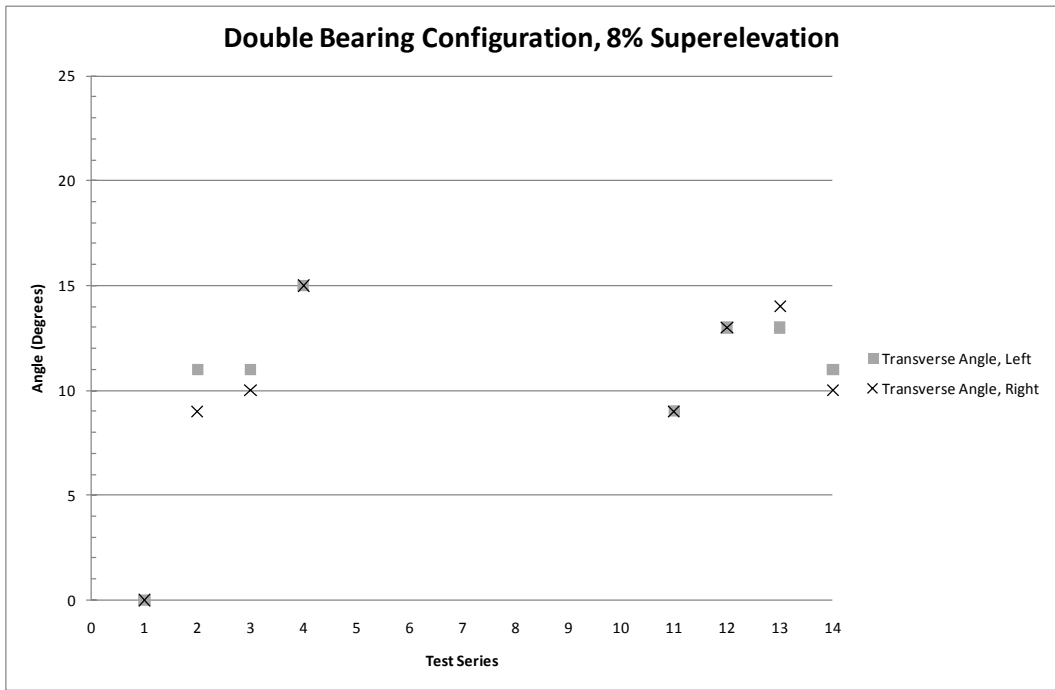


Figure 5.34--Summary of Transverse Displacement, 8% Double Pad Configuration

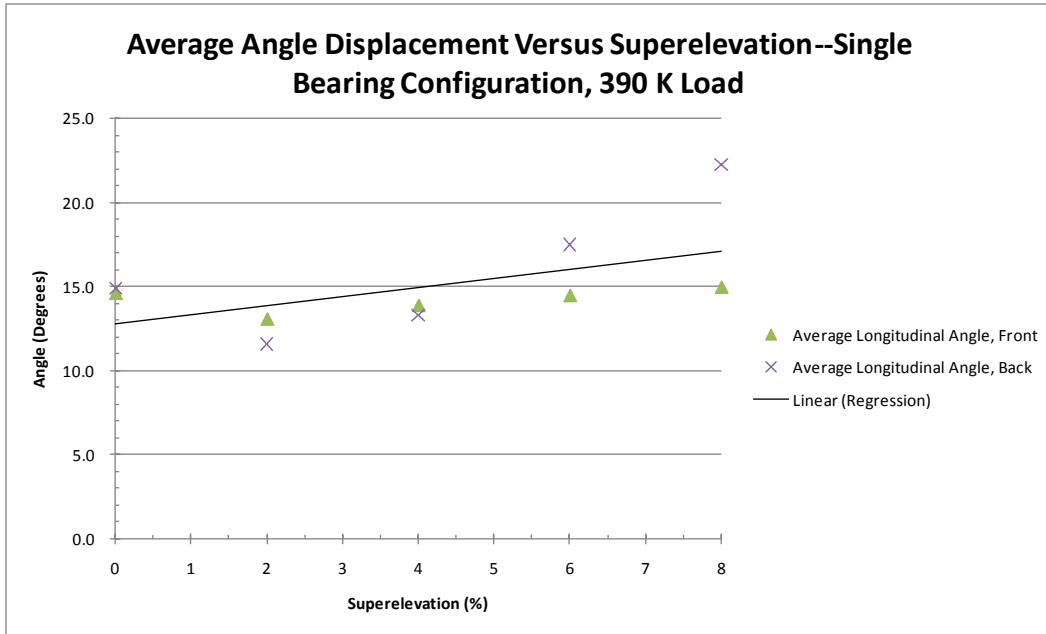


Figure 5.35--Summary of Longitudinal Displacement, Single Pad Configuration

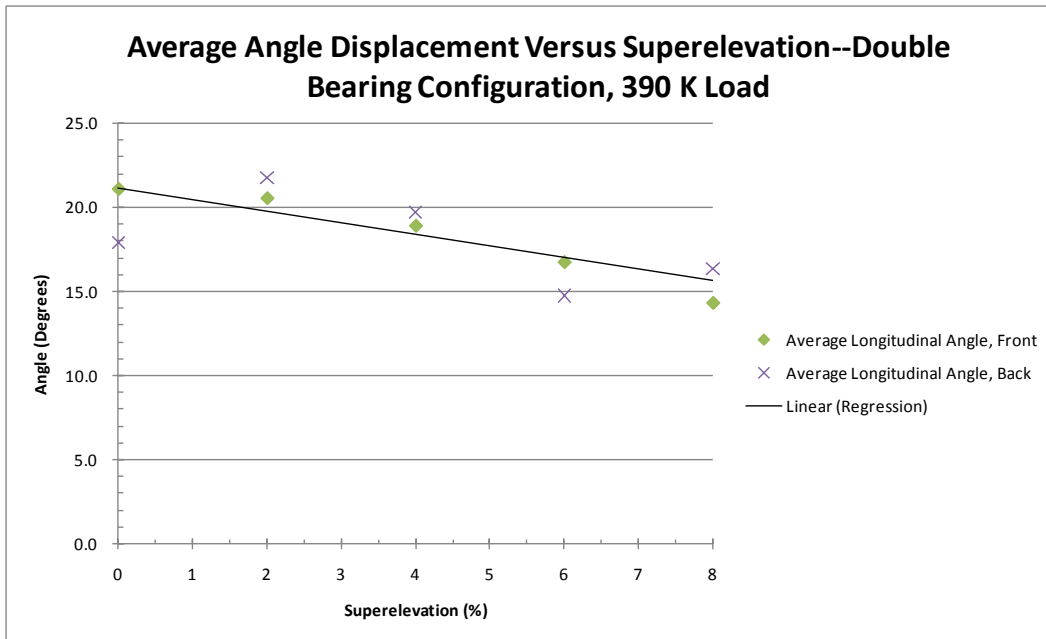


Figure 5.36--Summary of Longitudinal Displacement, Double Pad Configuration

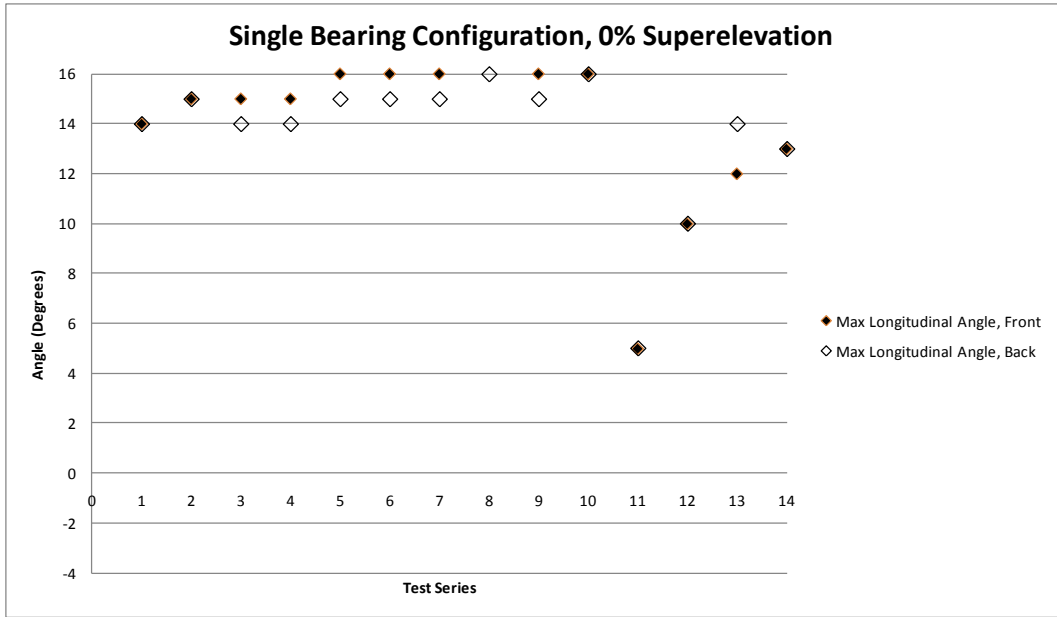


Figure 5.37--Summary of Longitudinal Displacement, 0% Single Pad Configuration

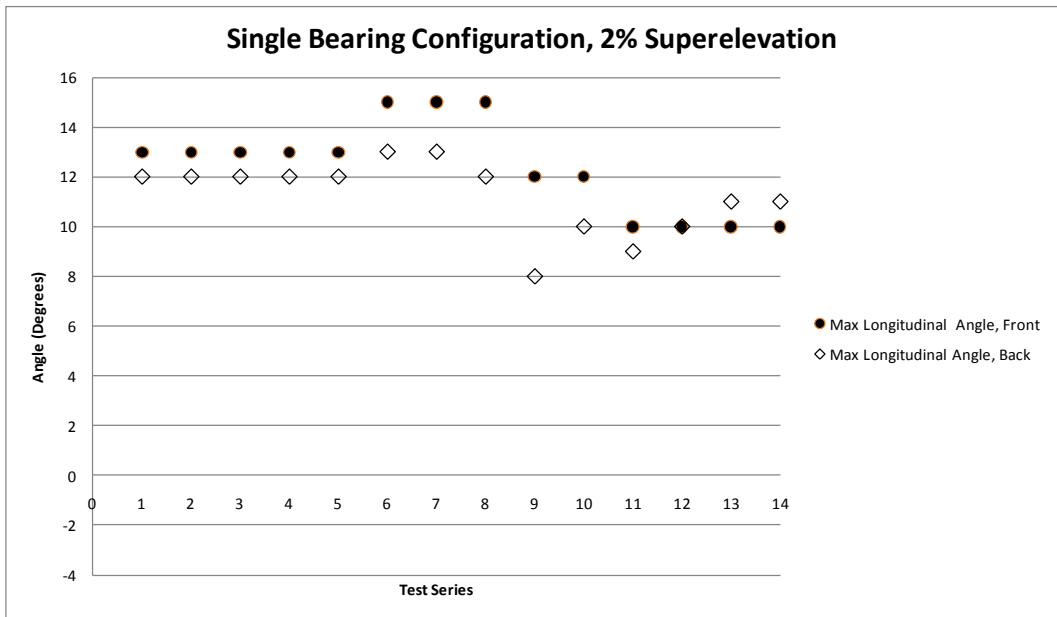


Figure 5.38--Summary of Longitudinal Displacement, 2% Single Pad Configuration

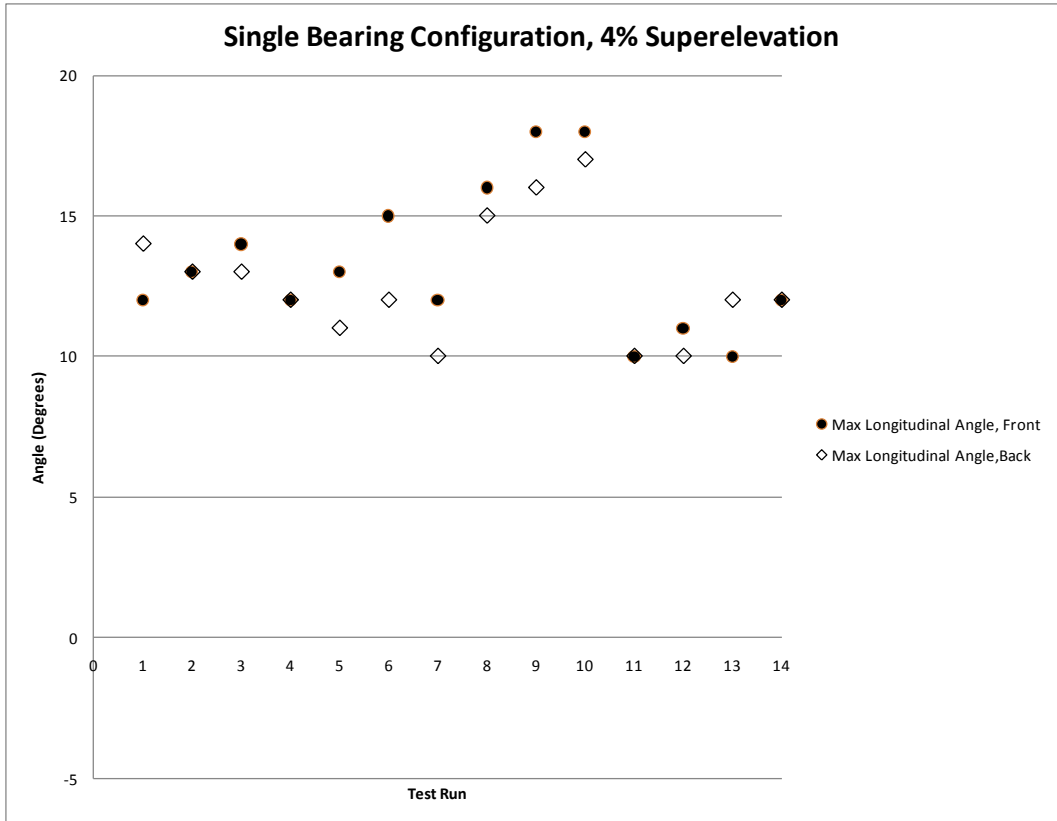


Figure 5.39--Summary of Longitudinal Displacement, 4% Single Pad Configuration

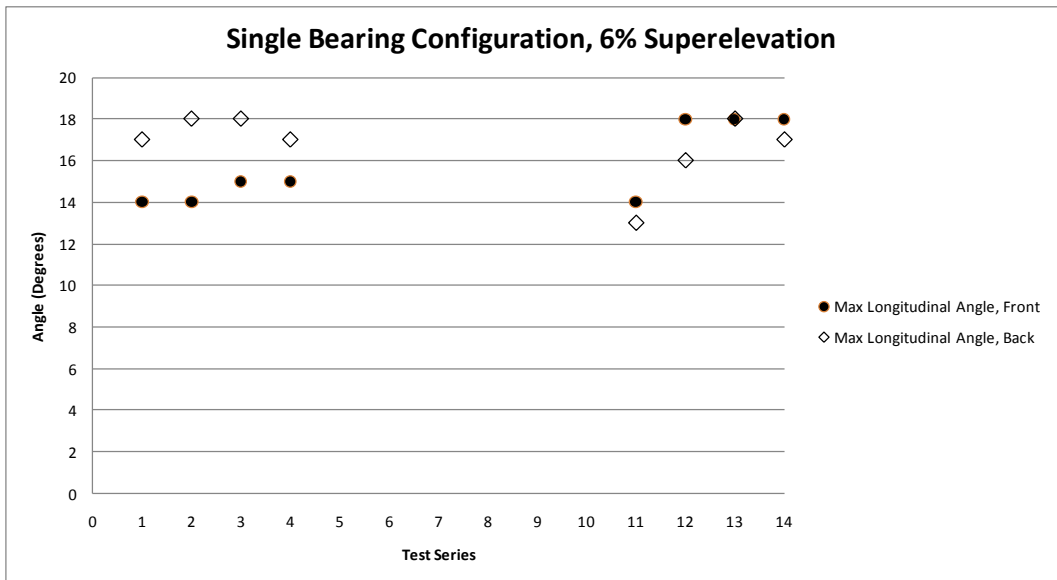


Figure 5.40--Summary of Longitudinal Displacement, 6% Single Pad Configuration

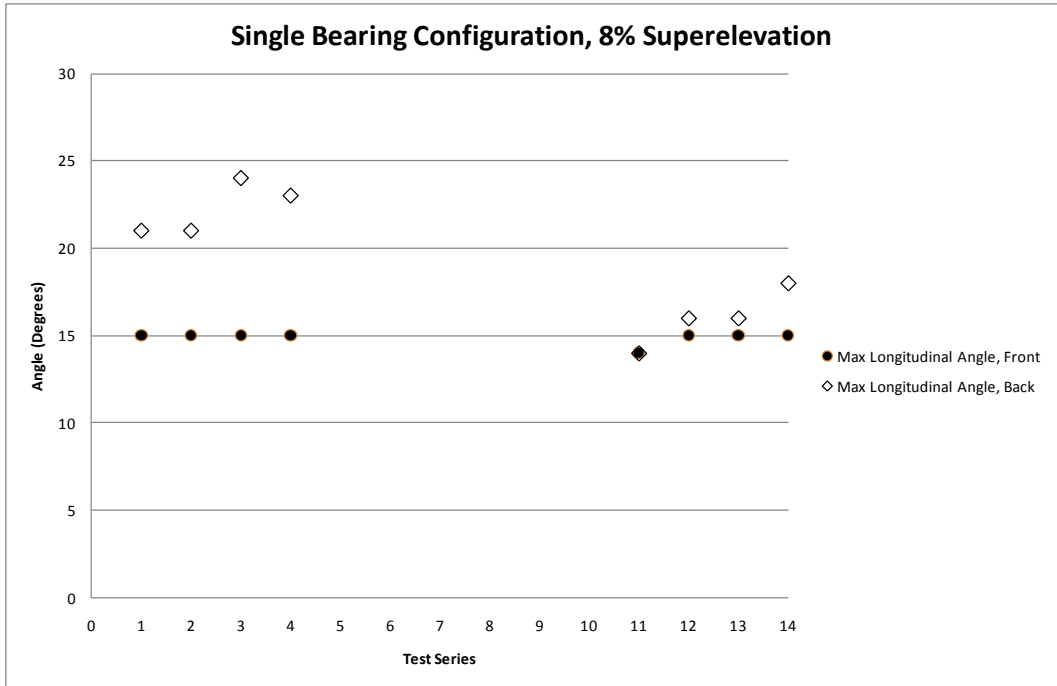


Figure 5.41--Summary of Longitudinal Displacement, 8% Single Pad Configuration

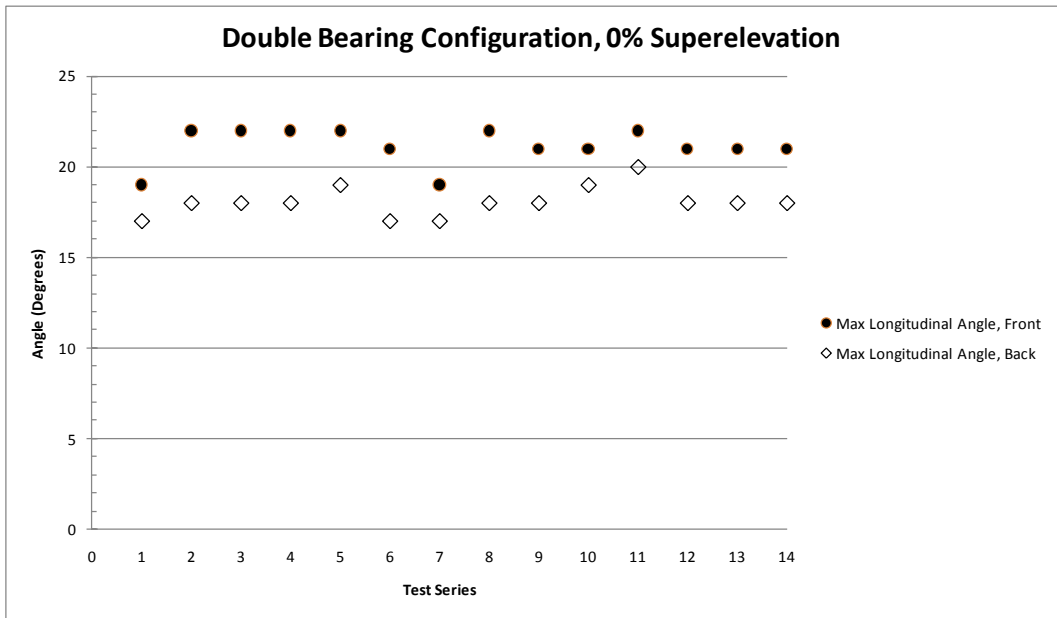


Figure 5.42--Summary of Longitudinal Displacement, 0% Double Pad Configuration

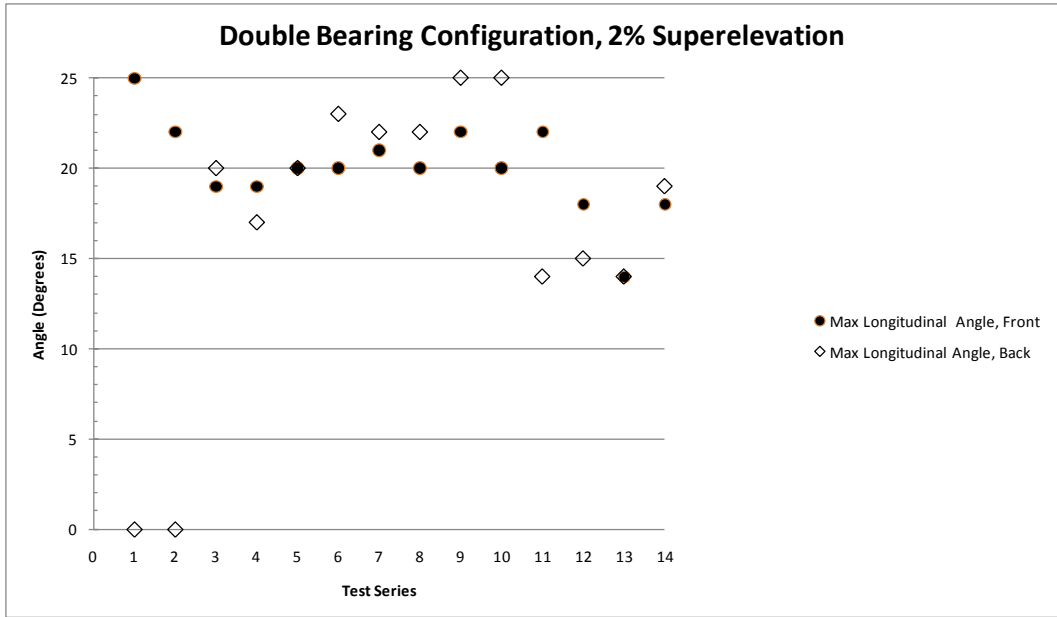


Figure 5.43--Summary of Longitudinal Displacement, 2% Double Pad Configuration

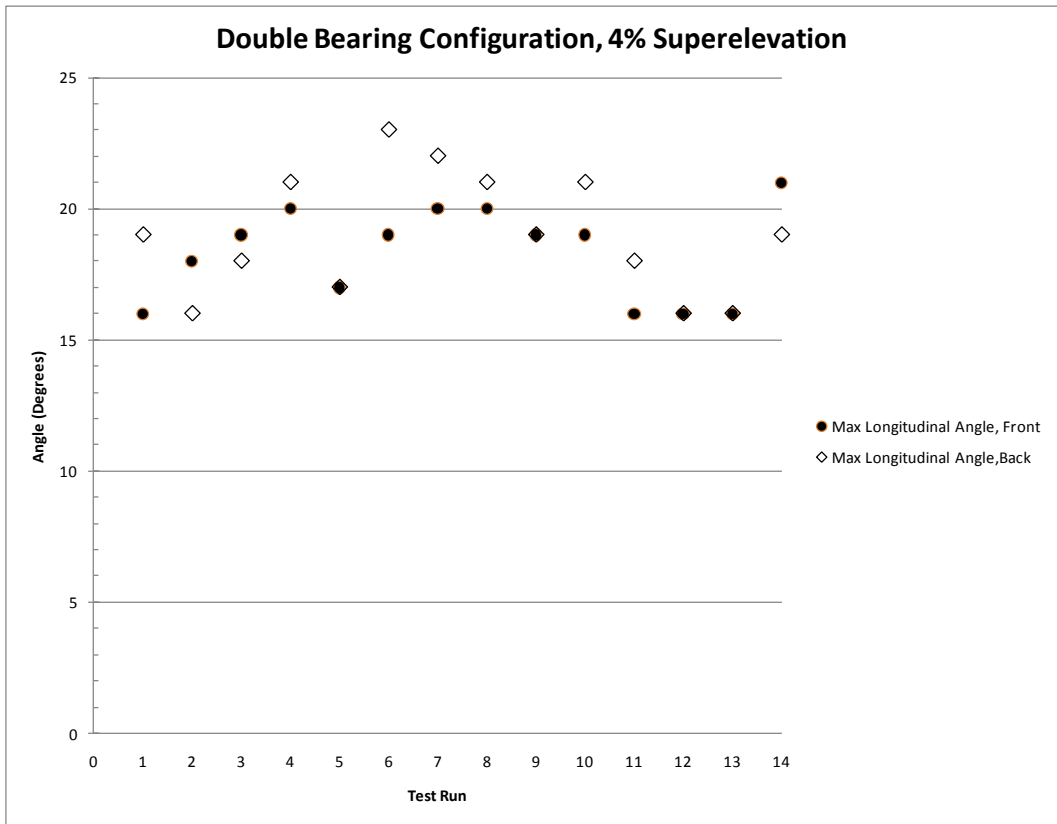


Figure 5.44--Summary of Longitudinal Displacement, 4% Double Pad Configuration

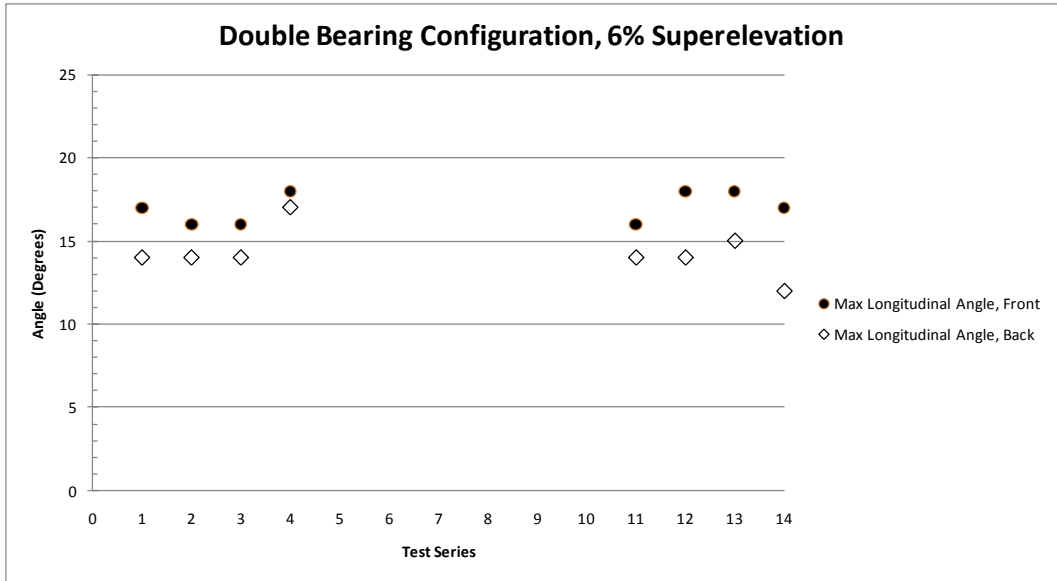


Figure 5.45--Summary of Longitudinal Displacement, 6% Double Pad Configuration

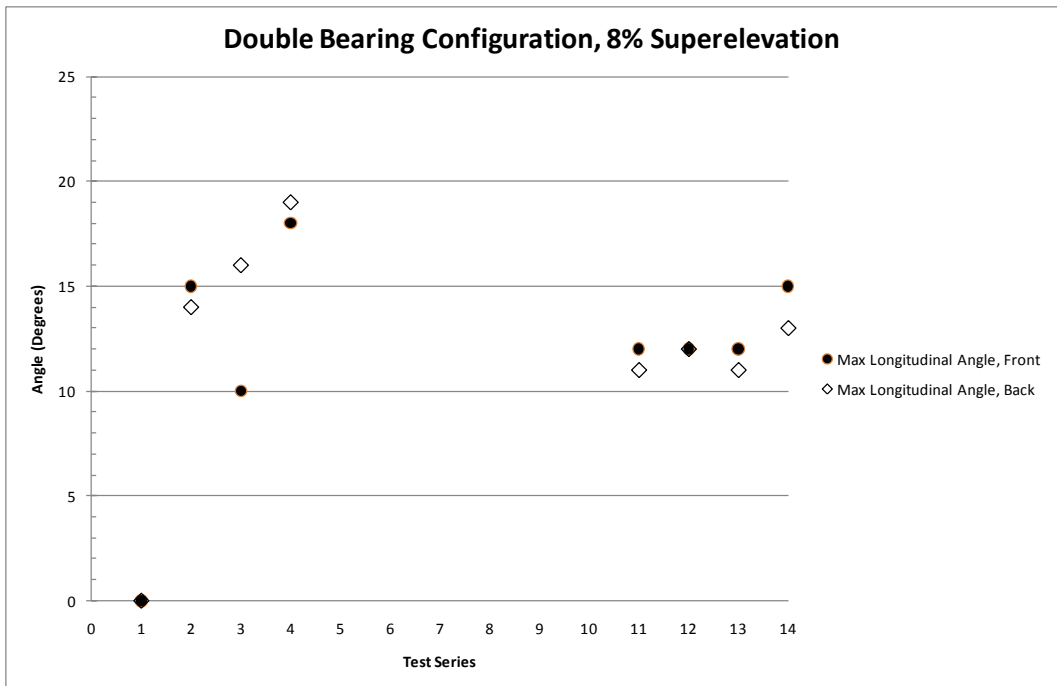


Figure 5.46--Summary of Longitudinal Displacement, 8% Double Pad Configuration

### 5.2.3. Regression Analysis of Laboratory Results

TechMRT conducted a regression analysis in order to determine if a prediction model for the transverse and longitudinal displacements could be developed. Table 5.1 shows the predictor variables used in the regression models analyzed. Initially, it was thought that separate models would need to be developed for the single pad and double pad configurations. With the addition of an indicator variable to account for the bearing pad configuration, this idea was decided against in favor of a single model that predicts the displacements. Two models were developed: first for the transverse displacement, Y1 in degrees, and second for the longitudinal displacement, Y2 in degrees.

Table 5.1—Predictor Variables used in Regression Analysis

Predictor Variable	Description
X1	The Transverse Superelevation of the beam, expressed as a percent.
X2	An Indicator Value to describe the bearing configuration, 0 for a single bearing and 1 for a double bearing
X3	Total Vertical Load Applied to Bearing Configuration in Kips
X12	The interaction of both the transverse superelevation and bearing configuration (X1 times X2)
X13	The interaction of both the transverse superelevation and total vertical load (X1 times X3)
X1sq	Square of the Transverse Superelevation

To begin the analysis, a stepwise procedure was used to determine which variable combinations best explain the observed data. Once the variables were identified, models were run to determine which model provided the best fit. TechMRT used the adjusted R-square value for each model to determine which model was the best. Statistically speaking, the R-square value for a specific model will generally increase when additional variables are added to the model. The adjusted R-square value takes into account the number of variables in the model, thus providing a better decision criterion to determine the best model. Ultimately, the best prediction model would be the simplest model having the highest adjusted R-square value.

It became apparent from the stepwise analysis that predictor variables representing the superelevation of the beam and the bearing pad configuration provide a good starting point for the prediction model of both the transverse and longitudinal displacements. This makes sense as it mirrors the results discussed in the previous section. From here, eleven models for the transverse displacement were run containing different combinations of additional variables beyond the two initial variables. The best models based upon the adjusted R-square value and the results of the regression analysis are shown in Figure 5.47 and Figure 5.48.

<b>Analysis of Variance</b>					
<b>Source</b>	<b>Degrees of Freedom</b>	<b>Sum of Squares</b>	<b>Mean Square</b>	<b>F-Value</b>	<b>Pr &gt; F</b>
Model	4	6351.02535	1587.756	176.13	<.0001
Error	223	2010.22026	9.01444		
Corrected Total	227	8361.24561			
R-Square: 0.7596 Adjusted R-Square: 0.7553					
<b>Parameter Estimates</b>					
<b>Variable</b>	<b>Degrees of Freedom</b>	<b>Parameter Estimate</b>	<b>Standard Error</b>	<b>t-Value</b>	<b>Pr &gt;  t </b>
Intercept	1	-4.90711	0.97775	-5.02	<.0001
X1	1	2.2331	0.10446	21.38	<.0001
X2	1	4.27978	0.63841	6.7	<.0001
X3	1	0.01358	0.00246	5.52	<.0001
x12	2	-0.61591	0.14909	-4.13	<.0001

Figure 5.47– Regression Summary for Model 7, Transverse Angle

The two models are very similar. Both models incorporate the superelevation of the bearing, the bearing pad configuration, and the interaction of these two variables. Model 7 incorporates the vertical load applied while Model 11 incorporates the interaction of the

<b>Analysis of Variance</b>					
<b>Source</b>	<b>Degrees of Freedom</b>	<b>Sum of Squares</b>	<b>Mean Square</b>	<b>F-Value</b>	<b>Pr &gt; F</b>
Model	4	6543.86817	1635.967	200.74	<.0001
Error	223	1817.37744	8.14967		
Corrected Total	227	8361.24561			
R-Square: 0.7826 Adjusted R-Square: 0.7787					
<b>Parameter Estimates</b>					
<b>Variable</b>	<b>Degrees of Freedom</b>	<b>Parameter Estimate</b>	<b>Standard Error</b>	<b>t-Value</b>	<b>Pr &gt;  t </b>
Intercept	1	-0.2915	0.42691	-0.68	0.4954
X1	1	0.96478	0.18755	5.14	<.0001
X2	1	4.24857	0.60703	7	<.0001
x12	1	-0.60155	0.14179	-4.24	<.0001
x13	2	0.00384	0.000507	7.58	<.0001

Figure 5.48 – Regression Summary for Model 11, Transverse Angle

superelevation and the vertical load applied. With only a three percent increase in adjusted R-square value from Model 7 to Model 11, one could argue that Model 7 is the better fit. However, absent a significant difference in which variables are used in the prediction of the transverse angle, the model with the higher adjusted R-square value should be chosen. Since both models used the same variables and take into account the vertical load applied in some form, Model 11 from Figure 5.48 was chosen as the best prediction model:

$$Y1 = -0.292 + 0.965*X1 + 4.25*X2 - 0.602*X1*X2 + 0.00384*X1*X3 \quad \text{Equation 5.3}$$

where the variables are described in Table 5.1. This prediction model is included in Figure 5.25 and Figure 5.26. While the fit is much better for the single pad configuration, the double pad

configuration fit is acceptable. With an adjusted R-square value approaching 0.8, this model is fairly good in predicting the transverse displacement considering the variability in the data. If the R-square value had not been so high, separate prediction models would have been justified for each pad configuration rather than one a single model that accounts for the pad configurations.

For the longitudinal angles observed, the same analysis used for the transverse angle was conducted to determine the best model. Again, the stepwise procedure yielded the same starting point of using the superelevation of the bearing and pad configuration as the base model to start with. From there, twelve different models were analyzed. The best two models, based on the adjusted R-square criteria, were for Models 5 and 7. These models are highlighted in Figure 5.49 and Figure 5.50, respectively.

<b>Analysis of Variance</b>					
<b>Source</b>	<b>Degrees of Freedom</b>	<b>Sum of Squares</b>	<b>Mean Square</b>	<b>F-Value</b>	<b>Pr &gt; F</b>
Model	3	1637.91092	545.9703	76.83	<.0001
Error	224	1591.80838	7.10629		
Corrected Total	227	3229.7193			
R-Square: 0.5071 Adjusted R-Square: 0.5005					
<b>Parameter Estimates</b>					
<b>Variable</b>	<b>Degrees of Freedom</b>	<b>Parameter Estimate</b>	<b>Standard Error</b>	<b>t-Value</b>	<b>Pr &gt;  t </b>
Intercept	1	12.29029	0.39801	30.88	<.0001
X1	1	0.47787	0.09224	5.18	<.0001
X2	1	8.30411	0.56683	14.65	<.0001
x12	1	-1.22941	0.13237	-9.29	<.0001

Figure 5.49– Regression Summary for Model 5, Longitudinal Angle

<b>Analysis of Variance</b>					
<b>Source</b>	<b>Degrees of Freedom</b>	<b>Sum of Squares</b>	<b>Mean Square</b>	<b>F-Value</b>	<b>Pr &gt; F</b>
Model	4	1938.86292	484.7157	83.74	<.0001
Error	223	1290.85638	5.78859		
Corrected Total	227	3229.7193			
<p>R-Square: 0.6003 Adjusted R-Square: 0.5932</p>					
<b>Parameter Estimates</b>					
<b>Variable</b>	<b>Degrees of Freedom</b>	<b>Parameter Estimate</b>	<b>Standard Error</b>	<b>t-Value</b>	<b>Pr &gt;  t </b>
Intercept	1	7.2696	0.78351	9.28	<.0001
X1	1	0.54122	0.08371	6.47	<.0001
X2	1	8.30073	0.51158	16.23	<.0001
X3	1	0.01421	0.00197	7.21	<.0001
x12	2	-1.21939	0.11947	-10.21	<.0001

Figure 5.50– Regression Summary for Model 7, Longitudinal Angle

The prediction models shown in Figure 5.49 and Figure 5.50 contain the predictor variables of the bearing’s superelevation, pad configuration, and the interaction of these two effects. The difference is that Model 7 also utilizes the total vertical load applied in accounting for the prediction of the longitudinal angle observed. Remember that slight trends accounting for the total vertical load did appear in the figures in the previous section. This fact combined with a significantly higher adjusted R-square value (a nearly 20% increase) led TechMRT to chose Model 7 as the best prediction model for the longitudinal displacement. The model is shown in Equation 5.4. This prediction model is also included in Figure 5.35 and Figure 5.36 and appears to fit very well.

$$Y_2 = 7.27 + 0.541 * X_1 + 8.30 * X_2 + 0.0142 * X_3 - 1.22 * X_1 * X_2 \quad \text{Equation 5.4}$$

where the variables are described in Table 5.1.

#### **5.2.4. Summary of Transverse and Longitudinal Displacements**

In summary, both the transverse and longitudinal displacements of the bearing pads are affected by the bearing's superelevation and pad configuration, along with the interaction of these two variables. Both displacements are also affected by the total vertical load applied to the bearing; however, they differ in the way the load affects the displacement. For the transverse displacement, the total vertical load applied interacts with the superelevation to account for the angle displaced while just the total vertical load itself accounts for the longitudinal angle's displacement. The prediction equations for the transverse and longitudinal displacements are provided in Equation 5.3 and Equation 5.4, respectively.

### **5.3. Prediction of Uplift and/or Slipping**

Each bearing was tested under identical conditions for the first ten test runs consisting of a 390 kip vertical load. Test runs 11, 12, 13, and 14 had 150 kip, 210 kip, 270 kip, and 330 kip vertical loads respectively. The superelevations of 0%, 2%, 4%, 6%, and 8% were evaluated for both the single bearing and double bearing conditions. In addition to the forces required to cause the transverse and longitudinal displacements expected, any slip of the bearing with respect to the center block was measured. This slip represents the movement of the bearing with respect to the beam that is transferring its load to the pier via the elastomeric bearing. In essence, this is a measurement of the walking of the elastomeric bearing with respect to the beam.

#### **5.3.1. Measurement of Slip**

Slip measurements were taken for each test run at various points during the tests to determine if a pattern existed in the resulting slip. Slip was measured at each superelevation of 0%, 2%, 4%, 6%, and 8% for each test run until the maximum transverse slope for each test series was reached. For example, if the test run being conducted was to see a maximum superelevation of 6%, slip was measured at the 0%, 2%, 4%, and 6% transverse superelevation points respectively.

Slip was measured with a ruler. Bearings were placed on the concrete blocks according to TxDOT provisions. The bearing positions were lined with a black, permanent marker in order to place the bearings in the same position at the start of each test series. Measuring slip consisted of recording the linear change of position of the bearing with respect to the reference lines for the original placement of the bearing. An illustration of bearing slip is shown in Figure 5.51 and Figure 5.52. The reference lines show the original placement of the bearing.



Figure 5.51 – Illustration of Slip, Transverse Front

Slip measurements were obtained at three different locations for each test run as shown in Figure 5.53. Two transverse measurements were obtained at the front and back of the bearing with reference to the line heading into the photo. One longitudinal measurement was obtained at the back of the bearing with respect to the line parallel to the photograph. The three slip measurements were labeled the transverse front, transverse back, and longitudinal slips. The transverse front measurement recorded the transverse displacement of the bearing measured at the corner opposite of where the transverse force was applied, and on the side of the bearing where the longitudinal force was applied to the bearing. The transverse back slip measurement



Figure 5.52 – Illustration of Slip, Transverse Back



Figure 5.53—Slip Measurement Locations

recorded the transverse displacement of the bearing at the corner of the bearing opposite the application of both the longitudinal and transverse forces. The longitudinal slip measured the longitudinal slip of the bearing at the same corner as the transverse back measurement. These locations were chosen because a ruler could be placed at these locations to facilitate measuring the actual displacement. The ruler easily fit in these locations and could be read accurately. Also, these locations were not crowded with wires connected to any strain gages. Measurements

taken from areas with wires present might have interfered with the ability to obtain accurate, consistent measurements.

It was difficult to determine when slipping first occurred during each test. When loaded, the corners of the bearings began to ‘curl’ which looked very similar to movement of the bearing. Figure 5.54 below shows the curling action. The curl is easily noticeable on the bottom right corner of the bearing in the picture. The difference between slip and curl was difficult to define. Thus, TechMRT defined slip as a displacement of at least 0.25 inches, and at this point the curling action leads way to a measurable slip. Trying to differentiate between curling and slip prior to this limit proved too difficult and would not provide beneficial information to the project.



Figure 5.54 – Bearing Corner Undergoing Curling

### **5.3.2. Analysis of Slip Data**

The investigation into the slip behavior of the bearings started with determining if the vertical load on a bearing at a specific transverse slope had an effect on the resulting slip. The results revealed that slip occurs without consideration of the total vertical load applied to the bearing. As shown in Figure 5.55 through Figure 5.60, little variation exists between the test runs. Tests runs one through ten represent a 390 kip load and test runs 11, 12, 13, and 14 represent the application of a 150 kip, 210 kip, 270 kip, and 330 kip loads respectively. For

example, Figure 5.56 shows that while the slip did vary some for each test run, no pattern or trend exists for the 8% transverse slope, double bearing configuration shown in this figure. In addition, Figure 5.57 through Figure 5.60 show that the same trendless pattern exists for the single bearing configuration.

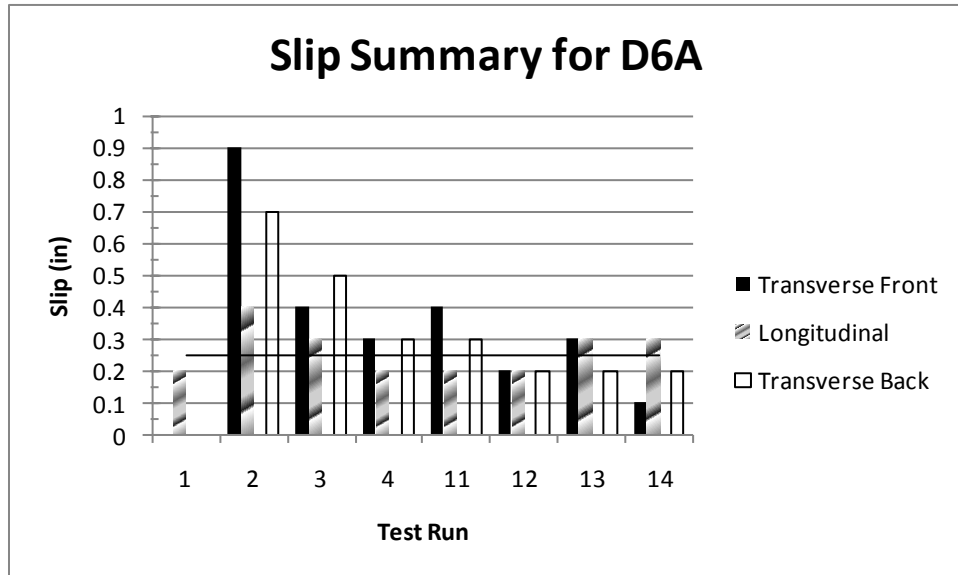


Figure 5.55 – Summary of Slip Results for 6% Transverse Slope, Double Pad Configuration

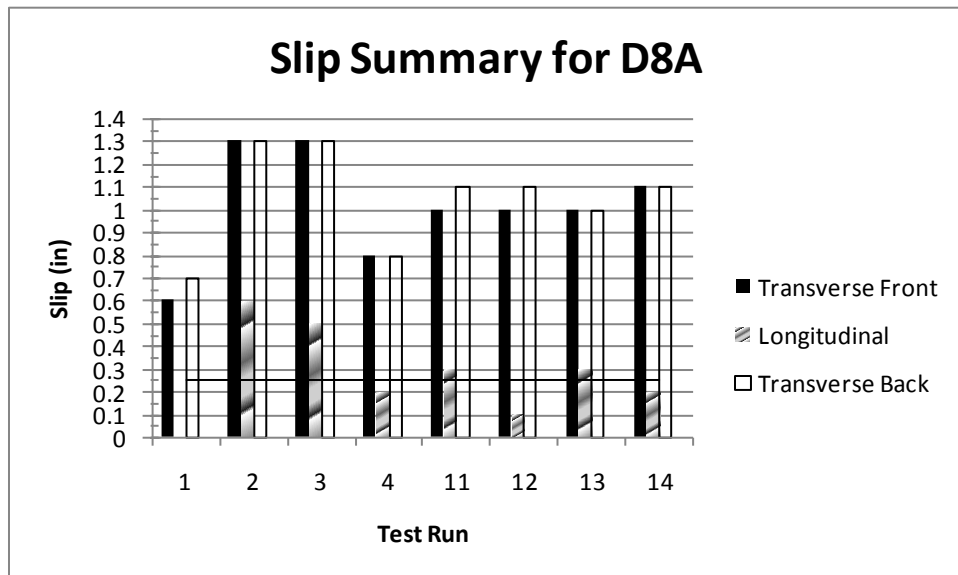


Figure 5.56 – Summary of Slip Results for 8% Transverse Slope, Double Pad Configuration

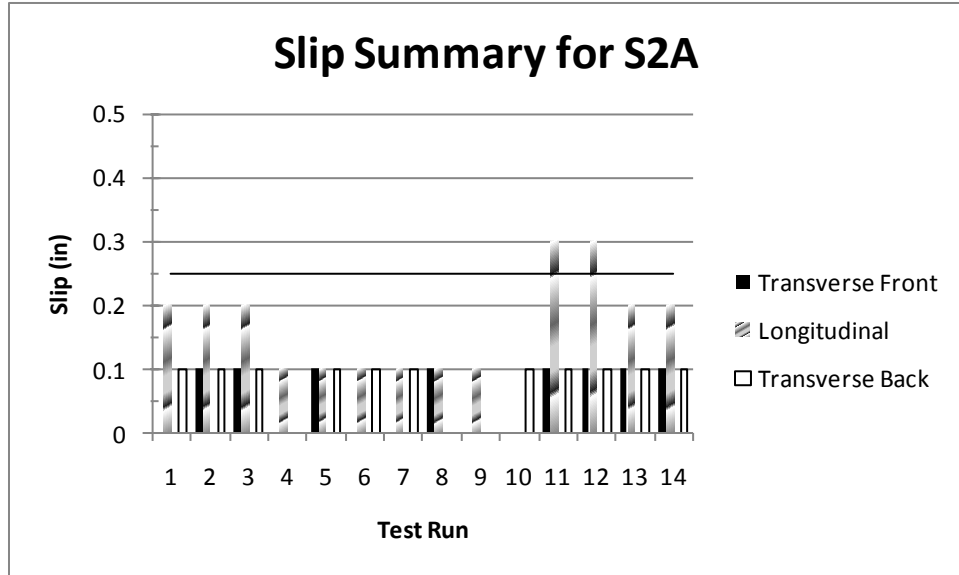


Figure 5.57 – Summary of Slip Results for 2% Transverse Slope, Single Pad Configuration

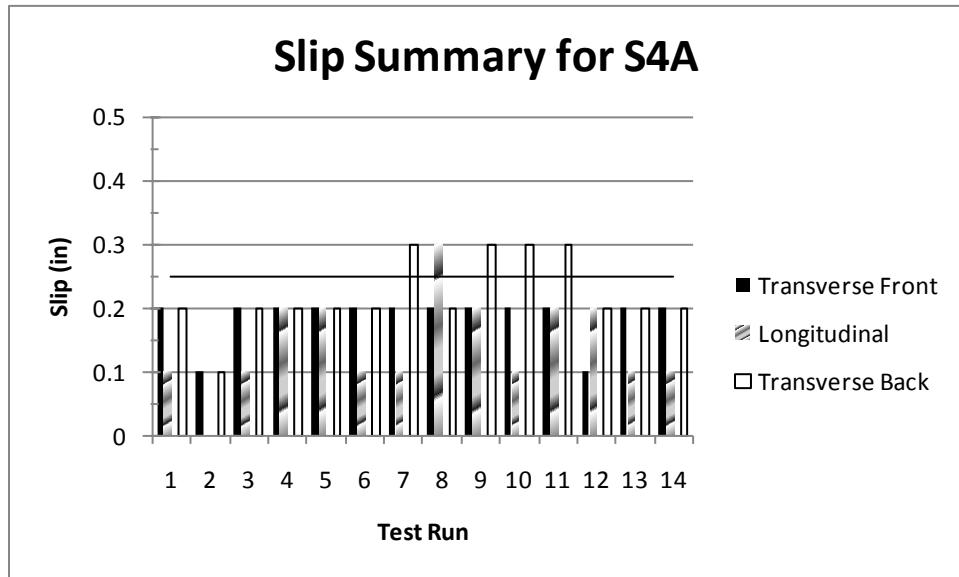


Figure 5.58– Summary of Slip Results for 4% Transverse Slope, Single Pad Configuration

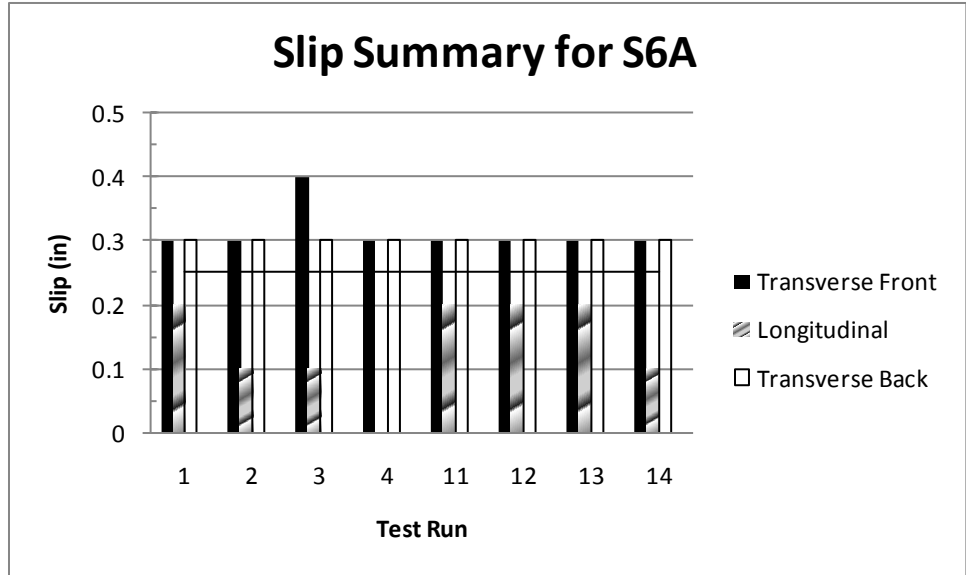


Figure 5.59 – Summary of Slip Results for 6% Transverse Slope, Single Pad Configuration

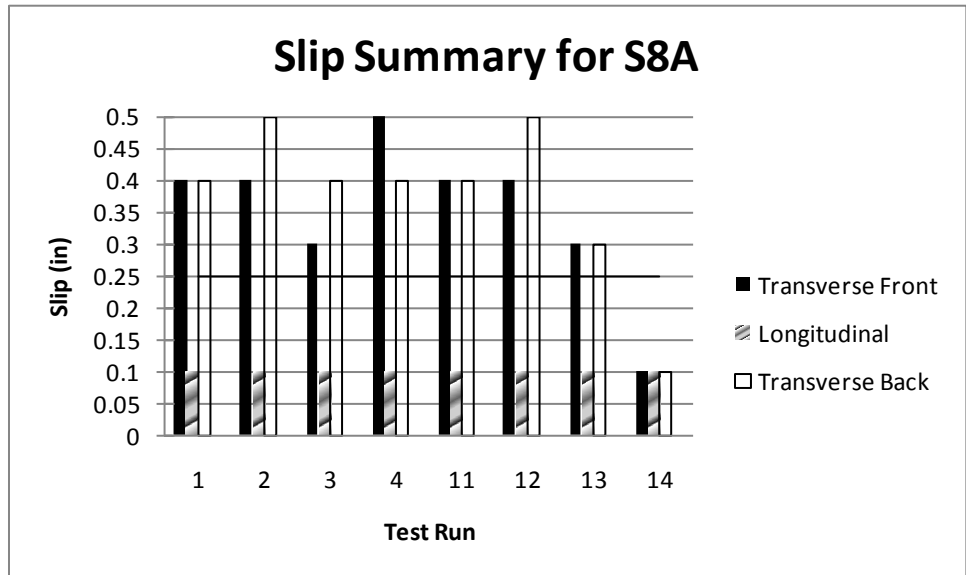


Figure 5.60 – Summary of Slip Results for 8% Transverse Slope, Single Pad Configuration

The fact that the data does not show a trend in the amount of slip that occurs based on the vertical load applied does not seem to fit intuitively. Researchers originally thought more slip would occur when a lower vertical load was applied to the bearings. Since the friction force generated by the vertical load is less when a smaller normal force is applied, it would seem logical that the slip potential would be greater when subjected to the transverse force resulting from the superelevation. However, this is not the case because the transverse force required to

simulate the transverse slope does show a decreasing trend with a lighter vertical load. Thus, since less transverse force is applied when the vertical load is lighter, the slip remains fairly constant regardless of the applied vertical load. Variations in the slip must occur due to some other unknown conditions.

While the amount of slip does not appear to vary due to the vertical load within a specific transverse slope, the same cannot be said when comparing the slip of a bearing under identical loads with different superelevations. These results are summarized in Figure 5.61 and Figure 5.62. These charts illustrate that there is definitely an increase in slip with an increase in transverse slope. For the single pad configuration, the pattern is readily apparent. For the double pad configuration, slip appears to start only after the slope exceeds 4%. However, this most likely is not the case. Slip became apparent to the test observers during the 6% superelevation series of the double pad configuration. While the bearings were inspected while conducting the 2% and 4% superelevation tests with the double bearing configuration, it was not readily apparent to the testers that slip might be of concern. Slip, if it did occur, was likely less than 0.25 in. at this point and not necessarily noticed. Slip was measured, rather than just observed, for all subsequent double bearing tests.

The difference between curling and slip, as mentioned earlier in this section, was the next item investigated. Slips less than 0.25 in. are difficult to distinguish from edge curling. For this reason, a line representing 0.25 in. is shown on all graphs. When considering this threshold, slip becomes apparent and very likely at transverse superelevations greater than 4%. Again, while slip was not recorded for the double bearing configurations of 2% and 4% superelevation, the slip that occurred, if any, was small (i.e., 0.25 in. or less) otherwise the movement of the bearings would have been noticed.

For the 0%, 2%, and 4% test runs, ten tests were conducted at the 390 Kip load resulting in 20 transverse slip observations and 10 longitudinal slip observations. For the six percent and eight percent transverse slopes, 4 tests were conducted at the 390 kip vertical load, resulting in 8 transverse and 4 longitudinal slip observations, respectively.

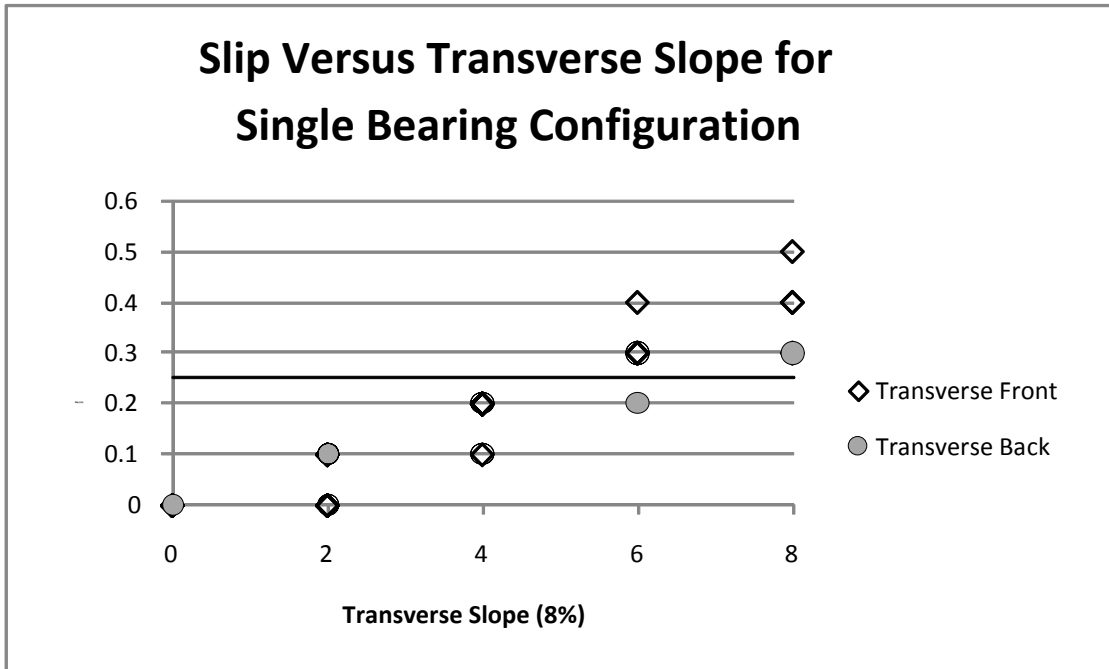


Figure 5.61– Summary of Slip Results, Single Bearing Configuration

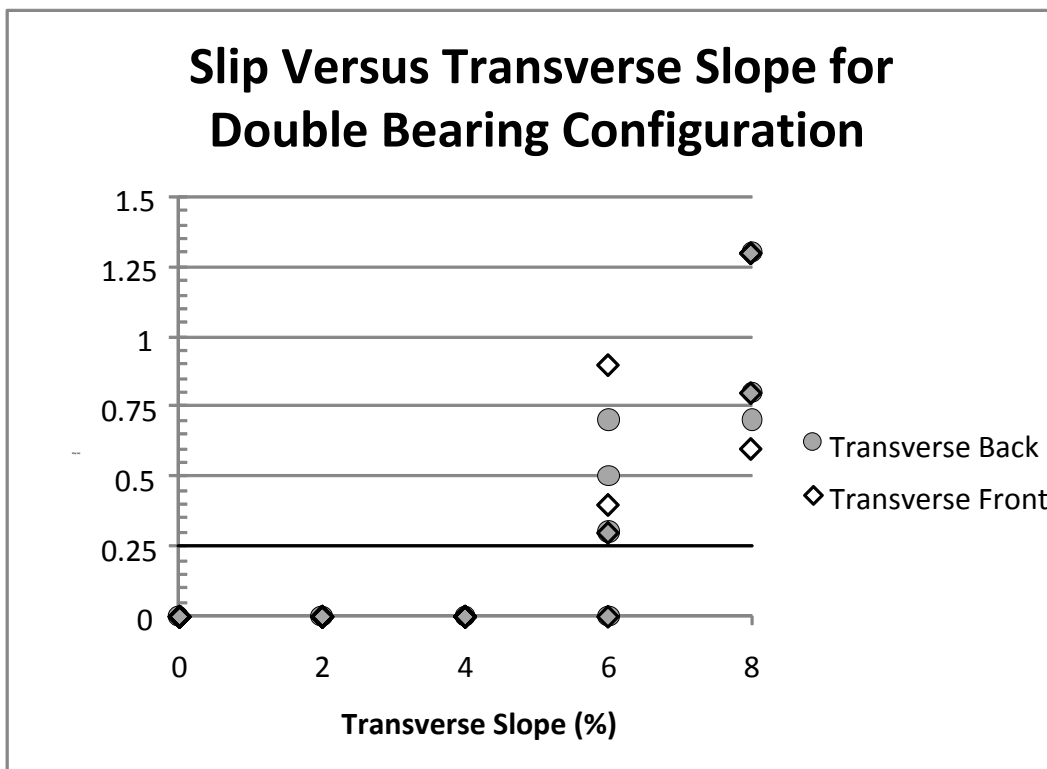


Figure 5.62 – Summary of Slip Results, Double Bearing Configuration

Table 5.2 shows a summary of the percentage of locations where slip was found during each test run. The first column identifies the specific superelevation. The second and third columns provide the percent of test runs within the single pad test series where slip in the transverse and longitudinal slip was noticed. The last two columns provide the same slip percentages for the double pad configuration test series. The table was created by using the 0.25-in. threshold to qualify as slip occurring.

Table 5.2 – Slip Summary for Test Series, 390 Kip Load

Transverse Slope	Single Bearing Configuration		Double Bearing Configuration	
	Percent Transverse Slip	Percent Longitudinal Slip	Percent Transverse Slip	Percent Longitudinal Slip
0%	0%	10%	0%	0%
2%	0%	0%	0%	0%
4%	15%	10%	0%	0%
6%	100%	0%	75%	50%
8%	100%	0%	100%	75%

Table 5.2 reinforces the idea that transverse slip is a limited occurrence at transverse superelevations equal to or below 4% percent. Additionally, a significant increase in the likelihood of transverse slip clearly occurs as the superelevation is increased from 4% to 6%. The results for longitudinal slip are less clear. While interpreting the data recorded, longitudinal slip does not appear to occur for the single bearing configuration. Longitudinal slip does appear to be more likely for the double bearing configuration, especially when the superelevations exceed 4%. The most likely explanation for the difference comes from the difference in the pad configurations. The longitudinal forces were applied as shown in Figure 4.13. With the double pad configuration, the longitudinal forces were applied at the centroid of each of the smaller bearings whereas this is not the case with the single pad configuration. While the contact area for the two pad configurations is the same, the single pad configuration has a single, larger bearing resisting movement versus two, smaller bearings each resisting the movement applied at their respective centroids. Thus, the difference in slip between bearing pad configurations could be a result of the individual bearing pad configurations. The single pad configuration is better at resisting the tendency to slip and results in smaller displacements.

What effect, if any, the bearing configuration had on the amount of slip observed was investigated. As previously indicated, the transverse slope appears to have an effect on the amount of transverse slip observed for each test run. Table 5.3 shows the average values for transverse and longitudinal displacement observed. The first column identifies the superelevation of the test series. Columns two and three display the average transverse and longitudinal slip observed for the single pad test series while the fourth and fifth columns provide the same information for the double pad test series. When presented in this manner, the data again show that as the transverse slope increases, so does the average amount of transverse slip. Slip for the double pad configuration, when observed, is larger than that of the single pad configuration. As with the likelihood of slip, no definitive conclusion can be drawn for the longitudinal slip prediction. The single bearing configuration shows no discernable pattern of behavior with respect to longitudinal slip while the double bearing configuration tends to show that the amount of longitudinal slip tends to increase with an increase in transverse slope.

Table 5.3 – Summary of Slip Details, 390 Kip Load

Transverse Slope	Single Bearing Configuration		Double Bearing Configuration	
	Average Transverse Slip (in)	Average Longitudinal Slip (in)	Average Transverse Slip (in)	Average Longitudinal Slip (in)
0%	0%	20%	0%	0%
2%	6%	12%	0%	0%
4%	21%	14%	0%	0%
6%	31%	10%	39%	28%
8%	41%	10%	101%	43%

In summary, transverse slip appears to increase as the superelevation of the U-beam is increased. Prediction of longitudinal slip does not appear to be possible with the data from this experiment. The observed data indicates that transverse slip is most likely to occur at superelevations greater than 4%.

### 5.3.3. Regression Analysis for Slip

TechMRT conducted a linear regression analysis for the prediction of a bearing's transverse slip using the dependent variables of bearing configuration and superelevation. For

the initial regression analysis, only first order terms for each predictor variable were used. Based upon the slip data presented in the previous section, this seemed like the most reasonable place to start. The observed slip, in inches, was modeled as the dependent variable, Y. The predictor variables used are shown in Table 5.1. The regression analysis was conducted with the aid of Statistical Analysis Software, version 9.2.

In order to find the best model that could predict the outcome of the dependent variable, five multiple regression models were initially considered. These models were:

Model 1: Use of Superelevation and Bearing Configuration to predict slip

Model 2: Use of Superelevation only to predict slip

Model 3: Use of Bearing Configuration only to predict slip

Model 4: Use of Superelevation, Bearing Configuration, and the interaction of Superelevation and Bearing Configuration to predict slip.

Model 5: Use of Superelevation and the interaction of the Superelevation and Bearing Configuration.

From these five models, the two models that seemed to fit the best were the second and fourth models. As with the earlier regression analysis discussed, the best models were done by looking at the adjusted R-square value and determining if a significant increase in the adjusted R-square value occurred with the addition of additional predictor variables. Summaries of the regression analysis are shown in Figure 5.63 and Figure 5.64 for Models 2 and 4 respectively. The regression equations for each model are as follows:

$$\text{For Model 2: } Y = -0.089 + 0.077 * X1 \quad \text{Equation 5.5}$$

$$\text{For Model 4: } Y = -0.158 + 0.100 * X1 + 0.139 * X2 - 0.0463 * X1 * X2 \quad \text{Equation 5.6}$$

In Equations 5.5 and 5.6, Y is the slip, in inches, predicted. X1 is the superelevation of the bearing, expressed in percent, and X2 is an indicator value for the bearing pad configuration (X2 is input as zero for a single pad configurations and one for a double pad configuration).

For a corresponding superelevation of zero percent, the linear fit for both models would predict a slip in the opposite direction of the applied load. This is impossible and lends itself to the belief that the model shown is really appropriate for superelevations between 2% and 8%. This is acceptable since the lab data suggests that transverse slip can be considered negligible at superelevations below 2%.

Further investigation leads to the conclusion that Model 4 is the better of the two models. The reason for this is that the adjusted R-square value for Model 4 is greater than that for Model 2. Model 2 predicts the slip based on the superelevation alone, yet a better fit is obtained if the bearing configuration and the interaction term for X1 and X2 in Model 4 are added to the regression model. The interpretation of this phenomenon is that the predicted slip depends on superelevation of the bearing, the bearing pad configuration, and the interaction of the two terms. Removal of the interaction term between the transverse superelevation and bearing configuration detracts from the fit of the model and yields an adjusted R-square value less than that of the full model.

After completing the initial analysis and looking at the scatter plot of slip versus transverse superelevation, TechMRT decided to investigate the possibility that the slip observed may exhibit a higher order relationship to a bearing's corresponding superelevation. Thus, two more models were analyzed to determine if they may provide a better explanation. The scatter plot of slip versus transverse slope showed a trend that the slip may be related to the square of the transverse superelevation. Model 6 was created to determine if the square of the bearing's transverse superelevation would result in a better prediction of the resulting slip.

<b>Analysis of Variance</b>					
<b>Source</b>	<b>Degrees of Freedom</b>	<b>Sum of Squares</b>	<b>Mean Square</b>	<b>F-Value</b>	<b>Pr &gt; F</b>
Model	1	5.81563	5.81563	177.96	<0.0001
Error	150	4.902	0.03268		
Corrected Total	151	10.71763			
R-Square: 0.5426 Adjusted R-Square: 0.5396					
<b>Parameter Estimates</b>					
<b>Variable</b>	<b>Degrees of Freedom</b>	<b>Parameter Estimate</b>	<b>Standard Error</b>	<b>t-Value</b>	<b>Pr &gt;  t </b>
Intercept	1	-0.00868	0.0229	-3.87	0.0002
X1	1	0.07689	0.00576	13.34	<0.0001

Figure 5.63 – Regression Summary for Model 2

<b>Analysis of Variance</b>					
<b>Source</b>	<b>Degrees of Freedom</b>	<b>Sum of Squares</b>	<b>Mean Square</b>	<b>F-Value</b>	<b>Pr &gt; F</b>
Model	3	6.34393	2.11464	71.56	<0.0001
Error	148	4.3737	0.02955		
Corrected Total	151	10.71763			
R-Square: 0.5919 Adjusted R-Square: 0.5836					
<b>Parameter Estimates</b>					
<b>Variable</b>	<b>Degrees of Freedom</b>	<b>Parameter Estimate</b>	<b>Standard Error</b>	<b>t-Value</b>	<b>Pr &gt;  t </b>
Intercept	1	-0.15809	0.0308	-5.13	<.0001
X1	1	0.10006	0.00775	12.91	<.0001
X2	1	0.13883	0.04356	3.19	0.0018
X12	1	-0.04634	0.01096	-4.23	<.0001

Figure 5.64 – Regression Summary for Model 4

Model 4 was also edited and rerun as Model 7. Here, TechMRT checked into whether using the square of the bearing’s superelevation provides a better explanation for slip in conjunction with the other variables in Model 4. A similar approach was taken during the earlier regression analysis for the displacement prediction; however, the square of the superelevation detracted from prediction models fit and was discarded. As demonstrated in Figure 5.65 and Figure 5.66, the adjusted R-square value for Model 7 is the highest and thus provides the best explanation for the slip of a bearing. As such, Model 7 provides the best prediction model for the slip that will occur. The resulting model is:

$$Y = -0.0721 + 0.0139*X1^2 + 0.144*X2 - 0.0481*X1*X2 \quad \text{Equation 5.7}$$

Another important discussion is whether the magnitude of the vertical load affects the amount of slip that occurs. When analyzed as part of the regression models, the magnitude of the vertical load does not seem to be a significant factor in explaining the slip behavior observed. If a

<b>Analysis of Variance</b>					
<b>Source</b>	<b>Degrees of Freedom</b>	<b>Sum of Squares</b>	<b>Mean Square</b>	<b>F-Value</b>	<b>Pr &gt; F</b>
Model	1	7.14471	7.14471	299.95	<.0001
Error	150	3.57292	0.02382		
Corrected Total	151	10.71763			
<p>R-Square: 0.6666 Adjusted R-Square: 0.6644</p>					
<b>Parameter Estimates</b>					
<b>Variable</b>	<b>Degrees of Freedom</b>	<b>Parameter Estimate</b>	<b>Standard Error</b>	<b>t-Value</b>	<b>Pr &gt;  t </b>
Intercept	1	-0.02732	0.01603	-1.7	0.0903
X1sq	1	0.01098	0.000634	17.32	<.0001

Figure 5.65 – Regression Summary for Model 6

<b>Analysis of Variance</b>					
<b>Source</b>	<b>Degrees of Freedom</b>	<b>Sum of Squares</b>	<b>Mean Square</b>	<b>F-Value</b>	<b>Pr &gt; F</b>
Model	3	7.77536	2.59179	130.37	<.0001
Error	148	2.94227	0.01988		
Corrected Total	151	10.71763			
<p>R-Square: 0.7255 Adjusted R-Square: 0.7199</p>					
<b>Parameter Estimates</b>					
<b>Variable</b>	<b>Degrees of Freedom</b>	<b>Parameter Estimate</b>	<b>Standard Error</b>	<b>t-Value</b>	<b>Pr &gt;  t </b>
Intercept	1	-0.07211	0.0203	-3.55	0.0005
X1sq	1	0.0139	0.000777	17.88	<.0001
X2	1	0.14406	0.03467	4.16	<.0001
X12	1	-0.04805	0.00853	-5.63	<.0001

Figure 5.66 – Regression Summary for Model 7

variable, X3, representing the vertical load applied to the bearing in kips, is added to the model, the adjusted R-square value decreases (to a value of 0.706). In addition, the alpha level for the X3 variable was 0.840, which is not significant. When these two factors are considered, there is no reason to believe that the vertical load applied has a significant effect on the slip observed.

In summary, the best prediction model takes into account a bearing's transverse superelevation, the bearing pad configuration, and the interaction of the two variables. The model in Equation 5.7 provides the best prediction model for the slip that occurs based on the adjusted R-square criteria. While the addition of the applied vertical load to the model does improve the adjusted R-square value, the increase is not significant.

#### **5.3.4. Measurement of Uplift**

Uplift, also called “liftoff,” occurs when a bearing is loaded eccentrically, either by a load not acting through the centroid of the bearing or by an applied moment or rotation. Uplift has been a concern in the past for the load combination of low vertical loads applied with a high rotation. Previous editions of the AASHTO design considerations for bearings did not allow for any liftoff. Stanton et al. (2008) recently concluded through research that uplift may not be a problem for bearings and recommend the removal of the “no lift-off” clause. As such, TechMRT investigated whether uplift was present as a result of the triaxial loading state introduced by superelevating the beams and if any patterns emerged in the uplift behavior.

TechMRT measured uplift with a ruler and recorded the data on the Laboratory Bearing Hard Copy Data Information Sheet seen in Figure 4.24. Data from four areas were recorded and labeled as transverse top, transverse bottom, longitudinal top, and longitudinal bottom liftoff. As shown in Figures 4.12 and 4.13, the beam is represented by the center block and the bearing seat is represented by the top block of the loading apparatus. As such the transverse top and longitudinal top measurements represent any uplift that occurs between the bearing and the bearing seat in their respective directions. By the same manner, the longitudinal and transverse bottom measurements represent any uplift that occurs between the bearing and the beam the bearing supports. An example of observed uplift can be seen in Figure 5.67. The transverse top liftoff occurring between the bearing and simulated bearing seat at the upper right corner of the bearing is noticeable. In addition, one can see that no liftoff occurs between the bearing and the



Figure 5.67 – Example of Observed Transverse Top Uplift

simulated beam in this photograph. A ruler was used to measure the uplift to the nearest tenth of an inch.

### 5.3.5. Analysis of Uplift

Analysis of the uplift measurements yielded interesting results. No real trends in uplift exist for uplift occurring in the longitudinal direction; however, a trend does exist in the transverse direction. The transverse bottom uplift recorded, when observed, was small. The measurements are on the order of 0.3 to 0.5 inches. However, TechMRT believes that this uplift is more the result of the curling action discussed earlier rather than true uplift. As such, the transverse bottom uplift will not be analyzed.

Trends do exist with analysis of the data for the case of transverse top uplift. Figure 5.68 through Figure 5.72 show a summary of the liftoff observed for each test run. It is important to note that transverse uplift was not observed for superelevations less than 4%. In addition, no uplift was observed for the single bearing configuration at the 4% superelevation.

An interesting trend can be seen in the aforementioned figures. Considering the single bearing configuration, it appears that as the magnitude of the applied vertical load is increased the resulting uplift also increases. In addition, the magnitude of the uplift seems to be proportionally related to the superelevation of the bearing. However, the opposite appears to be true for the double bearing configuration. For the double bearing configuration, the uplift tends

to be inversely proportional to the magnitude of the applied vertical load as well as inversely proportional to the superelevation of the bearings.

At first, it seemed counterintuitive to see that the trends for the different bearing configurations to be opposite each other. Looking at Figure 5.68 and Figure 5.69, one may notice that the magnitude of the uplift that occurred with the single pad configuration tended to increase with a corresponding increase in superelevation. The reverse is true for the double bearing configuration. Keep in mind that slip was higher for the double bearing configuration. TechMRT believes that uplift tends to be lower as the superelevation is increased as a result of the slip occurring at higher superelevations. The slip that occurs tends to re-center the application of the loads and reduces the uplift that occurs.

As far as comparing the magnitudes of uplift for the single pad configuration to that of the double pad, it is important to remember that the double pad configuration has the same contact area as the single pad configuration. However, in the double pad configuration, the two smaller bearings are placed further out beneath the supported beam. This creates a support system that is more likely to be stable when subject to moment or rotation than that of the single bearing configuration. This is believed to be the reason that uplift, when it occurs for both bearing configurations at a specified superelevation, is smaller for the double bearings when compared to the magnitude for the single bearings.

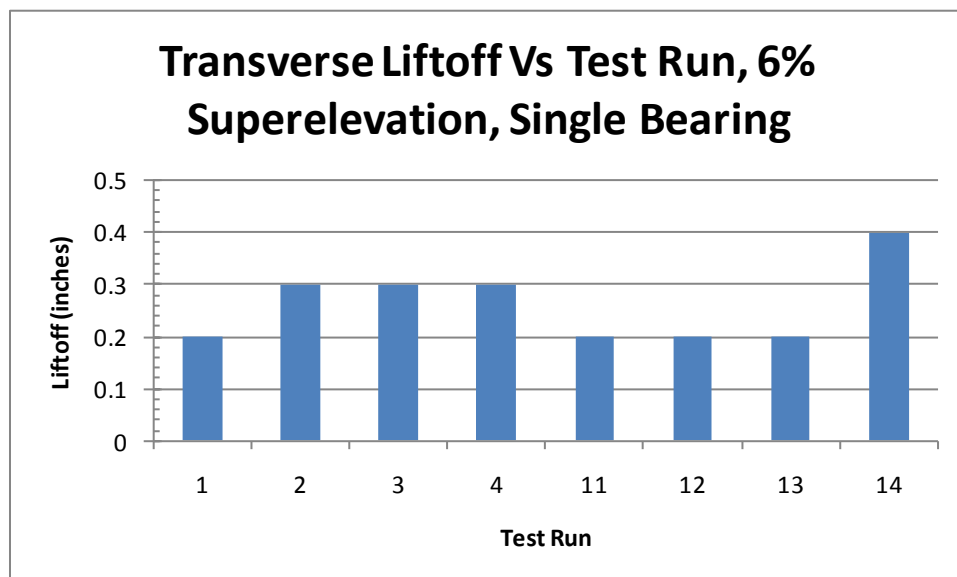


Figure 5.68—Uplift Summary, Test Series S6A

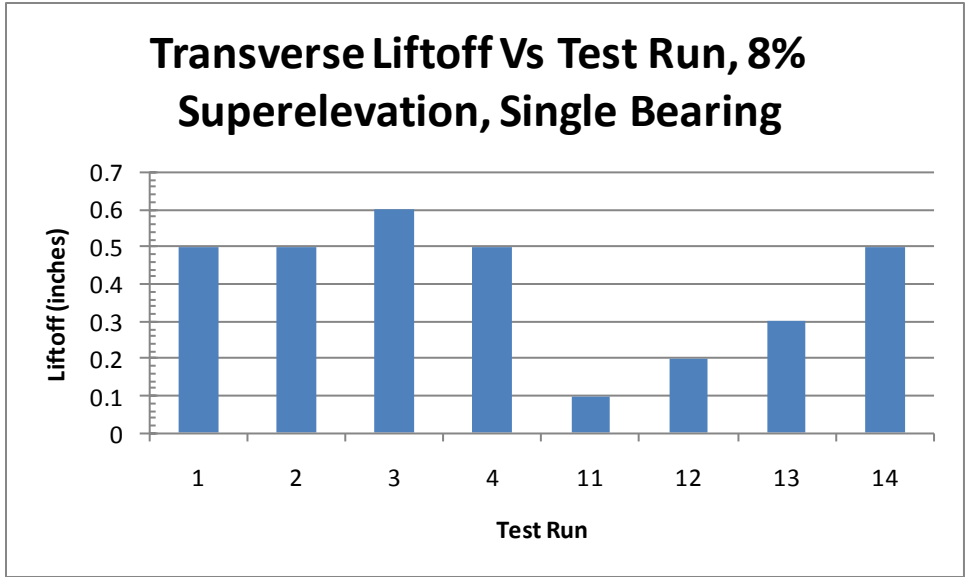


Figure 5.69—Uplift Summary, Test Series S8A

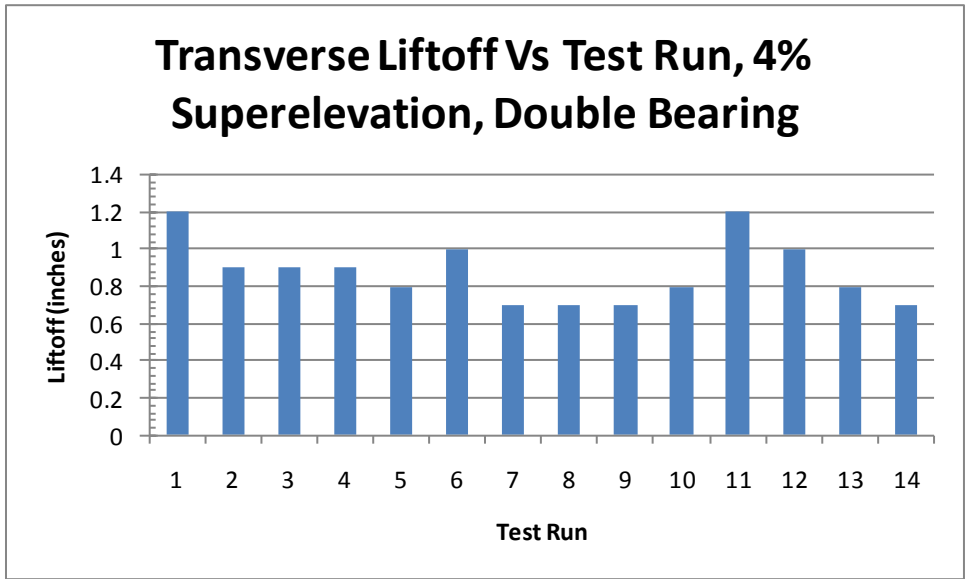


Figure 5.70—Uplift Data for Test Series D4A

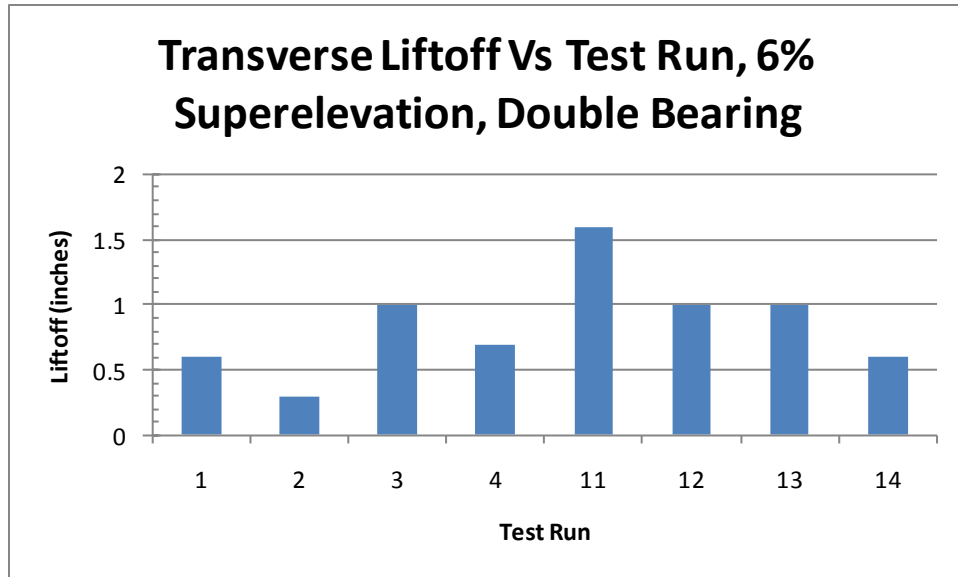


Figure 5.71—Uplift Summary, Test Series D6A

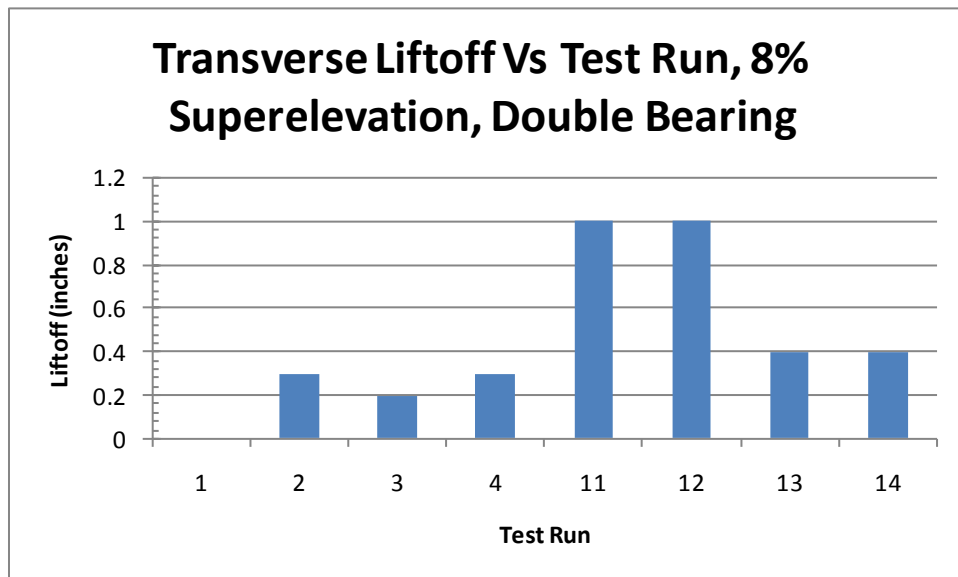


Figure 5.72—Uplift Summary, Test Series D8A

### 5.3.6. Prediction of Uplift

Prediction of uplift proves to be more difficult than that of a bearing’s slip or transverse displacement. Uplift seems to be affected by many factors including the bearing pad configuration, the magnitude of the load applied, the superelevation of the bearing, and whether or not slip occurs while loading the bearing. Due to the intricacies involved in the resulting uplift behavior, TechMRT does not feel that a sufficient model can be developed at this time.

### **5.3.7. Summary of Uplift and Slip**

Slip was found to be related to the square of the superelevation of the bearing and the interaction of the bearing configuration with the corresponding superelevation. The relationship is shown in Equation 5.4. Uplift appears more complicated to predict. For this reason, a prediction for uplift is not feasible at this time. The amount of slip occurring appears to affect the amount of uplift that occurs among other factors and more information needs to be investigated in order to make a good prediction.

## **5.4. Prediction of Damage**

TechMRT's original intent while conducting the experiment was to investigate the effect that the superelevation of a U-beam has on the bearings upon which they are placed. TechMRT noticed that a certain amount of shear strain was permanently applied in the case where the bearings are superelevated along with the bearing seat. The permanent shear strain was noticeable while inspecting the bridges in both Wichita Falls and Lubbock. The shear strain was large enough that one could measure the strain with a ruler.

In a sense, TechMRT designed an experiment that would allow for the simulation of superelevation while also allowing for inspection of the bearings throughout each test run. One item documented during the experiment was if any damage to the bearing was readily apparent. The following section of this report will provide details on the summary of the damage noted and whether or not any trends can be identified to predict.

### **5.4.1. Reporting of Observed Damage to Bearings**

Each elastomeric bearing was inspected for damage after all loads were applied during each test run. The thought behind waiting until all loads were applied stems from observing a worst case scenario where the superelevated beam sees the maximum dead and traffic loads while having undergone longitudinal deflections due to the thermal effects. The inspection consisted of visually checking the bearing to search for any signs of cracking, debonding, delamination, or rupture of the shims. Each bearing was inspected on all four sides with the aid of a flashlight. In cases where damage was present, photographs were obtained to catalog the damage. Any damage present was recorded on the Laboratory Bearing Hard Copy Data Information Sheet seen in Figure 4.24.

In order to present the data in an organized, meaningful way, the authors categorized observed damage into one of five categories:

- 1) No visible damage was observed
- 2) Minor, hairline cracking was observed
- 3) Significant, heavier cracking was observed
- 4) Tension debonding occurred
- 5) Delamination occurred

These categories are progressive; the damage followed the distinct order of the categories created. This is important to remember as its impact will be discussed in later sections.

#### **5.4.2. Categorization of Observed Damage**

Generally, hairline cracking is not a serious issue. The cracking appears to be confined to the surface and is illustrated in Figure 5.73. Hairline cracks originate in the valleys corresponding to the locations of the shim in the middle of the photograph. Previous research by Stanton et al. (2008) suggests that hairline cracks do not inhibit a bearing's ability to function properly. Should moisture be present in this situation, it is doubtful that the moisture would penetrate the elastomer and begin to corrode the steel shims. As the cracking becomes more pronounced, the chance of water penetrating through the elastomer and coming in contact with the shim becomes greater. Water that comes in contact with steel can begin to corrode the steel and diminish the capacity of the bearing. This phenomenon is compounded by the fact that bearings are placed in locations where direct sunlight is an unusual occurrence so moisture in the vicinity is not likely to dissipate quickly. As such, heavier, more pronounced cracks are categorized separately. These thicker, heavier cracks are illustrated in Figure 5.74. The cracks become more pronounced in the valleys between the bulges. Note that evidence of delamination is lacking in Figure 5.74 since five distinct valleys are visible. These valleys correspond to the locations of the five steel reinforcing shims.



Figure 5.73 – Hairline Surface Cracks on Elastomeric Bearing

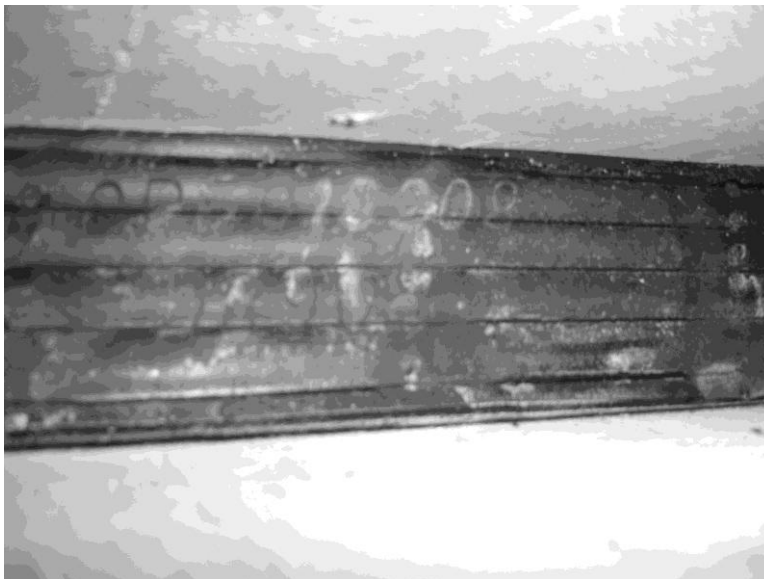


Figure 5.74 – Heavy Surface Cracking on an Elastomeric Bearing

The next stage of failure observed was tension debonding. Tension debonding occurs when the elastomer separates from the bearing at the end of the shims. The obvious sign of this phenomenon is when two or more smaller bulges present on a loaded bearing combine to form a larger, single bulge. Debonding is illustrated in Figure 5.75. In this photo, the proof that debonding occurred is noticeable in the areas near both fingertips where only three distinct valleys remain on the surface of the bearing. The debonding is more pronounced adjacent to the



Figure 5.75 – Tension Debonding at Shims

finger at the bottom of the photograph. Since the elastomer is no longer in contact with the shim, the formation of an additional valley in the profile of the bearing no longer exists.

If the load is increased further after debonding occurs, this can lead to delamination. Delamination is considered the continuation of the debonding down the length of the shim. Figure 5.76 displays a bearing that has likely experienced delamination. The phenomenon can be seen along the top shim as identified by the paperclip. The elastomer here has completely separated from the shim and would continue along its length into the bearing under more severe loading or increased cyclic loading. Typically, it is hard to distinguish between tension debonding and delamination without taking apart the bearing. However, the technicians did notice the penetration of shims through the elastomer as shown on the right side of the photograph in Figure 5.77. This phenomenon was, for the most part, limited to the indentions in the bearing used to remove it from the mold when cast. This area has less elastomer providing cover for the shims. Shim penetration is categorized as delamination since this is the result of the elastomer debonding along the shim. Tension debonding and delamination are serviceability issues for the bearing. While the elastomeric bearings will continue to sustain the loads and will not result in a catastrophic failure, the bearing is no longer performing its intended capacity. Further cyclic loading may cause more delamination and in extreme cases the elastomer may



Figure 5.76 – Delamination of Elastomer



Figure 5.77 – Exposure of Shims

walk out from between the shims completely. Consequently, TechMRT believes that bearings should not be placed under conditions that may cause either tension debonding or delamination.

#### **5.4.3. Analysis of Damage**

Damage to the bearing observed while conducting each test run was noted on the bearing worksheet and compiled. A summary of the damage noted is shown in Table 5.4. This table

Table 5.4 – Raw Summary of Damage by Test Series

Configuration	Superelevation	Number of Test Runs With Noticeable Damage				Delamination
		No Damage	Hairline Cracking	Heavy Cracking	Tension Debonding	
Double	0%	1	11	0	0	0
Double	2%	3	9	0	0	0
Double	4%	0	12	7	0	0
Double	6%	0	8	6	2	0
Double	8%	0	8	8	7	2
Single	0%	3	9	0	0	0
Single	2%	2	10	0	0	0
Single	4%	1	11	3	3	3
Single	6%	3	5	3	1	1
Single	8%	2	6	6	6	4

summarizes the total number of test runs where each level of damage observed was present. The first two columns designate the pad configuration and superelevation of the test series while the remaining five columns list the number of test runs where each category of damage was observed.

Table 5.5 summarizes the same information, but provides the percentages of each test series for each level of damage in the last five columns of the table instead of the raw number of observations. The raw data is important, but the data in Table 5.5 presents a clearer picture pertaining to the behavior of the bearing. The first topic of discussion is that damage or wear of bearings is going to happen when the bearings are placed on a transverse superelevation. These tests show that hairline cracking is almost a certainty. Heavy cracking does not appear to be an issue at small transverse superelevations. The first occurrence of heavy cracking for both bearing configurations occurs at 4% superelevation. As the amount of superelevation is increased beyond 4%, more significant damage is noticed. Tension debonding and delamination begin to occur. Tension debonding is prevalent at 6% superelevation and delamination becomes apparent at 8% superelevation. The results follow the same trend regardless of the bearing pad configuration. From this data, it can be predicted that a serviceability failure would be much more likely at higher superelevations.

It is important to remember that damage is a progressive phenomenon. Once damage occurs, the bearing cannot repair itself. Thus, it is also important to look at the time history of

Table 5.5 – Percentage Based Summary of Damage by Test Series

Configuration	Superelevation	Percentage of Test Runs With Noticeable Damage				delamination
		No Damage	Hairline Cracking	Heavy Cracking	tension debonding	
Double	0%	8%	92%	0%	0%	0%
Double	2%	25%	75%	0%	0%	0%
Double	4%	0%	100%	58%	0%	0%
Double	6%	0%	100%	75%	25%	0%
Double	8%	0%	100%	100%	88%	25%
Single	0%	25%	75%	0%	0%	0%
Single	2%	17%	83%	0%	0%	0%
Single	4%	8%	92%	25%	25%	25%
Single	6%	38%	63%	38%	13%	13%
Single	8%	25%	75%	75%	75%	50%

the damage noted in Table 5.6. The first two columns show the pad configuration and superelevation of the bearings. The next five columns show the number of test runs conducted within each test series before each level of damage was observed. The data suggests that as the superelevation of the bearing seat is increased, the numbers of runs required before each damage level is observed is reduced. Thus, as the superelevation of a bearing is increased, the time to significant damage is reduced. This time can be thought of as requiring less loading cycles. Table 5.6 reinforces the idea that superelevation is not a significant concern for bearings that have a superelevation of 4% or less.

Table 5.6 – Progressive Damage Summary by Test Series

Configuration	Superelevation	Number of Test Runs Until First Sign of Damage			
		Hairline Cracking	Heavy Cracking	tension debonding	Delamination
Double	0%	3	N/A	N/A	N/A
Double	2%	6	N/A	N/A	N/A
Double	4%	3	8	N/A	N/A
Double	6%	1	3	6	N/A
Double	8%	1	1	3	8
Single	0%	6	N/A	N/A	N/A
Single	2%	5	N/A	N/A	N/A
Single	4%	4	12	12	12
Single	6%	3	5	8	8
Single	8%	3	3	3	5

#### **5.4.4. Summary of Damage Analysis**

Analysis of the bearing damage information provided throughout the experiment lends itself to two conclusions. First, the data in Table 5.4 through Table 5.6 reinforce the damage principles discussed in NCHRP Report 596 (Stanton et al., 2008). This is because once a bearing has experienced damage of some sort the damage will remain throughout the life of a bearing. With the addition of more loading cycles, the severity of the damage observed increases. The other conclusion is that placing bearings at a superelevation of 6% or greater seems to be an unconservative practice when considering the potential for damage. While some would say that allowing a bearing to be loaded in the transverse direction at any level is not wise, analysis of the data resulting from this experiment suggest that small superelevations do not reduce the serviceability of the bearing significantly. It appears that moderation is the key with transverse loads. When combining the results of the damage analysis with that of the slip behavior, bearings placed at an elevation of 6% or greater tend to result in more damage and higher slip displacements. These issues lead to questions about the serviceability of elastomeric bearings subjected to transverse superelevations equal to or greater than 6%.

#### **5.5. Finite Element Analysis**

As mentioned in Section 4.5, TechMRT conducted a finite element analysis for each bearing pad configuration at the same superelevations that were tested in the laboratory. The resulting angular displacements shown in Section 4.5 do appear to match well with the laboratory data illustrating that finite element analysis of the bearing pads can be an effective research tool.

When looking at the results of the finite element analysis, the damage noticed during the laboratory can be explained through investigating the shear strains within the elastomeric bearing. Figure 5.78 through Figure 5.83 illustrate the strain profile within the elastomeric bearing along one of the transverse faces of the bearing. The transverse face in these figures is the face opposite the application of the transverse forces. Within each figure, the strain patterns are similar. The strain illustrated is the strain in the vertical, or z-direction. The strain occurring within the bearing is generally compressive in nature, except for localized areas of tension near the extreme top and bottom elements of the pad and areas along the shims.

Notice as the superelevation increases for each bearing pad configuration the size of the area undergoing the localized tension effects increases and the magnitude of the tension strains increases. As the local tensile strains increase, damage to the elastomer occurred. This started out as hairline cracks in the elastomer and proceed through the range of damage discussed in section 5.4. Debonding occurred when the tensile force exceeded that of the bonding forces between the elastomer and the shims at the edges of the bearing, and delamination occurred as this phenomenon continued down the length of the shims. Each level of damage observed in the laboratory generally occurred along the top and bottom shims first, then appeared along adjacent shims toward the centerline of the bearing. This behavioral pattern is explained through the strain patterns illustrated in Figure 5.78 through Figure 5.83. While these figures show the strain profiles for one transverse face, similar patterns exist on the other faces.

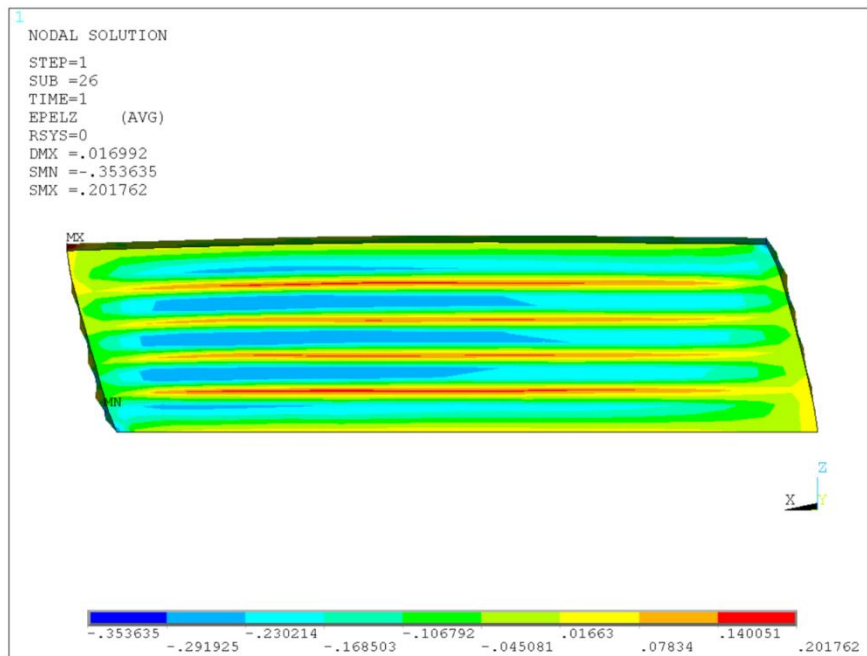


Figure 5.78--Strains in Z-direction (Transverse Face), 0% Single Pad Configuration

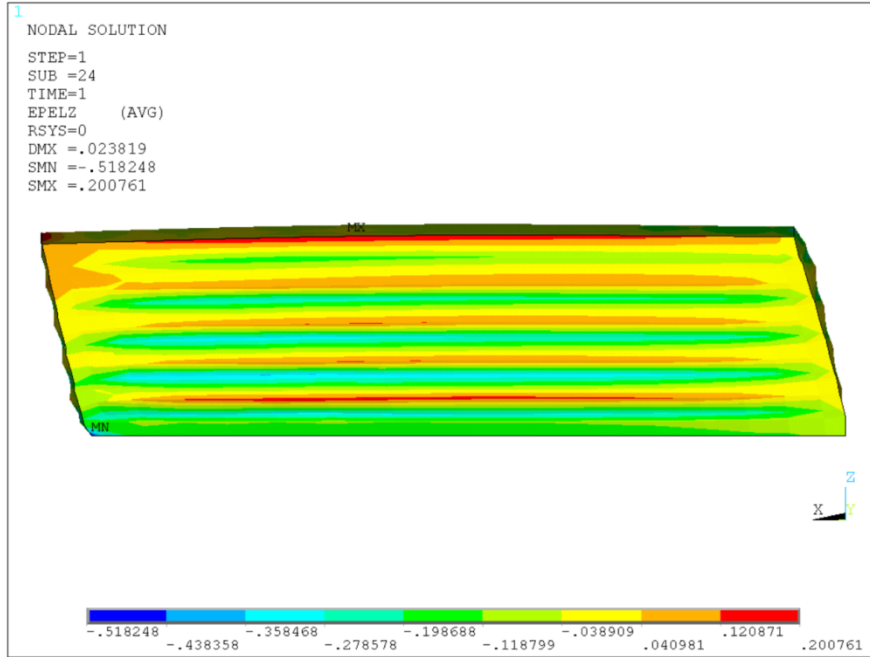


Figure 5.79--Strain in Z-direction (Transverse Face) 4% Single Pad Configuration

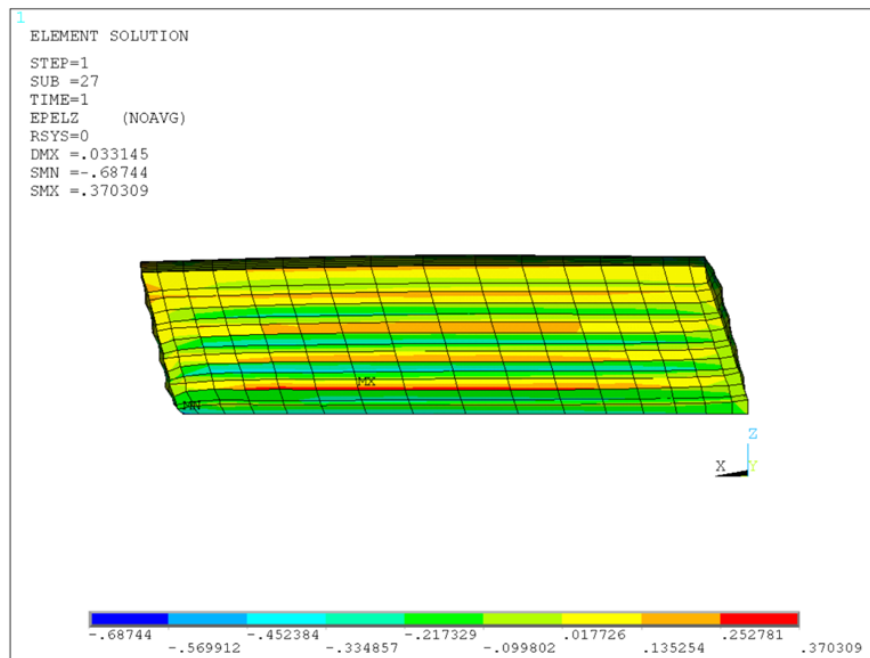


Figure 5.80--Strain in Z-direction (Transverse Face), 8% Single Pad Configuration

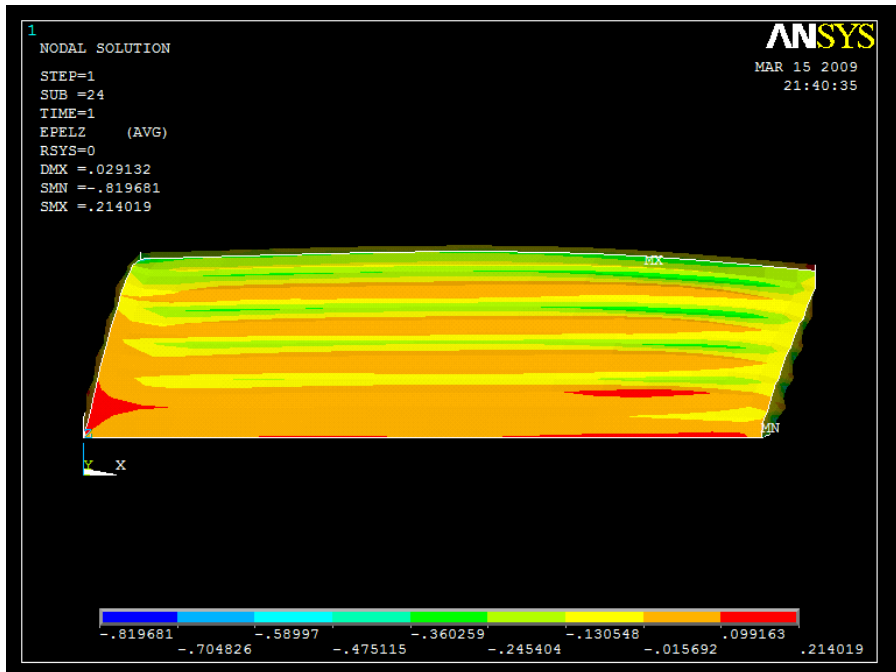


Figure 5.81--Strain in Z-direction (Transverse Face), 0% Double Pad Configuration

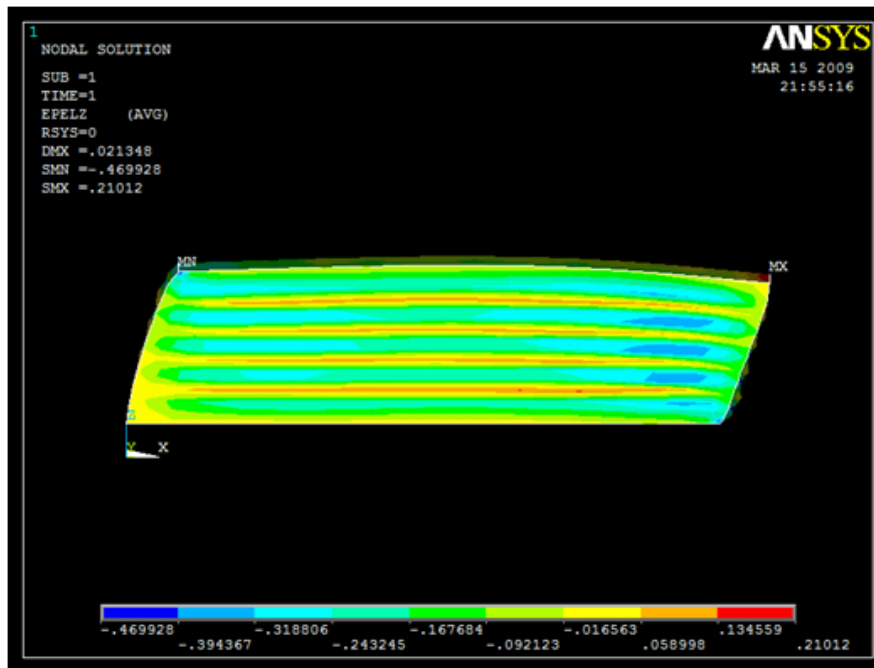


Figure 5.82--Strain in Z-direction (Transverse Face), 4% Double Pad Configuration

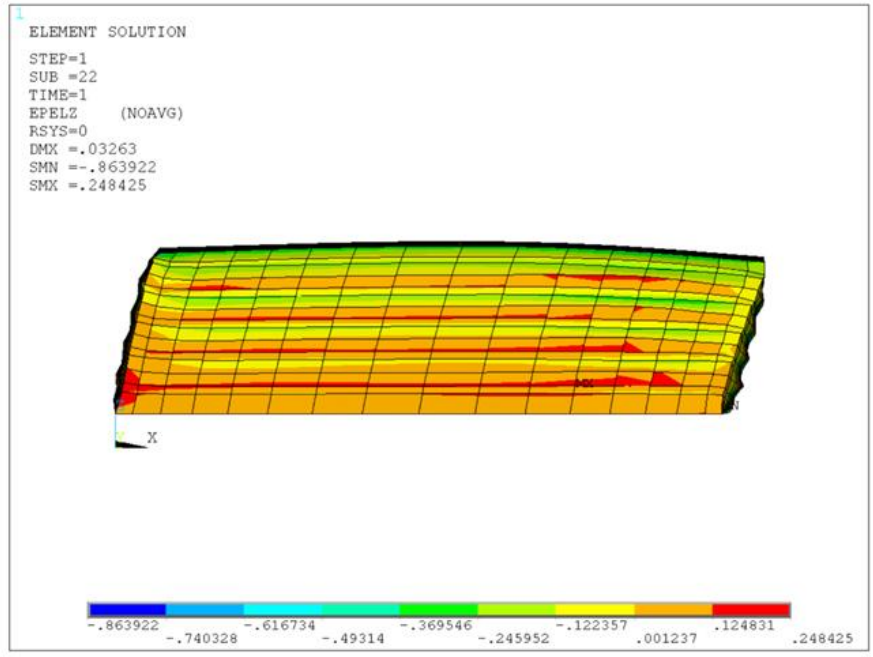


Figure 5.83--Strain in Z-direction (Transverse Face), 8% Double Pad Configuration

## 6. Conclusions and Recommendations

### 6.1. Research Objective No. 1 (New Design)

The first research objective was to determine if there was a need to consider the transverse superelevation in design, and if so, how it should be considered. In response to this objective, the following conclusions and recommendations are offered:

1. The transverse slope should be considered in new designs. A method utilizing two terms, the Delta1 and Delta2 terms, has been proposed in Section 3.2 that considers the effect of the transverse slope on the five applicable AASHTO Method “A” Elastomeric Bearing Design limit states. In order to incorporate the terms into TxDOT design provisions, modifications to the TxDOT LRFD Bridge Design Manual have been suggested. These provisions were submitted as Product P1 and are included in Appendix 6-1 “Product P1-Modifications to the LRFD Design of U-Beam Bearings”.
2. Field observations confirmed the presence of both the Delta1 and Delta2 deflections. The deflections were observed in bearings immediately after the placement of the U-beams and in bearings exposed to loading for several years.
3. Tables 3.4 through 3.13 were developed using the proposed modifications to the LRFD Design of U-Beam Bearings in order to show the impact of the proposed modifications to the normally designed span/spacing arrangements. In general, many of the design provisions exceed one or more of the allowable limit states when the transverse slope exceeds 4%. The tables also show the influence of the effective length required for thermal expansion and/or contraction. These tables, combined with the laboratory results, indicate that using transverse slopes greater than 4% have the potential for detrimental effects. Therefore, unless provisions are designed to mitigate the effects of the transverse slope, uniform-height steel-reinforced elastomeric bearings for U-beams should not be used for transverse slopes exceeding 4%.

4. A review of the existing literature revealed that some, but not much, information exists on the triaxial state of stress/strain in steel-reinforced elastomeric bearings. Much of the information that does exist pertains to natural rubber bearings which are not used in Texas.
5. The existing literature indicates that damage to elastomeric bearings is progressive. Results of the laboratory tests confirm this assessment.
6. Results of a nationwide survey indicate that eight states, in addition to Texas, currently use a U or Tub shaped section. The country is divided nearly evenly in response to the question “Does your state allow beam sections to be placed on a slope matching the slope of the roadway ...?”, with twenty (50%) responding “Yes” and 19 (47.5%) responding “No”. The response to “Does your state use uniform height elastomeric bearing pads to support members placed on a slope matching the slope of the roadway?” was identical, with twenty (50%) responding “Yes” and 19 (47.5%) responding “No”. One state, Florida, indicated that the transverse slope was limited to 2%. This limit most likely evolved from the rule-of-thumb 2% limit for longitudinal slopes which has historically worked well.
7. Theoretically, the double bearing arrangement should perform slightly better than the single bearing arrangement when required to resist a transverse moment. The resisting moment of inertia in the transverse direction is 2.4 times larger for the double bearing than the single bearing and the resisting section modulus in the transverse direction is 1.8 times larger.
8. Considering the combination of transverse and longitudinal deflections, the double bearing arrangement performed better in laboratory tests by allowing for nearly twice as much longitudinal displacement (for a given ratio of observed to predicted load) as compared to the single pad arrangement. Therefore, designers should consider placing the double pad arrangement on the end of the U-beam expected to undergo the highest longitudinal displacement.
9. The laboratory tests revealed that significant slip tended to occur for transverse slopes of 6% and higher.

10. Dapped beam configurations may impact the ability to inspect and/or monitor the performance of elastomeric bearings subjected to transverse slopes. This end condition prevents TxDOT from being able to inspect the bearings to determine the conditions of the bearings. TechMRT recommends that dapped beams should be avoided if possible for the cases when U-beams and their bearings are superelevated transversely.
11. A finite element analysis method has been developed that matches the laboratory results well and can be used for future research.

## **6.2. Research Objective No. 2 (Existing Bearings)**

The second research objective was to determine if there was a need to address existing U-beam bridges that have already been constructed on a significant transverse superelevation using standard steel-reinforced elastomeric bearing pads. If a need was determined, then recommendations for inspecting and documenting the condition were to be developed.

1. Electronic monitoring of existing steel-reinforced elastomeric bearings for U-beams is not recommended. Strain gages applied to the exterior of the bearings, although capable of undergoing high strains while remaining attached, provide information that is not useful because of localized bulging of the bearings on the sides between the internal shim plates.
2. In lieu of electronic monitoring, TechMRT recommends that existing bearings be monitored as a part of the routine inspection program. The following four items should be recorded:
  - a. The transverse angles on the front right and left faces of a bearing can be easily and accurately measured to the nearest degree by using a transparent two-inch-tall protractor as shown in Figure 4.1.
  - b. The longitudinal angles on the front of the bearing should be measured. Obtaining accurate readings for the longitudinal angles is often difficult, especially if the bearing is further back on the bearing seat. The inspector should use a flashlight and small, 2 inch standard 30-60-90 and 45-45-90 triangles to aid in the inspection. If a reading with the protractor is impossible, the triangles can be used to determine the approximate longitudinal angle (i.e. less than 30° or between 30° and 45°).

- c. The transverse and longitudinal slopes of the U-beam can be obtained by using a digital level.
  - d. Any visible damage including: cracking, tension debonding, or delamination.
3. TxDOT occasionally uses shear keys to limit or prevent the transverse displacement caused when a transverse slope exists. Limited observations and discussions with contractors have lead to the conclusion that shear keys perform only marginally well. Since a U-beam placed on a transverse slope instantaneously deflects the bearing as the U-beam is placed, it is difficult for U-beams to be placed in a way that does not cause some transverse deflection in the bearings. Also, limited inspections revealed that the up-slope side of a shear key is usually in full contact with localized spalling along the contact surface. A gap usually exists on the down-slope side of a shear key. The unusual phenomena observed where the superstructure pivoted about the shear key causing the bearing furthest from the pivot point to be dynamically compressed enough to be heard from the ground in one inspection was an alarming and unwanted side effect of using a shear key.
4. It is recommended that the wording in the TxDOT “Elements” Field and Coding Manual be revised in order to provide the inspector with more specific guidance on how to code Element No. 310 Elastomeric Bearings. (Texas Department of Transportation 2001) First, the wording for Condition State No. 3 which appears to be incorrectly copied from a different element, needs the basic wording corrected. Second, a sentence should be considered for each condition state that provides numeric guidance on the slope of the bearing. Third, although TxDOT does not consider Feasible Actions in the “Elements” Field and Coding Manual, three feasible actions are suggested. These recommendations are shown in Table 6.1.

Table 6.1 – Recommended Revisions to “Elements” Field Inspection and Coding Manual –  
Element No. 310

Condition	Description	Feasible Actions
1	The element shows little or no deterioration. Shear deformations are correct for existing temperatures. <b><i>The vertical slope is less than or equal to 10 degrees in the transverse direction and 30 degrees in the longitudinal direction.</i></b>	1. Do Nothing
2	Minor cracking, splitting or other deterioration may be present. Shear deformation may be slightly excessive. Strength and/or serviceability are not affected. <b><i>The vertical slope is between 10 and 20 degrees in the transverse direction and 30 and/or 45 degrees in the longitudinal direction.</i></b>	1. Do Nothing 2. Monitor Bearing
3	Advanced deterioration, debonding and/or delamination. Shear deformations may be excessive. Top and bottom surfaces may no longer be parallel. Loss of bearing support is imminent. <b><i>The vertical slope is greater than or equal to 20 degrees in the transverse direction and/or 45 degrees in the longitudinal direction.</i></b>	1. Do Nothing 2. Monitor Bearing 3. Reset/Replace Bearing

## References

- Abe, Masato, Yoshia, Junji, and Fujino, Yozo, (2004). "Multiaxial Behavior of Laminated Rubber Bearings and Their Modeling I: Experimental Study," *Journal of Structural Engineering*, Vol. 130, No. 8, pp 1119-1132.
- Abe, Masato, Yoshia, Junji, and Fujino, Yozo, (2004). "Multiaxial Behavior of Laminated Rubber Bearings and Their Modeling II: Modeling," *Journal of Structural Engineering*. Vol. 130, No. 8, pp 1133-1144.
- American Association of State Highway Officials (2007). *AASHTO LRFD Bridge Design Specifications, 4<sup>th</sup> Edition. Customary U.S. Units*. Washington D.C.
- American Association of State Highway Officials (2006). *LRFD Bridge Design Specifications, 3rd Edition with Interims*. Washington D.C.
- Arditzoglou, Y.J., Yura, J.A., and Haines, A.H., (1995). "Research Report No. 1304-2: Test Methods for Elastomeric Bearings on Bridges," Texas Department of Transportation.
- Chen, R. and Yura, J., (1995). "Research Report No. 1304-4: Wax Build-up on the Surfaces of Natural Rubber Bridge Bearings," Texas Department of Transportation.
- Cox, Randy, Homann, David, Eskridge, Amy, Hyzak, Michael, Freeby, Gregg, Wolf, Lloyd, Merrill, Brian, and Holt, John (2007). "Concrete Bridges in Texas," *Aspire*, Vol. 1, No. 2, pp 43 – 45.
- Doody, Micheal E. and Noonan, James E., (1999). "Long-Term Performance of Elastomeric Bridge Bearings," *Transportation Research Record*, No. 1688, pp 139-146.
- English, B.A., Klingner, R.E., and Yura, J.A. (1994). "Research Report No. 1304-1: Elastomeric Bearings: Background Information and Filed Study," Texas Department of Transportation.
- Green, Tanya, Yazdani, Nur, Spainhour, Lisa, and Cai, Chun S., (2001). "Effect of Bearing Stiffness and Skew Angle on Performance of Precast Concrete Bridge," *Transportation Research Record*, No. 1770, pp 27-33.
- Hamzeh, O., Tassoulas, J.L., and Becker, E.B., (1995). "Research Report No. 1304-5: Analysis of Elastomeric Bridge Bearings," Texas Department of Transportation.
- Hamzeh, O., Tassoulas, J.L., and Becker, E.B., (1998). "Behavior of Elastomeric Bridge Bearings: Computational Results," *Journal of Bridge Engineering*, Vol. 3, No. 3, pp 140 – 146.
- Heymsfield, Ernest, McDonald, Jamie, and Avent, Richard R., (2001). "Neoprene Bearing Pad Slippage at Louisiana Bridges," *Journal of Bridge Engineering*, Vol. 6, No. 1, pp 30 - 36.
- Herrmann, Leonard R., Ramaswamy, Ananth, and Hamidi, Ramin, (1989). "Analytical Parameter Study for Class of Elastomeric Bearings," *Journal of Structural Engineering*. Vol. 115, No. 10, pp 2415 – 2434.

Holt, John (June 8<sup>th</sup>, 2006). "Study of Elastomeric Bearings for Superelevated U-Beam Bridges." TxDOT (RTI).

Holt, John and Medlock, Ronald (2004). "Standardized Concrete Bridges in Texas," Proceedings from 2004 Concrete Bridge Conference, Charlotte North Carolina.

McDonald, Jamie, Heymsfield, Ernest, and Avent, Richard R., (2000). "Slippage of Neoprene Bridge Bearings," *Journal of Bridge Engineering*, Vol. 5, No. 3, pp 216 – 223.

Mozkah, A., Constantinou, C., and Reiaborn, A. (1990). "Teflon Bearings in Base Isolation I: testing." *Journal of Structural Engineering*. Vol. 116, No. 2, pp 438 – 454.

Muscarella, J.V. and Yura, J.A., (1995). "Research Report No. 1304-3: An Experimental Study of Elastomeric Bridge Bearings with Design Recommendations," Texas Department of Transportation.

Stanton, John F., Roeder, Charles W., Mackenzie-Helnwein, Peter, White, Christopher, Kuester, Colin and Craig, Brianne (2008). *National Cooperative Highway Research Program Report 596: Rotation Limits for Elastomeric Bearings*. Transportation Research Board, Washington D.C.

Texas Department of Transportation, (2006). "[Design Example for Elastomeric Bearings for Prestressed Concrete Beams](http://www.dot.state.tx.us/services/bridge/ex_other.htm)," [http://www.dot.state.tx.us/services/bridge/ex\\_other.htm](http://www.dot.state.tx.us/services/bridge/ex_other.htm).

Texas Department of Transportation, (2006). *LRFD Bridge Design Manual*, Texas Department of Transportation.

Texas Department of Transportation, (2007). *Superstructure Design Recommendations*, [http://www.dot.state.tx.us/publications/bridge/span\\_tables\\_ubeams.pdf](http://www.dot.state.tx.us/publications/bridge/span_tables_ubeams.pdf).

TxDOT Expressway, (2006). Bridge Standards, "Standard UBEB: Elastomeric Bearing and Bearing Seat Details," <http://www.dot.state.tx.us/insdtdot/orgchart/cmd/cserve/standard/bridge-e.htm>

TxDOT. *TxDOT Expressway British Standards (English)*. 2009.

<http://www.dot.state.tx.us/insdtdot/orgchart/cmd/cserve/standard/bridge-e.htm> (accessed 2009).

—. *Bridge Design Manual*. 2001.

—. "Bridge Detailing Manual." August 2001.

—. "LRFD Bridge Design Manual." April 1, 2007.

—. *Superstructure Design*. 2009.

[http://www.txdot.gov/business/contractors\\_consultants/bridge/super\\_design.htm](http://www.txdot.gov/business/contractors_consultants/bridge/super_design.htm) (accessed 2009).

—. *Superstructure Design Information*. 2009.

[http://www.txdot.gov/business/contractors\\_consultants/bridge/super\\_design.htm](http://www.txdot.gov/business/contractors_consultants/bridge/super_design.htm) (accessed 2009).

—. *Texas Department of Transportation: Other Design Information*. 2006.

[http://www.txdot.gov/business/contractors\\_consultants/bridge/other\\_design.htm](http://www.txdot.gov/business/contractors_consultants/bridge/other_design.htm) (accessed 2009).

Topkaya, Cem, and Yura, Joseph A., (2002). “Test Method for Determining the Shear Modulus of Elastomeric Bearings,” *Journal of Structural Engineering*, Vol. 128, No. 6.

Yakut, Ahmet, and Yura, Joseph A., (2002). “Evaluation of Low-Temperature Test Methods for Elastomeric Bridge Bearings,” *Journal of Bridge Engineering*, Vol. 7, No. 1, pp 50 - 56.

Yakut, Ahmet, and Yura, Joseph A., (2002). “Parameters Influencing Performance of Elastomeric Bearings at Low Temperatures,” *Journal of Structural Engineering*, Vol. 128 No. 8, pp 986 – 994.

Yakut, Ahmet, and Yura, Joseph A., (2002). “Evaluation of Elastomeric Bearing Performance at Low Temperature,” *Journal of Structural Engineering*, Vol. 128 No. 8, pp 986 – 994.

Yazdani, Nur, Eddy, Scott., and Cai, Chun S., (2000). “Effect of Bearing Pads on Precast Prestressed Concrete Bridges,” *Journal of Bridge Engineering*, Vol. 5, No. 3, pp 224 – 232.

Yazdani, Nur, Eddy, Scott M., and Cai, Chun S., (2000). “Validation of AASHTO Bearing Stiffness for Standard Precast Concrete Bridge Girders,” *ACI Structural Journal*, Vol. 97, No. 3, pp 436 – 442.

Yura, J., Kumar, A., Yakut, A., Topkaya, C., Becker, E. and Collingwood, J., (2001). *NCHRP Report 449: Elastomeric Bridge Bearings: Recommended Test Methods*. Washington D.C.: National Academy Press.

Appendix 2-1

Responses to Questionnaire Survey

State and Address	1. Does your state use a precast, prestressed U ...?	2. Do you know of any other states ...?	3. Does your state allow ... a slope matching the roadway ...?	4. Does your state use uniform height elastomeric pads ...?	5. If there is someone in your office that is familiar ... please provide their contact information.
Alabama Department of Transportation 1409 Coliseum Boulevard P. O. Box 303050 Montgomery, AL 36130	No	No	Yes	Yes	Fred Conway conwayf@dot.state.al.us 334-242-6007
Alaska Department of Transportation 3132 Channel Drive P. O. Box 12500 Juneau, AK 99519	No	Washington, Oregon	Yes	Yes	Elmer E. Marx elmer.marx@alaska.gov 907-465-6941
Arizona Department of Transportation 205 South 17th Avenue Mail Drop 613E Phoenix, AZ 85007	No	No	No	No	602-712-7391
Arkansas Department of Transportation P. O. Box 2261 Little Rock, AR 72203	No	No	No	No	501-569-2000
California Department of Transportation P. O. Box 942873 Sacramento, CA 94273-0001	-	-	-	-	916-227-7000
Colorado Department of Transportation  4201 E. Arkansas Avenue  Denver, CO 80222	Yes	California, Florida, Washington	Yes	Yes, Most designed simple span made continuous; only leveling pad is req'd	Jamal I. Elkaiss jamal.elkaissi@dot.state.co.us  303-757-9486
Connecticut DOT 2800 Berlin Turnpike Newington, CT 06131-7546	-	-	-	-	860-594-2000

State and Address	1. Does your state use a precast, prestressed U ...?	2. Do you know of any other states ...?	3. Does your state allow ... a slope matching the roadway ...?	4. Does your state use uniform height elastomeric pads ...?	5. If there is someone in your office that is familiar ... please provide their contact information.
Delaware Department of Transportation P. O. Box 778 Dover, DE 19903	No	No	No	No	302-760-2299
District of Columbia Dot Frank D. Reeves Municipal Center 2000 14th Street NW, 6th Floor Washington, DC 20009	-	-	-	-	202-673-6813
Florida Department of Transportation 605 Suwannee Street Tallahassee, FL 32399-0450	Yes	No	Yes - slopes < .02, then use tapered steel sole plates	Yes	Andre Pavlov andre.pavlov@dot.state.fl.us 850-414-4293
Georgia Department of Transportation No. 2 Capitol Square SW Atlanta, GA 30334	-	-	-	-	404-363-7512
Hawaii Department of Transportation Aliiamoku Building 869 Punchbowl Street Honolulu, HI 96813	No	No	No	No - We don't place member on slope. Bearings are horiz. But may match slope of bridge in long. direction	Paul Santo paul.santo@hawaii.gov 808-692-7611
Idaho Transportation Department 3311 W. State Street P. O. Box 7129 Boise, ID 83707-1129	No	No	Yes	Yes	
Illinois Department of Transportation 2300 S. Dirksen Parkway Springfield, IL 62764	No	No	No	No	Thomas Domagalski thomas.domagalski@illinois.gov 217-785-2913

State and Address	1. Does your state use a precast, prestressed U ...?	2. Do you know of any other states ...?	3. Does your state allow ... a slope matching the roadway ...?	4. Does your state use uniform height elastomeric pads ...?	5. If there is someone in your office that is familiar ... please provide their contact information.
Indiana Department of Transportation 100 N. Senate Avenue Room IGCN 755 Indianapolis, IN 46204	-	-	-	-	317-232-5474
Iowa Department of Transportation 800 Lincoln Way Ames, IA 50010	-	-	-	-	515-239-1564
Kansas Department of Transportation D.D. Eisenhower State Office Bldg. 700 S.W. Harrison Street Topeka, KS 66603-3754	No	No	No	Yes	785-296-3761
Kentucky Transportation Cabinet 200 Mero Street Frankfort, KY 40622	-	-	-	-	502-564-4560
Louisiana Department of Transportation P. O. Box 94245 Baton Rouge, LA 70804-9245	Yes - 2 projects so far	Yes - Texas	Yes	Yes	Paul Fossier pfossier@dotd.la.gov 225-374-1323
Maine Department of Transportation Child Street 16 State House Station Augusta, ME 04333-0016	No	No	Yes	Yes	Leanne Timberlake leanne.timberlake@maine.gov 207-624-3422
Maryland Department of Transportation 7201 Corporate Center Drive Hanover, MD 21076	No	No	No	NA	
Massachusetts Highway Department The Executive Office of Trans. 10 Park Plaza, Ste. 3170 Boston, MA 02116	-	-	-	-	617-973-7800

State and Address	1. Does your state use a precast, prestressed U ...?	2. Do you know of any other states ...?	3. Does your state allow ... a slope matching the roadway ...?	4. Does your state use uniform height elastomeric pads ...?	5. If there is someone in your office that is familiar ... please provide their contact information.
Michigan Department of Transportation State Transportation Building P. O. Box 30050 Lansing, MI 48909	No	No	Yes	Yes	Steve Beck beck52@michigan.gov
Minnesota Department of Transportation Transportation Building 395 John Ireland Boulevard St. Paul, MN 55155	No	No	No	No	Manjula Louis 631-366-4487
Mississippi Department of Transportation 401 North West Street Jackson, MS 39201	No	No	No	No	
Missouri Department of Transportation Central Office P. O. Box 270 Jefferson City, MO 65102-0270	No	No	Yes	Yes	
Montana Department of Transportation 2701 Prospect Avenue P. O. Box 201001 Helena, MT 59620-1001	No	No	Yes - Certain types of sections	No	Kent Barnes Kbarnes@mt.gov 406-444-6260
Nebraska Department of Roads P. O. Box 94759 Lincoln, NE 68509-4759	No	Colorado, Washington	Yes	Yes	Fouad Jaber: Fjaber@dot.state.ne.us 402-479-3967
Nevada Department of Transportation 1263 South Stewart Street Carson City, NV 89712	Yes	No	No	No	Mark Elicegui melicegui@dot.state.nv.us 775-888-7540
New Hampshire DOT John O. Morton Building 7 Hazen Drive Concord, NH 03302-0483	-	-	-	-	Mark Richardson 603-271-2551

State and Address	1. Does your state use a precast, prestressed U ...?	2. Do you know of any other states ...?	3. Does your state allow ... a slope matching the roadway ...?	4. Does your state use uniform height elastomeric pads ...?	5. If there is someone in your office that is familiar ... please provide their contact information.
New Jersey DOT P. O. Box 600 Trenton, NJ 08625-0600	No	No	NA	NA	
New Mexico DOT 1120 Cerrillos Road Santa Fe, NM 87504-1149	Yes	No	No	Yes	Jimmy D. Camp jimmy.camp@state.nm.us 505-827-5532
New York Department of Transportation 50 Wolf Road Albany, NY 12232-0203	No	No	No	No	Arthur Yannotti ayannotti@dot.state.ny.us 518-457-4453
North Carolina DOT 1503 Mail Service Center Raleigh, NC 27699-1503	No	No	No	No	
North Dakota DOT 608 East Boulevard Avenue Bismarck, ND 58505-0700	No	No	Yes	No	Larry Schwartz lschwartz@nd.gov 701-328-4446
Ohio Department of Transportation 1980 W. Broad Street Columbus, OH 43223	No	No	Yes	No	Tim Keller tim.keller@dot.state.oh.us 614-446-2463
Oklahoma Department of Transportation 200 N. E. 21st Street Oklahoma City, OK 73105	yes	No	No	-	Jack Schmiedel jschmiedel@odot.org 405-521-6488
Oregon Department of Transportation 355 Capitol Street. N.E. Salem, OR 97301-3871	Yes	Washington	No - Beam seats are level	NA	Bruce Johnson / Bruce.V.Johnson @odot.state.tx.od.us 503-986-3344
Pennsylvania DOT Bridge Quality Assurance Division P. O. Box 3560 Harrisburg, PA 17105-3560	No	No	Yes	Yes - only prestressed concrete adjacent box beams are placed parallel to roadway	Patti Kiehl pkiehl@state.pa.us 717-772-0586

State and Address	1. Does your state use a precast, prestressed U ...?	2. Do you know of any other states ...?	3. Does your state allow ... a slope matching the roadway ...?	4. Does your state use uniform height elastomeric pads ...?	5. If there is someone in your office that is familiar ... please provide their contact information.
Rhode Island DOT Two Capitol Hill Providence, RI 02903	No	No	Yes	Yes	Michael L. Savella msavella@dot.ri.us 401-222-2053 X. 4080
South Carolina DOT P. O. Box 191 Columbia, SC 29202-0191	No	No	yes - precast Ubeams placed on slope	yes - For precast deck beam units	
South Dakota Department of Transportation Becker-Hansen Building 700 E. Broadway Avenue Pierre, SD 57501	No	No	No	No	
Tennessee Department of Transportation James K. Polk Building Ste. 700 Nashville, TN 37243-0349	No	Yes -Washington State	Yes	Yes	
Utah Department of Transportation 4501 South 2700 West Mail Stop 141200 Salt Lake City, UT 84114-1200	No	No	No	No	Ray Cook raycook@utah.gov 801-964-4466
Vermont Agency of Transportation One National Life Drive Montpelier, VT 05633-5001	-	-	-	-	Wm. Michael Hedges mike.hedges@state.vt.us 802-828-2621
Virginia Department of Transportation Struc. & Bridge Division, Room 1011 1401 E. Broad Street Richmond, VA 23219	No	No	No	No	Julius Volgyi, Jr. julius.volgyi@vdot.virginia.gov 814-786-7537
Washington State DOT P. O. Box 47300 Olympia, WA 98504-7300	Yes	Yes - Colorado	Yes	Yes	Bijan Khaleghi khalegb@wsdot.wa.gov 360-705-7181

State and Address	1. Does your state use a precast, prestressed U ...?	2. Do you know of any other states ...?	3. Does your state allow ... a slope matching the roadway ...?	4. Does your state use uniform height elastomeric pads ...?	5. If there is someone in your office that is familiar ... please provide their contact information.
West Virginia DOT Building 5 1900 Kenawha Boulevard E. Charleston, WV 25305	No	Yes - Tennessee (did in the '80's)	Yes	Yes	Jim Shook jshook@dot.state.wv.us
Wisconsin Department of Transportation Hill Farms State Transportation Bldg. P. O. Box 7910 Madison, WI 53707-7910	No	Indiana Maybe	No	No	
Wyoming Department of Transportation 5300 Bishop Boulevard Cheyenne, WY 82009-3340	No	No	Yes - Precast I Sections	Yes	Gregg Fredrick

Appendix 3-1

Standard Texas U-beam Sheets



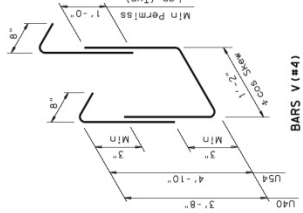






**BARS U(#5)**

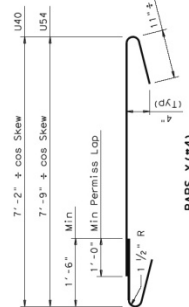
Bars U may be placed with multiple segments, provided no segment is less than 10 ft in length and 40 ft Min C-C splices.



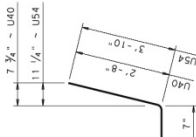
**BARS V (#4)**  
(ISOMETRIC VIEW)

**GENERAL NOTES:**

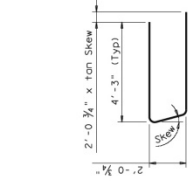
Designed according to AASHTO LRFD Specifications. Concrete must be Class H, Use Class H (HPC) if required elsewhere in plans. Steel must be Grade 60. An equal area of welded wire reinforcement, conforming to ASTM A 997, may be used in lieu of bars U, V, W, X, and Y. All reinforcing steel unless shown otherwise shall be covered to all reinforcing steel unless shown otherwise. Chamfer all outside corners for skew over 20 degrees. Provide a chamfer or 1/8" radius at all corners noted to require a chamfer. Shop drawings can be prepared with horizontal skew angles up to 15 degrees. Bars U, V, W, X, and Y shall be provided in addition to the fabrication tolerances (fabrication). #24, "Precast Concrete Structures (Fabrication)".



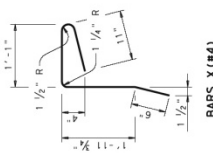
**BARS Y (#4)**



**BARS P (#4)**

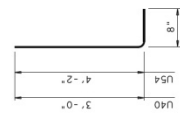


**BARS W (#4)**



**BARS X (#4)**

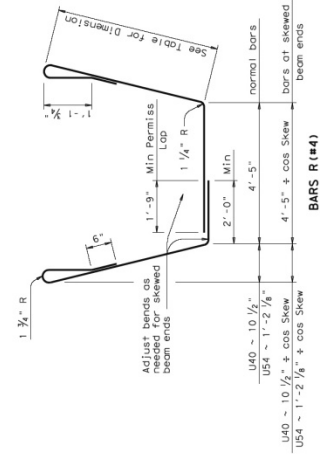
BAR R DIMENSION		Beam Type
Skew Angle	U40	U54
0° thru 15°	3'-9 1/4"	4'-11 1/2"
15° thru 30°	3'-9 1/2"	5'-0"
30° thru 45°	3'-10 1/4"	5'-1"



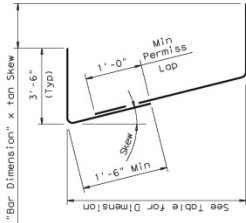
**BARS F (#4)**

BAR DS DIMENSION		Beam Type
Bar	U40	U54
DS1	4'-8"	4'-9"
DS2	4'-11"	5'-0"
DS3	5'-2"	5'-5"
DS4	5'-4 1/4"	5'-9 1/2"
DS5	5'-6 1/2"	6'-1 1/2"

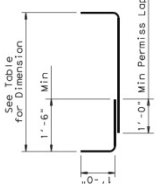
BAR D DIMENSION		Beam Type
Bar	U40	U54
D1	4'-8"	4'-9"
D2	4'-11 1/2"	5'-1"
D3	5'-2"	5'-5 1/2"
D4	5'-4"	5'-10"
D5	5'-6 1/2"	6'-1 1/2"



**BARS R (#4)**



**BARS DS1-5 (#4)**



**BARS D1-5 (#4)**

DISCLAIMER: The use of this drawing is governed by the Texas Engineering Practice Act. No warranty of any kind is made by KDOT for any purpose whatsoever. KDOT assumes no responsibility for the conversion of this drawing to other formats or for incorrect results or damages resulting from its use.

DATE	DESCRIPTION	BY	CHECKED

HL93 LOADING SHEET 3 OF 3

**Texas Department of Transportation**  
Bridge Division

**PRESTRESSED CONCRETE U-BEAM DETAILS**

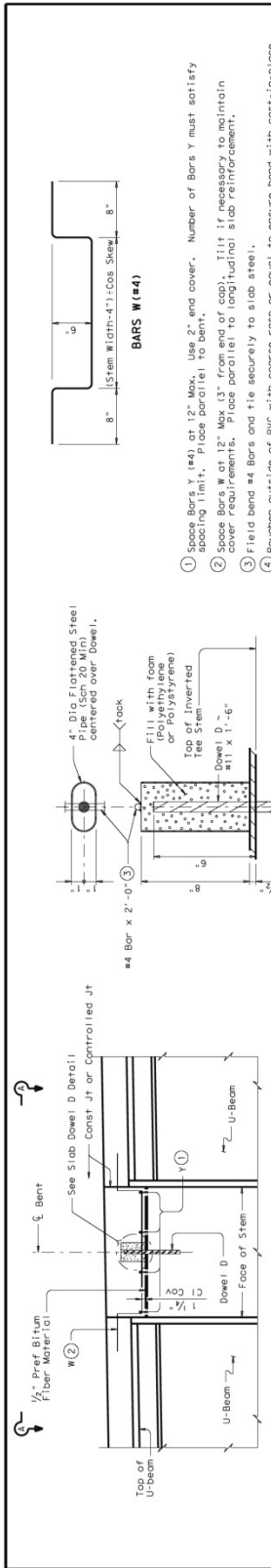
UBD

FILE	CONTRACT	NO.	PROJECT	NO.	DATE

REV	DATE	DESCRIPTION

QUANTITY	CONTROL	SHEET

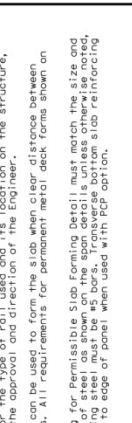




**CONTINUOUS SLAB OVER INVERTED TEE BENT**

Slab reinforcement not shown for clarity.

See standard PMDF for connection details



**C-I-P DRAIN DETAIL**

See "C-I-P Drain Detail"



**DRAIN DETAILS**

(Saw-cutting is not allowed)



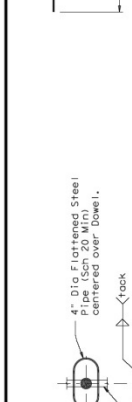
**CHAMFER AND DRIP BEAD DETAIL**

See standard PMDF for connection details



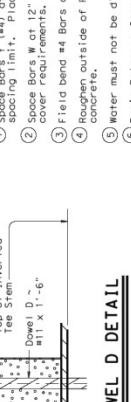
**PERMISSIBLE SLAB FORMING DETAIL**

See standard PMDF for connection details



**SLAB DOWEL D DETAIL**

See Bent Details for number and location.



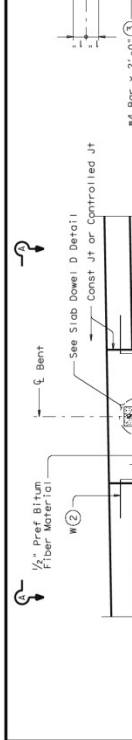
**CONTROLLED JOINT DETAIL**

(Saw-cutting is not allowed)



**VIEW A-A**

Applies to sloped overhang only



**BARS W (#4)**

- Space Bars Y (#4) at 12\"/>

- Drain Entrance formed in Rail or Sidewalk.
- All openings and fittings to be at slantwater (See 401 PVC. See Item 481. PVC Pipe for Drains for slope, connections and solvent welding. Bend reinforcing steel to clear PVC 1\"/>

- Bottom slab reinforcing for Permissible Slab Forming Detail must match the size and location of the top slab reinforcing. The bottom slab reinforcing steel must be as bars. Transverse bottom slab reinforcing must have 1\"/>

**GENERAL NOTES:**

Specify fasteners in accordance with AASHTO LRFD

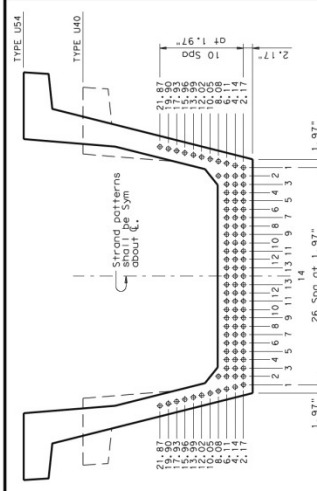
Texas Department of Transportation  
 Bridge Division  
**MISCELLANEOUS  
 SLAB DETAILS**  
**PRESTR. CONC U-BEAM SPANS**

UJRM  
 FEDERAL AID PROJECT  
 FEDERAL AID DISTRICT  
 FEDERAL AID COUNTY  
 FEDERAL AID CITY

DATE: 07/17/2008  
 DRAWN BY: J. J. JONES  
 CHECKED BY: J. J. JONES  
 DESIGNED BY: J. J. JONES

DISCLAIMER: The use of this standard is governed by the Texas Engineering Practice Act. No warranty of any kind is made by TxDOT for any purpose whatsoever. TxDOT assumes no responsibility for the accuracy or the appropriateness of other formats or for incorrect results or damages resulting from the use.

NO.	DATE	BY	DESCRIPTION
1	07/17/2008	J. J. JONES	ISSUED FOR CONSTRUCTION







## Appendix 3-2

TxDOT Design Example for Elastomeric Bearings for Prestressed Concrete Beams

County: Any      CSJ: Any      Design: BRG      Date: 12/2006  
 Hwy: Any      Ck Dsn: BRG      Date: 12/2006

Design: Bridge Bearing Pad Design Example

Design based on AASHTO LRFD Bridge Design Specifications - 3rd Ed. - 2006 Interims and TxDOT LRFD Bridge Design Manual and Standards

The usual starting place for "designing" elastomeric bearings is an analysis of the standard pad configurations for applicability to the superstructure geometry. In particular, the pads must satisfy slip requirements for the designed unit length. Other factors such as compressive stress, stability, rotation, and bearing seat geometry are accounted for in the standard pad design and therefore do not need to be checked as long as the standard pad is not altered.

The intention of the original design for the bearings represented on the IBEB Standard sheet was to make the pads usable for all simple spans, all two span units, and a large number of three span units. Due to all the conditions that can reduce the dead load on the end bearings (narrow beam spacing, short end span, severe beam slope) and thereby increase the chance for slip, good engineering judgement dictates checking the standard pad for suitability on any continuous unit with three or more spans.

For purposes of illustrating TxDOT's design method, the example below will examine all the requirements, even though for a standard pad a slip check alone will usually suffice if the unit is under 400' in length. In general, designers should be more conservative on stability (both construction and final) and slip, and liberal on compressive allowables.

**Unit Information:** (4-Span Prestressed Concrete I-Beam Unit)

The design example will consider the first span of 60ft with prestressed concrete beams (Type C) and a T501 rail.

NoSpans = 4  
 UnitLength = 60ft + 80ft + 80ft + 70ft

UnitLength = 290 ft

Span = 60ft

BeamSpacing = 8ft

SlabThickness = 8in

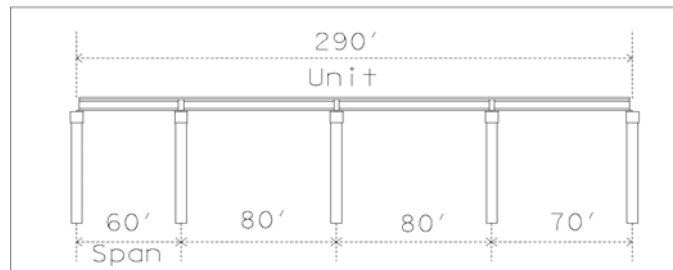
UnitWeight<sub>Concrete</sub> =  $150 \frac{\text{lb}}{\text{ft}^3}$

BeamWeight =  $0.516 \frac{\text{k}}{\text{ft}\cdot\text{beam}}$

RailWeight =  $0.326 \frac{\text{k}}{\text{ft}\cdot\text{rail}}$

BeamSlope = 1.03%

Skew = 30deg



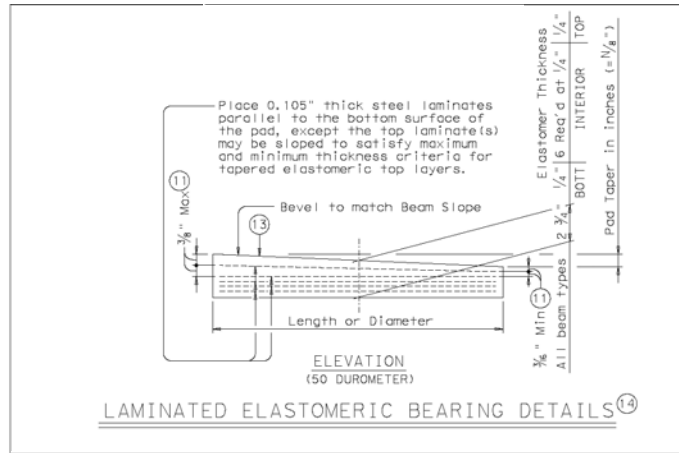
(Max Beam Slope From RDS)

Although the skew is shown in this design example and would affect the pad area, it is not used in any of the below calculations since the area reduction of no more than 10%, due to clipped pads, is not a concern. For further explanation see Appendix A on pg. 8.

## Bearing Pad Information:

The minimum overall thickness for a bearing pad should be at least 1 1/2" of elastomer (i.e., excluding plate thickness) to help the bearing compensate for beam and bearing seat build-up non parallelism, and/or surface irregularities. Certain cases where the designer needs to accommodate tight construction clearance limitations, match existing profile grades using existing caps, etc., may also be sufficient reason to violate this general rule of thumb for minimum elastomer thickness.

(Check Standard Pad for Ty C Beam (Ref. IBEB Standard))



Elastomer = 50 Durometer Neoprene

$h_s$  = Elastomer reinforcement;  
Grade 36, 12 gauge steel plates;

$$h_s = 0.105 \text{ in}$$

$h_{ro}$  = Individual thickness of the outer (top and bottom) layers of elastomer

$$h_{ro} = 0.25 \text{ in}$$

$n_{ro}$  = Number of the outer layers of elastomer

$$n_{ro} = 2$$

$h_{rto}$  = Total thickness of the outer layers of elastomer

$$h_{rto} = h_{ro} \cdot n_{ro}$$

$$h_{rto} = 0.5 \text{ in}$$

$h_{ri}$  = Individual thickness of the interior layers of elastomer

$$h_{ri} = 0.25 \text{ in}$$

$n_{ri}$  = Number of the interior layers of elastomer

$$n_{ri} = 6$$

$h_{rti}$  = Total thickness of the interior layers of elastomer

$$h_{rti} = h_{ri} \cdot n_{ri}$$

$$h_{rti} = 1.5 \text{ in}$$

$h_{rt}$  = Total thickness of the layers of elastomer

$$h_{rt} = h_{rto} + h_{rti}$$

$$h_{rt} = 2 \text{ in}$$

$$\text{TotalPadHeight} = h_{rt} + (n_{ro} + n_{ri} - 1) \cdot h_s$$

$$\text{TotalPadHeight} = 2.735 \text{ in}$$

(50 Durometer Neoprene is standard, but for beams on a severe grade and horizontal displacement 60 or 70 Durometer Neoprene may be desired. For additional information see report 1304-3.)

$$\text{Length}_{\text{Pad}} = 7\text{in}$$

$$\text{Width}_{\text{Pad}} = 16\text{in}$$

$$\text{PlanArea}_{\text{Pad}} = \text{Length}_{\text{Pad}} \cdot \text{Width}_{\text{Pad}}$$

$$\text{PlanArea}_{\text{Pad}} = 112\text{in}^2$$

For additional information on tapers, overall geometry and general information see Appendix A starting on pg. 8.

### Shape Factor:

$A_b$  = The area of perimeter free to bulge for an individual layer of elastomer

$$A_b = (\text{Length}_{\text{Pad}} + \text{Width}_{\text{Pad}}) \cdot 2 \cdot h_{ri}$$

$$A_b = 11.5\text{in}^2$$

$$S = \frac{\text{PlanArea}_{\text{Pad}}}{A_b}$$

$$S = 9.739$$

### Loads:

#### Dead Load:

$$\text{Beam}_{\text{DL}} = \text{BeamWeight} \cdot \frac{\text{Span}}{2}$$

$$\text{Beam}_{\text{DL}} = 15.48\text{ k}$$

$$\text{Slab}_{\text{DL}} = \text{UnitWeight}_{\text{Concrete}} \cdot \text{SlabThickness} \cdot \text{BeamSpacing} \cdot \frac{\text{Span}}{2}$$

$$\text{Slab}_{\text{DL}} = 24\text{ k}$$

$$\text{Rail}_{\text{DL}} = \text{RailWeight} \cdot \frac{\text{Span}}{2} \cdot \frac{1}{3\text{beams}}$$

$$\text{Rail}_{\text{DL}} = 3.26\text{ k}$$

$$\text{Total}_{\text{DL}} = \text{Beam}_{\text{DL}} + \text{Slab}_{\text{DL}} + \text{Rail}_{\text{DL}}$$

$$\text{Total}_{\text{DL}} = 42.74\text{ k}$$

(Refer to Appendix B on pg. 11, Table B-1 or IBEB Standard for pad size)  
(Width is Parallel to bridge long axis)

(LRFD 14.7.5.1)

(The target shape factor range is 10.0 to 12.0, to utilize the compressive capacity. If the shape factor is below 10.0 the capacity decreases, and if the shape factor is above 12.0 it does not supply any extra capacity due to the 1.2ksi cap on the compressive capacity. )

(TxDOT Design Manual)  
Overlay is not considered in bearing pad design since the lightest dead load is conservative for slip, the typical controlling factor, and compressive allowables have a large factor of safety.

Distribute rail load to a maximum of 3 outer beams.

### Live Load:

-No impact loading is considered when calculating compressive stress (LRFD C14.7.5.3.2; TxDOT Design Manual)

$$R_{x_{Truck}} = 32k + 32k \cdot \left( \frac{\text{Span} - 14\text{ft}}{\text{Span}} \right) + 8k \cdot \left( \frac{\text{Span} - 28\text{ft}}{\text{Span}} \right) \quad (\text{LRFD 3.6.1.2.2})$$

$$R_{x_{Truck}} = 60.8 \text{ k}$$

$$R_{x_{Lane}} = 0.64 \frac{\text{k}}{\text{ft} \cdot \text{lane}} \cdot \frac{\text{Span}}{2} \quad (\text{LRFD 3.6.1.2.4})$$

$$R_{x_{Lane}} = 19.2 \frac{\text{k}}{\text{lane}}$$

$$LLDF_{\text{Shear}} = 0.814$$

$$\text{BearingLiveLoad} = (R_{x_{Truck}} + R_{x_{Lane}}) \cdot LLDF_{\text{Shear}}$$

$$\text{BearingLiveLoad} = 65.12 \text{ k}$$

*(The Live Load Reactions are assumed to be the Shear Live Load Distribution Factor multiplied by the Lane Load Reaction. The Shear Live Load Distribution Factor was calculated using the "LRFD Live Load Distribution Factors" Spreadsheet)*

### Compressive Stress Check: (Service Limit)

#### Shear Modulus:

$$G_{73} = 95\text{psi} \quad \text{at } 73^{\circ}\text{F}$$

$$G_0 = 175\text{psi} \quad \text{at } 0^{\circ}\text{F}$$

(LRFD 14.7.6.3.2)

*(LRFD 14.7.5.2; Use TxDOT criteria for shear modulus from Design Manual)*

There is a range of values for the shear modulus (95psi-130psi) that you may actually receive from the fabricator when you specify 50 Durometer. After the research for Report 1304-3, TxDOT decided to use Yura's suggested value of 95psi since it is conservative.

#### Allowable Stress :

$$S = 9.739 \quad (\text{Calculated on pg. 8})$$

MaxStress<sub>DL</sub> is the smaller of:

$$1.2 \text{ ksi}$$

$$1.2\text{ksi} \times (G_{73}) \times (S) = 1.11\text{ksi}$$

$$\text{MaxStress}_{DL} = 1.11 \text{ ksi}$$

$G_S$  = Total compressive load stress

$G_S$  is the smaller of:

$$1.5 \text{ ksi}$$

$$1.5\text{ksi} \times (G_{73}) \times (S) = 1.39\text{ksi}$$

$$G_S = 1.39 \text{ ksi}$$

(LRFD 14.7.6; TxDOT Design Manual)

*The 1200 psi dead load stress maximum should not be exceeded by more than 5%, and only if the shape factor permits. For further explanation see Appendix A on pg.9.*

*The 1500 psi limit, is not an absolute max, and overages of up to 15% above this limit are not cause to resize the pad. For further explanation see Appendix A on pg.9.*

**Actual Stress:**

Dead Load Stress:

$$\sigma_{DL} = \frac{\text{Total}_{DL}}{\text{PlanArea}_{pad}}$$

$$\sigma_{DL} = 0.382 \text{ ksi}$$

MaxStress <sub>DL</sub> is greater than $\sigma_{DL}$ therefore OK.
---

Total Load Stress:

$$\sigma_{TL} = \frac{\text{BearingLiveLoad} + \text{Total}_{DL}}{\text{PlanArea}_{pad}}$$

$$\sigma_{TL} = 0.963 \text{ ksi}$$

G <sub>S</sub> is greater than $\sigma_{TL}$ therefore OK.
--

**Shear Check (Strain):** (Service Limit)

(LRFD 14.7.6.3.4)

 $\Delta s$  = max. total shear deformation of the elastomer at service limit state

$$\text{CoefThermalExpan}_{\text{Concrete}} = 0.000006 \frac{\text{in}}{\text{in}\cdot\text{degF}} \quad (\text{LRFD 5.4.2.2})$$

$$\Delta s = \text{CoefThermalExpan}_{\text{Concrete}} \cdot \frac{\text{UnitLength}}{2} \cdot 70 \text{degF} \quad (\text{TxDOT Desgin Manual - use } \Delta T=70 \text{degF})$$

$$\Delta s = 0.731 \text{ in}$$

Current AASHTO specifications suggest a 50% maximum shear strain limit. Therefore, the pad elastomer material (steel plate thickness not included) total thickness must be twice the expected thermal movement at the bearing.

$$h_{rt} = 2 \text{ in} \quad (\text{calculated on pg. 2})$$

$$2\Delta s = 1.462 \text{ in}$$

$h_{rt}$ is greater than $2\Delta s$ therefore OK.
--

**Anchorage Check (Slip):** (Strength Limit)

(LRFD 14.7.6.4; Use TxDOT Design Manual)

TxDOT uses the shear modulus "G<sub>0</sub>" (modulus at 0 deg F) for the slip check because the pad is stiffer at colder temperatures and therefore produces larger shear forces when the beam contracts thermally.

$$\gamma_{pmin} = \text{Minimum permanent load factor} \quad (\text{LRFD 3.4.1-2})$$

$$\gamma_{pmin} = 0.9$$

$$\text{FactoredTotal}_{DL} = \gamma_{pmin} \cdot \text{Total}_{DL}$$

$$\Delta s_{allow} = \frac{(0.2 - \text{BeamSlope}) \text{FactoredTotal}_{DL} h_{rt}}{G_0 \cdot \text{PlanArea}_{pad}}$$

$$\Delta s_{allow} = 0.745 \text{ in}$$

$\Delta s_{allow}$ is greater than $\Delta s$ therefore OK.
---

If the slip check were to fail, increasing the height of the bearing pad is the typical solution. F or more solutions for slip check failure refer to Appendix A on pg.10.

**Stability:**

$$h_{rt} = 2 \text{ in}$$

$h_{rtallow}$  is the smaller of:

$$\frac{\text{Length}_{\text{Pad}}}{3} = 2.333 \text{ in}$$

$$\frac{\text{Width}_{\text{Pad}}}{3} = 5.333 \text{ in}$$

$$h_{rtAllow} = 2.333 \text{ in}$$

$h_{rtAllow}$  is greater than  $h_{rt}$  therefore OK.

**Compressive Deflection:** (Service Limit)

Compressive deflection is usually not a concern from a functionality standpoint since the 4% to 5% range of deflection that most of TxDOT's standard pads undergo, yields a hardly noticeable 3/32" vertical compression. For further explanation refer to Appendix A on pg.10.

$$\varepsilon_i = 4.4\%$$

( $\varepsilon_i=4\%$  for shape factors approaching 10.0)

$$\sigma_{TL} = 0.963 \text{ ksi}$$

$$S = 9.74$$

(Use  $S$  and  $\sigma_{TL}$  to get  $\varepsilon_i$  from Figure C14.7.5.3.3-1, which can be found in Appendix C on pg. 12, Figure C-1.)

$$\delta = \sum \varepsilon_i h_i = \sum \delta_i$$

$$h_{ri} = 0.25 \text{ in} \quad (\text{Calculated on pg. 2})$$

Since all layers in the bearing pad are the same thickness and shape,  $\varepsilon_i$  is the same for every layer and therefore the below equations are true.

$$\delta_i = \varepsilon_i \cdot h_{ri}$$

$$\delta_i = 0.011 \text{ in}$$

$$h_{rt} = 2 \text{ in}$$

$$\delta = \varepsilon_i \cdot h_{rt}$$

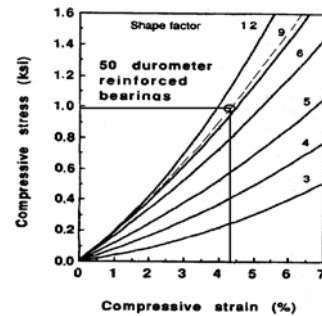
$$\delta = 0.088 \text{ in}$$

$$\delta_{iwithCreep} = 1.25 \cdot \delta_i$$

$$\delta_{iwithCreep} = 0.0138 \text{ in}$$

(LRFD 14.7.6.3.6; According to the LRFD Design Manual it is acceptable to use  $h_{rt}$  instead of the total pad height.)

(TxDOT Design Manual-"estimate compressive deflection using AASHTO LRFD Bridge Design Specifications, Figure C14.7.5.3.3-1.)



(LRFD 14.7.5.3.3-1)

$$0.07h_{ri} = 0.018 \text{ in}$$

$0.07h_{ri}$  is greater than  $\delta_{iwithCreep}$  therefore OK.

(LRFD Table 14.7.5.2-1)

(LRFD 14.7.6.3.3)

**Rotation:** (Service Limit)

(Use TxDOT Design Manual)

AASHTO has strict guidelines for rotation that TxDOT does not adhere to. AASHTO seeks to prevent any amount of lift off, a requirement that TxDOT does not support. Most TxDOT reinforced elastomeric bearing pads are used under prestressed concrete beams that rotate little (less than 0.005 radians) and impart a fairly heavy dead load on a relatively narrow (9" max) pad, making uplift due to rotation an improbable event. The research for Report 1304-3 has shown rotations close to 0.030 radians can be accommodated by our standard pads with less than 20% lift off, and even with that amount of lift off the pad will function normally. We regularly encounter cases in construction where it is noted that the pad is not in contact with a bearing surface for a considerable portion of the pad area (usually due to construction tolerances, mis-matches in surface slopes, etc.) with no apparent detriment to the bearing performance in final service.

Non-Composite I-Beam Properties:

$$E = 5000\text{ksi}$$

$$I = 82602\text{in}^4$$

$$q = \text{BeamWeight} + \frac{\text{RailWeight}}{3} + \text{SlabThickness} \cdot \text{BeamSpacing} \cdot \text{UnitWeight}_{\text{Concrete}} \quad (\text{Weight of the superstructure})$$

$$q = 1.425 \frac{\text{k}}{\text{ft}}$$

$$\theta_{\text{DL}} = \frac{q \cdot \text{Span}^3}{24 \cdot E \cdot I}$$

$$\theta_{\text{DL}} = 0.0045 \text{ rad}$$

$$\text{camber} = 2\text{in}$$

$$\theta_{\text{camber}} = \frac{4 \cdot \text{camber}}{\text{Span}}$$

$$\theta_{\text{camber}} = 0.011 \text{ rad}$$

$\theta_{\text{camber}}$  is greater than  $\theta_{\text{DL}}$  therefore:

$$\theta_{\text{DL}} = 0 \text{ rad}$$

$$\Delta_{\text{LL}} = \frac{\text{Span}}{800}$$

$$\theta_{\text{LL}} = \frac{4 \cdot \Delta_{\text{LL}}}{\text{Span}}$$

$$\theta_{\text{LL}} = 0.005 \text{ rad}$$

$$\theta_{\text{Total}} = \theta_{\text{LL}} + \theta_{\text{DL}} + 0.005\text{rad}$$

$$\theta_{\text{Total}} = 0.01 \text{ rad}$$

$$\frac{\theta_{\text{Total}} \cdot (0.8 \cdot \text{Length}_{\text{Pad}})}{2} = 0.028 \text{ in}$$

$$\delta = 0.088 \text{ in} \quad (\text{Calculated on pg. 6})$$

$\delta \text{ is greater than } \frac{\theta_{\text{Total}} \cdot (0.8 \cdot \text{Length}_{\text{Pad}})}{2} \text{ therefore OK.}$
--

(Camber From  
PSTRS14/PGSuper output)

(Assuming camber is  
the result of uniform  
moment caused by  
prestressing)

(For the LL Midspan  
deflection use  
PSTRS14/PGSuper or  
assume Span/800 to be  
conservative)

(0.005 radians is added to  
account for construction  
uncertainties) (TxDOT  
Design Manual)

(TxDOT Design Manual)

## Appendix A

### Unit Information:

#### *Skew:*

In general, the clipped pad areas do not decrease by more than approximately 10%. The pad plan dimensions were increased when more severe clips were needed. The 10% reduction for clips or the area for dowel holes is not a concern for the following reasons:

- 1.) TxDOT is extremely conservative (greater than a factor of 10 for compressive failure) on compressive allowables, thus increasing slip prevention.
- 2.) Shape factor controlled D.L. compressive allowables vary minimally from the assumptions in the standards due to the altered perimeter to area ratios when clipped.
- 3.) Compressive deflections are usually around  $3/32$ " for standard pads.

### Bearing Pad Information:

#### *Bearing Pad Taper:*

Taper is usually not specified by the designer for TxDOT jobs. The fabricators typically extract this information from the contract plans by calculating the beam slope from bearing seat elevations on the bridge "Bearing Seat Elevations and Quantities" sheet. The fabricator then determines which load application "platten" satisfies the slope tolerance specifications and can be used in the pad vulcanization process. The standard pads listed on the IBEB sheet will deflect around 4% on average, or about  $5/32$ " for the 2" of elastomer in them, which typically is sufficient to accommodate a slope mis-match from fabrication or construction sources. ( $5/32$ " in 9" is equivalent to a slope of 1.74%.)

#### *Design Recommendations:*

- 1.) For beams on grades of between 1 and 3%, taper the pads accordingly. The top layer only shall be tapered. (all shims parallel)
- 2.) For beams on grades of between 3 and 6%, taper the top two layers, limiting the top layer thickness to  $3/8$ " at the thick end. (all shims parallel except top shim)
- 3.) Beams on grades greater than 6% will require special consideration (ie, span restraints, pad restraints, higher durometer elastomer, custom shim placement, etc.; see Report 1304-3, Chapter 8 for conclusions concerning heavily tapered pads). 6% beam slope is the upper limit that TxDOT will design tapered pads for without special precautions, such as locking the "low" end of the unit in place and forcing the structure to expand uphill.

### *Bearing Seat Geometry:*

For custom applications, the designer needs to be aware of the specified minimum cap edge and beam edge distances. The centerline of bearing is a nominal distance and the pads will function satisfactorily if placed off center from it as long as the load is not placed close to a cap edge to induce spalling or overlapping a beam chamfer edge to pinch the elastomer and induce a "walking" phenomena on the cap surface. When checking the required edge distances for custom designs, also take note of the beam end clearance values listed on the standard. Beam end clearance values vary with cap type and are increased on cap types such as inverted tee interior bents, where field experience with construction/fabrication errors and resulting beam end trimming has dictated the need for more room.

### *General:*

Continue to "round" layer thicknesses to 1/8" increments within shape factor constraints. Pad width (transverse to beam longitudinal axis) for custom designs should not be less than approximately 3/4 of the bottom beam flange width without a more thorough analysis. TxDOT currently has some exceptions to this guideline - round pads, pads for smaller beams, etc - but have had feedback that in general there have been no construction related stability problems with these particular pads. A general rule of thumb is to design the width of the pad so that the c.g. will always fall within the middle third of the pad. If construction tolerances, i.e. horizontal beam sweep, variance from plumb, out of level bearing seats and so on, can vary the c.g. a four inch total width, then the pad should be at least 12" wide.

### *Bearing Pad Material:*

TxDOT currently prohibits the use of "Polyisoprene" (Natural Rubber) for the manufacture of bearing pads. This is due to a slip problem experienced in the late 1980's and early 1990's that was caused by a "blooming" of paraffin wax used in the formulation to the surface of the pad. This wax can be used in "Polychloroprene" (Neoprene) but is usually present in much smaller amounts than in natural rubber, and as yet there have been no documented cases of neoprene-associated slip due to a wax bloom in Texas.

## **Compressive Stress and Deflection Checks:**

### *Compressive Stress Allowables:*

The Live Load check is intended to keep the maximum stresses within a reasonable "range"; it is believed that the temporary nature of a live load has little effect on long term serviceability of the bearing. Thus, the 1500 psi limit, is not an absolute max and overages of up to 15% above this limit are not cause to resize the pad. Reinforced elastomeric bearing pads in the configurations that TxDOT uses have failed in laboratory compression tests at stresses of between 15,000 and 20,000 psi and therefore have large factors of safety against compressive failure. Of greater concern is the loading that the pad sees on a permanent basis, such as under dead load, the consequent side face bulging, and how well the pad functions in combination with cycles of thermally-induced shear strain. For this reason the 1200 psi dead load stress maximum should not be exceeded by more than 5% and only if the shape factor permits. Unlike AASHTO requirements for Method A or Method B, TxDOT design practice places no additional requirement on materials testing when using these compressive allowables. Instead, material quality is insured via prequalification of fabricators, the elastomer formulation and 100% load testing of pads produced for TxDOT.

### *Compressive Deflection:*

Compressive deflection is usually not a concern from a functionality standpoint, since the 4% to 5% range of deflection that most TxDOT standard pads undergo yields a hardly noticeable 3/32" vertical compression. Severely tapered pads can deflect up to 60% more (close to 5/32" total), but still not enough to induce a "bump" at the end of a bridge. This information becomes useful when determining if a pad can absorb construction mis-matches and/or to check rotation ability. Creep will add as much as 25% more deflection, but this is not a concern as it will add a maximum 3/16" total deflection.

### **Anchorage Check (Slip):**

#### *Slip failure solutions:*

Typically slip problems are controlled by increasing the pad thickness. In some cases this may not be desirable from an economic standpoint (fabricator re-tooling) or if the resulting height violates stability criteria. Alternative solutions might include the following:

- 1) Increasing the beam spacing to increase bearing dead load if the beams can handle the additional load.
- 2) Increasing the end span length if feasible.
- 3) Reducing the number of spans in the unit if the resulting increase in cost of deck joints does not offset the cost of custom pads. (Standard pads cost approximately \$65 to \$100 each, custom pads cost almost double the amount of standard ones. Both items usually represent, a very small percentage of overall bridge cost and therefore, the decision on which item to purchase is not critical.)
- 4) As a last resort, decrease the pad plan area to increase slip resistance. The least expensive way to do this is to pick a standard pad for the next smallest beam on the IBEB sheet. For a Type "C" beam case that does not work, try a pad from the table for "B" beams or "A" beams. If none of the standard pads solve the problem, design new pad plan dimensions. This requires the fabricator to order new forms or shim the insides of existing forms, so a large volume job is preferable for this option. When reducing the plan area, do so by decreasing the pad length to preserve pad stability. Construction stability of the beam on the bearing prior to construction bracing installation may be a concern when calculating the pad length reduction. There have been no reports of construction instability associated with relatively narrow pad widths such as that for an AASHTO Type IV beam when using the 15" diameter round pad. Another rule of thumb is to make the pad wide enough so that the center of gravity will never fall outside of the middle third of the pad. This calculation would be based on the designer's estimate of how out of plumb the beam may tilt in the field due to bearing seat construction tolerances, beam mis-fabrication, beam "warping", and etc. In the absence of a more refined approach, experience with the existing pad geometries is probably the best guide.

## Appendix B

ELASTOMERIC BEARING DATA TABLE								
Bent Type	Beam Type	Brg Type (13)	Beam End Skew Angle Range	Pad Size Lgth x Wdth	Pad Clip Dimensions		"C" (9)	
					"A"	"B"		
AT ABUTMENTS, INVERTED - T & TRANSITION BENTS WITH BACKWALLS	A	A-1-"N"	0° thru 15°	7" x 12"	—	—	—	
	A	A-2-"N"	15° + thru 45°	7" x 12"	1 1/4"	1 1/4"	3/4"	
	A	A-3-"N"	45° + thru 60°	7" x 12"	1 1/2"	2"	1"	
	B	B-1-"N"	0° thru 15°	7" x 14"	—	—	—	
	B	B-2-"N"	15° + thru 45°	7" x 14"	2 1/4"	2 1/4"	3/4"	
	B	B-3-"N"	45° + thru 60°	7" x 14"	3 3/4"	2 1/4"	1"	
	C	C-1-"N"	0° thru 15°	7" x 16"	—	—	—	
	C	C-2-"N"	15° + thru 45°	7" x 16"	3 1/4"	3 1/4"	3/4"	
	C	C-3-"N"	45° + thru 60°	8" x 16"	6"	4"	1"	
	IV	IV-1-"N"	0° thru 15°	7" x 22"	—	—	1"	
	IV	IV-2-"N"	15° + thru 29°	7" x 22"	2 1/2"	4 1/2"	1"	
	IV	IV-3-"N"	30° (16)	15" Dia	—	—	2 3/8"	
	IV	IV-4-"N"	40° (16)	15" Dia	—	—	2 5/8"	
	IV	IV-5-"N"	50° (16)	15" Dia	—	—	3 1/8"	
	IV	IV-6-"N"	60° (16)	15" Dia	—	—	4"	
	VI	VI-1-"N"	0° thru 15°	9" x 24"	—	—	2"	
	VI	VI-2-"N"	15° + thru 29°	9" x 24"	3 1/4"	5 1/2"	2"	
	VI	VI-3-"N"	30° (16)	17" Dia	—	—	3 3/4"	
	VI	VI-4-"N"	40° (16)	17" Dia	—	—	4"	
	VI	VI-5-"N"	50° (16)	17" Dia	—	—	5 1/2"	
VI	VI-6-"N"	60° (16)	17" Dia	—	—	6"		
AT CONVENTIONAL INTERIOR BENTS	Sq Bm Ends	A	A-4-"N"	Not Applicable	7" x 12"	—	—	—
		B	B-4-"N"	Not Applicable	7" x 14"	—	—	—
		C	C-4-"N"	Not Applicable	7" x 16"	—	—	—
		IV	IV-7-"N"	Not Applicable	7" x 22"	—	—	—
		VI	VI-7-"N"	Not Applicable	9" x 24"	—	—	—
		Skewed Bm Ends	A	A-5-"N"	0° thru 15°	7" x 12"	—	—
	A		A-6-"N"	15° + thru 60°	7" x 12"	1"	1"	—
	B		B-5-"N"	0° thru 15°	7" x 14"	—	—	—
	B		B-6-"N"	15° + thru 45°	7" x 14"	1 3/4"	1 3/4"	—
	B		B-7-"N"	45° + thru 60°	7" x 14"	2 3/4"	1 3/4"	—
	C		C-5-"N"	0° thru 15°	7" x 16"	—	—	1/2"
	C		C-6-"N"	15° + thru 45°	7" x 16"	2 3/4"	2 3/4"	—
	C		C-7-"N"	45° + thru 60°	7" x 16"	4 1/2"	2 3/4"	—
	IV		IV-8-"N"	0° thru 15°	7" x 22"	—	—	1"
	IV		IV-9-"N"	15° + thru 29°	7" x 22"	1 1/4"	2"	—
	IV		IV-10-"N"	29° + thru 60°	15" Dia	—	—	—
	VI		VI-8-"N"	0° thru 15°	9" x 24"	1"	3 3/4"	1 1/2"
	VI	VI-9-"N"	15° + thru 29°	9" x 24"	1"	2"	—	
VI	VI-10-"N"	29° + thru 60°	17" Dia	—	—	—		

**Table B-1. Elastomeric Bearing Data from the IBEB Standard**

## Appendix C

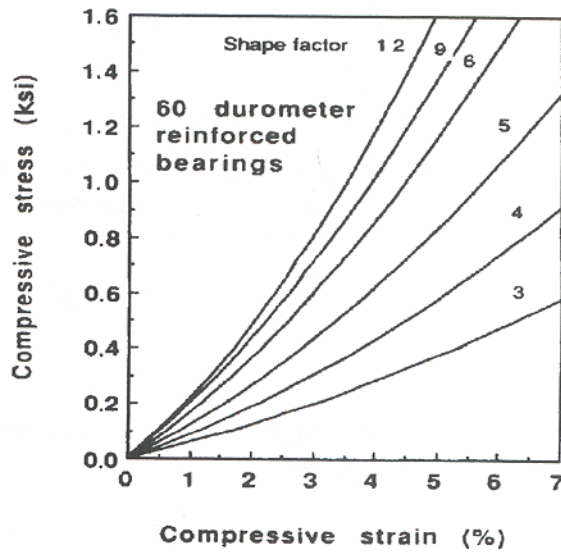
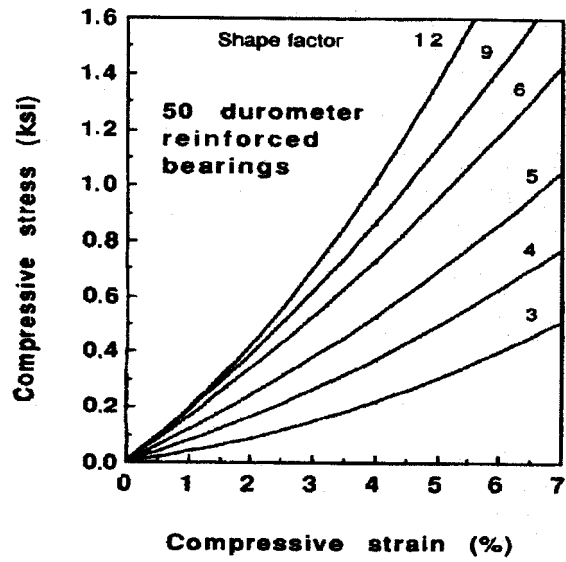


Figure C14.7.5.3.3-1 Stress-Strain Curves.

Figure C-1. Stress-Strain Curves from AASHTO LRFD

Appendix 4-1

Bearing Condition Sheets for Wichita Falls Inspection and Protractor

# Bearing Condition Sheet

Mark:	A
Plan:	371
Skew:	0

Date:	20-Feb-08
Looking:	Upstation
Joint:	No Joint

Temp:	57 °F
-------	-------



## Beam Slopes

Transverse:	5.80%
Longitudinal:	1.80%
Bearing Seat:	6.60%

Down to the:	Left
Down to the:	Upstation (Left)
Down to the:	Left

## Heights: (The total height is 2 and X/32 inches)

	Left
Front	15
Back	N/A

	Right
	16
	N/A

## Transverse Slopes (degrees from bearing seat)

	Left
Front	108
Back	

	Right
	104

## Longitudinal Slopes (degrees from bearing seat)

	Left
Front	92
Back	

	Right
	92

## Uplift

Left	None Visible
------	--------------

Minor Uplift for about 1/2 in.

Right	0.50
-------	------

# Bearing Condition Sheet

Mark:	B
Plan:	371
Skew:	

Date:	20-Feb-08
Looking:	
Joint:	

Temp:	58 °F
-------	-------



## Beam Slopes

Transverse:	3.70%
Longitudinal:	0.10%
Bearing Seat:	4.10%

Down to the:	Left
Down to the:	Upstation
Down to the:	Left

## Heights: (The total height is 2 and X/32 inches)

	Left
Front	13
Back	N/A

	Right
	16
	N/A

## Transverse Slopes (degrees from bearing seat)

	Left
Front	102
Back	

	Right
	99

## Longitudinal Slopes (degrees from bearing seat)

	Left
Front	
Back	

	Right

## Uplift

Left	None Visible
------	--------------

Right	None Visible
-------	--------------

# Bearing Condition Sheet

Mark:	C
Plan:	371
Skew:	

Date:	20-Feb-08
Looking:	
Joint:	

Temp:	58 °F
-------	-------



## Beam Slopes

Transverse:	3.00%
Longitudinal:	0.40%
Bearing Seat:	2.40%

Down to the:	Left
Down to the:	Upstation
Down to the:	Left

## Heights: (The total height is 2 and X/32 inches)

	Left
Front	17
Back	N/A

	Right
	12
	N/A

## Transverse Slopes (degrees from bearing seat)

	Left
Front	110
Back	

	Right
	110

## Longitudinal Slopes (degrees from bearing seat)

	Left
Front	
Back	

	Right

## Uplift

Front	None Visible
-------	--------------

	Minor uplift for 1/2 in
Right	0.50

# Bearing Condition Sheet - Bearing D1

Mark:	D1
Plan:	371
Skew:	

Date:	20-Feb-08
Looking:	
Joint:	

Temp:	65 °F
-------	-------



## Beam Slopes

Transverse:	1.00%
Longitudinal:	0.80%
Bearing Seat:	1.00%

Down to the:	Right
Down to the:	Downstation
Down to the:	Right

## Heights: (The total height is 2 and X/32 inches)

	Left
Front	12
Back	N/A

	Right
	12
	N/A

## Transverse Slopes (degrees from bearing seat)

	Left
Front	100
Back	

	Right
	100

## Longitudinal Slopes (degrees from bearing seat)

	Left
Front	
Back	

	Right

## Uplift

Left	None Visible
------	--------------

Right	None Visible
-------	--------------

# Bearing Condition Sheet

Mark:	D2
Plan:	371
Skew:	

Date:	20-Feb-08
Looking:	
Joint:	

Temp:	65 °F
-------	-------



## Beam Slopes

Transverse:	1.00%
Longitudinal:	0.80%
Bearing Seat:	0.70%

Down to the:	Right
Down to the:	Downstation
Down to the:	Right

## Heights: (The total height is 2 and X/32 inches)

	Left
Front	16
Back	N/A

Right
14
N/A

## Transverse Slopes (degrees from bearing seat)

	Left
Front	100
Back	

Right
100

## Longitudinal Slopes (degrees from bearing seat)

	Left
Front	
Back	

Right

## Uplift

Left	None Visible
------	--------------

Right	None Visible
-------	--------------

# Bearing Condition Sheet

Mark:	E
Plan:	371
Skew:	

Date:	20-Feb-08
Looking:	
Joint:	

Temp:	65 °F
-------	-------



## Beam Slopes

Transverse:	6.10%
Longitudinal:	0.10%
Bearing Seat:	6.00%

Down to the:	Left
Down to the:	Upstation
Down to the:	Left

## Heights: (The total height is 2 and X/32 inches)

	Left
Front	14
Back	N/A

Right
18
N/A

## Transverse Slopes (degrees from bearing seat)

	Left
Front	105
Back	

Right
100

## Longitudinal Slopes (degrees from bearing seat)

	Left
Front	
Back	

Right
1.25

## Uplift

Left	None Visible
------	--------------

Good amount for 1.25"

Right	None Visible
-------	--------------

# Bearing Condition Sheet

Mark:	F
Plan:	371
Skew:	

Date:	20-Feb-08
Looking:	
Joint:	

Temp:	65 °F
-------	-------



## Beam Slopes

Transverse:	5.20%
Longitudinal:	0.10%
Bearing Seat:	6.50%

Down to the:	Left
Down to the:	Upstation
Down to the:	Left

## Heights: (The total height is 2 and X/32 inches)

	Left
Front	17
Back	N/A

Right
18
N/A

## Transverse Slopes (degrees from bearing seat)

	Left
Front	105
Back	

Right
104

## Longitudinal Slopes (degrees from bearing seat)

	Left
Front	
Back	

Right

## Uplift

Left	None Visible
------	--------------

Right	None Visible
-------	--------------

# Bearing Condition Sheet

Mark:	G (G1)
Plan:	185
Skew:	

Date:	20-Feb-08
Looking:	
Joint:	

Temp:	75 °F
-------	-------



## Beam Slopes

Transverse:	6.40%
Longitudinal:	1.20%
Bearing Seat:	4.70%

Down to the:	Right
Down to the:	DownStation
Down to the:	Right

## Heights: (The total height is 2 and X/32 inches)

	Left
Front	19
Back	N/A

Right
14
N/A

## Transverse Slopes (degrees from bearing seat)

	Left
Front	100
Back	

Right
100

## Longitudinal Slopes (degrees from bearing seat)

	Left
Front	
Back	

Right

## Uplift

Left	Yes
------	-----

Right	None Visible
-------	--------------

# Bearing Condition Sheet

Mark:	H (G2)
Plan:	185
Skew:	

Date:	20-Feb-08
Looking:	
Joint:	

Temp:	75 °F
-------	-------



## Beam Slopes

Transverse:	6.40%
Longitudinal:	1.20%
Bearing Seat:	4.70%

Down to the:	Right
Down to the:	DownStation
Down to the:	Right

## Heights: (The total height is 2 and X/32 inches)

	Left
Front	16
Back	N/A

Right
14
N/A

## Transverse Slopes (degrees from bearing seat)

	Left
Front	103
Back	

Right
105

## Longitudinal Slopes (degrees from bearing seat)

	Left
Front	
Back	

Right

## Uplift

Left	Yes
------	-----

Right	Crunched
-------	----------

# Bearing Condition Sheet

Mark:	I
Plan:	185
Skew:	

Date:	20-Feb-08
Looking:	
Joint:	

Temp:	76 °F
-------	-------



## Beam Slopes

Transverse:	5.30%
Longitudinal:	1.10%
Bearing Seat:	5.80%

Down to the:	Right
Down to the:	DownStation
Down to the:	Right

## Heights: (The total height is 2 and X/32 inches)

	Left
Front	17
Back	N/A

Right
15
N/A

## Transverse Slopes (degrees from bearing seat)

	Left
Front	108
Back	

Right
110

## Longitudinal Slopes (degrees from bearing seat)

	Left
Front	
Back	

Right

## Uplift

Left	Little at corner
------	------------------

Right	None Visible
-------	--------------

# Bearing Condition Sheet

Mark:	I
Plan:	185
Skew:	

Date:	20-Feb-08
Looking:	
Joint:	

Temp:	76 °F
-------	-------



## Beam Slopes

Transverse:	5.30%
Longitudinal:	1.10%
Bearing Seat:	5.80%

Down to the:	Right
Down to the:	DownStation
Down to the:	Right

## Heights: (The total height is 2 and X/32 inches)

	Left
Front	14
Back	N/A

Right
15
N/A

## Transverse Slopes (degrees from bearing seat)

	Left
Front	105
Back	

Right
105

## Longitudinal Slopes (degrees from bearing seat)

	Left
Front	
Back	

Right

## Uplift

Left	Little
------	--------

Right	None Visible
-------	--------------

# Bearing Condition Sheet

Mark:	K
Plan:	185
Skew:	

Date:	20-Feb-08
Looking:	
Joint:	

Temp:	66 °F
-------	-------



## Beam Slopes

Transverse:	6.60%
Longitudinal:	0.40%
Bearing Seat:	6.60%

Down to the:	Left
Down to the:	Upstation
Down to the:	Left

## Heights: (The total height is 2 and X/32 inches)

	Left
Front	13
Back	N/A

	Right
	15
	N/A

## Transverse Slopes (degrees from bearing seat)

	Left
Front	105
Back	

	Right
	100

## Longitudinal Slopes (degrees from bearing seat)

	Left
Front	
Back	

	Right

## Uplift

Left	Crushed Lower Left Corner
------	---------------------------

Right	None Visible
-------	--------------

# Bearing Condition Sheet

Mark:	L
Plan:	185
Skew:	

Date:	20-Feb-08
Looking:	
Joint:	

Temp:	66 °F
-------	-------



## Beam Slopes

Transverse:	6.20%
Longitudinal:	1.20%
Bearing Seat:	5.90%

Down to the:	Right
Down to the:	Downstation
Down to the:	Right

## Heights: (The total height is 2 and X/32 inches)

	Left
Front	17
Back	N/A

Right
18
N/A

## Transverse Slopes (degrees from bearing seat)

	Left
Front	99
Back	

Right
100

## Longitudinal Slopes (degrees from bearing seat)

	Left
Front	
Back	

Right

## Uplift

Front	None Visible
-------	--------------

Right	4.25"
-------	-------

# Bearing Condition Sheet

Mark:	M
Plan:	185
Skew:	

Date:	20-Feb-08
Looking:	
Joint:	

Temp:	65 °F
-------	-------



## Beam Slopes

Transverse:	6.20%
Longitudinal:	1.20%
Bearing Seat:	7.00%

Down to the:	Right
Down to the:	Downstation
Down to the:	Right

## Heights: (The total height is 2 and X/32 inches)

	Left
Front	17
Back	N/A

	Right
	18
	N/A

## Transverse Slopes (degrees from bearing seat)

	Left
Front	100
Back	

	Right
	100

## Longitudinal Slopes (degrees from bearing seat)

	Left
Front	
Back	

	Right

## Uplift

Left	1.5"
------	------

Right	Crushed upper Right Corner
-------	-------------------------------

# Bearing Condition Sheet

Mark:	N
Plan:	185
Skew:	

Date:	20-Feb-08
Looking:	
Joint:	

Temp:	65 °F
-------	-------



## Beam Slopes

Transverse:	5.30%
Longitudinal:	1.00%
Bearing Seat:	4.90%

Down to the:	Right
Down to the:	South
Down to the:	Right

## Heights: (The total height is 2 and X/32 inches)

	Left
Front	15
Back	N/A

	Right
	14
	N/A

## Transverse Slopes (degrees from bearing seat)

	Left
Front	97
Back	

	Right
	96

## Longitudinal Slopes (degrees from bearing seat)

	Left
Front	
Back	

	Right

## Uplift

Left	None Visible
------	--------------

Right	None Visible
-------	--------------

# Bearing Condition Sheet

Mark:	O
Plan:	185
Skew:	

Date:	20-Feb-08
Looking:	
Joint:	

Temp:	65 °F
-------	-------



## Beam Slopes

Transverse:	5.30%
Longitudinal:	1.00%
Bearing Seat:	5.40%

Down to the:	Right
Down to the:	South
Down to the:	Right

## Heights: (The total height is 2 and X/32 inches)

	Left
Front	16
Back	N/A

	Right
	16
	N/A

## Transverse Slopes (degrees from bearing seat)

	Left
Front	96
Back	

	Right
	99

## Longitudinal Slopes (degrees from bearing seat)

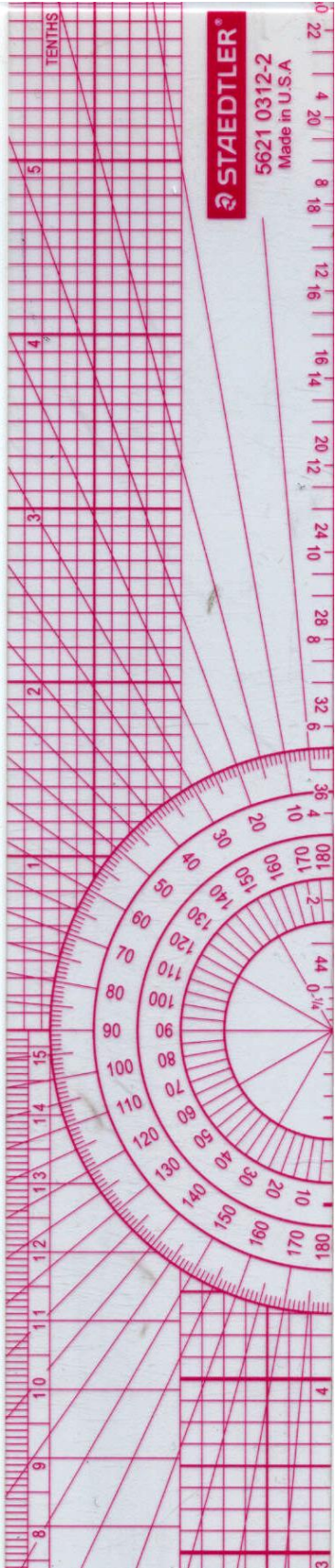
	Left
Front	
Back	

	Right

## Uplift

Front	None Visible
-------	--------------

Right	None Visible
-------	--------------



Appendix 4-2  
Additional Strain Gage Information

## Material List for Strain Gage Application

### Strain Gages

Name: SR-4 General Purpose Strain Gages, GF=2.06  
Manufacturer: Vishay Micro-Measurements  
Part Number: EP-08-125RA-120

### Cellophane Tape

Name: M-Line Accessories Cellophane Tape  
Manufacturer: Vishay Micro-Measurements  
Part Number: PCT-2A 6599, Control #0002

### Terminals

Name: M-Line Bondable Terminals  
Manufacturer: Vishay Micro-Measurements  
Part Number: CPF-75C

### Strain Gage and Terminal Bonding Material

Name: M-Bond AE 10 Adhesive Kit  
Manufacturer: Vishay Micro-Measurements  
Part Number: F015578, Control #000800

### Wire Connecting Strain Gage to Terminal

Name: 34 Gage Red ETP Single Conductor Wire  
Manufacturer: Vishay Micro-Measurements  
Part Number: 134-AQP6484

### Wire Connecting Strain Gage to Terminal

Name: 34 Gage Red ETP Single Conductor Wire  
Manufacturer: Vishay Micro-Measurements  
Part Number: 134-AQP6484

### Soldering Station

Name: Temperature Controlled Soldering Station  
Manufacturer: Tenma  
Part Number: Model #21-7935

### Solder

Name: M-Line 6619 Solder  
Manufacturer: Vishay Micro-Measurements  
Part Number: 361A-20R-25, Control #144

## **Material List for Strain Gage Application (Cont.)**

### Wire Connecting Terminal to P3

Name: 26 AWG 3 Conductor Wire  
Manufacturer: Vishay Micro-Measurements  
Part Number: 326-DFV

### Strain Gage Recorder

Name: P3 Strain Indicator and Recorder  
Manufacturer: Vishay Micro-Measurements  
Part Number: P3

### Rubber Protective Covering

Name: Strain Gage Protective Covering  
Manufacturer: Vishay Micro-Measurements  
Part Number: M-coat F Kit, 6692, Control #0647

### Keystone Jacks

Name: Cat 5E keystone Jack T568 A/B Ivory  
Manufacturer: Cat 5E  
Part Number: NKJ-5107



## Dead Loads

### General Information

$$\text{span} = 87.59\text{ft} \quad \text{spa} = 12.25 \text{ ft} \quad \text{DFV} = 1.175$$

### Dead Loads

$$w_{\text{self}} = 1.167 \text{ klf} \quad w_{\text{rail}} = 0.0 \text{ klf} \quad w_{\text{bolster}} = 0.0 \text{ klf}$$

$$w_{\text{slab}} = 0.0 \frac{\text{kip}}{\text{ft}^2} \text{ spa} \quad w_{\text{slab}} = 0 \text{ klf}$$

$$w_{\text{overmin}} = 0 \text{ klf} \quad w_{\text{overmax}} = 0.0 \frac{\text{kip}}{\text{ft}^2} \text{ spa} \quad w_{\text{overmax}} = 0 \text{ klf}$$

$$P_{\text{ebmin}} = 4.06 \text{ kip} \quad P_{\text{ebmax}} = 5.41 \text{ kip}$$

$$P_{\text{intdiamin}} = 1.35 \text{ kip} \quad P_{\text{intdiamax}} = 3 \text{ kip}$$

$$R_{D\text{min}} = \left( \frac{\text{span}}{2} \right) (w_{\text{self}} + w_{\text{rail}} + w_{\text{bolster}} + w_{\text{slab}} + w_{\text{overmin}}) + P_{\text{ebmin}} + P_{\text{intdiamin}}$$
$$R_{D\text{min}} = 56.519 \text{ kip}$$

$$R_{D\text{max}} = \left( \frac{\text{span}}{2} \right) (w_{\text{self}} + w_{\text{rail}} + w_{\text{bolster}} + w_{\text{slab}} + w_{\text{overmax}}) + P_{\text{ebmax}} + P_{\text{intdiamax}}$$
$$R_{D\text{max}} = 59.519 \text{ kip}$$

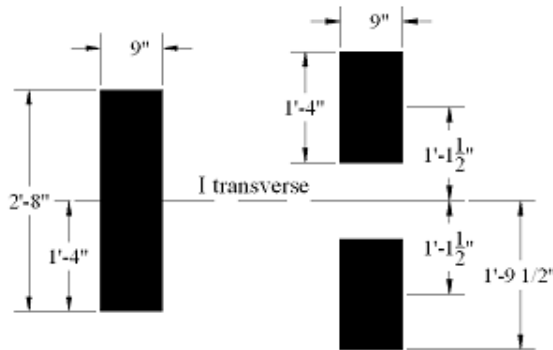
Note: Per the contractor, actual beam weight was estimated at 139.5 kips. The crane measured weight was less, approximately 140 kips less the lifting equipment (7 or 17 kips)

$$R_{D\text{min}} = \frac{139.5 \text{ kip}}{2} \quad R_{D\text{min}} = 69.75 \text{ kip}$$
$$R_{D\text{max}} = \frac{139.5}{2} \text{ kip} \quad R_{D\text{max}} = 69.75 \text{ kip}$$

Calculations for Prediction of Transverse Angle – US 82 BOS-W Overpass Ramp

### Bearing Properties

$$\begin{aligned}
 h_s &= 0.105 \text{ in} & h_{ro} &= 0.25 \text{ in} & n_{ro} &= 2 & h_{rto} &= h_{ro} n_{ro} \\
 h_{rto} &= 0.5 \text{ in} & h_{ri} &= 0.375 \text{ in} & n_{ri} &= 4 & h_{rti} &= h_{ri} n_{ri} \\
 h_{rti} &= 1.5 \text{ in} & h_{rt} &= h_{rto} + h_{rti} & h_{rt} &= 2 \text{ in} & T &= h_{rt} + (n_{ro} + n_{ri} - 1) h_s \\
 T &= 2.525 \text{ in} & d_2 &= 13.5 \text{ in} & & & &
 \end{aligned}$$



### One Pad Properties

$$\begin{aligned}
 W_1 &= 32 \text{ in} & L_1 &= 9 \text{ in} & A_1 &= W_1 L_1 & A_1 &= 288 \text{ in}^2 \\
 A_{1b} &= (W_1 + L_1) 2 h_{ri} & A_{1b} &= 30.75 \text{ in}^2 & S_1 &= \frac{A_1}{A_{1b}} & S_1 &= 9.366 \\
 I_{T1} &= \frac{L_1 W_1^3}{12} & I_{T1} &= 24576 \text{ in}^4 & S_{T1} &= \frac{I_{T1}}{\frac{W_1}{2}} & S_{T1} &= 1536 \text{ in}^3
 \end{aligned}$$

### Two Pad Properties

$$\begin{aligned}
 W_2 &= 16 \text{ in} & L_2 &= 9 \text{ in} & A_2 &= W_2 L_2 & A_2 &= 144 \text{ in}^2 \\
 A_{2b} &= (W_2 + L_2) 2 h_{ri} & A_{2b} &= 18.75 \text{ in}^2 & S_2 &= \frac{A_2}{A_{2b}} & S_2 &= 7.68 \\
 I_{T2} &= 2 \frac{L_2 W_2^3}{12} + 2 (L_2 W_2) d_2^2 & I_{T2} &= 58632 \text{ in}^4 \\
 S_{T2} &= \frac{I_{T2}}{d_2 + \frac{W_2}{2}} & S_{T2} &= 2727 \text{ in}^3
 \end{aligned}$$

Calculations for Prediction of Transverse Angle – US 82 BOS-W Overpass Ramp (Cont.)

## Transverse Loads

### *Delta1 Displacement*

$$\Theta_T = 0.038 \quad \Theta_L = 0.0 \quad G_{\text{low}} = 0.095 \text{ksi} \quad G_{\text{high}} = 0.175 \text{ksi}$$

$$P_D = R_{D\text{max}} \quad P_D = 69.75 \text{kip} \quad P_{LL} = R_{LL} \quad P_{LL} = 0 \text{kip}$$

$$\text{Delta1}_D = \frac{P_D \Theta_T h_{rt}}{G_{\text{low}} A_1} \quad \text{Delta1}_D = 0.19 \text{in}$$

$$\text{Delta1}_{LL} = \frac{P_{LL} \Theta_T h_{rt}}{G_{\text{low}} A_1} \quad \text{Delta1}_{LL} = 0 \text{in}$$

### *Delta2 Displacement*

$$Y_{\text{bott}} = 22.36 \text{in} \quad \text{Delta2} = Y_{\text{bott}} \Theta_T \quad \text{Delta2} = 0.85 \text{in}$$

$$M_{\text{TDL}} = \left[ \text{Delta1}_D + \text{Delta2} \right] P_D \quad M_{\text{TDL}} = 72.779 \text{kip in}$$

$$M_{\text{TLL}} = \left[ \text{Delta1}_{LL} + \text{Delta2} \right] P_{LL} \quad M_{\text{TLL}} = 0 \text{kip in}$$

$$M_T = M_{\text{TDL}} + M_{\text{TLL}} \quad M_T = 72.779 \text{kip in}$$

### *Angle Predicted*

$$\beta_D = \text{atan} \left( \frac{\text{Delta1}_D}{T} \right) \quad \beta_D \frac{180}{\pi} = 4.388$$

Calculations for Prediction of Transverse Angle – US 82 BOS-W Overpass Ramp (Cont.)

## Appendix 6-1

Product P1 - Modifications to the LRFD Design of U-Beam Bearings

---

## Section 6

### Prestressed Concrete U Beams (Types U40 and U54)

#### Materials

Use Class H concrete with a minimum  $f'_{ci} = 4.0$  ksi and  $f'_c = 5.0$  ksi.

Design beams for 0.5-in, low-relaxation strands. You may use 0.6-in, low-relaxation strands for unusual cases but should check its availability with fabricators.

Use prestressing strand with a specified tensile strength,  $f_{pu}$ , of 270 ksi.

You need not increase section properties of the beam to account for the transformed area of strands or mild steel.

#### Geometric Constraints

The maximum skew angle for U-beam bridges is 45 degrees.

The maximum allowable transverse slope for U-beam bridges using standard uniform-height steel-reinforced elastomeric bearings is 4 percent.

#### Structural Analysis

Beam designs must meet the following requirements:

- ◆ Include the overlay at the discretion of the designer or if the bridge will receive the overlay immediately after construction. Recognize that including the overlay in the design of U beams can significantly limit their ability to span longer span lengths.
- ◆ Distribute 2/3 of the rail dead load to the exterior beam and 1/3 of the rail dead load to the adjacent interior beam applied to the composite cross section.
- ◆ Each U beam has two interior diaphragms at a maximum average thickness of 13 in. They are located as close as 10 ft. from midspan of the beam. Account for each diaphragm as a 2-kip load for U40 beams and as a 3-kip load for U54 beams applied to the non-composite cross section.
- ◆ Use section properties given on the standard drawings.
- ◆ Composite section properties may be calculated assuming the beam and slab to have the same modulus of elasticity (for beams with  $f'_c < 8.5$  ksi). Do not include haunch concrete placed on top of the beam when determining section properties. Section properties based on final beam and slab modulus of elasticity may also be used.

- ◆ Live load distribution factors must conform to *AASHTO LRFD Bridge Design Specifications*, Article 4.6.2.2.2 for flexural moment and Article 4.6.2.2.3 for shear, except for exterior beam design. For exterior beam design, use a distribution factor

for two or more design lanes loaded only. Do not use the distribution factor for one design lane loaded unless the clear roadway width is less than 20.0 ft. Use 1.0 for the multiple presence factor for one lane loaded. For exterior beams, multiply the result of the lever rule by 0.9 to account for continuity. The live load used to design the exterior beam must never be less than the live load used to design an interior beam.

- ◆ For bridges with less than three girders in the cross section, assume the live load distribution factors for flexural moment and shear are equal to the number of lanes divided by the number of girders. Determine the number of lanes as required by *AASHTO LRFD Bridge Design Specifications*, Article 3.6.1.1.1.

### Design Criteria

Standard beam designs must meet the following requirements:

- ◆ Stresses at the ends of the beam are controlled with the use of debonding. Draped strands are not permitted in U beams.
- ◆ The maximum amount of debonding is limited to 75% of the strands per row and per section.
- ◆ The maximum debonded length is the lesser of the following:
  - Half-span length minus the maximum development length specified in the AASHTO LRFD Bridge Design Specifications, Article 5.11.3.
  - 0.2 times the span length
  - 15.0 ft.
- ◆ Grouping of U-beam designs are at the discretion of the designer. However, no exterior U beam may have less carrying capacity than that of an interior U beam of equal length. If the designer chooses to group beams, a general rule is to group beams with no more than a four-strand difference.
- ◆ See [“Prestressed Concrete I Beams”](#) and [“Steel-Reinforced Elastomeric Bearings for Prestressed Concrete Beams”](#) for other design criteria.

### Detailing

Detail span sheets for a cast-in-place slab with precast concrete panels.

---

## Section 2

### Steel-Reinforced Elastomeric Bearings for Prestressed Concrete Beams

#### Materials

Use 50-durometer neoprene for steel-reinforced elastomeric bearings.

Use a shear modulus range of 95 to 175 psi for design, using the least favorable value for the design check.

Make steel shims 0.105 in. thick.

Do not use adhesives between bearings and other components.

#### Geometric Constraints

See standard drawings available at <http://www.dot.state.tx.us/insdot/orgchart/cmd/cserve/standard/bridge-e.htm> for standard pad details.

You may use tapered bearings if the taper does not exceed 0.055 ft./ft. For beams on steeper grades, use a beveled steel sole plate field-welded (1/4-in, fillet) to a 1/2-in, steel plate embedded in and anchored to beams with headed stud anchors. Use a minimum of four 1/2-in.-by-3-in. stud anchors with studs located between strands and reinforcement. The minimum thickness of sole plate should be 1.5 in. of steel between weld and elastomer. The sole plate should extend at least 1 in. beyond the beam flange. Sole plates should not be vulcanized to the bearing to allow slip to occur at the beam/bearing interface.

Use 1/4-in, exterior pad layers. If using 1/4-in, interior pad layers, disregard the requirements in the *AASHTO LRFD Bridge Design Specifications*, Article 14.7.6.1, specifying exterior layers no thicker than 70% of internal layers.

#### Structural Analysis

Assume a temperature change of 70 degrees Fahrenheit after erection when calculating thermal movement in one direction (not total). This provides a conservative estimate of thermal movement after erection in most regions of Texas based on the minimum and maximum temperature contour maps in the *AASHTO LRFD Bridge Design Specifications*, Article 3.12.2.2.1 (the panhandle region is the most extreme case with  $T_{min}$  at 10 degrees F and  $T_{max}$  at 115 degrees F).

Do not include shrinkage, creep, and elastic shortening when determining maximum movement, which will be accommodated through infrequent slip.

Do not apply IM to live load when checking compressive stress (see *AASHTO LRFD Bridge Design Specifications*, Commentary C 14.7.5.3.2).

Use appropriate shear live load distribution, modified for skew.

Use the critical DL condition (the lightest predicted DL) when checking against slip as required by *AASHTO LRFD Bridge Design Specifications*, Article 14.7.6.4.

Use Load Combination Service I for all gravity loads.

For the design of steel-reinforced elastomeric bearings for U-beam bridges placed on a transverse slope, the effect of the transverse slope shall be considered by including:

- ◆ The transverse displacement,  $\Delta_1$ , caused by the horizontal component of the end reaction;
- ◆ The distance from the centerline of the bearing and the center of gravity of the composite U-beam and deck section,  $\Delta_2$ , determined as the product of the transverse slope and the perpendicular distance from the bottom of the composite U-beam and deck section to its center of gravity;
- ◆ The transverse moment,  $M_t$ , determined by the product of the end reaction and the sum of the  $\Delta_1$  and  $\Delta_2$  distances for the Compressive Stress, Compressive Deflection, and the Rotation checks;
- ◆ The effective displacement,  $\Delta_{s, \text{Eff}}$ , determined as the square root of the sum of the  $\Delta_1$  and the thermal expansion displacements for the Shear Strain check;
- ◆ The effective slope,  $\Theta_{\text{Eff}}$ , determined as the square root of the sum of the transverse and longitudinal slopes for the Anchorage Slip check.

### Design Criteria

Follow Design Method A in *AASHTO LRFD Bridge Design Specifications*, Article 14.7.6, with the following exceptions:

- ◆ DL compressive stress limit is the lesser of 1.20 ksi and 1.2 GS.
- ◆ Total compressive stress limit is the lesser of 1.50 ksi and 1.5 GS. This limit can be exceeded up to 15% at the engineer's discretion.
- ◆ For rotation check, disregard *AASHTO LRFD Bridge Design Specifications*, Article 14.7.6.3.5. Rotation is acceptable if the total compressive deflection equals or exceeds  $\frac{\Theta_x(0.8xL)}{2}$ , where L is the pad length defined in *AASHTO LRFD Bridge Design Specifications*, and  $\Theta$  is the total rotation. Estimate compressive deflection using *AASHTO LRFD Bridge Design Specifications*, Figure C14.7.5.3.3-1.

- ◆ Calculate total rotation for dead and live load plus 0.005 radians for construction uncertainties as required by *AASHTO LRFD Bridge Design Specifications*, Article 14.4.2.1. Take maximum live load rotation as  $4 \Delta / (\text{span length})$ , where  $\Delta$  is midspan LL deflection.
- ◆ Account for pad taper when checking against slip as required by *AASHTO LRFD Bridge Design Specifications*, Article 14.7.6.4, as follows:  $\Delta_s \leq (0.2 - Gr) \times DL \times h_{rt} / (G \times A)$ , where Gr = beam grade in ft./ft.
- ◆ You may use  $h_{rt}$  instead of total pad height when checking stability as required in *AASHTO LRFD Bridge Design Specifications*, Article 14.7.6.3.6.

### Detailing

Use standard drawing IBEB for guidance on detailing custom bearing pad designs.